UNIVERSITÉ DE STRASBOURG

ÉCOLE DOCTORALE DES SCIENCES DE LA VIE ET DE LA SANTE

Institut de Biologie Moléculaire des Plantes

UPR CNRS 2357

THÈSE présentée par :

Thibaut HACQUARD

soutenue le : **21 Septembre 2018**

pour obtenir le grade de : **Docteur de l'université de Strasbourg**
Discipline/ Spécialité : Aspects Moléculaires et Cellulaires de la Biologie

---

Molecular characterization of the F-box protein FBW2 in the RNA silencing in *Arabidopsis thaliana*

THÈSE dirigée par :
   M. Pascal GENSCHIK   Directeur de recherches, CNRS

RAPPORTEURS :
   Mme. Erika ISONO   Professeur, Université de Constance
   M. Thierry LAGRANGE   Directeur de recherches, CNRS

AUTRES MEMBRES DU JURY :
   Mme. Catherine RECHENMANN   Directrice de recherches, CNRS
   Mme. Izabela SUMARA   Directrice de recherches, CNRS
   M. Hervé VAUCHERET   Directeur de recherches, INRA
   M. Grégory VERT   Directeur de recherches, CNRS

Table of contents

Abbreviations

AD	Activation Domain
APC/C	Anaphase Promoting Complex or cyclosome
AGO	ARGONAUTE
AGO1	ARGONAUTE1
AMN1	Antagonist of Mitotic exist Network 1
AMSH3	Associated Molecule with the SH3 domain of STAM3
ASK	Arabidopsis Skp1 homologue
ASK1	Arabidopsis Skp1 homologue 1
ATG	Autophagy
ATG7	Autophagy 7
ATG8	Autophagy 8
ATI1	ATG8-Interacting Protein 1
BCTV	*Beet Curly Top Virus*
BD	Binding Domain
BTB/POZ	Bric-a-brac, Tramtrack, Broad-complex / Pox virus and Zinc finger
BUL1-BUL2	Binds to Ubiquitin Ligase 1 and 2
CAND1	Cullin Associated and Neddylation Dissociated 1
CDS	Coding Sequence
CHIP	C terminus of Hsc70-Interacting Protein
CHX	Cycloheximide
CLINK	Cell cycle Link
CMA	Chaperone-Mediated Autophagy
COP1	Constitutive Photomorphogenic
CP	Coat Protein
CRL	Cullin RING Ligases
CRL3s	Cullin3 RING Ligases
CTD	C-Terminal Domain
CUL1	Cullin 1
CUL3	Cullin 3
CUL4	Cullin 4
DCAF	DDB1 CUL4 Associated Factor
DDB1	DNA Damaging Binding 1
DDB2	DNA Damaging Binding 2
DRB4	DsRNA Binding protein 4
DRM2	Domains Rearranged Methyltransferase 2
DUBs	Deubiquitination enzymes
DUF1785	Domain of Unknown Function 1785
DWD	DDB1 binding WD40
E1	Ubiquitin-activating enzyme
E2	Ubiquitin-conjugating enzyme
E3	Ubiquitin-ligase
ER	Endoplasmic Reticulum
ERAD	Endoplasmic Reticulum-Associated Degradation
FBNYV	*Faba bean necrotic yellow virus*
FBW2	F-box with WD40
GFP	Green Fluorescent Protein
GUS	β-glucuronidase
GW	Glycine-Tryptophan
HA	Human influenza Hemagglutinin

HC	HindIII-ClaI
HECT	Homologous to E6-AP Carboxyl Terminus
HEN1	HUA ENHANCER 1
HIGS	Host Induced Gene Silencing
HSP90	Heat Shock Protein 90
HST	HASTY
HYL1	Hyponastic Leaves 1
LRR	Leucine-Rich Repeats
MAPK	Mitogen-activated protein kinase
MATH	Meprin And TRAF Homology
MID	Middle
MS	Murashige and Skoog
MSI1	Suppressor of IRA1
MSI4	Suppressor of IRA4
MUSE1	Mutant *snc1*-Enhancing 1
MVBs	Multi Vesicular Bodies
NBR1	Neighbor of BRCA 1
NDP52	Nuclear Dot Protein 52
NES	Nuclear Export Signal
NLS	Nuclear Localization Signal
NRPE1	Nuclear RNA Polymerase E1
nts	Nucleotides
PABP	poly(A)-binding protein
PAZ	Piwi-Argonaute-Zwille
pb	base pair
PCR	Polymerase Chain Reaction
PE	Phosphatidylethanolamine
PNK	Polynucleotide kinase
PRT1	PROTEOLYSIS 1
PRT6	PROTEOLYSIS 6
PSRP1	Phloem Small RNA binding Protein 1
PUB4	E3 Plant U-Box 4
PUBs	Plant U-Box proteins
RBX1	RING Box Protein 1
RBX2	RING Box Protein 2
RDR6	RNA-dependent RNA polymerase 6
RFP	Red Fluorescent Protein
RING	Really Interesting New Gene
RISC	RNA Induced Silencing Complex
RITS	RNA-Induced Transcriptional Silencing complex
ROC1	Regulator of Cullin 1
RP	Regulatory Particle
RPN10	Regulatory Particle Non-ATPase 10
RPS2	Resistance to *Pseudomonas syringae* 2
RPT5	Regulatory Particle Triphosphatase 5
RUB1	Related to Ubiquitin 1
SCF	Skp1, Cullin and F-box
SE	SERRATE
SGS3	Suppressor of Gene Silencing 3

Skp1	S-phase kinase-associated protein 1
SNC1	Suppressor of *npr1-1*, constitutive 1
SPT5	Suppressor of Ty insertion 5
SQN	SQUINT
TAAR	TIR1 / AFB Auxin Receptor
TE	Transposable Element
TGS	Transcriptional Gene Silencing
TOR	Target Of Rapamycin
tRFs	tRNA-derived RNA fragments
TYLCSV	*Tomato yellow leaf curl Sardinia virus*
TYLCV	*Tomato yellow leaf curl virus*
TYMV	*Turnip yellow mosaic virus*
UBC	Ubiquitin-conjugating
UBP	Ubiquitin-specific processing protease
UCH	Ubiquitin C-terminal Hydrolase
UFD2	Ubiquitin Fusion Degradation 2
UPL	Ubiquitin-Protein Ligase
VIP1	VirE2-Interacting Protein 1
VSR	Viral Suppressor of RNA silencing
YFP	Yellow Fluorescent Protein
Zeo	Zeocin

Introduction

Every living being grows and lives between the boundaries defined by its genetic information. But genetic information itself is not the actor of life, just the imprint. The real actors are the proteins which are encoded within. They control the structure, the functioning, the replication, the adaptation, ... every aspect of any physiological process. But in order for them to perform their tasks correctly, they need to be present where and when they are needed and absent where and when they could be deleterious. Hence, proteins need to be regulated.

I interested myself in two major mechanisms regulating proteins ; the first is the ubiquitin-dependent proteolysis which controls proteins degradation and the second is the RNA silencing which regulates proteins synthesis. Both mechanisms are essential for the development and adaptation of plants, more widely eukaryotes, and affect each other since they are themselves composed by proteins.

My work focused on the regulation of a key protein from the RNA silencing, AGO1 by FBW2, a component from the ubiquitin-dependent proteolysis pathway.
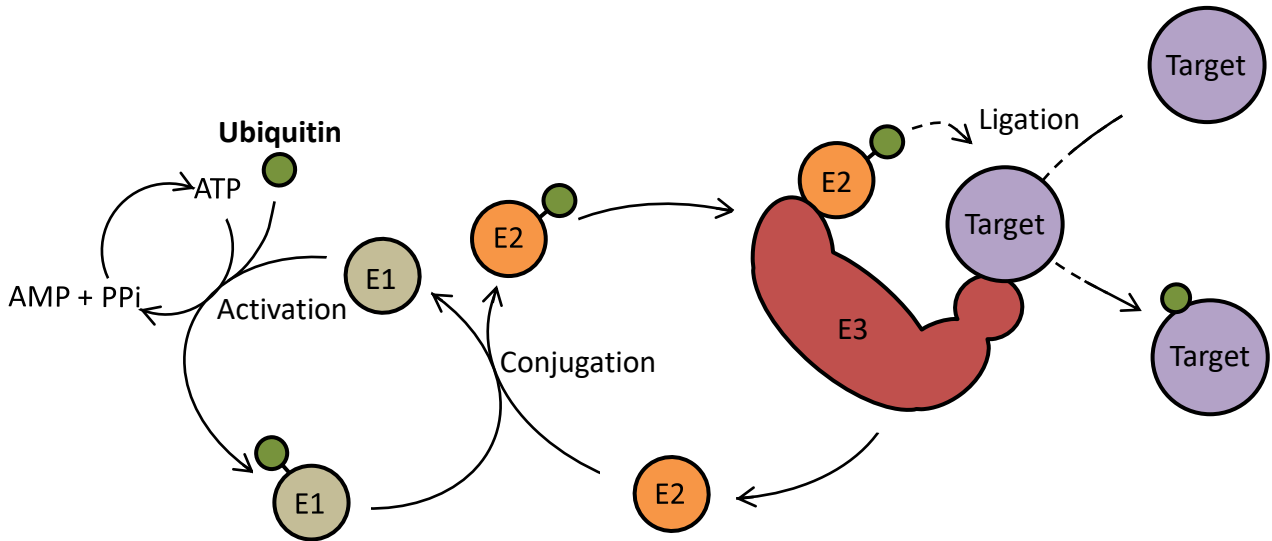
Figure 1 : Mechanism of the ubiquitination

Ligation of ubiquitin to a target protein requires three molecular steps. First, ubiquitin needs to be activated by an enzyme called E1. This step is ATP dependent. Then, ubiquitin is transferred on a E2 enzyme at the conjugation step. Lastly, ubiquitin is ligated on a target protein recognized by an E3 enzyme.

Figure 2 : Structure of the ubiquitin

Ubiquitin is composed of 76 amino acids organized in a β-sheet and an α-helix. In red are the amino acids corresponding to the lysine residues that can be linked to other ubiquitin moieties. The C-terminal end of the protein is indicated by the glycine 76 in blue, which is covalently linked to the target protein.
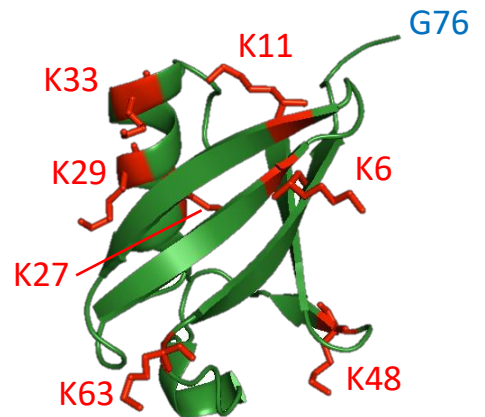
1 Ubiquitin-dependent proteolysis

The ubiquitin-dependent proteolysis is a molecular mechanism that allows the targeting and degradation of proteins (Hershko, 1998). Similarly to a labelling system, ubiquitin is used by the cell to label proteins in a specific manner. Ubiquitin conjugation to proteins is used in many ways by the cell, the most well known being proteasomal degradation. Indeed, specific degradation of proteins at specific time points and locations is crucial for cellular functions. Ubiquitin is widely used by Eukaryotes and similar mechanisms exists in Archea and Bacteria (Maupin-Furlow, 2013; Striebel et al., 2009). More than 1400 genes involved in ubiquitin-dependent proteolysis can be found in the model plant *Arabidopsis thaliana*, which represent more than 5% of its proteome (Smalle and Vierstra, 2004).

1.1 Molecular components

Before being attached to a target protein, the ubiquitin needs to be processed by several enzymes called E1, E2 and E3. These enzymes catalyze respectively its activation, conjugation and ligation to the target (Figure 1). A fourth category of enzyme, called E4, is required for subsequent polyubiquitination.

1.1.1 Ubiquitin

Ubiquitin is a small and compact protein composed of 76 amino which form a β-sheet and an α-helix folded around a hydrophobic core (Figure 2) (Vijay-kumar et al., 1987). This structural feature, called β-grasp, is specific to ubiquitin and can be found in other proteins called ubiquitin-like proteins (van der Veen and Ploegh, 2012). Ubiquitin can be post-translationally modified by phosphorylation and covalently linked to other ubiquitin proteins, forming chains as a result of several steps of ubiquitination (Kane et al., 2014; reviewed in Pickart and Fushman, 2004). Highly conserved in eukaryotes with only one amino acid difference in plants vs. Chlamydomonas, two in comparison to *Saccharomyces cerevisiae* and three between plants and animals, ubiquitin is highly conserved and ubiquitous, hence its

name. It is encoded by 12 genes in *A. thaliana* ecotype Columbia, five of which code for tandem repeats of identical ubiquitin monomers while two others correspond to ubiquitin-like genes where there is an amino acid substitution in at least one of the ubiquitin repeats (Callis et al., 1995; reviewed in Callis, 2014). The four remaining genes are called ubiquitin-extension genes and code for one ubiquitin co-translated to one or two ribosomal proteins (Callis et al., 1990; reviewed in Callis, 2014). Ubiquitin genes are widely expressed with individual variations depending on developmental and environmental factors, among them UBQ10 is the most constitutively expressed (Sun and Callis, 1997; reviewed in Callis, 2014).E1

1.1.2 E1

In order to be linked to a substrate, the ubiquitin firstly needs to be activated. This step is catalyzed by an biquitin-activating enzyme called E1, which is composed of three domains ; one adenylation domain which adenylates the ubiquitin through the use of ATP, one catalytic Cys domain, which then binds the ubiquitin from its C-terminal end through a thioesther bond and one E2-binding ubiquitin-fold domain, which recruits the E2 enzyme (Haas and Rose, 1982; Lee and Schindelin, 2008). The E1 then transfers ubiquitin to the E2 enzyme though a transthioesterification process (Haas et al., 1982). E1 enzymes are strongly conserved in evolution and two genes can be found in Arabidopsis (Hatfield et al., 1997). Worthy of note, ubiquitin-like proteins are also activated by E1-like enzymes (Schulman and Wade Harper, 2009).

1.1.3 E2

After its activation, ubiquitin needs to be brought to the substrate. This ubiquitin carrier enzyme or ubiquitin conjugation protein is called E2. E2 enzymes contains an ubiquitin conjugating (UBC) domain with a conserved cysteine that accepts the ubiquitin from the E1 through a thioesther bond (Hershko, 1983; Hershko and Ciechanover, 1992). In Arabidopsis, 48 proteins contain the UBC domain, among them eight lack the cysteine residue needed to carry the ubiquitin (these are called Ubiquitin conjugating Enzymes Variants [UEVs]) and three have been described to act as ubiquitin-like protein conjugating enzymes. Of the 37 remaining,
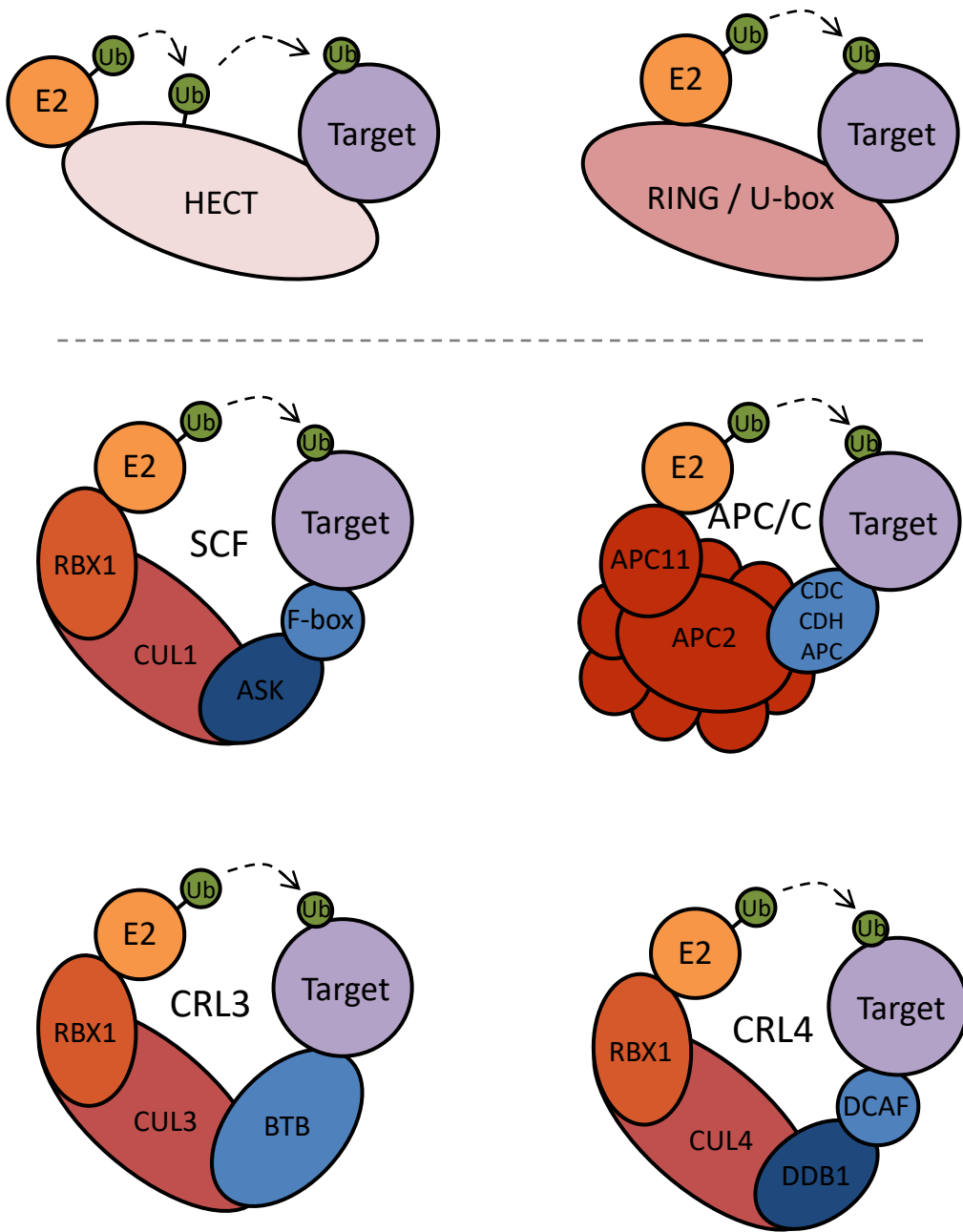
Figure 3 : Composition of plant E3 ligases

Six different types of E3 ubiquitin ligases are found in plants. The monomeric E3 ligases are presented on top. They use an HECT, RING or, closely related, U-box domain to interact with the E2 and target proteins. On the contrary to monomeric E3 ligases, the multimeric E3s shown below use adaptor proteins (in light blue) to recognize a variety of substrates. Among all, the HECT-based ligases is the only one to catalyze ubiquitination with an intermediary step where ubiquitin is directly linked to the E3.

24 have shown E2 activity so far (Callis, 2014). The diversity of E2 compared to E1 can be explained by their diversity of functions; although they recover the ubiquitin from the same E1, they interact with different E3 enzymes in order to transfer the ubiquitin to a bigger variety of substrates (Callis, 2014).

1.1.4 E3

Except rare exceptions, the E2 alone is not able to recognize protein substrates. The protein target recognition is the role of ubiquitin protein ligase (E3) enzymes, which are responsible for the specificity of the mechanism. E3 enzymes bring together the E2 and substrate allowing the transfer of the ubiquitin to the substrate. The ligation of the ubiquitin onto the substrate is called ubiquitination. Plants have more than 1000 different E3 genes (reviewed in Chen and Hellmann, 2013 and papers cited therein) and proteomic analysis of the ubiquitome (ubiquitinated proteins) shows more than 940 substrates involved in a wide range of physiological and developmental processes, particularly in metabolism and hormone signaling (Kim et al., 2013). Depending on their structure, plants E3 ligases have been divided in 3 main classes; HECT, RING and U-box (Hua and Vierstra, 2011) (Figure 3).

1.1.4.1 HECT

Homologous to E6-AP Carboxyl Terminus (HECT) is a protein domain of 350 amino acids that was discovered in human (Huibregtse et al., 1995). HECT are monomeric E3 ligases that have the particularity to transfer the ubiquitin from the E2 on the target through an intermediate thioester bond on the HECT domain (Scheffner et al., 1995; Kumar et al., 1997). While the human genome encodes over 50 of them, only 5 can be found in yeast and 7 in Arabidopsis where they are named Ubiquitin-Protein Ligases (UPL1 to UPL7) (Downes et al., 2003). Most of their roles are unknown apart from UPL3, also called KAKTUS, which is involved in endoreplication control in trichomes (Perazza et al., 1999) and UPL5 which negatively regulates leaf senescence by triggering the degradation of the transcription factor WRKY53 (Miao and Zentgraf, 2010).
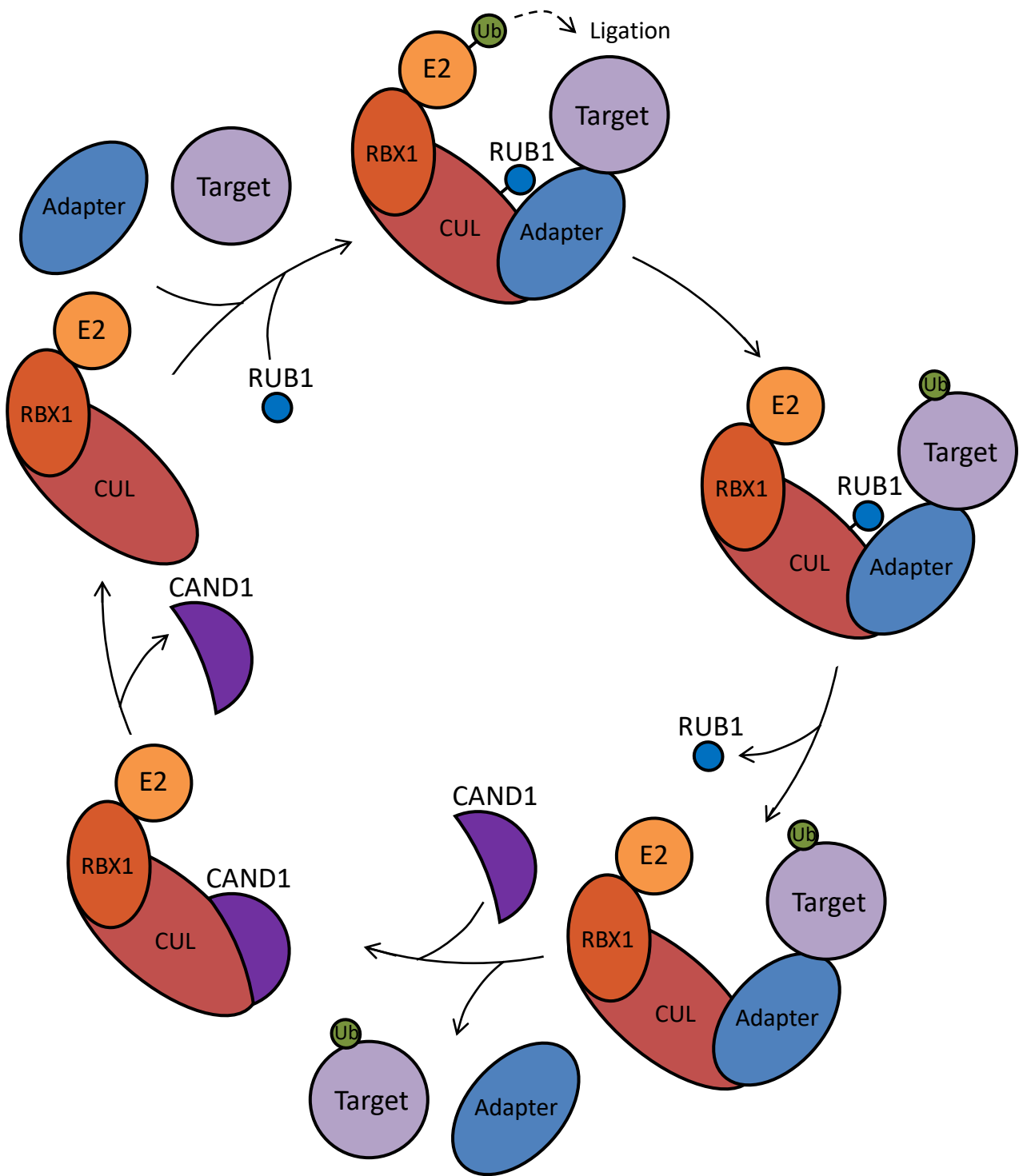
Figure 4 : Model of the regulation of CUL-based E3 ligase by rubylation

The adaptor and the target proteins are recruited on the CULLIN to allow ubiquitin ligation. When RUB1/NEDD8 (here indicated as RUB1) is removed from the CULLIN, the interaction with the adaptor subunit is destabilized. In absence of RUB1, CAND1 interacts with the CULLIN and prevent further interaction with adaptor proteins. Novel rubylation of the CULLIN hinders CAND1 interaction and stabilizes the interaction with a new adaptor protein for further ubiquitination.

1.1.4.2 RING

The largest diversity of E3 ligases is found within the RING family. The Really Interesting New Gene (RING) domain has been discovered in the nineties and was firstly thought to bind DNA instead of mediating protein-protein interaction (Freemont et al., 1991; Lovering et al., 1993). There are actually several types of RING domains, 8 can be found in Arabidopsis (Stone et al., 2005). Among them, the RING-H2 and RING-HC groups compose 90% of the family and are mostly linked to the class of ubiquitin E3 ligases (Lorick et al., 1999). RING E3 ligases can be monomeric, and directly interact with the substrate or multimeric protein complexes that use adaptor proteins to interact with a bigger variety of substrates. Both promote the transfer of the ubiquitin onto the substrate without intermediate reaction (reviewed in Deshaies and Joazeiro, 2009).

In plants, monomeric RING E3 ligases have been found to be implicated in various physiological processes such as drought stress tolerance, nodulation, gravitropism and metabolism (reviewed in Chen and Hellmann, 2013). They also act in a particular protein degradation process called the N-end rule pathway, where proteins beginning with particular amino acids instead of the N-terminal methionine are recognized by specific E3 ligases, called N-recognins that trigger their degradation (Varshavsky, 1996). In plants, PRT1 and PRT6 have been demonstrated to act as N-recognins (reviewed in Graciet and Wellmer, 2010).

On the contrary to monomeric RING, multimeric RING E3 ligases are composed of at least three proteins with a Cullin protein as scaffold. Mammals make use of 7 Cullins, yeast of 3 and Arbadidopsis of 5 (CUL1, CUL2, CUL3a, CUL3b and CUL4) (Risseeuw et al., 2003; Thomann et al., 2005). Cullins possess a Carboxy-Terminal Domain (CTD) which interact with Regulator of Cullin 1 or 2 (ROC1 or ROC2 also called RING Box Protein [RBX1 or RBX2]) and three Cullin Repeat which recruit a substrate recognition subunit (Lechner et al., 2002; reviewed in Sarikas et al., 2011). The whole protein complex is called Cullin RING Ligase (CRL), with RBX1 or RBX2 in charge of recruiting the E2. They are the major class of E3 ligases in plants and their activity has been shown to be regulated at several levels; phosphorylation of the target recognition site, phosphorylation of the E3,

A. Species: F-box domain (IPR001810)

Key Species

Key species	Number of proteins
Arabidopsis thaliana (Mouse-ear cress)	1420
Oryza sativa subsp. japonica (Rice)	1156
Caenorhabditis elegans	396
Mus musculus (Mouse)	203
Homo sapiens (Human)	200
Danio rerio (Zebrafish)	171
Drosophila melanogaster (Fruit fly)	62
Schizosaccharomyces pombe (strain 972 / ATCC 24843) (Fission yeast)	13
Saccharomyces cerevisiae (strain ATCC 204508 / S288c) (Baker's yeast)	11

B.

# of Genes	AGI#	F-box	Domain
160	At4g27050		LRR_PD
107	At3g18980		A Type-I
107	At3g04660		A Type-II
97	At4g38940		Kelch
97	At1g78100		Unknown
42	At5g67250		LRR
26	At4g22060		C5 Type-I
18	At5g24040		C5 Type-II
18	At3g61060		Lectin-related
10	At1g76900		TUB
3	At5g57360		PAS/LOV Kelch
2	At2g44900		LRR Armadillo
2	At3g52030		WD-40
2	At5g06550		Jmj C
1	At1g70590		TPR repeats
1	At5g56180		Actin-related
1	At5g56180		DEAD-like Helicase

200 a.a.

Figure 5 : Diversity of F-box proteins

A. Number of F-box proteins referenced in the InterPro database. This amount is significantly higher in plants compared to model organisms of other kingdoms.
B. Examples of plant F-box protein domain composition. On the left is indicated the number of genes annotated similarly to the gene presented. On the right are represented the domains that likely mediate the target recognition. The Leucine Rich Repeats (LRR) is the most commonly found in F-boxes (adapted from Gagne et al., 2002)

autoubiquitination, rubylation of Cullins and involvement of protein or small molecules as cofactors (reviewed in Deshaies and Joazeiro, 2009). The rubylation (also called neddylation in mammals) is a post-translational modification particularly known to regulate Cullin-based E3s (Figure 4). It uses the ubiquitin-like protein Related to Ubiquitin 1 (RUB1), NEDD8 in mammals, to post-translationally modify the Cullin and promote the activity of the E3 by preventing its association with the negative regulator Cullin Associated and Neddylation Dissociated 1 (CAND1) (reviewed in Hotton and Callis, 2008). In turn, RUB1/NEDD8 deconjugation is also important as it destabilizes the cullin RING ligase complex allowing for the exchange of the substrate recognition subunits (reviewed in Mergner and Schwechheimer, 2014)

The following RING-type ubiquitin protein E3 ligase complexes are found in plant:

- SCF

This ubiquitin protein E3 ligase complex is essential for the plant as knock-out mutant of its scafflod subunit CUL1 are lethal (Shen et al., 2002). It is named based on its composition by the Skp1, Cullin and F-box (SCF) proteins. In plants, the closely related protein CUL2 can also replace CUL1 to interact with Skp (Risseeuw et al., 2003). Homologous genes for S-phase kinase-associated protein 1 (Skp1) in Arabidopsis are called Arabidopsis Skp1 homologue (ASK) and form a family of 21 genes (Kalde et al., 2003; Marrocco et al., 2003; Dezfulian et al., 2012). These proteins serve as adaptors between the Cullin and the F-box protein, which defines the substrate specificity. The F-box motif was discovered in yeast with the cell cycle regulator protein cyclin F (Chang et al., 1996). It forms the biggest protein family in Arabidopsis with more than 700 predicted proteins, which amounts to 2,3 % of the genome, while only 68 can be found in human (reviewed in Hua and Vierstra, 2011) (Figure 5A). Often found in the N-terminal part of the protein, the F-box motif is followed by another protein-protein interaction domain, such as WD40 or Leucine-Rich Repeats (LRR), which recognizes the target protein (reviewed in Kipreos and Pagano, 2000) (Figure 5B). F-box proteins are involved in many physiological processes in plants, the most well known being hormone signalling where the F-boxes TIR1, COI1, SLY1 & SNE, EBF1 & EBF2 regulate auxin, jasmonate, gibberrelin and ethylene responses respectively (reviewed in Lechner et al., 2006). F-box proteins often target phosphorylated substrates, allowing another layer of

regulation in this mechanism (Skowyra et al., 1997). Moreover, F-box proteins are often unstable in the absence of their target and degraded by the proteasome, either by auto-ubiquitination or targeting by another E3 ligase (Li et al., 2004; Zhou and Howley, 1998; Galan and Peter, 1999).

- CUL3-BTB

The CUL3 proteins interact with proteins containing the Bric-a-brac, Tramtrack, Broad-complex / Pox virus and Zinc finger (BTB/POZ) domain to form this E3 ligase (reviewed in Pintard et al., 2004; and in Genschik et al., 2013). Similarly to F-box proteins, BTB proteins use a secondary protein-protein interaction domain to recognize the substrate (Stogios et al., 2005). In Arabidopsis, counts 2 CUL3 (CUL3a and b) and 80 BTB genes, which have been classified in subfamilies depending on their secondary domain (Dieterle et al., 2005; Gingerich et al., 2005). Some BTBs have been found to control the stability of transcriptional regulators like the BTB/POZ-MATH (BPMs, MATH standing for Meprin And TRAF Homology) family, which regulates the abscisic acid response in Arabidopsis (Weber et al., 2005; Lechner et al., 2011).

- CUL4-DDB1

Like Skp1 in the SCF complex, DNA Damaging Binding 1 (DDB1) serves as adaptor between the Cullin4 (CUL4) and a DDB1 CUL4 Associated Factor (DCAF) protein (Bernhardt et al., 2006; reviewed in Higa and Zhang, 2007). DCAFs interact with DDB1 through a modified WD40 domain called DDB1 binding WD40 (DWD) (Lee and Zhou, 2007; Lee et al., 2008). In Arabidopsis, 119 of them can be found and are involved in various physiological processes such as photomorphogenesis with Constitutive Photomorphogenic 1 (COP1), parental imprinting with Multi-copy Suppressor of IRA 1 (MSI1) or floral transition with MSI4 (reviewed in Chen and Hellmann, 2013).

1.1.4.3 APC/C

Essential to the cell cycle progression, the Anaphase Promoting Complex or cyclosome (APC/C) is an E3 ubiquitin ligase composed by 11 to 13 different proteins (Gieffers et al., 2001; reviewed in Peters, 2006). The APC2 and APC11 proteins act

in a similar manner to Cullin and RBX1 as scaffold and E2-interactant proteins (Leverson et al., 2000; Tang et al., 2001). The APC/C has been discovered as a key E3 ubiquitin ligase triggering the degradation of cyclin proteins (Gieffers et al., 2001; Murray, 1995). While the primary role of the APC/C is to control the progress of mitosis, it has also been shown to act in the RNA silencing pathway where it regulates the Arabidopsis DsRNA Binding protein 4 (DRB4) (Marrocco et al., 2012).

1.1.4.4 U-box

The U-box domain is a modified RING where the zinc atoms are replaced by a hydrogen bond network (Aravind and Koonin, 2000; Andersen et al., 2004). It was discovered in yeast in an E4 enzyme (Koegl et al., 1999). U-box E3s are monomeric ligases, which are called Plant U-Box proteins (PUBs) in plants. They have been classified in 8 subfamilies depending on the nature of the secondary protein-protein interaction domain in charge of the target recognition. PUBs seem to be mostly involved in stress response (Yee and Goring, 2009).

1.1.5 E4

A more discrete but nonetheless important function is carried out by the E4 proteins, which help some E3 ligases to build extension of ubiquitin marks, forming polyubiquitin chains. E4s were discovered in yeast with the Ubiquitin Fusion Degradation 2 (UFD2) protein (Koegl et al., 1999). Some of them comport a U-box domain, such as UFD2 and a C terminus of Hsc70-Interacting Protein (CHIP) in yeast and human while others are wholly different like the complex Binds to Ubiquitin Ligase 1 and 2 (BUL1-BUL2) and p300, still in yeast and human respectively (reviewed in Hoppe, 2005). In plants, the E4 Mutant *snc1*-Enhancing 1 (MUSE1) has been shown to complement the *ufd2Δ* yeast mutants and is required for the homeostatic control of two proteins involved in pathogen resistance; Suppressor of *npr1-1*, constitutive 1 (SNC1) and Resistance to *Pseudomonas syringae* 2 (RPS2) (Huang et al., 2014).

1.1.6 Deubiquitination

Instead of promoting ubiquitin ligation, some enzymes can cleave polyubiquitin chains in order to release ubiquitin monomers, they are called Deubiquitination
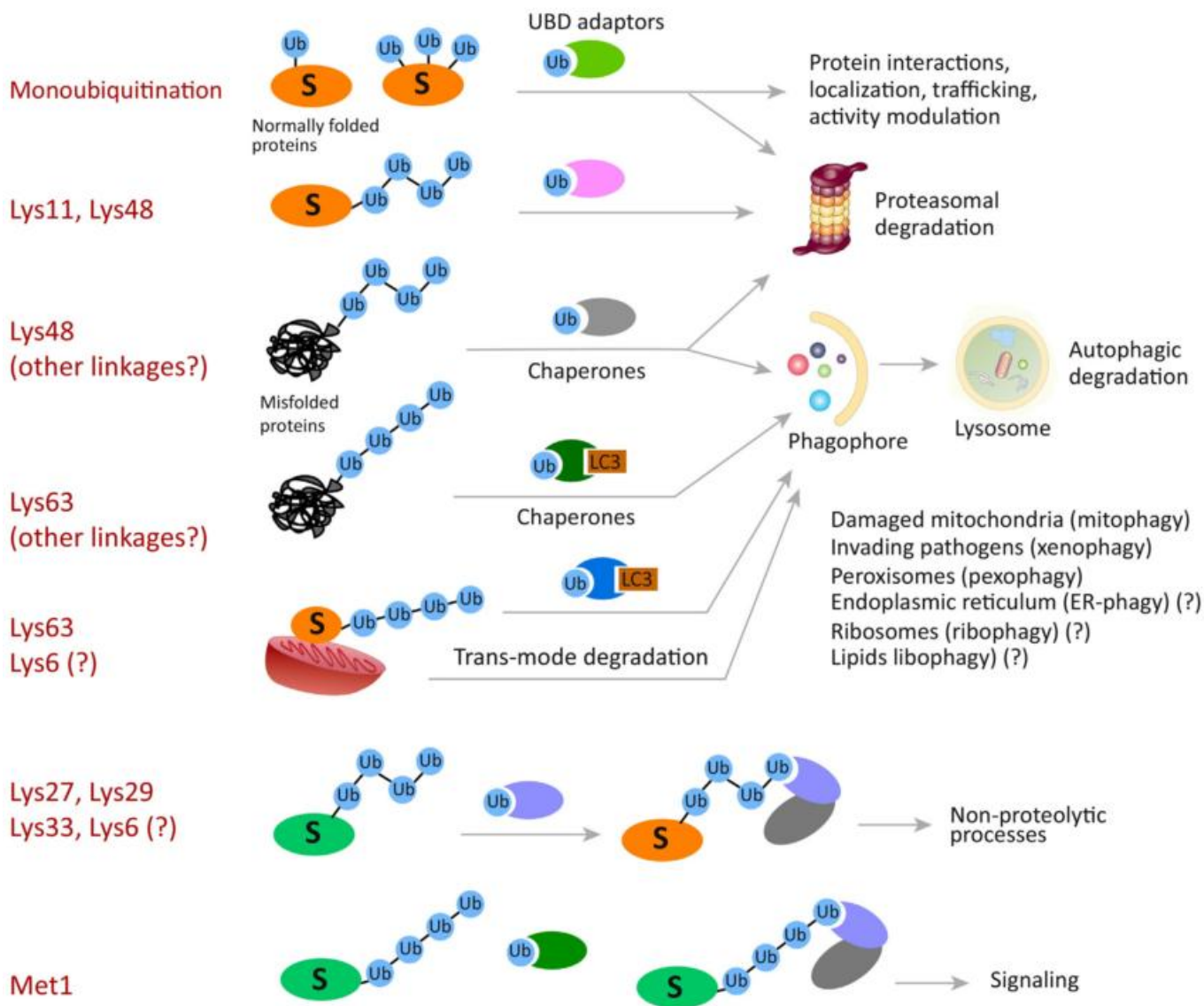
Figure 6 : The ubiquitin code

Substrates can harbour different types of ubiquitination (indicated on the left), which differentially affects their fate (on the right). Lys11 and Lys48 polyubiquitin chains typically trigger proteasomal degradation while Lys63 polyubiquitin chains are associated to autophagy (from Kwon and Ciechanover, 2017).

enzymes (DUBs) (D'Andréa and Pellman, 1998). DUBs are classed in two groups depending on their activity; the Ubiquitin C-terminal Hydrolase (UCH) and the Ubiquitin-specific processing protease (UBP). UCH are in general required for the processing of the polyubiquitin translational products and recycling of the ubiquitin from degradation intermediates. UBP have been observed to cleave ubiquitin from substrate conjugated polyubiquitin chains thus delaying its degradation, an activity that is also called editing (reviewed in Wilkinson, 2000). In Arabidopsis, a notable DUB called Associated Molecule with the SH3 domain of STAM 3 (AMSH3) does not interfere with proteasomal degradation, but is required for vacuole biogenesis and intracellular trafficking, underlying the importance of ubiquitination in processes other than proteolysis (Isono et al., 2010).

1.2 Ubiquitin code

Ubiquitination does not always trigger degradation of the substrate. In fact, only certain types of ubiquitination promote degradation through the proteasome. Substrates can either be monoubiquitinated or polyubiquitinated depending on the substrate, the E3 or the E2 (reviewed in Komander and Rape, 2012). More complexity is added by the fact that ubiquitin can be attached on several residues of the substrate, sometimes of different nature. Serine, threonine or N-terminal residues are possible substrate ubiquitin acceptor sites, but lysines are overall preferred (Wang et al., 2012; Pao et al., 2018; Ciechanover and Ben-Saadon, 2004). The nature of the ubiquitin chains, also called the ubiquitin code, is interpreted by subsequent reader proteins, which will determine the fate of the substrates (reviewed in Kwon and Ciechanover, 2017) (Figure 6).

1.2.1 Monoubiquitination

Like other post-translational modification, monoubiquitination can cause conformational changes, resulting in activation or inactivation of the substrate for protein interaction or simply enzymatic activity. By example, this modification has been described to trigger internalization and endocytosis of extracellular receptors, such as Ste2p in yeast, and regulate gene expression through histone modification, such as H2B during mitosis and meiosis in yeast or in photomorphogenesis and

circadian clock control in Arabidopsis (Sigismund et al., 2004; Bourbousse et al., 2012; Himanen et al., 2012).

1.2.2 Polyubiquitination

The chains of polyubiquitin can be of different types depending on how the ubiquitin are linked together. Indeed, ubiquitin contain 7 lysines which can serve as basis for further ubiquitination either as a single chain or multiple branching (reviewed in Ikeda and Dikic, 2008; and in Kwon and Ciechanover, 2017). Polyubiquitin chains are classed according to the lysine residue used for the chain extension; K6, K11, K27, K29, K33, K48, and K63. Elements determining the type of polyubiquitin chain formed are still unclear; preformed polyubiquitin chains have been shown to be directly attached to the substrate but the E2 specificity seems to be involved as well as UEVs cofactors (Li et al., 2007; Christensen et al., 2007). While all kind of linkages have been observed, the vast majority of polyubiquitin chains are composed by the K11, K48 and K63 types (Kim et al., 2013; reviewed in Kwon and Ciechanover, 2017).

Lys-11–linked chains are known to be synthesized by the APC/C and are needed for the proper progress of the cell cycle (reviewed in Wickliffe et al., 2011). They are also involved in the Endoplasmic Reticulum-Associated Degradation (ERAD) pathway where misfolded proteins are selectively discarded (Xu et al., 2009). K11 chains are recognized by the 26S proteasome which degrades the substrate onto which they are attached (Baboshina and Haas, 1996).

Lys-48–linked chains are the most well known type of polyubiquitination. This linkage forms a "compact" conformation where adjacent ubiquitin moieties interact with each other (reviewed in Komander and Rape, 2012). It was discovered in yeast where mutation of the lysine 48 is lethal and is thought to be the major proteolysis pathway linked to ubiquitin (Chau et al., 1989). K48 chains are recognized by the proteasome starting from 4 ubiquitins linked together and are produced by many E3 ligases (reviewed in Finley, 2009).

Lys-63-linked chains are involved in DNA-damage response, kinase activation, protein trafficking, and ribosomal protein synthesis (reviewed in Ulrich, 2002;
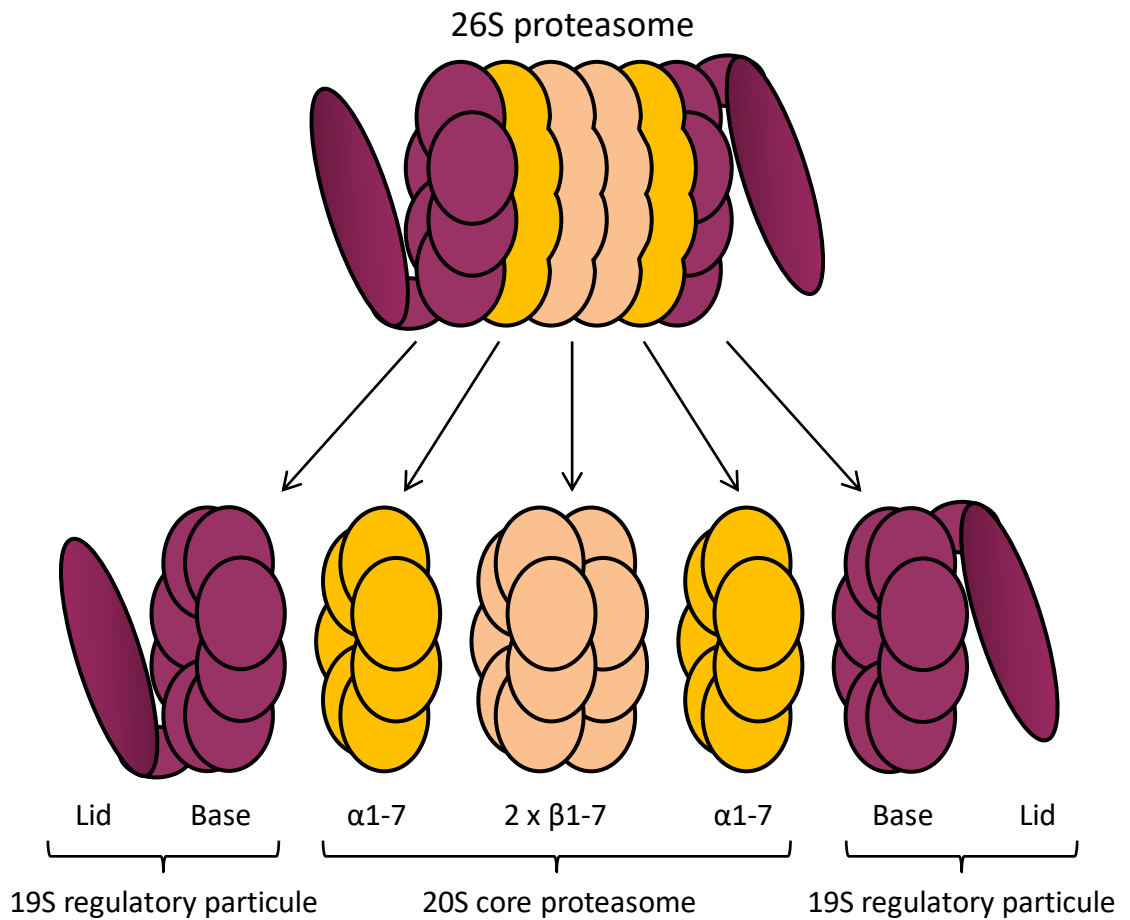
Figure 7 : Structure of the 26S proteasome

The 26S proteasome is composed of a 20S core and two 19S regulatory particle. The 20S core houses the protease activities in the β rings while the α rings restrict its access only to unfolded proteins. The regulatory particles are formed by a lid and a base, which recognize and unfold target proteins and recycle ubiquitin.

Erpapazoglou et al., 2014; Hicke and Dunn, 2003; Spence et al., 2000). On the contrary to K48 chains, they adopt an "open" conformation, are less prone to 26S proteasomal degradation but can be used to address substrates to proteolytic compartments such as the lysosome or the vacuole (reviewed in Komander and Rape, 2012). UEVs seem to play an important role in K63 chain formation by orienting the ubiquitin in a position favourable to K63 linkage (reviewed in Callis, 2014).

1.2.3 Proteolysis

Ubiquitination has been linked to proteolysis since its discovery. Proteasomal degradation is still the most well known ending for ubiquitinated proteins, but other ubiquitin-dependent degradation pathways have also been unravelled, often related to the autophagy.

1.2.4 Proteasomal degradation

This type of proteolysis uses the 26S proteasome as a dismantling machinery to recycle ubiquitinated proteins. Proteasomes are found archaea and eukaryotes and at the cellular level, in the nucleus and the cytoplasm. As the major mean for proteolysis, the proteasome is of critical importance for the cell. Hence, loss of function of most proteasome subunits is lethal or triggers pleiotropic effects (reviewed in Kurepa and Smalle, 2008).

1.2.4.1 Structure

The 26S proteasome is a 2.4 MDa barrel-shaped protein complex, highly conserved in eukaryotes, where proteins enter on one side and exit from the other side cleaved in small peptides (Yang et al., 2004). It is formed by two elements; a 20S core protease (CP) and a 19S regulatory particle (RP) (Voges et al., 1999) (Figure 7).

- Regulatory particle

The regulatory particle is composed by 17 subunits, which can be divided in two structures; the base and the lid. The base consists of 6 ATPases and 3 non-ATPase proteins that notably include Regulatory Particle Triphosphatase 5 (RPT5)

and Regulatory Particle Non-ATPase 10 (RPN10), which bind polyubiquitin chains and RPN1 which binds ubiquitin-like proteins (Fu et al., 1998; Elsasser et al., 2002). The lid is formed by 8 proteins with notably the DUB RPN11 which disassemble polyubiquitin chains (Verma et al., 2002).

- Core protease

The core protease is composed of four heptameric rings; two central rings each formed by seven β subunits and two peripheral rings formed by seven α subunits. The β subunits carry ATP-independent protease activities (β1: peptidyl glutamyl-peptide hydrolase, β2: trypsin-like protease, β3: chymotrypsin-like protease) while the α subunits restrict the access to unfolded polypeptides (reviewed in Smalle and Vierstra, 2004).

1.2.4.2 Mode of action

Several types of proteasomes have been found *in vivo* and vary depending on their subunits composition and the presence, absence or replacement of the regulatory particle (reviewed in Kurepa and Smalle, 2008). The core protease alone forms the 20S proteasome and is involved in degrading unstable and oxidized damaged proteins in a ubiquitin and ATP independent manner (Asher et al., 2006; Voss and Grune, 2007). The regulatory particle allows it to recognize ubiquitinated proteins and to release the ubiquitin in the cytosol through the use of ATP while directing the substrate inside the core protease (Verma et al., 2002; reviewed in Voges et al., 1999). In addition in vertebrates, the immunoproteasome, a specific proteasome isoform induced by interferons, is exclusively involved with the adaptive immune response and improved MHC class I antigen presentation (reviewed in Krüger and Kloetzel, 2012). Interestingly, the 26S proteasome controls its own activity through a self-regulation loop where it constitutively degrades the yeast transcription factor RPN4 which regulates the 26S proteasome genes expression (Ju et al., 2004). Although no RPN4 ortholog is present in plants, a similar regulation mechanism has been proposed (Yang et al., 2004).

Figure 8 : Mechanism of the macroautophagy

The TOR kinase promotes the dissociation of ATG13/ATG1 kinase complex depending on cellular signals. When it is formed, this complex activates the macroautophagy. ATG9 is responsible for the formation and expansion of a double membrane called the phagophore. ATG8 is activated and ligated to phosphatidylethanolamine (PE) by an ubiquitination-like process. It then serves as docking platform for various proteins including cargo receptors. Closed phagophores form vesicles called autophagosomes that are delivered to the vacuole where they are degraded (from Marshall and Vierstra, 2018).
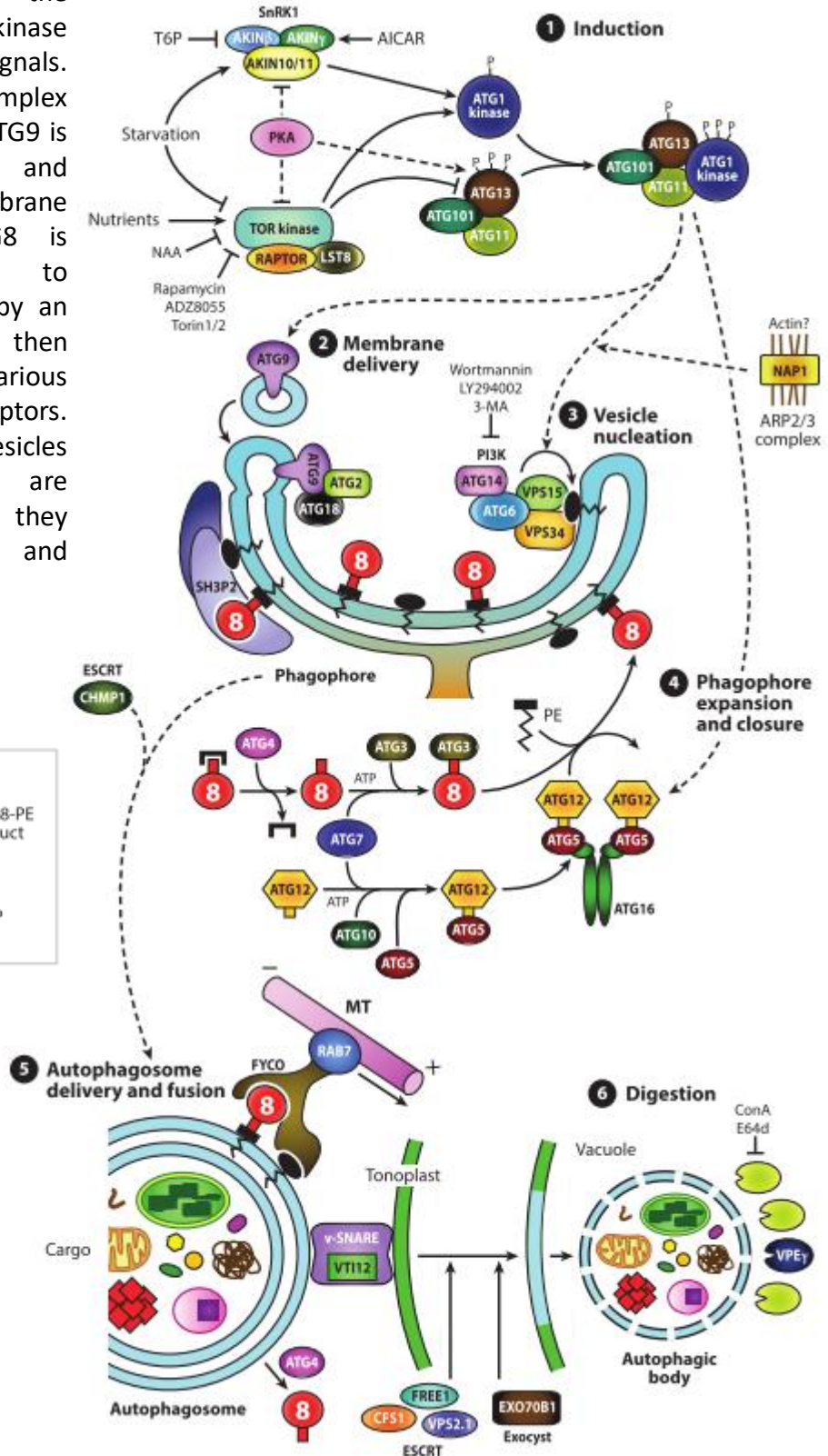
1.2.5 Autophagy

While the proteasome is dedicated to the breakdown of proteins, autophagy, from the greek "self eating", is able to degrade various cytoplasmic elements from RNA molecules to protein complexes and even organelles, which the proteasome cannot. Autophagy makes use of a special acidic cellular compartment, which hosts various degradations enzymes including proteases; the lysosome in animals or the vacuole in plants and fungi. This catalytic process is well known to recycle elements indiscriminately in times of starvation in order to remobilize resources, but it can also become highly specific (reviewed in Khaminets et al., 2016; and in Grumati and Dikic, 2018). Autophagy uses several import pathways to the lysosome/vacuole, which are nowadays classed in different categories, including chaperone-mediated autophagy (CMA), microautophagy, macroautophagy and mega-autophagy.

Chaperone-mediated autophagy seems to be absent in plants since no orthologs to the key proteins in charge of this process have been found (reviewed in Marshall and Vierstra, 2018). Mega-autophagy corresponds to vacuolar membrane breakdown, which triggers a global degradation of the cell components promoting cell death and has been involved in the plant innate immune response (reviewed in Bassham et al., 2006). Microautophagy traps cytosolic components by invaginating the vacuolar membrane and internalizing it while macroautophagy forms vesicles in the cytosol and import them inside the vacuole. The macroautophagy in particular shows links with the ubiquitin and specific proteolysis. I will focus on this one.

1.2.5.1 Mechanism

Over 40 Autophagy related (ATG) proteins taking part in the macroautophagy have been identified in yeast and most of these proteins have orthologs in plants (reviewed in Ohsumi, 2001; and in Marshall and Vierstra, 2018) (Figure 8).

To summarize briefly, in nutrient sufficient conditions, the Target Of Rapamycin (TOR) kinase controls the activation of the system by phosphorylating ATG13, preventing it to activate the kinase ATG1 (Suttangkakul et al., 2011; Dobrenel et al., 2016). ATG1 activation promotes 1) the creation and expansion of a double membrane structure called the phagophore, 2) the decoration of the
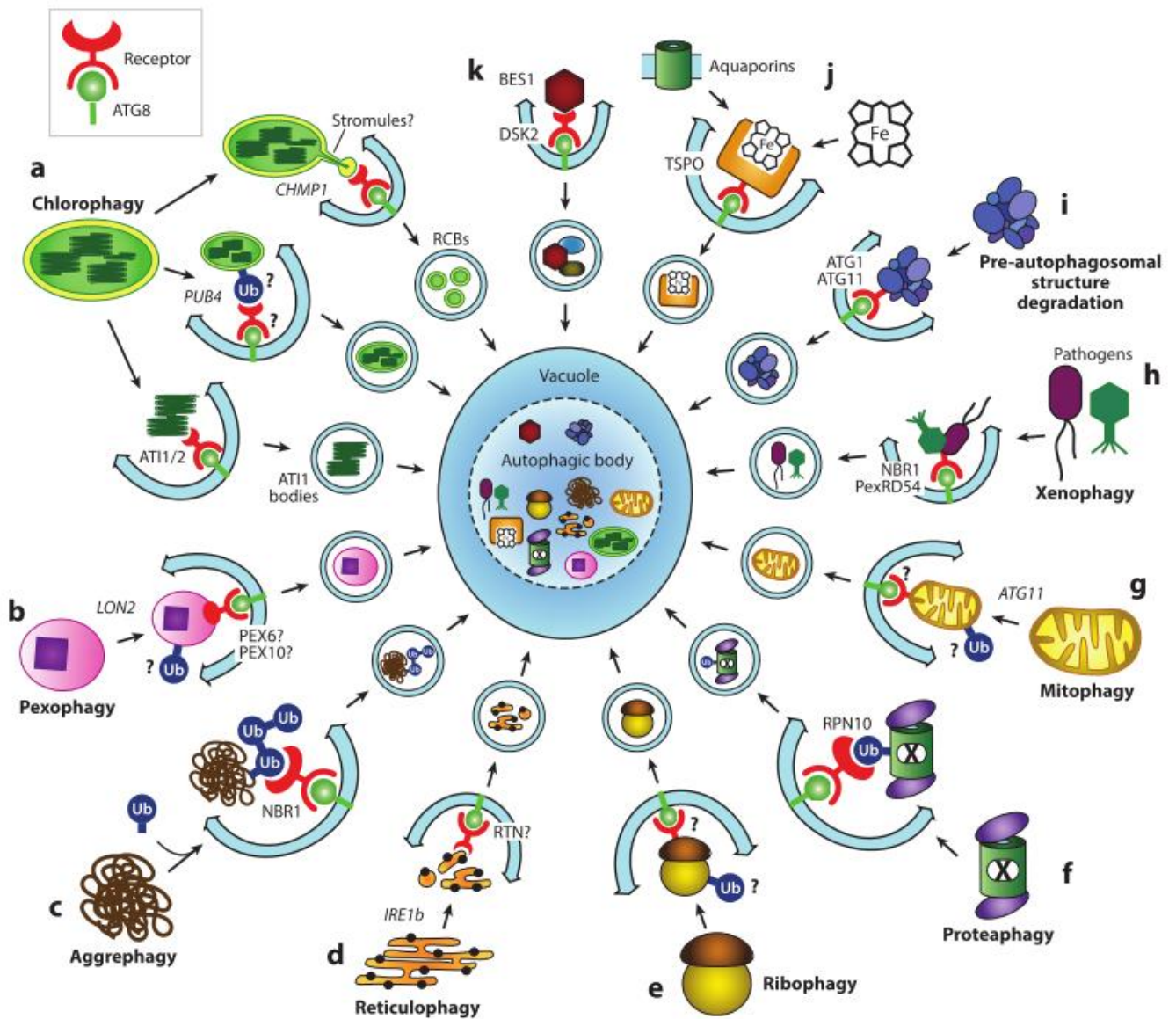
Figure 9 : Targets of the macroautophagy

The macroautophagy pathway regulates many cellular components. ATG8 serves as docking platform for cargo receptors that recognize these elements. Note the implication of the ubiquitin in several of these processes such as a) chlorophagy, c) aggrephagy, e) ribophagy, f) proteophagy and g) mitophagy (from Marshall and Vierstra, 2018).

phagophore with phosphatidylinositol-3-phosphate (PI3P) and ATG8 proteins. ATG8 is of particular interest; it is an ubiquitin-like protein which, similarly to the ubiquitin, is activated by ATG7, conjugated by ATG3 and linked to lipid phosphatidylethanolamine (PE) on the phagophore membrane by the ligase complex ATG5, ATG16 and ATG12. Once on the membrane, ATG8 serves as a docking platform for cargo receptor proteins that interact with the specific cargo to be degraded (reviewed in Michaeli et al., 2016; and in Marshall and Vierstra, 2018). The phagophore then closes and is imported into the vacuole.

1.2.5.2 Ubiquitin in the autophagy

Numerous selective autophagy pathways have been characterized and named according to the type of targeted cellular material and many of them depend on ubiquitination (Figure 9).

- Protein aggregates (aggrephagy)

Upon recognition by Hsp70 and subsequent ubiquitination by the E3 Hsc70-Interacting Protein (CHIP), aggregates of toxic, non-functional or misfolded proteins too big to be processed by the proteasome are recognized by Neighbor of BRCA 1 (NBR1). NBR1 is a cargo receptor which interacts with polyubiquitin chains and anchor ubiquitinated protein aggregates in the phagophore for their delivery to the vacuole (Zhou et al., 2014; reviewed in Lamark and Johansen, 2012).

- Chloroplasts (chlorophagy) / Mitochondra (mitophagy)

When facing irreversible damages, chloroplasts and mitochondria are sent to the vacuole to be recycled. Although this pathway still needs to be deciphered, the E3 Plant U-Box 4 (PUB4) has been shown to ubiquitinate chloroplast surface and the protein ATG8-Interacting 1 (ATI1) proved to be a cargo receptor involved in bringing plastids to the vacuole (Michaeli et al., 2014; Izumi et al., 2017). Damaged mitochondria are known to be ubiquitinated by the E3 (PARKIN) in mammals and then recognized by the cargo receptor Nuclear Dot Protein 52 (NDP52) (Yamano et al., 2016). Mitochondria recycling appears to also depend on the autophagy in plants but no counterparts of PARKIN and NDP52 have been found yet (Li et al., 2014).

- Ribosomes (ribophagy)

The cell needs to adapt its protein production in absence of nutrient, one way to achieve this is to diminish the number of ribosomes and recycle the one in excess. In yeast, the ubiquitin has been linked to the import of ribosomes in the vacuole (Kraft et al., 2008). In plants, ribosomal RNAs are known to be degraded in the vacuole but whether ribosomal proteins are also selectively degraded is unknown so far (Floyd et al., 2015).

- Proteasomes (proteaphagy)

Additionally to the proteasome self-regulation presented previously (section 1.3.1.2), malfunctioning proteasomes are ubiquitinated and sent to the vacuole. This process also happens upon nutrient deficiency and uses RPN10, the ubiquitin binding protein from the proteasomal regulatory particle, as cargo receptor (Marshall et al., 2015).

As illustrated with the protein aggregates example, some redundancy between proteasomal degradation and autophagy are possible, especially when proteasomes are not available. There is a crosstalk between the two pathways allowing the upregulation of one pathway when the other is lacking. This seems particularly true when the proteasome is inhibited, less when autophagy is impaired (Korolchuk et al., 2010).

1.3 Exogenous hijacking

The evolutionary success of the ubiquitin system in plants, particularly the SCF, makes it a target of choice for pathogens who seek to manipulate plant cellular functions. Thus microbes have evolved E3 ligases components to target and trigger the degradation of resistance-associated key proteins during the infection (reviewed in Magori and Citovsky, 2011; and in Alcaide-Loridan and Jupin, 2012). These exogenous E3 are of particular importance since they can be used as molecular tools to study the pathway they affect. Here are some examples:

1.3.1 From bacteria

Bioinformatics analysis of the InterPro database revealed 74 bacterial F-box genes, the majority of them coming from pathogens species (Price and Abu Kwaik, 2010). Since some already studied F-box pathogens were not detected in this analysis, the uncovered 74 genes likely represent an underestimation of the diversity of microbial F-box proteins.

The F-box protein virF encoded by *Agrobacterium tumefaciens* was the first bacterial F-box discovered. Agrobacteria are able to transfer and integrate a part of their DNA, called T-DNA, in the genome of the plant cell they infect. This process is widely used to insert engineered DNA sequenced in plants. virF hijacks the host SCF and triggers the degradation of VirE2-Interacting Protein 1 (VIP1), which is required for the T-DNA import in the nucleus but prevent its integration in the genome (Tzfira et al., 2004).

Another example concerns the bacterial plant pathogens from the *Ralstonia* genus which encode a family of seven F-box proteins called GALAs named after the conserved GAxALA amino acid sequence they share (Angot et al., 2006). GALAs are needed for *Ralstonia solanacearum* pathogenicity but it is not known yet what are their targets. Mutations of these genes suggests that they share overlapping functions but may also be specialized to different hosts (reviewed in Magori and Citovsky, 2011).

1.3.2 From viruses

Since the ubiquitin-dependent proteolysis is involved in the defence against pathogens, it is not a surprise that pathogens have developed ways to counteract it.

The *Turnip yellow mosaic virus* (TYMV) produces a DUB protein that specifically prevents its viral polymerase to be send to the proteasome (Chenon et al., 2012). Another strategy has been identified in the *Tomato yellow leaf curl Sardinia virus* (TYLCSV), *Tomato yellow leaf curl virus* (TYLCV), and *Beet curly top virus* (BCTV), where the C2/L2 protein deregulates the rubylation of Cullin based E3 ligases (Lozano-Duran et al., 2011).

Viruses also encode F-box proteins, such as Cell cycle Link (CLINK) from the *Faba bean necrotic yellow virus* (FBNYV) or P0 from the *Turnip Yellows Virus* (TuYV). CLINK targets the Retinoblastoma tumor-suppressor protein (pRB), which forces cells to enter the DNA synthesis phase preceding mitosis and facilitate viral replication (Lageix et al., 2007). For poleroviruses, the P0 F-Fbox protein triggers the degradation of ARGONAUTE 1 (AGO1) but in a proteasome-independent way by sending it instead in a specific manner to the vacuole (Bortolamiol et al., 2007; Baumberger et al., 2007; Derrien et al., 2012). AGO1 is a key protein of the anti-viral RNA silencing mechanism but also for the control of gene expression.

Ubiquitin-dependent proteolysis is not the only way to regulate the amount of proteins and it acts together with other mechanisms. One of them is RNA silencing which, like the ubiquitin, is very well conserved and extensively used by eukaryotes.
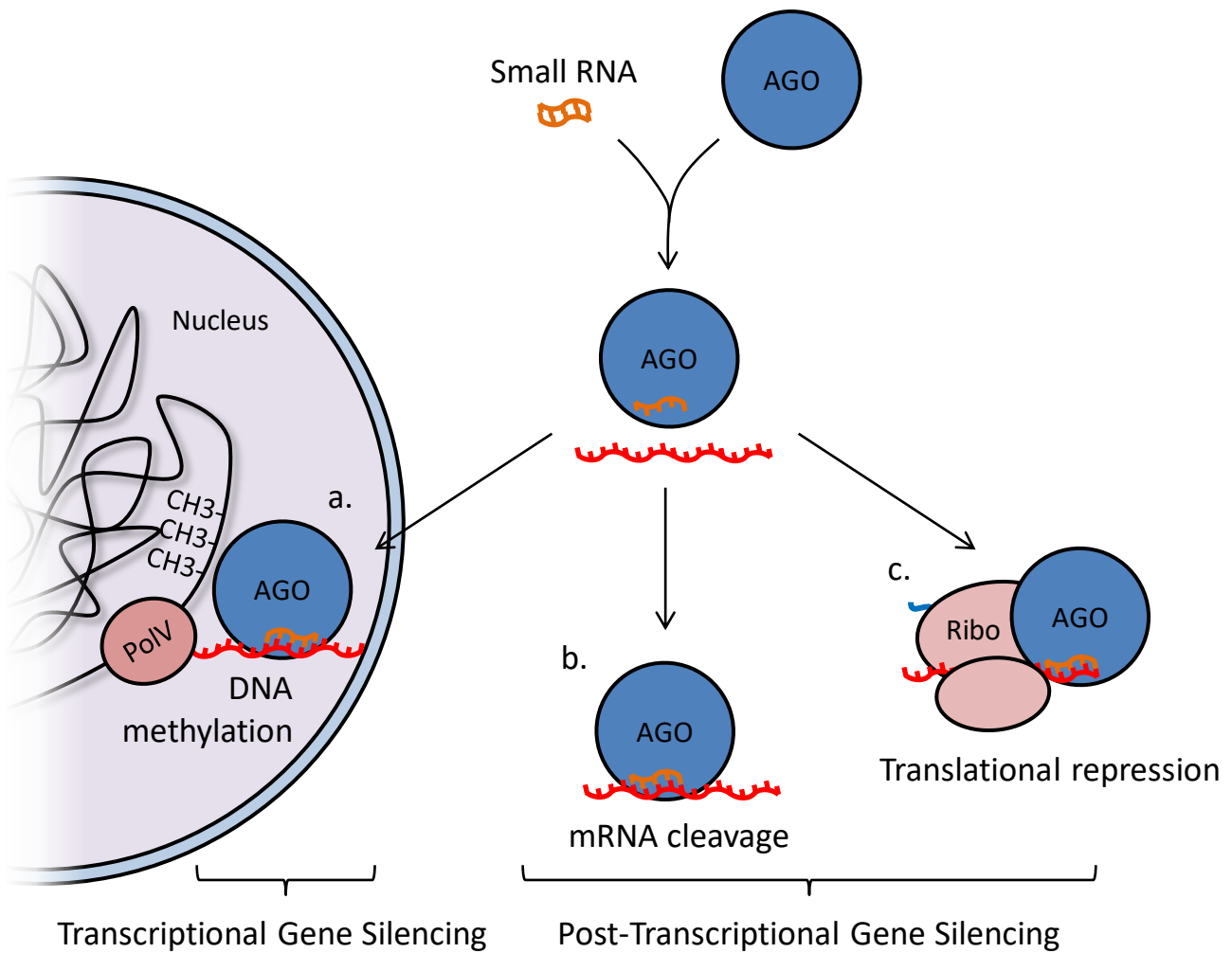
Figure 10 : Mechanisms for the RNA silencing

ARGONAUTE proteins are the main effectors of the RNA silencing. They use small RNAs as probe to target single stranded RNA molecule in a sequence-specific manner. The ARGONAUTE protein can either a) trigger methylation of genomic DNA, b) catalyse target RNA cleavage or c) inhibit the translation of the recognized mRNA. The first activity is called Transcriptional Gene Silencing (TGS) and the two other are named Post-Transcriptional Gene Silencing (PTGS) .

2 RNA silencing

Firstly discovered in plants, RNA silencing is a regulatory mechanism conserved in eukaryotes (reviewed in Tijsterman et al., 2002). Its manifestation was first observed in plants with the acquisition of resistance against the ringspot virus in newly formed tobacco leaves and in petunia when attempting to over-express a gene controlling pigment synthesis in flowers by introgressing a transgene gave the opposite result (Wingard, 1928; Napoli, 1990). The molecular mechanism was revealed later in *Caenorhabditis elegans* with the discovery of a small RNA controlling the expression of developmental genes (Reinhart et al., 2000).

2.1 Mechanism

The principle of RNA silencing implies a single stranded small RNA which serves as a probe to recognize other target RNA molecules in a sequence specific manner. Following recognition, the target RNA can either be cleaved, prevented from being translated or used as signal to trigger the methylation of the corresponding genomic DNA (Krol et al., 2010; Axtell, 2013; Borges and Martienssen, 2015). This way, RNA silencing acts at the post-transcriptional level (Post-Transcriptional Gene Silencing; PTGS) or directly at the transcriptional level (Transcriptional Gene Silencing; TGS) (Figure 10).

The small RNAs are produced from double stranded RNA structures cut by RNase-III-type endonucleases called Dicer (Bernstein et al., 2001; Hutvágner et al., 2001). In plants, the resulting small RNA duplex is methylated by HUA ENHANCER 1 (HEN1) to protect it from uridylation and subsequent degradation (Boutet et al., 2003; Yu et al., 2005; Ren et al., 2014). The duplex is then incorporated in a RNA-Induced Silencing Complex (RISC), more specifically bound in an ARGONAUTE protein (AGO), with the help of the chaperone Heat Shock Protein 90 (HSP90) and through the use of ATP (Iwasaki et al., 2010; Johnston et al., 2010). In plants, another co-chaperone named SQUINT (SQN) has been shown to act with HSP90 and facilitate small RNA loading (Iki et al., 2011; Earley and Poethig, 2011). The AGO protein then
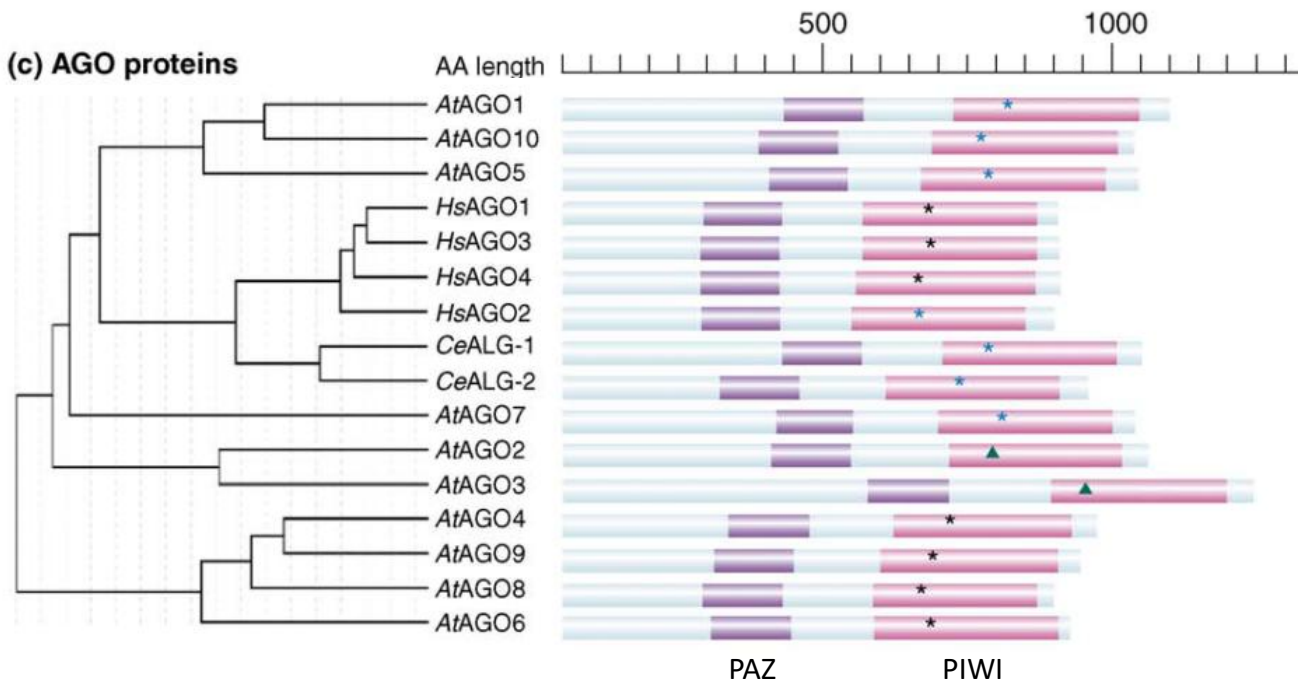
Figure 11 : Phylogeny of Arabidopsis ARGONAUTE proteins

Phylogenic tree of ARGONAUTE proteins from human, *Caenorhabditis elegans* and *Arabidopsis thaliana*. Three different clades are formed in Arabidopsis. AGO1, 5 and 10 form a group, AGO2, 3 and 7 form another and AGO4, 9, 8 and 6 compose the last group. Blue asterisks indicate verified slicer activity, black asterisks indicate cleavage inability and green triangles hypothetical slicer activities. The PAZ and the PIWI domains are shown in purple and pink respectively (adapted from Vazquez, 2006).

unwinds the duplex and keeps only the strand complementary to the RNA target (also called guide strand). The choice of the strand to keep seems to be associated Swith the thermodynamic instability of the 5' end compared to the 3' end (reviewed in Meister and Tuschl, 2004). With the help of the small RNA, the RISC targets RNA molecules and triggers different regulation mechanisms depending on its protein composition which can vary from 160 to 550 kDa (Sontheimer, 2005). The core AGO protein is common to all RISC complexes and is well conserved in eukaryotes (reviewed in Murphy et al., 2008). While vertebrates use one Dicer and 4 AGO proteins, Arabidopsis possess four Dicer Like (DCL1 to 4) and 10 AGO proteins (reviewed in Vazquez, 2006; and in Mallory and Vaucheret, 2010) (Figure 11).

2.2 Activities

Although RNA silencing components are present in most eukaryotes, its activities are not all conserved. For example, RNA silencing in fission yeast is only involved in DNA methylation but is absent in budding yeast. In animals, DNA methylation and messenger regulation are effective but only traces of antiviral activity have been observed while all three activities are well conserved in plants (reviewed in Baulcombe, 2004).

2.2.1 Messenger regulation

Transcriptional inactivation or targeted proteolysis is not enough to efficiently shutdown the cellular amount of a protein since protein synthesis can still occur as long as the messenger RNA exists. RNA silencing directly acts on messenger RNAs and uses dedicated small RNAs to target key genes in various cellular processes. Around 60% of protein coding genes are regulated by RNA silencing in animals, while this amount falls to less than 1% in plants coding mostly for transcription factors (Friedman et al., 2009; reviewed in Jones-Rhoades et al., 2006; German et al., 2008; Addo-Quaye et al., 2008).

- miRNA produced by DCL1

Messenger RNAs are commonly targeted by a class of small RNA called microRNA (miRNA). This class of small RNA has the particularity to be

complementary to the target RNAs allowing some mismatches. miRNA are encoded by dedicated genes that are transcribed by the RNA polymerase II (Pol II) or in introns of protein-coding genes (Xie et al., 2005a; Lee et al., 2004). They are produced from long fold-back structured RNA molecules called pri-miRNA, which are cut in stem-loop precursors called pre-miRNA. These pre-miRNA are then cut in small RNA duplexes. In animals, the RNase-III-type endonuclease Drosha process the pri-miRNA in the nucleus (Lee et al., 2003). The pre-miRNA is then exported in the cytoplasm by the Exportin 5 and cut by Dicer in small RNA duplex (Lund et al., 2004; Hutvágner et al., 2001). Whereas in plants, the pri-miRNA is cut twice by the same enzyme DCL1 in the nucleus (Kurihara and Watanabe, 2004). Another difference concerns the size of the miRNA ; animals miRNA are generally 22 to 23 nucleotides long while in plants DCL1 tends to produce 18 to 21 nucleotides long miRNA (reviewed in Bartel, 2004; and in Voinnet, 2009). Also, some pri-miRNA require the double stranded RNA binding protein Hyponastic Leaves 1 (HYL1) to be processed by DCL1 but the reason why other do not is still an open question (Han et al., 2004; Vazquez et al., 2004a; Dong et al., 2008; Szarzynska et al., 2009). The protein SERRATE (SE) has also been shown to interact with DCL1 and HYL1 and participate in miRNA synthesis (Yang et al., 2006).

- RISC formed with AGO1, 7 and 10

The miRNA loading step in plants was first thought to occur in the cytoplasm since an ortholog of Exportin 5, HASTY (HST), was found to impact miRNA biogenesis (Park et al., 2005). But more recently, AGO1 has been shown to enter, load miRNA and exit the nucleus thanks to a Nuclear-Localization Signal (NLS) and a Nuclear-Export Signal (NES) (Bologna et al., 2018). Notably, AGO1 is the main AGO protein in plants implicated in post-transcriptional gene regulation (Vaucheret et al., 2004; Baumberger and Baulcombe, 2005). For instance, AGO1 controls roots architecture depending on nitrogen availability and leaves development through the use of the miR393 which targets the F-box proteins from the TIR1 / AFB Auxin Receptor (TAAR) family (reviewed in Jones-Rhoades et al., 2006; Vidal et al., 2010; Si-Ammour et al., 2011). Other AGO proteins also load and use miRNAs such as AGO7 with the miR390 (discussed later) or AGO10 which sequesters miR165 and

miR166 to prevent them from silencing class III HomeoDomain-Leucine Zipper (HD-ZIP III) transcription factors, thus allowing proper development of shoot apical meristem (Montgomery et al., 2008; Zhu et al., 2011).

- Translational inhibition or cleavage

Once the RISC recognizes a target, it can exert two kind of activities; translational repression or mRNA cleavage. Translational repression is the main regulation used by animals, while plants prefer mRNA cleavage (reviewed in Meister, 2013). The choice between the two activities was first though to depend on the degree of complementarity between the small RNA and the target, but more recent studies rather favour the RISC composition as the determining factor. In animals, the GW182 protein family is required for translational repression (reviewed in Ding and Han, 2007). These proteins interact with mammalian AGO2 through a motif called ago hook which is composed of glycine next to tryptophan (GW) repeats (Till et al., 2007). GW182 has been shown to interfere with the poly(A)-binding protein (PABP) activity and recruits the enzyme CAF1 to deadenylate messenger RNAs (Fabian et al., 2009; Zekri et al., 2009). Deadenylation of messenger RNAs tail promotes their decaping and subsequent degradation, while interfering with PABP binding to eIF4G is supposed to prevent circularization of the messenger RNAs which prevents their translation (reviewed in Meister, 2013). Although the GW182 protein family is not conserved in plants, the protein SUO ("shuttle" in Chinese) has been proposed to act as their equivalent (Yang et al., 2012). At the opposite, the cleavage activity is independent of protein co-factors and is solely catalyzed by the AGO protein (Martinez and Tuschl, 2004; Nakanishi et al., 2012). The 5' part of the cleaved mRNA is degraded by the exosome and the 3' part by exoribonucleases (Orban and Izaurralde, 2005).

- Signal amplification

Plants display some particularity in RNA silencing. Thus some plant miRNA are produced as 22 nucleotides long and used to cleave target RNAs but in this case, the cleaved RNA is not degraded but instead used as a template for the production of further small RNAs (Chen et al., 2010). This happens with the *TAS* gene family
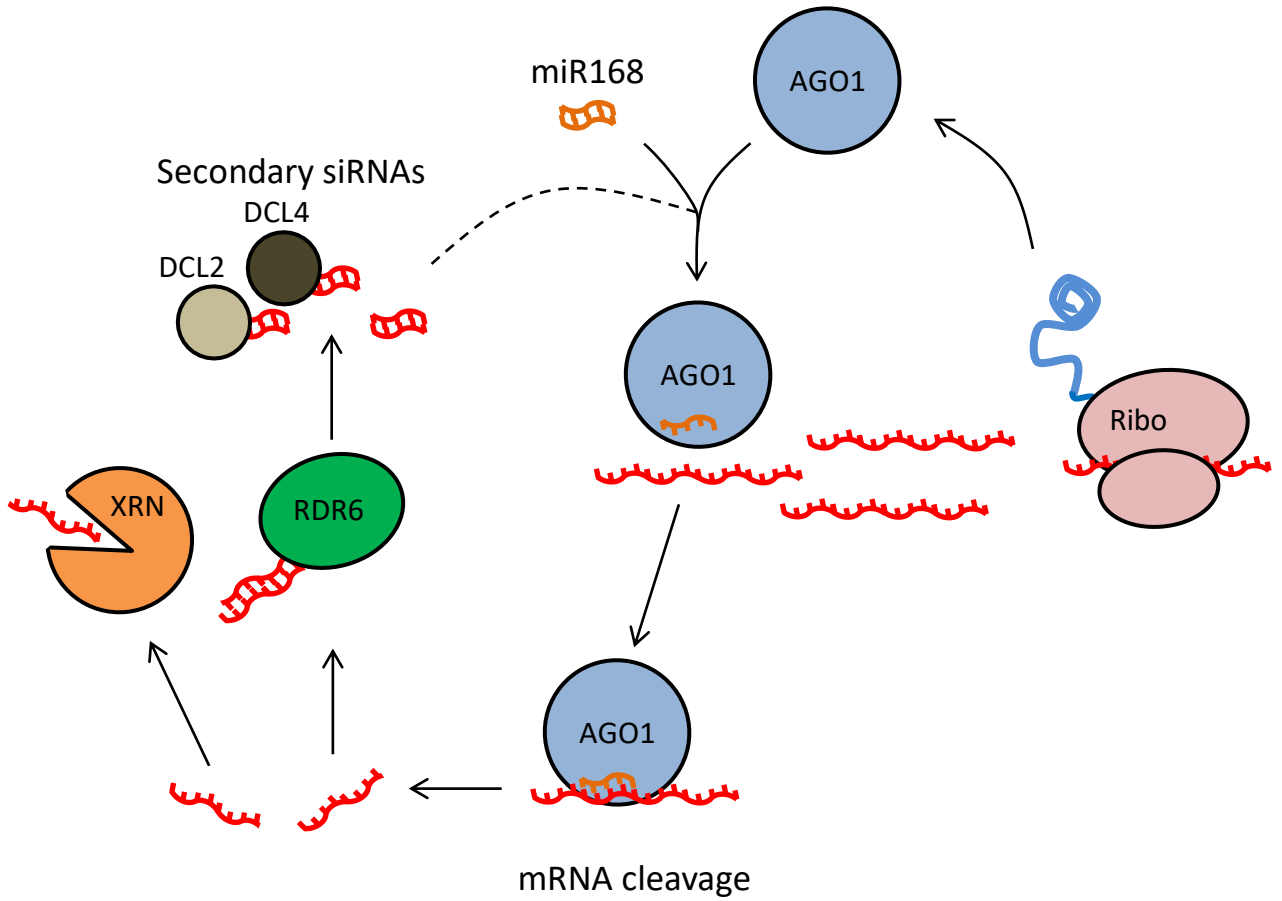
Figure 12 : AGO1 self regulation

ARGONAUTE1 targets and cleaves its own messenger RNA using miR168. The resulting cleavage products are either digested by Exoribonucleases (XRN) or transformed in double stranded RNA by the RNA-dependent RNA polymerase 6 (RDR6). This molecule is then cleaved in small RNA duplexes by DICER 2 and 4 and subsequently loaded in AGO1 to target its own transcript.

whose non-coding RNAs are specifically recognized by miRNAs and cleaved by AGO1 and AGO7 (Allen et al., 2005; Montgomery et al., 2008). The cleavage fragments are then converted to double stranded RNA (dsRNA) by the RNA-dependent RNA polymerase 6 (RDR6) with the help of Suppressor of Gene Silencing 3 (SGS3) (Peragine et al., 2004). The resulting dsRNA is subsequently cut in 21 nucleotides long small RNA mostly by DCL4 and are referred as secondary small RNAs called trans-acting short interfering RNAs (ta-siRNAs) (Vazquez et al., 2004b; Gasciolli et al., 2005; Xie et al., 2005b; Yoshikawa et al., 2005). The ta-siRNAs can, in turn, be loaded in RISCs to target messenger RNAs. A well-known example concerns the *TAS3*-derived ta-siRNAs, which are produced following a miR390 AGO7-mediated targeting in the leaves dorsal layer. These small RNAs diffuse to nearby cells and target, in a gradient dependant manner, the messenger RNAs of Auxin Response Factor 3 and 4 (ARF3 and ARF4) participating in leaf dorso-ventral polarity (Schwab et al., 2009; Pulido and Laufs, 2010; reviewed in Skopelitis et al., 2012). Like-wise production of secondary small RNAs can also occur directly on messenger RNA of coding genes as it is the case with the miR168 which is loaded in AGO1 and targets the messenger RNA of AGO1 forming an self-regulatory loop (Vaucheret et al., 2006; Mallory and Vaucheret, 2009) (Figure 12). Interestingly, some genes have been found to overlap in an antisense manner, producing complementary transcripts when co-expressed. This happens with the Δ^1-pyroline-5-carboxylate dehydrogenase (P5CDH) and the SRO5 genes, which are both expressed under salt stress condition. The resulting dsRNA is cut by DCL2 in 24 nucleotides long small RNAs that trigger the production of further secondary small RNAs termed natural short interfering RNAs (nat-siRNAs) (Borsani et al., 2005).

2.2.2 Antiviral defense

Amplification of RNA silencing by the production of secondary small RNAs is also widely used by plants as antiviral defence mechanism (reviewed in Szittya and Burgyán, 2013). RNA silencing targets viral RNA, which as a consequence hinders viral replication and diffuses a signal preparing non-infected cells for antiviral defence (reviewed in Mlotshwa et al., 2008).

- siRNA produced by DCL4 and 2

Replication of RNA viruses, bi-directional transcription of DNA viruses or folding of viral RNA can produce double stranded RNA molecules, which are potentially recognized and cut by Dicer proteins (reviewed in Mlotshwa et al., 2008; Molnar et al., 2005). All DCL proteins are involved in this process, but DCL4, and in its absence DCL2, stand out to massively generate 21 and 22, respectively, nucleotides long small RNAs, called viral interfering short RNAs (viral siRNAs or sometimes vi-siRNAs or vsiRNAs) (Blevins et al., 2006; Deleris et al., 2006). Antiviral silencing also requires RDR1, RDR2 and RDR6 for the production of secondary siRNA and are necessary for proper antiviral defence (Xie et al., 2001; Mourrain et al., 2000; Diaz-Pendon et al., 2007; Qu et al., 2005; reviewed in Qu, 2010).

- RISC formed with AGO1, 2, 5 and 7

As with miRNA, a primary effector of antiviral RNA silencing is AGO1 (Morel et al., 2002; Zhang et al., 2006). AGO2, AGO5 and AGO7 are also involved but to a lesser degree (Harvey et al., 2011; Jaubert et al., 2011; Wang et al., 2011; Takeda et al., 2008; Brosseau and Moffett, 2015; Qu et al., 2008). Notably, AGO2 and AGO5 favour the loading of small RNA with 5' terminal adenosine and cytosine, respectively, while AGO1 prefers 5' terminal uridine in the guide strand (Mi et al., 2008; Takeda et al., 2008). Once active, the RISC catalyzes the cleavage of viral RNA and/or prevents its translation (reviewed in Szittya and Burgyán, 2013).

- Silencing spreading

The mobility RNA silencing is of particular importance in the antiviral defence as it moves ahead of viral infection to prepare non-infected cells for viral uptake. Spreading of RNA silencing in the plants tissue has been observed in two different ways; short-range and systemic (reviwed in Mermigka et al., 2016). Observation of cell to cell movement of RNA silencing suggests that small RNAs travel through plasmodesmata (Voinnet et al., 1998; Himber et al., 2003; Kalantidis et al., 2006; Kobayashi and Zambryski, 2007). Systemic silencing uses the phloem to transport the silencing signal (Tournier et al., 2006). Various small RNAs have been observed in the phloem alongside the Phloem Small RNA binding Protein 1 (PSRP1) in pumpkin suggesting that here again, small RNA constitute the signal (Yoo et al.,

2004). Nevertheless, no clear orthologs of PSRP1 have yet been identified in Arabidopsis.

- Suppressors of RNA silencing

In order to counter the antiviral silencing, viruses have evolved specialized proteins know as Viral Suppressors of RNA silencing (VSRs) (reviewed in Pumplin and Voinnet, 2013; and in Csorba et al., 2015). Almost every plant virus produces VSRs, sometimes several, displaying a variety of mode of action which can be used as tool to dissect the RNA silencing mechanism (Díaz-Pendón and Ding, 2008). Three kind of strategies are usually employed: (1) reduce small RNA availability, (2) block the activity of RNA silencing core proteins and (3) prevent systemic spreading of silencing. P19 form the *tombusviruses* is probably the most well known VSR (Silhavy et al., 2002). It forms homodimers to seclude 21 nucleotides long small RNA from being loaded and used by RISC complexes (Vargason et al., 2003; West et al., 2003). Another VSR from the *poleroviruses*, P0, hijacks the SCF complex to target, ubiquitinate and trigger the degradation of AGO1 and several other AGO proteins (Pfeffer et al., 2002; Pazhouhandeh et al., 2006; Bortolamiol et al., 2007; Baumberger et al., 2007; Csorba et al., 2010; Derrien et al., 2012). P38 from the *Turnip crinckle virus* mimics the ago hook motif with GW repeats to interact with AGO1 and prevents its loading with small RNAs (Azevedo et al., 2010). Interestingly, P38 also interacts with AGO2 independently of its ago hook motif but does not interact with AGO4 (Zhang et al., 2012; Azevedo et al., 2010). The 2b protein *cucumoviruses* acts on the silencing at several levels (reviewed in Csorba et al., 2015). Among others, it prevents silencing systemic spreading, seclude single and double stranded small RNAs and interacts with and blocks AGO1 slicer activity (Guo and Ding, 2002; Goto et al., 2007; Chen et al., 2008; Zhang et al., 2006).

2.2.3 DNA methylation

Beside its antiviral activity, RNA silencing has also been shown to repress at the transcriptional level the expression of genes involved in pathogens defence (Li et al., 2011; Zhai et al., 2011; Shivaprasad et al., 2012). By this way, suppression of RNA silencing by viruses could activate secondary defences. Apart from this observation, transcriptional gene silencing (TGS) is mostly known to prevent the

activation of Transposable Elements (TE) in order to neutralize their mutagenic potential (reviewed in Fultz et al., 2015).

- siRNA produced by DCL3

DCL3 is the main Dicer involved in the production of small RNA. It generates 24 nucleotides long small RNAs, called heterochromatin-associated short interfering RNAs (hc-siRNAs), from dsRNA corresponding to silenced DNA regions (Herr et al., 2005; reviewed in Melnyk et al., 2011). These dsRNA are produced by Pol IV in partnership with RDR2 (Onodera et al., 2005; Kanno et al., 2005; Pontes et al., 2006). Since Pol IV is recruited by the methylation histone H3 lysine 9, a mark of transcriptional repression, DCL3 products are in this case more responsible of maintenance than *de novo* methylation (Cao et al., 2003; Lippman et al., 2003). In contrast, the initiation of TGS seems to rely on components of the antiviral silencing pathway. DCL4, RDR6, AGO1 and AGO2 have been shown to produce siRNAs from TE transcripts which are required to trigger transcriptional silencing (McCue et al., 2012; Nuthikattu et al., 2013).

- RITS formed with AGO3, 4, 6 and 9

AGO4 is the main AGO involved in TGS but AGO3, 6 and 9 have also been shown to load 24 nucleotides long small RNAs (Zilberman et al., 2003; Zheng et al., 2007; Havecker et al., 2010; Zhang et al., 2016). Additionally, AGO6 also takes 21 to 22 nucleotides long small RNAs (Nuthikattu et al., 2013). This particularity of AGO6 has been proposed to trigger initiation of TGS on active TE (McCue et al., 2015). Overall, these AGO proteins are supposed to be functionally different since *AGO4*, *AGO6*, and *AGO9* mutants have different molecular phenotypes (reviewed in Vaucheret, 2008). Even so, additive phenotypes in *AGO4* and *AGO6* double mutant suggest some functional redundancy as well as partial rescue of *AGO4* mutants by an *AGO4* promoter-driven *AGO3* construct (Zheng et al., 2007; Zhang et al., 2016). The RISC involved in TGS are generally called RNA-Induced Transcriptional Silencing complex (RITS).

- Methylation

The RITS is recruited to the DNA through Pol V activity (Kanno et al., 2005; Pontier et al., 2005; Lahmy et al., 2009). The mechanism here after is not completely understood. It is not known what transcription factors call for Pol V but Pol V stability on the DNA is linked to its ability to generate transcripts (reviewed in Fultz et al., 2015; Lahmy et al., 2016). AGO4 then recognize Pol V transcripts through the loaded small RNA (Wierzbicki et al., 2008, 2009). The Pol V subunit Nuclear RNA Polymerase E1 (NRPE1) recruits also AGO4 through a well conserved ago kook motif (El-shami et al., 2007; Trujillo et al., 2016). AGO4 also interacts with the Domains Rearranged Methytransferase 2 (DRM2) which triggers *de novo* DNA methylation but, in this process, only on the DNA strand complementary to the small RNA (Zhong et al., 2014; reviewed in Matzke et al., 2015). More recently, AGO4 has been shown to also directly interact with DNA, proposing a model where AGO4 is recruited in the Pol V vicinity through the NRPE1 ago hook motif, scans Pol V transcript and jumps to the corresponding DNA sequence where it recruits DRM2 (Lahmy et al., 2016). Apart from the well studied activity of AGO4 on routine TE regulation, TGS has also been shown to play a role in reproduction where AGO9 controls the specification of gametic cells (Olmedo-Monfil et al., 2010). It can also repress gene transcription by methylating their promoter sequence (Elmayan et al., 1998).

2.2.4 Discrete activities

Beside the RNA silencing main activities presented previously, some less understood functions have also been observed.

RNA silencing has also been implicated in DNA double strand break repair. The mechanism is still not well-understood but exists in both plants and animals (reviewed in Meister, 2013). In Arabidopsis, DCL2 generates 21 nucleotides long Double-strand bread Induced small RNAs (diRNAs) from sequences nearby the DNA damage which are loaded in AGO2 (Wei et al., 2012). The role of these small RNAs would be to trigger histone modification in the double-strand break vicinity in order to facilitate DNA repair or to recruit the DNA repair machinery. Still in Arabidopsis, small RNA may also be involved in the repair of UV-induced DNA lesions (Schalk et al.,

2017). This pathway involves the DNA Damage-Binding Protein 2 (DDB2) and AGO1.

Apart from their endogenous activities, small RNA have also been shown to move across kingdoms, a phenomenon call Host Induced Gene Silencing (HIGS) (Knip et al., 2014). Thus sRNAs can be transferred into pathogenic fungus and weaponized to target key genes and hinder fungal development (Nowara et al., 2010; Ghag et al., 2014; Koch et al., 2013). The opposite also exists, for instance, *Botrytis cinerea* exports small RNAs targeting genes controlling plant basal immunity (Weiberg et al., 2014).

Another still poorly understood class of small RNAs comes from tRNA-derived RNA fragments. Cleavage of tRNAs has been observed in many organisms and gives rise to fragments of 30-36 or 18-20 nucleotides long RNAs called tRFs (Dhahbi, 2015; reviewed in Sobala and Hutvagner, 2011; and in Schimmel, 2018; and in Martinez, 2018). In plants, tRFs are supposed to be processed by DCL1 and have been found loaded in AGO1, presumably to target TE transcripts (Loss-Morais et al., 2013; Martinez, 2018).

Among the 10 AGO proteins, only AGO8 activity has not been described so far. It is thought to be a pseudogene originating from recent duplication of AGO9 as it is weakly expressed and its mRNA exhibits frame-shift changes caused by alternative splicing (reviewed in Vaucheret, 2008). At the opposite, AGO1 is the most described plant AGO protein as it plays a central role by contributing to nearly all RNA silencing activities (Vaucheret et al., 2004; Baumberger and Baulcombe, 2005; Qi et al., 2005).
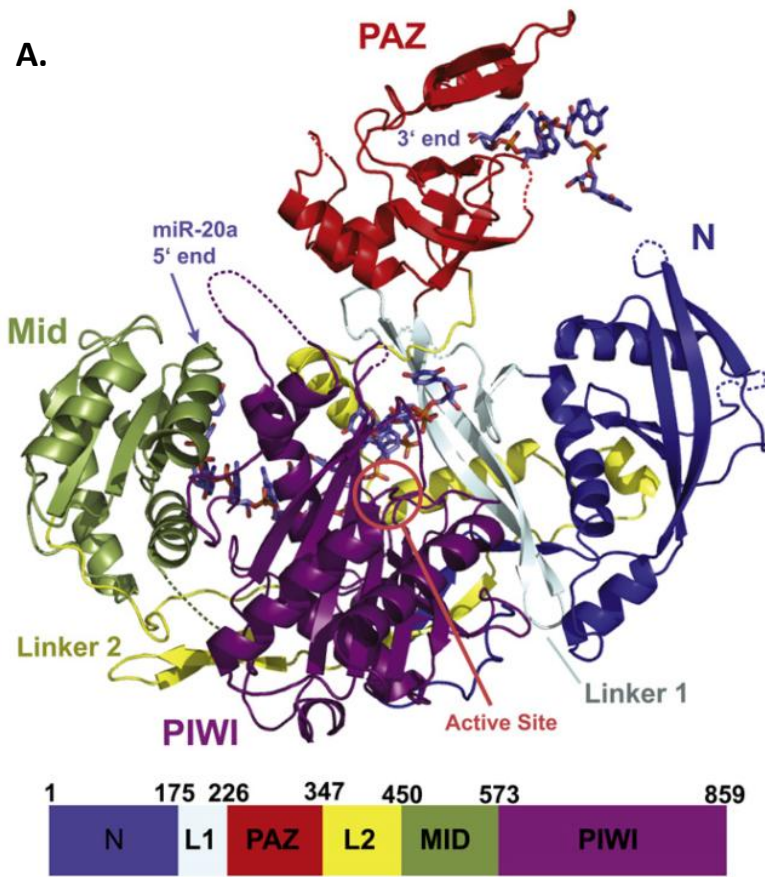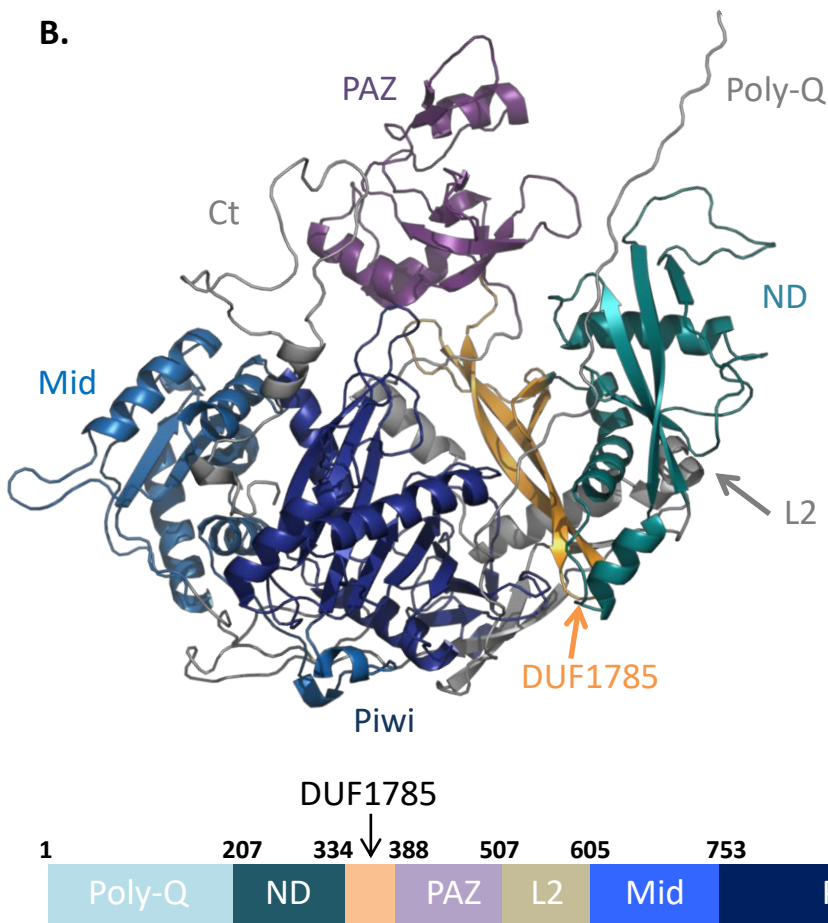
Figure 13 : ARGONAUTE structure

A. Structure of human AGO2 in complex with the miR-20a. The PAZ domain anchors the 3' end of the small RNA. The 5' end is caught between the Mid and the PIWI domains. On the side, the N domain helps the unwinding of the small RNA duplexes. The protein is organized around the Linker 1 while the Linker 2 envelops it from the outside (from Elkayam et al., 2012).

B. Predicted structure of Arabidopsis thaliana AGO1 by the PHYRE2 tool (Kelly et al., 2015). The protein domains are annotated according to Poulsen et al., 2013. The overall conformation of the protein is very similar to the one from human AGO2. The N-terminal part of the protein could not be structurally predicted and is referred here as Poly-Q but is also called N-terminal coil in the literature. The C-terminal end is extended compared to human AGO2 and is here named Ct. The linker 1 is called Domain of Unknown Function 1785 (DUF1785).

3 AGO1

AGO1 was the first AGO protein discovered and has been named after the shape of its mutant *ago1-1* which resembles an octopus (Bohmert et al., 1998). AGO1 importance is moreover highlighted by a strongly impaired development in null mutants (reviewed in Vaucheret, 2008).

3.1 Structure

AGO proteins are also found in prokaryotes where they load DNA instead of RNA, suggesting a common ancestor (Swarts et al., 2014). Since then, their overall structural characteristics remained unchanged (reviewed in Swarts et al., 2014). AGO proteins are roughly organized by four domains; The N-terminal domain, the Piwi-Argonaute-Zwille (PAZ) domain, the middle (MID) domain and the PIWI domain (reviewed in Höck and Meister, 2008). The PAZ domain anchors the 3' end of the small RNA (Lingel et al., 2003, 2004; Ma et al., 2004; Song et al., 2003; Yan et al., 2004). The 5' end is more specifically recognized and caught by the MID and the PIWI domains (Ma et al., 2005; Parker et al., 2005; Frank et al., 2010, 2012). Additionally, the PIWI possess a RiboNuclease H (RNase H) fold responsible of the cleavage activity in certain AGO proteins, as it is the case with Arabidopsis AGO1 (Cerutti et al., 2000; Parker et al., 2004; Yuan et al., 2005; Baumberger and Baulcombe, 2005). On the other hand, the N-terminal domain is required for the small RNA duplex unwinding (Kwak and Tomari, 2012).

The protein structure that has been solved and is the closest to plant AGO1, is the one from Human AGO2 (Schirle and MacRae, 2012; Elkayam et al., 2012). It reveals a two-lobed structure surrounding the loaded small RNA (Figure 13). The N-terminal domain can be subdivided in four elements; N-terminal coil, N domain, Domain of Unknown Function 1785 (DUF1785) and linker 1 which makes the connection with the PAZ domain. The N-terminal coil is variable among AGO proteins, the one from Arabidopsis AGO1 contains a Nuclear Localization Signal (NLS) and a Nuclear Export Signal (NES) (Bologna et al., 2018). As I will develop in

the Result section, the DUF1785 is particularly needed for the unwinding of perfectly matched sRNA duplexes and carries the recognition motif for the viral suppressor of silencing P0 (Derrien et al., 2018). The DUF1785 would also produce some flexibility to the structure, allowing the PAZ domain to change between an open or closed conformation (Poulsen et al., 2013). A second linker connects the PAZ and the MID domains and seems to be the scaffold of the protein by interacting with all domains (Poulsen et al., 2013).

3.2 Interactors

Proteomics analysis of RISCs composition in human has shown a great number of proteins (Meister et al., 2005; Höck et al., 2007). Among them, Dicer, DEAD/DEAH box helicases and GW182 proteins are commonly described. A growing number of GW proteins are being discovered and interact with AGO proteins through so-called ago hook / GW motifs (Meister et al., 2005). Mapping of this interaction showed that amino acids in proximity to the 5' end sRNA binding site form pockets that catch the tryptophan of this motif (Till et al., 2007; Elkayam et al., 2017). Two of such pockets are conserved from human AGO2 to Arabidopsis AGO1 (Schirle and MacRae, 2012; Poulsen et al., 2013). Only a single GW is required to interact with human AGO2 and favours interaction with loaded AGO2 (Till et al., 2007; Elkayam et al., 2017). Ago hook motifs often comprise several repeats of GW spaced by at least 10 amino acids, forming an unstructured region (Till et al., 2007). Several GW therefore improve the interaction with and allow the recruitment of several AGO proteins (Pfaff et al., 2013; Elkayam et al., 2017). Notably, the glycin next to the tryptophan can be replaced by amino acids with small or flexible chains, further enlarging the number of potential AGO interactors (Pfaff et al., 2013).

Human GW182, the first described GW protein, was found in cytoplasmic speckles distinct from endosomes, lysosomes, peroxisomes or golgi complexes (Eystathioy et al., 2002). The link between these GW / Processing bodies and RNA silencing was only later identified by showing GW182 interaction with AGO2 and its requirement for proper silencing (Jakymiw et al., 2005; reviewed in Ding and Han, 2007). GW182 is part the TNRC6 protein family where the ago hook motif is conserved but these proteins are only present in animals (Behm-Ansmant et al.,

2006). In plants, the SUO protein contains an ago hook motif, localizes in P bodies and has been proposed to fulfil the GW182 function in translation inhibition (Yang et al., 2012). Other ago hook motifs have been found implicated in the TGS pathway. The plant-specific Pol IV subunit NRPE1 uses an ago hook motif to recruit AGO4 on the chromatin (El-shami et al., 2007). Needed for RDR2-independent DNA methylation, the NERD protein interacts with AGO2 though an ago hook motif but also with the histone H3, revealing a novel chromatin-based RNA silencing pathway that links PTGS and TGS (Pontier et al., 2012). As a last example, Suppressor of Ty insertion 5 (SPT5)-like contains more than 40 GW repeats and supposedly serves as elongation factor for Pol V (Bies-Etheve et al., 2009). Apart from plants, the ago hook motif has also been found implicated in yeast TGS. Targeting complex subunit 3 (Tas3) recruits the RITS complex on the centromeres by interacting with the Chromodomain protein 1 (Chp1) and yeast Ago1 (Verdel et al., 2004; DeBeauchamp et al., 2008). Interestingly, the interaction with Tas3 also requires a sRNA to be loaded inside Ago1 (Holoch and Moazed, 2015).

3.3 Regulations

Several observations point out a strong control of AGO1 protein level; while null Arabidopsis *ago1* mutants are strongly affected in their development, often leading to precocious death, excess of AGO1 protein also leads to aberrant growth (Bohmert et al., 1998; Fagard et al., 2000; Morel et al., 2002; Vaucheret et al., 2004). Notably, the level of AGO proteins in both plants and animals is strongly correlated with sRNAs availability (Derrien et al., 2012; Smibert et al., 2013; Martinez and Gregory, 2013). Like human AGO2, plant AGO1 is regulated at both the transcriptional and post-translational levels (Adams et al., 2009; reviewed Mallory and Vaucheret, 2010).

GUS promoter trap analysis of Arabidopsis *AGO1* revealed the expression in vascular tissues and more strongly in meristems (Vaucheret et al., 2006). Moreover, AGO1 is globally expressed at the embryo stage (Mallory et al., 2009). At the post-transcriptional level, the expression of the miR168 overlaps *AGO1* expression to regulate AGO1 steady state through a self-regulatory loop where AGO1 targets its own transcript (Vaucheret et al., 2004).

NLS

```
AtAGO1  MVRKRRTDAPSEGGEGSGSREAGPVSGGGRGSQRGGFQQGGGQHQGGRGYTPQPQQGGRG  60
HsAGO2  ------------------------------------------------------------   0
AtAGO1  GRGYGQPPQQQQQYGGPQEYQGRGRGGPPHQGGRGGYGGGRGGGPSSGPPQRQSVPELHQ  120
HsAGO2  ------------------------------------------------------------   0
```
NES
```
AtAGO1  ATSPTYQAVSSQPTLSEVSPTQVPEPTVLAQQFEQLSVEQGAPSQAIQPIPSSSKAFKFP  180
HsAGO2  -------------------------------MYSGAGPALAPPAPPPPIQGYAFKPP   26
                                        *   *  :.    *  *  .. *** *

AtAGO1  MRPGKGQSGKRCIVKANHFFAELPDKDLHHYDVTITPEVTSRGVNRAVMKQLVDNYRDSH  240
HsAGO2  PRPDFGTSGRTIKLQANFFEMDIPKIDIYHYELDIKPEKCPRRVNREIVEHMVQHFKTQI   86
         **. * **:     ::**.*   ::*. *::**:* *.**    * *** ::::*::::.

AtAGO1  LGSRLPAYDGRKSLYTAGPLPFNSKEFRINLLDEEVGAGGQRREREFKVVIKLVARADLH  300
HsAGO2  FGDRKPVFDGRKNLYTAMPLPIGRDKVEL-----EVTLPGEGKDRIFKVSIKWVSCVSLQ  141
         :*.* *.:****.**** ***. .: .::      **   *:.:* *** ** *: ..*:

AtAGO1  HLGMFLEGKQSDAPQEALQVLDIVLRELPTSRYIPVGRSFYSPDIGKKQSLGDGLESWRG  360
HsAGO2  ALHDALSGRLPSVPFETIQALDVVMRHLPSMRYTPVGRSFFTASEGCSNPLGGGREVWFG  201
         .*  * .**:* .*:* :* **:*:*.**: ** ******::  *. .:  ** * ** *

AtAGO1  FYQSIRPTQMGLSLNIDMSSTAFIEANPVIQFVCDLLNRD---ISSRPLSDADRVKIKKA  417
HsAGO2  FHQSVRPSLWKMMLNIDVSATAFYKAQPVIEFVCEVLDFKSIEEQQKPLTDSQRVKFTKE  261
         *:**:**:   *:****:*:*** :*.**:***::*:      .::*:**:*.::*::*

AtAGO1  LRGVKVEVTHRGNMRRKYRISGLTAVATRELTFPVDERNT---QKSVVEYFHETYGFRIQ  474
HsAGO2  IKGLKVEITHCGQMKRKYRVCNVTRRPASHQTFPLQQESGQTVECTVAQYFKDRHKLVLR  321
         ::*:*** ** *.*:****:. :*     ::.***:  ** .   : :*:**:: *:.::

AtAGO1  HTQLPCLQVGNSNRPNYLPMEVCKIVEGQRYSKRLNERQITALLKVTCQRPIDREKDILQ  534
HsAGO2  YPHLPCLQVGQEQKHTYLPLEVCNIVAGQRCIKKLTDNQTSTMIRATARSAPDRQEEISK  381
          :.********:.:: .***:***:**.*** .*:** :*:**::* *..: :* ::.:

AtAGO1  TVQLNDYAKDNYAQEFGIKISTSLASVEARILPPPWLKYHESGREGTCLPQVGQWNMMNK  594
HsAGO2  LMRSASFNTDPYVREFGIMVKDEMTDVTGRVLQPPSILYGGRN-KAIATPVQGVWDMRNK  440
         ::   :.  .*.:****:: :.  *.*: *:* ** :*:  .. *  .* * * *:* **

AtAGO1  KMINGGTVNNWICINFSRQ--VQDNLARTFCQELAQMCYVSGMAFNPEPVLPPVSARPEQ  652
HsAGO2  QFHTGIEIKVWAIACFAPQRQCTEVHLKSFTEQLRKISRDAGMPIQGQPCFCKYAQGADS  500
         ::. .   :*  *.:* :    **  *:.*.:** :**  :.*** ::  * *  ::  .

AtAGO1  VEKVLKTRYHDATSKLSQGKEIDLLIVILPDNNGSLYGDLKRICETELGIVSQCCLTKHV  712
HsAGO2  VEPMFRHLK-------NTYAGLQLVVVILP-GKTPVYAEVKRVGDTVLGMATQCVQMKNV  552
         **  ::: *         *.**:*::***  **  :*.::**: :* **:.:** :*: *

AtAGO1  FKMSKQYMANVALKINVKVGGRNTVLVDALSRRIPLVSDRPTIIFGADVTHPHPGEDSSP  772
HsAGO2  QRTTPQTLSNLCLKINVKLGGVNNILLP---QGRPPVFQQPVIFLGADVTHPPAGDGKKP  609
          :   *::* :.*******:**.*..*:*    :.**.: .*:*:*******.. *: .*

AtAGO1  SIAAVVASQDWPEITKYAGLVCAQAHRQELIQDLFKEWKDPQKGVVTGGMIKELLIAFRR  832
HsAGO2  SIAAVVGSMDAH-PNRYCATVRVQQHRQEIIQDL-----------AAMVRELLIQFYK  655
         ******.* *.   *.*  .:* .* ****:****             *:::*** * :

AtAGO1  STGHKPLRIIFYRDGVSEGQFYQVLLYELDAIRKACASLEAGYQPPVTFVVVQKRHHTRL  892
HsAGO2  STRFKPTRIIFYRDGVSEGQFQQVLHHELLAIREACIKLEKDYQPGITFIVVQKRHHTRL  715
         **  ** ************** *** :** ***:**  ** .*** :**:*********

AtAGO1  FAQNHNDRHSVDRSGNILPGTVVDSKICHPTEFDFYLCSHAGIQGTSRPAHYHVLWDENN  952
HsAGO2  FCTDKNER--VGKSGNIPAGTTVDTKITHPTEFDFYLCSHAGIQGTSRPSHYHVLWDDNR  773
         *.  :*:.*   *.****  **.**:**.*********************:******:*.

AtAGO1  FTADGLQSLTNNLCYTYARCTRSVSIVPPAYYAHLAAFRARFYMEPETSDSGSMASGSMA  1012
HsAGO2  FSSDELQILTYQLCHTYVRCTRSVSIPAPAYYAHLVAFRARYHLVDKEHDSAEGSH---T  830
         *::* **.**  **:**.******** .********:*****: :. : *** ..*.   *

AtAGO1  RGGGMAGRSTRGPNVNAAVRPLPALKENVKRVMFYC  1048
HsAGO2  S-GQSNGRD-----HQALAKAV-QVHQDTLRTMYFA  859
         . *.  ***      *.: : :  ::::*. *.*::.
```

Poly-Q
ND
DUF1785
PAZ
L2
Mid
Piwi
Ct

1
207
334
388
507
605
753
997
1048

Figure 14 : Alignement of Arabidopsis AGO with Human AGO2

The protein sequences of Arabidopsis AtAGO1 and human HsAGO2 were aligned with Clustal Omega (https://www.ebi.ac.uk/Tools/msa/clustalo/). Amino acids with small side chains are displayed in red, acidic in blue, basic in magenta, hydroxyl or sulfhydryl or amine in green. Asterisks (*) indicate full conservation, colon (:) strong and period (.) weak similar properties. The domains are indicated by the colored background in accordance to the scheme on the right. Arabidopsis Nuclear Localization Signal (NLS) and Nuclear Export Signal (NES) (Bologna et al., 2018) are indicated with purple bars. Known post-translational modifications of human AGO2 are indicated with white arrows and specified here after ;

Phosphorylations
S387 (Zeng et al., 2008; Horman et al., 2013)
Y529 (Rüdel et al., 2011)
S824 to S834 (Quévillon Huberdeau et al., 2017)

Sumoylation
K402 (Josa-Prado et al., 2015)
Hydroxylation
P700 (Qi et al., 2008)

3.3.1 Post-translational modifications

Not much is known about AGO1 post-translational modifications in plants but their number and importance for human AGO2 function suggest that at least some may be conserved and open new avenues for research in the plant field (Figure 14).

- Hydroxylation

Human AGO2 has been shown hydroxylated on the proline 700 by type I collagen prolyl-4-hydroxylase (C-P4H(I)) (Qi et al., 2008). Interestingly, preventing this modification destabilizes AGO2 and impairs RNA silencing (Qi et al., 2008). On the other hand, AGO2 hydroxylation has been shown to improve the interaction with HSP90 and increases miRNA levels alongside AGO2 activity (Wu et al., 2011a). Hydroxylation has also been reproduced *in vitro* on AGO4 and to a lesser extent on AGO1 and AGO3 and is promoted *in vivo* by hypoxia (Qi et al., 2008; Wu et al., 2011a).

- Acetylation

Plant AGO1 has been identified by peptide affinity enrichment for acetylated lysine residues (Wu et al., 2011b). However, nothing is known about the function of this modification in plants. Acetylation also occurs on Drosha and prevents its degradation by the ubiquitin system (Tang et al., 2013).

- ADP-ribosylation

PolyADP-ribose is required for the formation of stress granules which are protein aggregates different from P-bodies (Leung et al., 2011; reviewed in Anderson and Kedersha, 2008). Among other proteins constituting the stress granules, human AGO proteins are ADP-ribosylated, particularly upon stress, which correlates with alleviation of RNA silencing (Leung et al., 2011).

- Phosphorylation

Several phosphorylation sites have been identified on human AGO2. For instance, the serine 387 has been shown to be phosphorylated by both the p38

mitogen-activated protein kinase (MAPK) and the proto-oncogene Akt3/PKBγ (Zeng et al., 2008; Horman et al., 2013). This modification favours the localization of AGO2 to the P-bodies and its interation with GW182 (Zeng et al., 2008; Horman et al., 2013). Interestingly, it also promotes translational repression over mRNA cleavage (Horman et al., 2013). The tyrosine 529 of human AGO2 can also be phosphorylated (Rüdel et al., 2011). As it participates in the sRNA binding in the MID domain, this modification prevents sRNA binding by generating a repulsive force and reduces localization to P-bodies (Rüdel et al., 2011). As such, Y529 phosphorylation has been proposed to be a molecular switch for sRNA loading (Rüdel et al., 2011). On the other hand, nearby phosphorylation of AGO2 threonine 555 and serine 561 abolishes the interaction with GW proteins, mRNA binding and localization to P-bodies but does not influence sRNA loading (Quévillon Huberdeau et al., 2017). Lastly, a cluster of serines and threonines (824 to 834) located in the C-terminal part of AGO2 is phosphorylated by Casein Kinase 1 Alpha 1 (CSNK1A1) and dephosphorylated by the Ankyrin Repeat Domain 52 Protein - Phosphatase 6 Catalytic Subunit complexe (ANKRD52–PPP6C) (Quévillon Huberdeau et al., 2017; Golden et al., 2017). These modifications also affect mRNA binding and form a cycle where phosphorylation/dephosphorylation promotes AGO2 activity by improving its availability for new targets (Quévillon Huberdeau et al., 2017; Golden et al., 2017). Still other phosphorylation on AGO2 have been reported but have not been studied so far (Rüdel et al., 2011; Quévillon Huberdeau et al., 2017).

- Sumoylation

The lysine 402 of human AGO2 is modified by SUMO1 and SUMO2 (Josa-Prado et al., 2015). Mutation of this amino acid does not affect AGO2 silencing activity but the mutation of the amino acids next to it prevents the docking of the E3 ligase responsible for the sumoylation and reduces AGO2 activity (Josa-Prado et al., 2015).

- Ubiquitination

While it is clear that both plant and metazoan AGO proteins are targeted for degradation, most probably through ubiquitination, these degradation pathways are
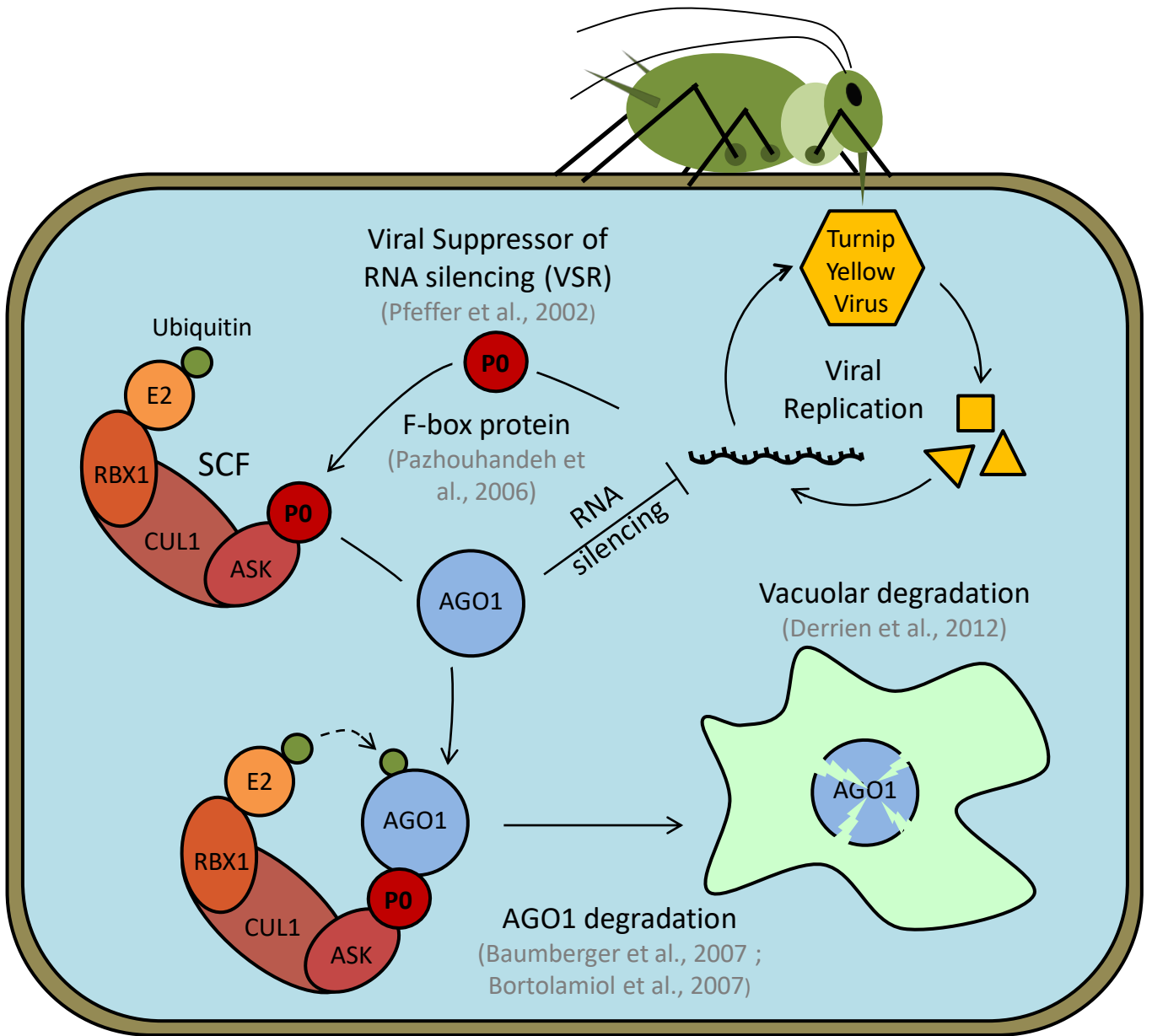
Figure 15 : Mode of action of the viral suppressor of silencing P0

The Turnip Yellows Virus is a single stranded RNA based virus notably transmitted by aphids. Its protein P0 is a viral suppressor of silencing that hijacks the SCF complex and triggers the degradation of AGO1. Instead of being degraded by the 26S proteasome, AGO1 is degraded in the vacuole.

still poorly characterized. Inhibition of the chaperone HSP90 activity, which is implicated in the sRNA loading, fosters human AGO2 protein destabilization in a proteasome-dependant manner (Johnston et al., 2010). Alternatively, human AGO2 has also been found associated with the Nuclear Dot Protein 52 (NDP52) which is a cargo receptor for autophagy (Gibbings et al., 2012). These two observations did not correlate with important changes in miRNA levels, suggesting that the unloaded form of AGO2 is degraded in both case (Johnston et al., 2010; Gibbings et al., 2012). In mouse, it was reported that the E3 ubiquitin ligase mLin41 interacts with AGO2 through its coiled-coil domain and promotes its ubiquitination in vitro and in vivo. Moreover, ectopic overexpression of mLin41 reduced the level of endogenous Ago2 in embryonic carcinoma cells and this effect was attenuated by inhibition of the proteasome. However more recent studies put into question the control of AGO2 stability by mLin41 (Chang et al., 2012; Chen et al., 2012) thus the role of this E3 ubiquitin ligase in the turnover of AGO2 still need further investigations. In Drosophila, the proteasome has also been found to regulate AGO2 stability as well as the Ubiquitin-conjugating enzyme E2 variant 1A (Uev1A), pointing out the implication of the ubiquitin-proteasome system (Chinen and Lei, 2017).

In plants, the viral suppressor of silencing P0 from the *Turnip Yellows Virus* (TuYV) triggers AGO1 degradation by sending it to the vacuole (Pfeffer et al., 2002; Pazhouhandeh et al., 2006; Bortolamiol et al., 2007; Baumberger et al., 2007; Csorba et al., 2010; Derrien et al., 2012) (Figure 15). To summarize, P0 proteins from Poleroviruses, have been shown to promote the degradation of AGO1 and presumably impair RNA-based anti-viral immunity (Baumberger et al., 2007; Bortolamiol et al., 2007). This mechanism was even extended to VSRs of other viruses (Chiu et al., 2010; Fusaro et al., 2012). Notably, P0 acts upstream of AGO1 loading and thus would prevent the formation of RISC (Csorba et al., 2010). At the molecular level, viral P0 VSRs encode F-box proteins (Pazhouhandeh et al., 2006) that hijack the host SCF E3 ubiquitin-protein ligase to promote AGO1 or an associated protein ubiquitination. Because ubiquitination of target proteins by SCF-type complexes often leads to their proteasomal degradation, it was a surprise to find that the degradation of AGO1 by P0 was insensitive to inhibition of the proteasome

(Baumberger et al., 2007). It was later reported that AGO1 was degraded in the vacuole most likely by an autophagy-related process (Derrien et al., 2012).

Because viruses usually highjack host cell machineries, it was likely that AGO1 protein degradation also occurs in a P0-independent context. Hence, an Arabidopsis endogenous F-box protein called F-box With WD40 2 (FBW2) has been shown to impact AGO1 protein level and activity (Earley et al., 2010). FBW2 was identified by a genetic suppressor screen of a null allele of SQUINT (SQN), encoding a Cyclophilin-40 chaperon, a positive regulator of AGO1 activity. While *FBW2* loss-of-function mutants do not exhibit an increase in AGO1 protein level, most likely because of the miR168-dependent feedback mechanism regulating AGO1 expression (Vaucheret et al., 2006), FBW2 overexpression significantly reduces AGO1 protein content (Earley et al., 2010). To a situation reminiscent to the VSR P0, the proteasome inhibitor MG132 was also unable to block the FBW2-mediated degradation of AGO1. At the molecular level however, we know very little about the mode of action of FBW2.

4 Research project

The laboratory in which I performed my PhD work has a long working history on plant ubiquitin E3 ligases and their involvement in various key physiological processes such as the cell cycle, hormone signalling or epigenetic regulation. Since 2006, the atypical degradation of AGO1 triggered by P0 is a topic of interest of the laboratory, and still forms a challenging topic nowadays. My PhD work focussed on the molecular mechanisms of AGO1 degradation in *Arabidopsis thaliana*, and is subdivided in the two following parts.

First, I contributed to the elucidation of the P0-mediated AGO1 decay pathway.In an attempt to generate P0-resistant AGO1 mutants, a genetic screen has been performed. One mutant, the *Sup149* (later called *ago1-57*), has been proven to be fully resistant to P0 but also affected in its silencing abilities. This mutation falls in the Domain of Unknown Function 1785 (DUF1785) of AGO1, which is part of the linker 1. I participated to the work aiming at characterizing this mutation and the functional relevance of the domain it affects. This work has been published in Plant Cell (Derrien et al., 2018), and will thus only be shortly discussed in this thesis.

Second, my main project focused on the regulation of AGO1 by the endogenous F-box protein FBW2. Since P0 hijacks the SCF to exert its silencing suppressor activity, we aimed to identify endogenous E3 ubiquitin ligases that are involved in the turnover of AGO1. One obvious candidate was FBW2, as it was previously shown that increased FBW2 levels lead to reduction in AGO1 protein levels (Earley et al., 2010). I thus investigated the molecular mechanism by which FBW2 could control AGO1 protein level. I showed that FBW2 and AGO1 interact and that FBW2 triggers AGO1 degradation through the SCF^{FBW2} activity. Intriguingly, neither the proteasome nor the classical autophagy pathway seemed to be responsible for AGO1 degradation in this process. Finally, I propose a physiological role for the FBW2-mediated AGO1 degradation. These results have not yet been published, and will be presented in detail in the following section.

Results

1 *ago1-57*, an AGO1 allele resistant to P0

The beginning of my PhD took part within an ongoing project studying a new allele of AGO1; the mutation *ago1-57*. This work was recently published in The Plant Cell (Derrien et al., 2018). The *ago1-57* mutant was recovered in a P0 suppressor genetic screen. In this screen, we took advantage of the severe phenotype caused by the expression of the viral F-box P0, which disable developmental programs that are normally controlled by AGO1-miRNA entities. The aim was therefore to find new components of the virus-induced AGO1 degradation pathway, and if possible to generate plants resistant to P0 and by extent to the Turnip Yellows Virus (TuYV). The mutation recovered, sup149.1, did indeed render AGO1 non-degradable by P0 and suppressed the developmental defects caused by P0 expression. Interestingly, the causal mutation turned out to be a missense mutation of AGO1 itself,

This work investigates the phenotype of the *ago1-57* mutation and highlights the importance of the Domain of Unknown Function 1785 (DUF1785), in which the *ago1-57* mutation is localized. *ago1-57* is the first AGO1 allele that is affected in the DUF1785 and despite limited effect on the miRNA-mediated regulation, is severely impaired in transgene silencing as well as in production of some secondary siRNA species. Explanation for this apparent discrepancy came from the extended molecular characterization of AGO1 behaviour in the mutant. Both *in vitro* and *in vivo* approaches showed that the *ago1-57* allele is affected at the unwinding step of the mature RISC formation, *i.e.* in the separation and subsequent removal of the passenger strand of the small RNA duplex. The effect is marginal and concerns only a fraction of miRNA duplexes, while perfectly matched duplexes like siRNA do not appear to be unwound by the mutated allele. This differential unwinding defect exhibited by small RNA duplexes of different stability explains the strong defects in siRNA-mediated regulation, since siRNA-RISCs will be unable to act.

The *ago1-57* mutation induces a change from a glycine residue in position 186 to an aspartic acid, in the degron of P0 (i.e., the minimal element within a protein that
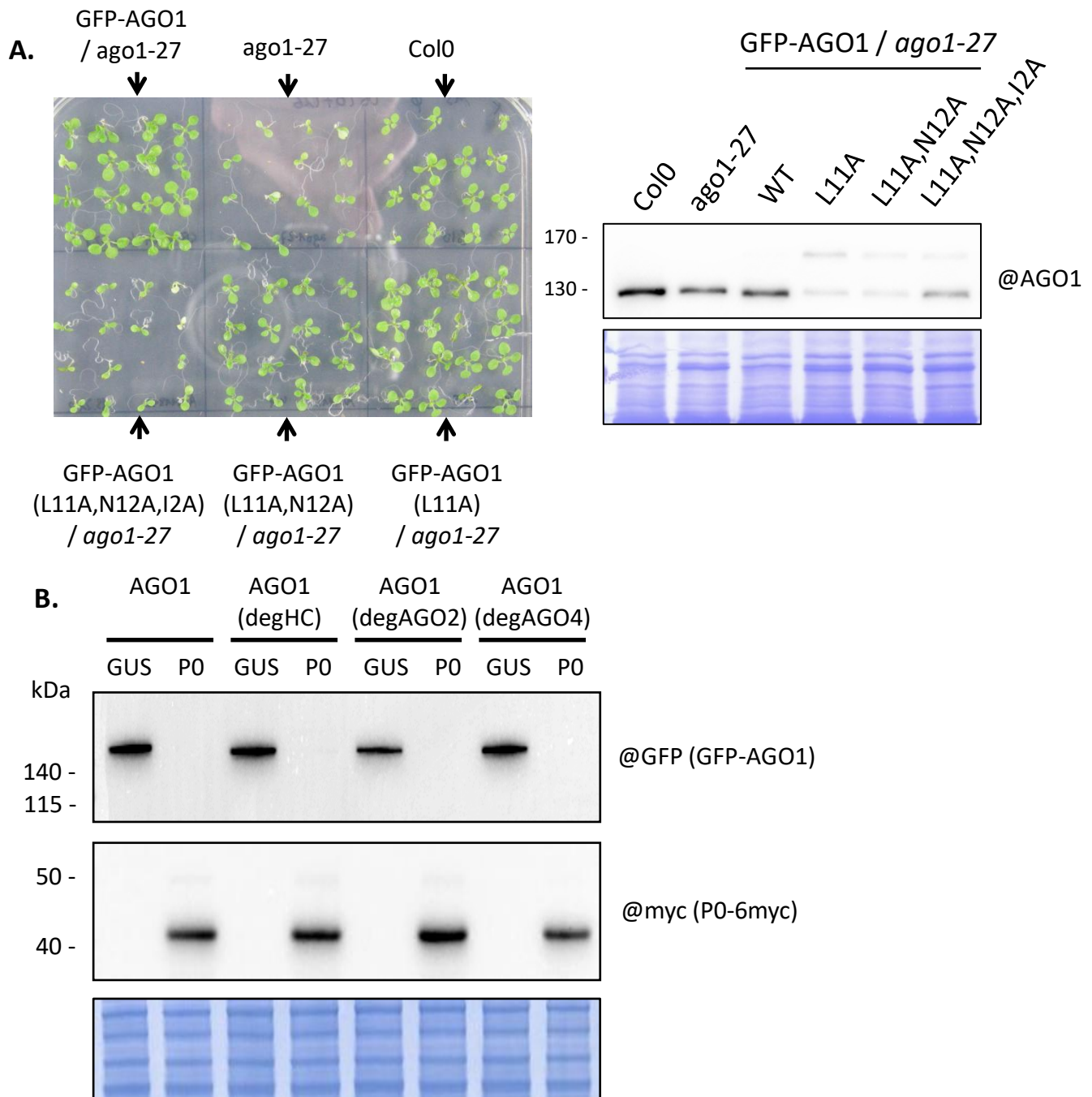
Figure 16 : Mutation and replacement of P0 degron in AGO1

The degron is the minimal element within a protein that is sufficient for recognition and degradation by a proteolytic apparatus (Varshavsky, 1991). Coomassie blue staining was used as a loading control for the Western blots. "@" indicates hybridization with antibody.

A. Complementation of *ago1-27* mutants with GFP-AGO1 and its versions with mutated degrons. The mutations are annotated according to Derrien et al., 2018. Left : 10 days old seedlings grown on MS medium. Right : Western blot of protein extracts from the same seedlings.

B. Western blot of protein extracts from four week old *Nicotiana benthamiana* agroinfiltrated leaves. Agrobacteria harbouring full length GFP-AGO1 or GFP-AGO1 with modified degron as specified and a 35S::P0-6myc constructs were infiltrated at an OD of 0,3. Tissues were sampled 3 days later. Expression of GUS serves as control. DegAGO2 and DegAGO4 correspond to AGO1 versions where the degron is replaced by the homologue sequence of AGO2 and AGO4 respectively. DegHC corresponds to the insertion of silent mutations, necessary to create an appropriate recombination site.

is sufficient for recognition and degradation by a proteolytic apparatus; Varshavsky, 1991), which had been concomitantly identified by expressing separate domains of AGO1 with P0 in a transient system, and scoring them for degradative ability. Once the degron was identified an alanine scanning mutagenesis of the AGO1 P0-degron was used to identify essential amino acid inside the degron, and this is an approach I participated in. Subsequently, as a strategy to render the full-size AGO1 resistant to P0, I also introduced in AGO1 other mutations found by the alanine scanning mutagenesis of the degron (the L11A, N12A and I2A, numbered after their position in the degron rather then from the start of the primary sequence) and tested their impact on plant development by introducing the mutant versions of GFP-AGO1 into the *ago1-27* mutant (Figure 16A). While the L11A mutation appears to complement the phenotypic defects of the mutant similarly to the WT GFP-AGO1, this is not the case of the double and triple mutation. Mutating both L11 and N12 leads to a phenotype that is intermediate between a WT plant and an *ago1-27*, while combining the three mutations fails to complement the mutant phenotype. This suggests that the L11A mutation does not compromise AGO1 function, but that the combination of several mutations affects the function of the DUF1785 domain, in perhaps a way that is similar to the *ago1-57* allele.

Next, I created AGO1 chimeras that contain the degron from other Arabidopsis ARGONAUTEs. This was done by swapping the paralogous sequence of the AGO of choice in place of the degron of AGO1. Since AGO4 was previously shown as being more resistant to P0 (Baumberger et al., 2007), its putative degron was selected to try to render the resulting chimera more stable, and so was the degron of AGO2, that belongs to a clade separate from the one of AGO1 (Vaucheret, 2008). These constructs were then tested in *Nicotiana benthamiana* transient expression but were equally susceptible to P0 (Figure 16B), suggesting that the putative degrons of AGO2 and AGO4 are also targeted by P0, a fact that was later confirmed for the two endogenous proteins (Derrien et al., 2018).
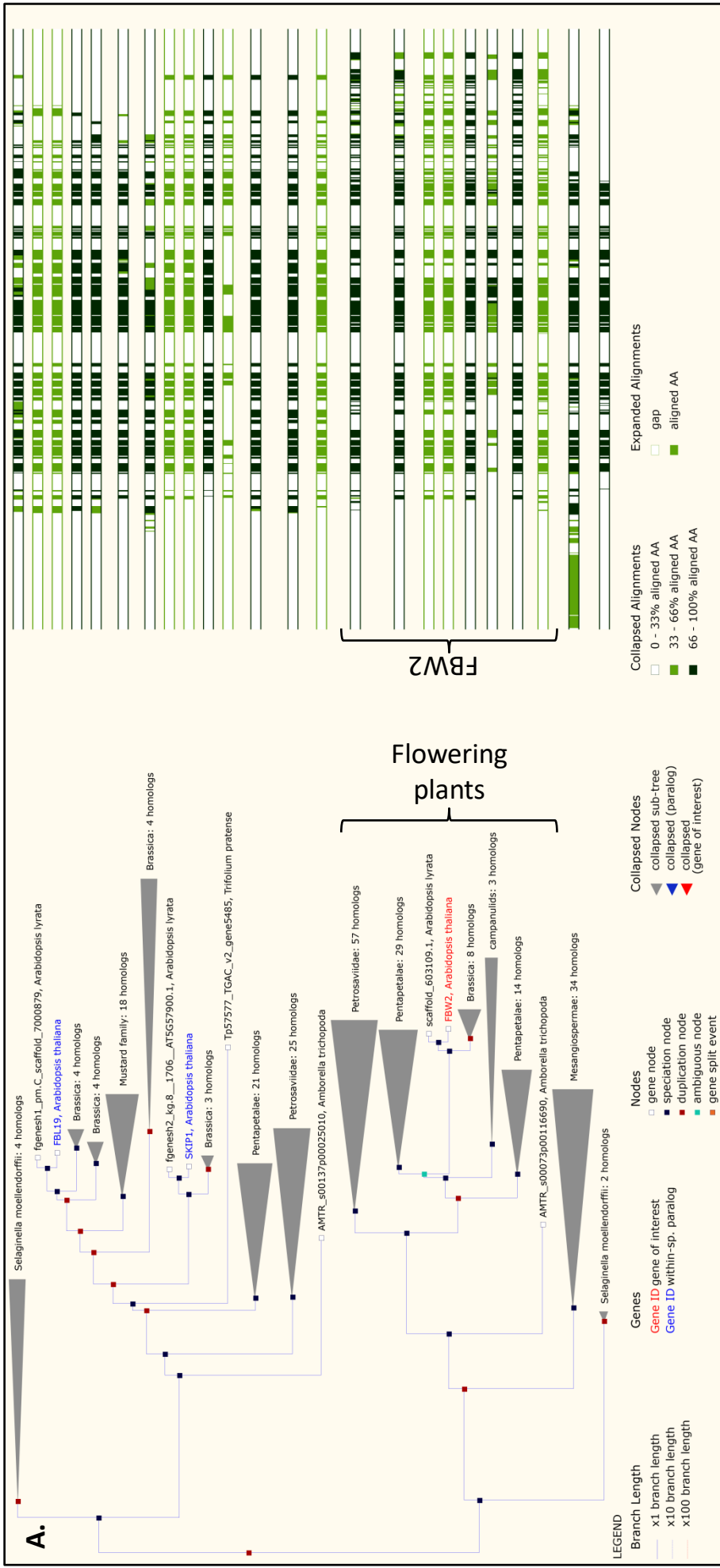
Figure 17 : FBW2 conservation and gene structure

A. FBW2 is conserved in flowering plants. Phylogenic analysis of FBW2 orthologs available at http://plants.ensembl.org/Arabidopsis_thaliana/Gene/Compara_Tree?g=AT4G08980;r=4:5758014-5760569. The amino acids conservation is illustrated on the right, pay attention to the C-terminal end.
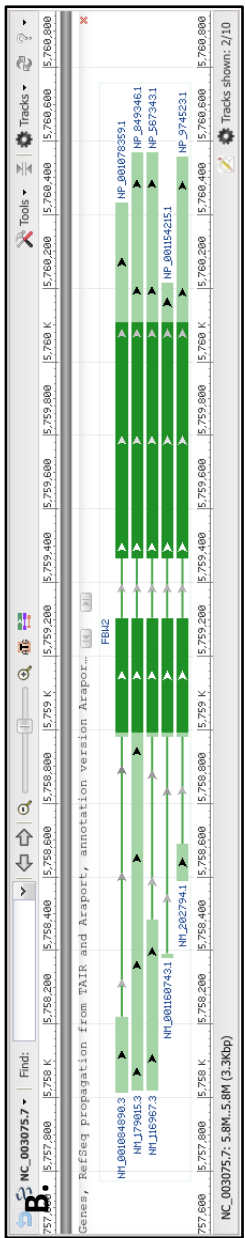
B. Structure of FBW2 gene. Five different transcript generate only one protein sequence. One intron is located in the coding sequence and is evenly spliced. The other introns are located in the 5' UTR and present alternative splicing.

2 FBW2, a novel regulator of AGO1

2.1 FBW2: a LRR-containing F-box protein

The main part of my PhD focussed on the protein FBW2. According to *in silico* generated phylogenetic trees, the F-BOX AND WD REPEAT DOMAIN-CONTAINING 2 (*FBW2*) is exclusively conserved among flowering plants (Figure 17A). This gene has also been called *SKIP18*. To be consistent, we will call it FBW2 along the thesis manuscript.

At RNA level, five different transcripts are reported for *FBW2*. They all code for the same protein, but they differentiate themselves by alternative splicing and different 3' UTRs (different transcription termination sites). Thus, the single intron implanted in the coding sequence is common to all transcripts and spliced evenly, while introns localized in the 5' UTR are spliced differently (Figure 17B).

The *FBW2* gene encodes a protein of 317 amino acids carrying an F-box domain at its N-terminal side. This domain is well-conserved among Arabidopsis F-boxes but shows some particularities compared to the canonical F-box motif (Figure 18A). In disagreement to its name, FBW2 does not contain a WD40 domain and has therefore been mis-annotated. However, the protein sequence of FBW2 contains many LRR repeats, a structure found commonly in plant F-box proteins (Gagne et al., 2002) and often providing a .... function to the protein. Submitting the FBW2 amino acids sequence to the Phyre2 tool (Kelly et al., 2015) allows the prediction, with high confidentiality, of a structure similar to the human SKP2 F-box protein, which contains leucine-rich repeats (LRR) belonging to the Antagonist of Mitotic exit Network 1 protein (AMN1) superfamily (Figure 18B). However, the C-terminal part of FBW2 does not resemble any annotated protein domain.
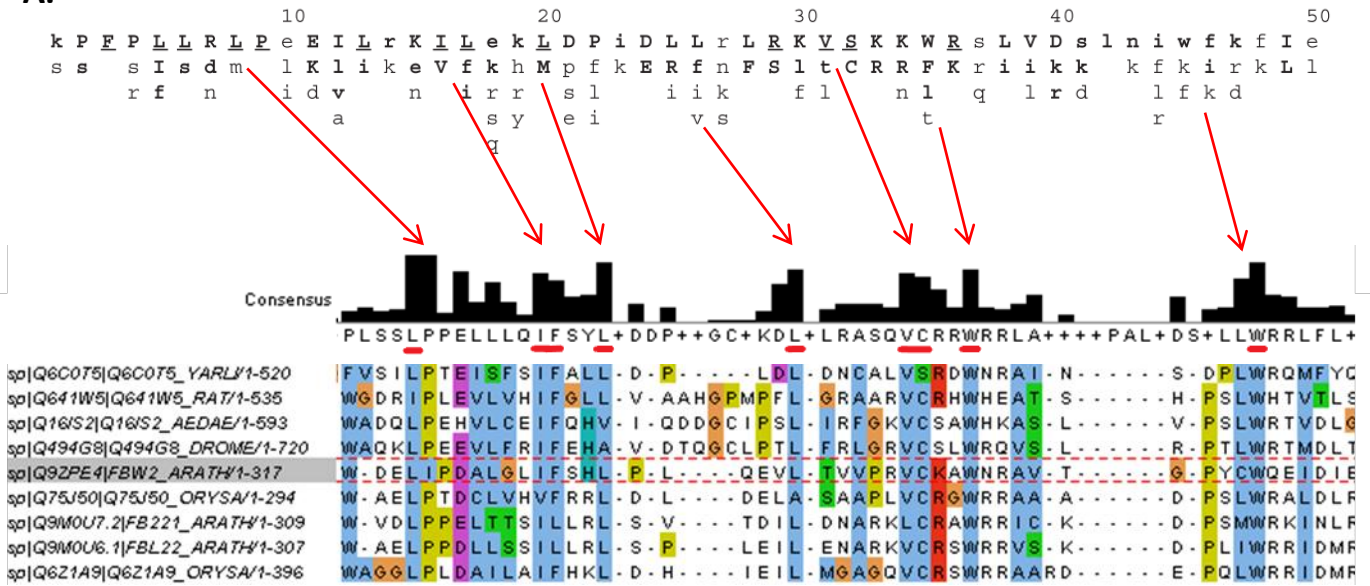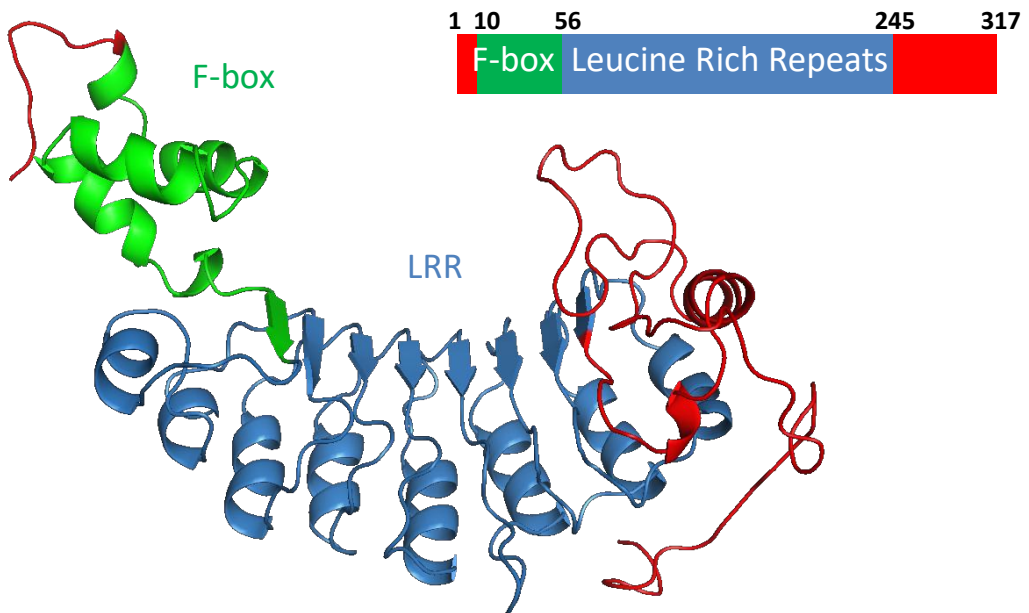
Figure 18 : FBW2 structure and F-box conservation

A. Top : consensus sequence of the F-box motif as published by Kipreos and Pagano., 2000. Residues conserved in over 40% of the F-box sequences are in bold and underlined capital letters, 20-40% in bold and non-underlined capital letters, 15-19% in bold lower case letters and 10-14% in non-bold lower case letters.

Bottom : Clustal Omega alignment of FBW2 with the 76 representative proteins of the F-box-like family (pfam12937) to whom it belongs. Conserved amino acids with hydrophobic side chains are in blue, positively charged in red, negatively charged in magenta, polar in green, aromatic in cyan, cysteines are in pink, prolines in yellow and glycines in orange.

Red arrows show correspondences between the F-box consensus sequence and the F-box-like consensus sequence. Conserved FBW2 amino acids are underlined in red.

B. Prediction of FBW2 3D structure by PHYRE2 (Kelly et al., 2015). The sequence from residue 8 to 248 is structured with a high confidence (99.9%) from other known structures of F-box protein such as Human SKP2. The F-box domain is indicated in green and the leucine-rich repeats (LRR) in blue. In red at the N-terminal and C-terminal ends are regions that could not be structured by prediction.
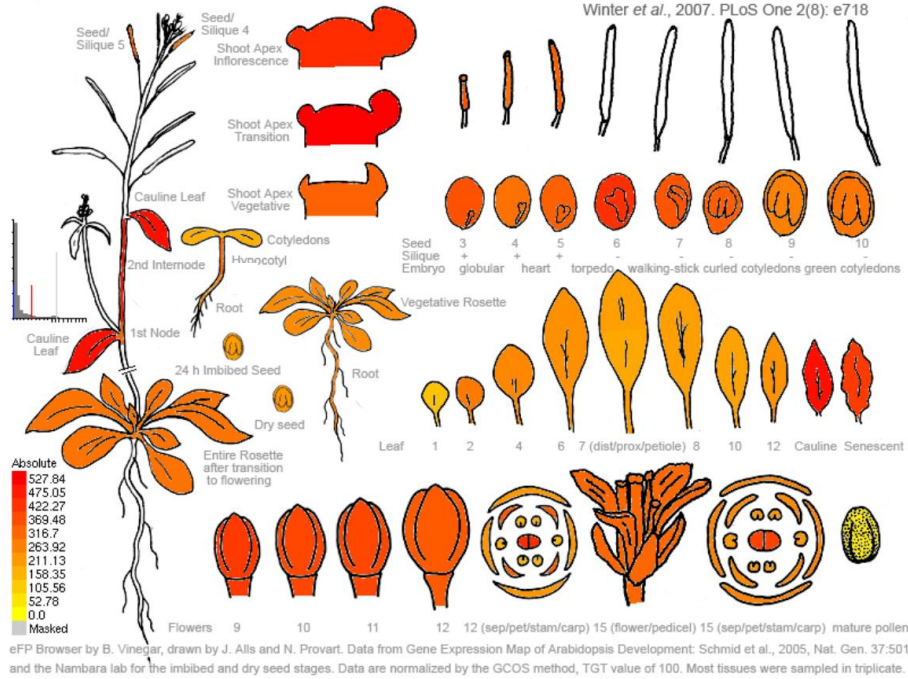
Figure 19 : eFP browser view of FBW2 expression during Arabidopsis development

Transcriptomic data from the Arabidopsis eFP Browser (Winter et al., 2007). The expression level was measured by Schmid et al., 2005 and the Nambara laboratory for seed stages. The absolute level of expression is indicated by colors ranging from yellow (no expression) to red (strong expression) as indicated on the bottom left corner.
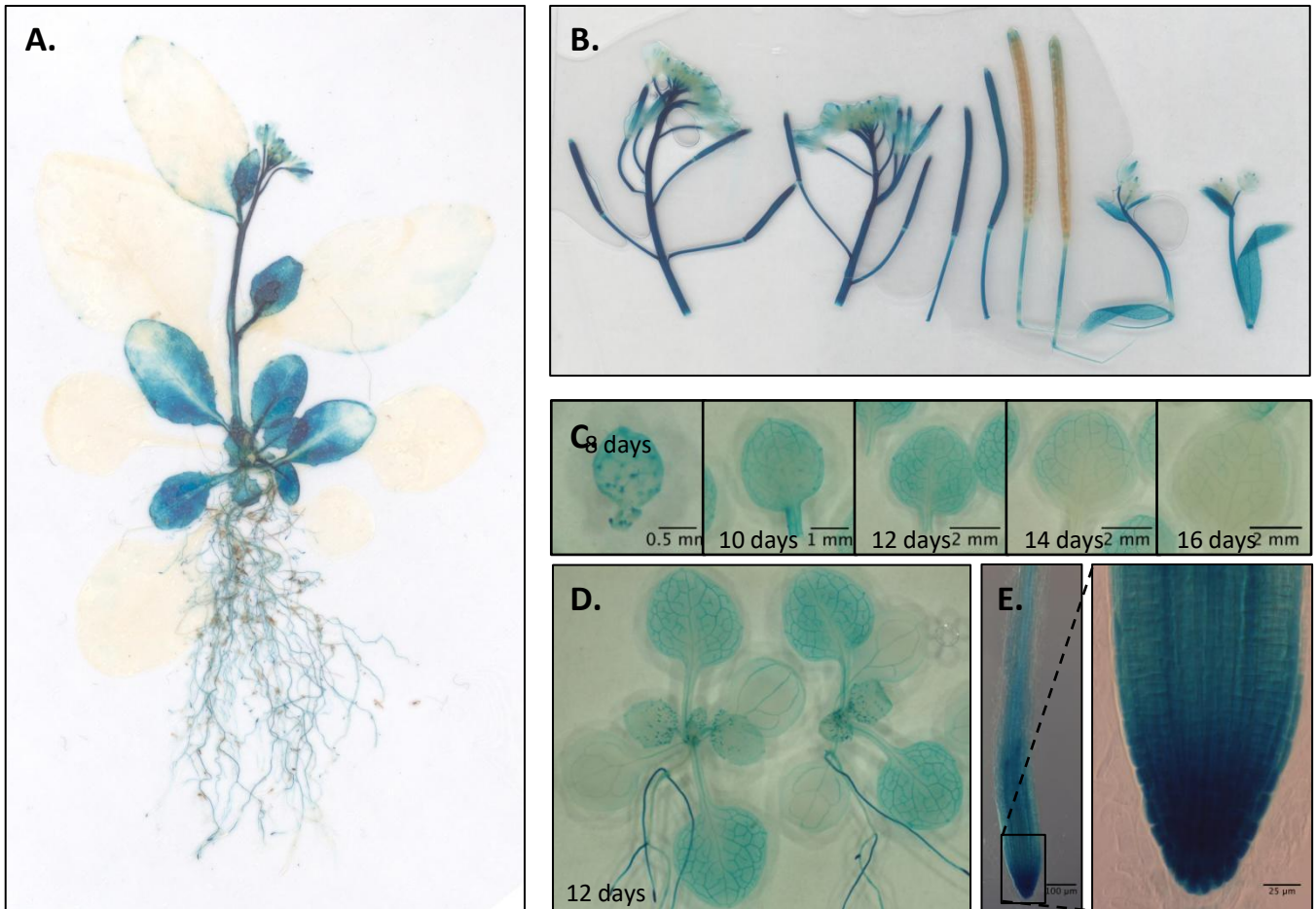
Figure 20 : Promoter-GUS analysis of *FBW2* expression

Analysis of FBW2 promoter-GUS lines showed *GUS* expression in
A. Young tissues of 40 days old plants.
B. Floral organs of 2 months old plants.
C. Trichomes and vascular tissues of leaf one and leaf two (8 to 16 days old plantlets).
D. Root vascular tissues and meristems.

2.1.1 *FBW2* expression and subcellular localization

Studying *FBW2* expression pattern and intracellular localization could give important insights concerning the function of the protein. For instance, an activity restricted to some organs or association to specific cell compartments could provide information to orient further research. Here, a promoter trap approach with the *β-glucuronidase (GUS)* reporter gene and fusion of FBW2 to different fluorescent proteins were used to answer these questions.

- Promoter activity

In silico data from the eFP browser suggest a ubiquitous expression of *FBW2* in different plant organs (Figure 19). This data also indicated that *FBW2* expression is in general insensitive to hormones or stresses (Supplementary Figures 1, 2 and 3). In order to complete these data that were generated by analysing different transcriptomics datasets, a promoter region of FBW2 including the 5'-UTR (2 kb upstream of the start codon) was cloned and inserted upstream of the *β-glucuronidase* (*GUS*) reporter gene in the plasmid pGWB633. This plasmid has already been used to study the promoter of another Arabidopsis F-box gene; *FBL3* (Nakamura et al., 2010) and also successfully used to assess the activity of various promoter sequences in *Nicotinana benthamiana* agro-infiltration assays (Bossi et al., 2017).

In total, 18 stable lines harbouring this construct (pFBW2:GUS) were generated. Among them, 5 lines with single insertion of the transgene were selected, and comparable results were obtained for 4 of them (T3) upon GUS staining. The analysis of these lines showed GUS activity in the trichomes of young leaves and in the vascular tissues of growing leaves, but the staining disappeared as leaves get older (Figure 20). In roots, the GUS activity is restrained to the vasculature, except in the meristem, where the staining is more intense and dispersed. The flowers are not stained except for the stigmas. We also observed that young siliques are well-coloured until they mature, but further reveal uncoloured seeds. Overall, our data obtained with the pFBW2:GUS lines are in agreement with the *in silico* data (Figure 19) ; FBW2 is ubiquitously expressed.
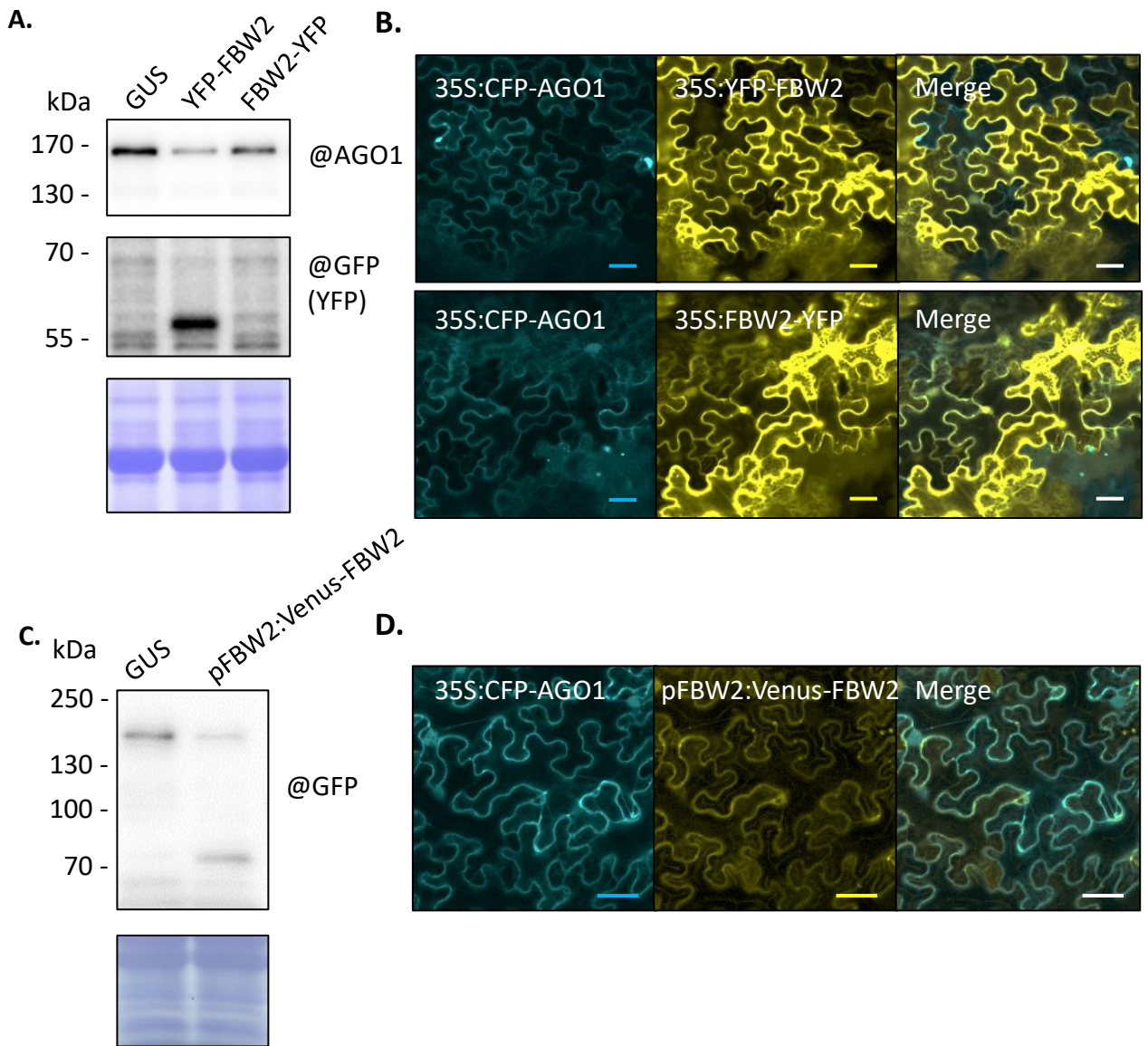
Figure 21 : Transient expression of fluorescent-tagged FBW2

Co-infiltration of four week-old *Nicotiana benthamiana* leaves with *Agrobacteria* harbouring binary vectors for the expression of fluorescent-tagged protein constructs. Bacteria were infiltrated at an OD of 0,1. Pictures were taken and tissues were sampled 3 days later.

A. Western blot of protein extracts from agroinfiltrated leaves with 35S::CFP-AGO1 and 35S::YFP-FBW2 constructs. Expression of GUS serves as negative control. Coomassie blue staining was used as a loading control. "@" indicates hybridization with the corresponding antibody.

B. Subcellular localization of CFP-AGO1 and YFP-FBW2 by confocal microscopy. CFP and YFP were excited at 458 and 514 nm, respectively. Emission signals were recovered between 465 and 510 nm for the CFP and 520 and 596 nm for the YFP. (Scale bars: 40 µm)

C. Western blot of protein extracts from agroinfiltrated leaves with 35S::CFP-AGO1 and pFBW2::Venus-FBW2 constructs. Expression of GUS serves as negative control. Coomassie blue staining was used as a loading control. "@" indicates hybridization with antibody.

D. Subcellular localization of CFP-AGO1 and Venus-FBW2 by confocal microscopy. CFP and Venus were excited at 458 and 514 nm, respectively. Emission signals were recovered between 465 and 510 nm for the CFP and 520 and 596 nm for the Venus. (Scale bars: 40 µm)

These observations also suggest that the *FBW2* promoter is mainly active in vascular and in young and dividing tissues. However, since the GUS staining revealed blue-saturated tissues already after one hour of staining, one can assume that the *FBW2* promoter is very strong in these tissues, but might still be fairly active also in other tissues, not clearly stained after 1 hour. Indeed, some promoters require more than 10 hours of staining treatment to reveal the GUS activity. Prolonging the GUS staining treatment with these pFBW2:GUS lines showed an extensive staining of all tissues of the plants (not shown), which could correspond to a weaker promoter activity in some tissues, but could also simply be explained by the diffusion over time of the strong GUS staining signal. Notably, the staining pattern published with the *FBL3* promoter (Nakamura et al., 2010) is similar to the one observed with *FBW2* promoter.

- FBW2 fusion to fluorescent proteins

To investigate FBW2 protein localization at the subcellular level, the coding sequence of FBW2 was fused to fluorescent proteins for confocal microscopy imaging. Scott Poethig (University of Pennsylvania, USA) kindly provided us with 35S promoter-driven N-terminal and C-terminal fusion of FBW2 with the Yellow Fluorescent protein (YFP) (unpublished material). We first transiently expressed these constructs in *Nicotiana benthamiana* leaves. Confocal imaging of transiently transformed leaves revealed a strong signal of the FBW2 fusion proteins in the cytosol (Figure 21A). Subsequently, we aimed to verify the functionality of these fusion constructs. As it was previously described that FBW2 is likely to cause degradation of the AGO1 protein, we co-infiltrated the YFP-FBW2 constructs together with CFP-AGO1. Infiltration of GUS alone was used as a negative control. Importantly, we observed that both fusion proteins colocalize, and that the expression of the 35S:YFP-FBW2 construct was the most efficient in degrading AGO1 (Figure 21B), validating that this constructis functional in *Nicotiana benthamiana*. The 35S:FBW2-YFP was in contrast not detectable on Western blot and less efficiently destabilized AGO1 (Figure 21B). This is not surprising as it is known that F-box proteins are more stable with protein tags at their N-terminus.

A.

- quiescent centre (QC)
- cortex/endodermis initials and daughter cell
- epidermis/lateral root cap initials
- columella initials
- pericycle initials
- vasculature initials
- columella
- lateral root cap
- epidermis
- cortex ⎤
- endodermis ⎦ ground tissue
- pericycle ⎤
- vasculature ⎦ stele

B.   Relative expression level of FBW2

Relative expression level of Venus

C.

mock   MLN4924   MG132   E-64d

Figure 22 : Expression of Venus-FBW2 under pFBW2 control

Analysis of Arabidopsis lines expressing Venus-FBW2 under the control of the endogenous promoter of FBW2.

A. Cellular localization of Venus-FBW2. A scheme of the root apical meristem organization is presented on top (from Stahl and Simon, 2005), its colour code is indicated on the right. Accordingly, FBW2 is expressed in the quiescent center area and in the root cap. The Venus was excited at 514 nm. The emission signal was recovered between 520 and 600 nm.

B. RT-qPCR analysis in promFBW2::Venus-FBW2 plants. Expression level of FBW2 relative to the wild type plant Col0 is shown on top, expression level of the Venus is indicated below. The null mutant *fbw2-4* was used as control, L.8 and L.10.1 correspond to two independent transgenic lines.

C. Pharmacological treatments of pFBW2:Venus-FBW2 transgenic line. The MNL4924 (25 μM) blocks the activity of CULLIN-based E3 ubiquitin ligases. MG132 (50 μM) inhibits proteasomal degradation. E-64d (50 μM) blocks cysteine proteases involved in the autophagy and vacuolar degradation. (Scale bars: 40 μm)

Next, we aimed to observe the expression and localization of FBW2 in stable transgenic Arabidopsis lines. Therefore, the coding sequence of FBW2 was fused to the Venus fluorescent protein at its N-terminus, and put under the control of its own promoter (pFBW2:Venus-FBW2). Venus is an improved version of the YFP yellow emission protein, but with decreased sensitivity to pH and an improved maturation rate (Nagai et al., 2002). Also this construct was expressed and functional in *N. Benthamiana* leaves (Figure 21C-D) and was thus used for Arabidopsis Col-0 plant transformation. In total, 20 stable lines harbouring this construct were generated and five lines were further selected for a single insertion of the transgene and comparable results were obtained with 3 different lines in T3 subjected to confocal imaging (Figure 22A). In contrast to the promoter-GUS staining experiments and the transient expression assays, only a very weak signal, visible from 520 to 600 nm, could be recovered near the quiescent center of the root apical meristems and also in the root cap. This fluorescent signal was visible in the cytosol, likely in some nuclei, but seems also present in the vacuole of cells in the root cap. As these results were surprising, we further verified whether the transgene is expressed in our lines. RNA was extracted and primers were designed for qRT-PCR to amplify the coding region of FBW2 (revealing the expression of both the transgene and the endogenous FBW2 transcript) and the Venus sequence (revealing only the expression of the transgene). As expected, no *FBW2* expression was observed for the *fbw2-4* null allele used here as a control (Figure 22B). Expression of the transgene was clearly confirmed (Venus primers) for 2 transgenic lines selected. Note however that in these lines, the global expression of *FBW2* (transgene and endogenous) was not increased, as could have been expected upon introducing an additional copy of the gene. Next, as many F-box proteins are known to be unstable (Galan and Peter, 1999; Petroski and Deshaies, 2005), we questioned the FBW2 stability, as this may at least partially explain the low abundance of the Venus-FBW2 signal detected. Therefore, we used different chemicals commonly used to block protein degradation. We treated our pFBW2:Venus-FBW2 lines with MG132 (an inhibitor of the proteasome), MLN4924 (a drug that efficiently inhibits CULLIN neddylation) and E-64d (a cysteine protease inhibitor, blocking autophagy and vacuolar protein degradation). However, none of these treatments significantly increased the fluorescent signal or changed the expression pattern (Figure 22C).
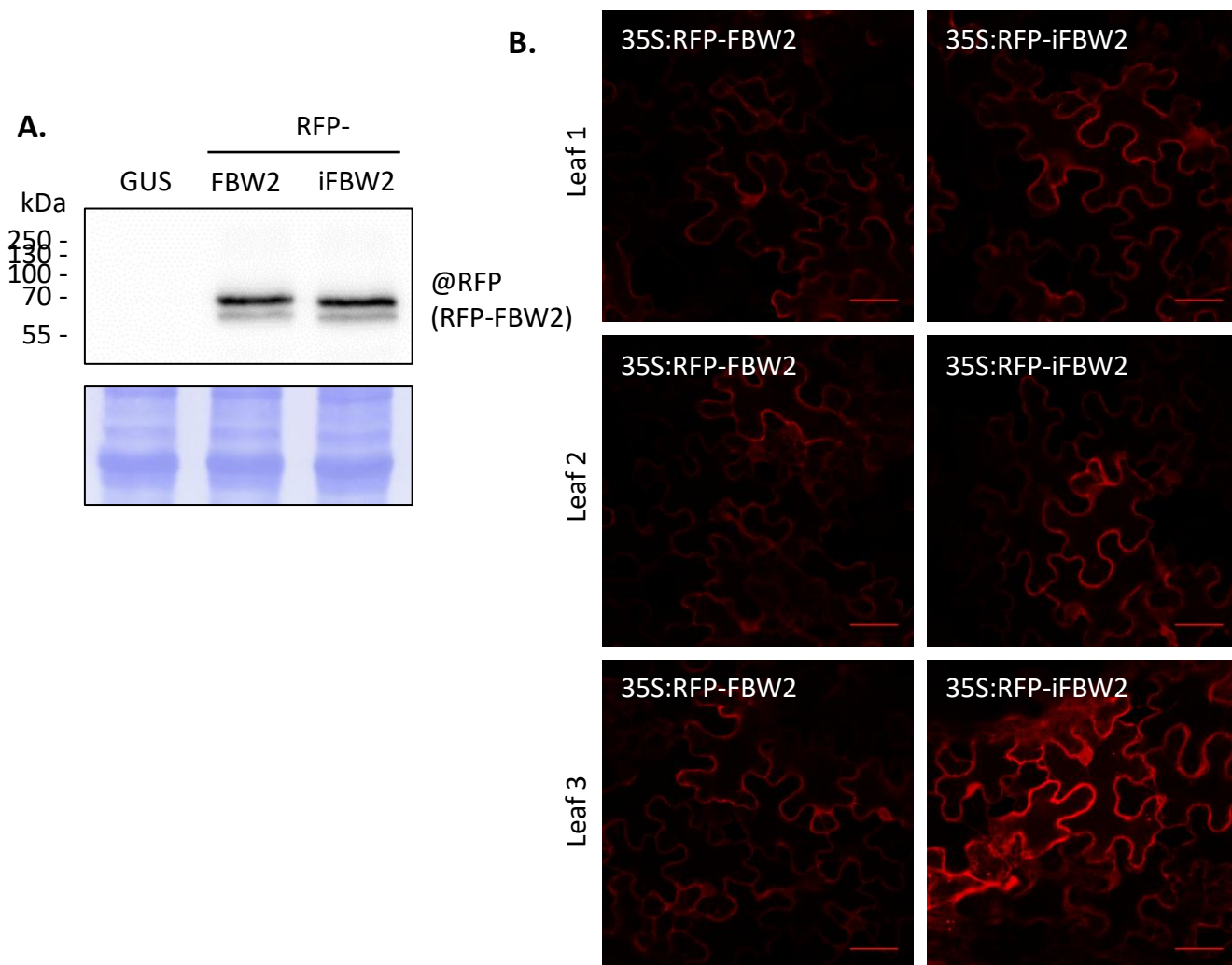
Figure 23 : Effect of the intron in the coding sequence on *FBW2* expression

Infiltration of four week-old *Nicotiana benthamiana* leaves with *Agrobacteria* harbouring binary vectors for the expression of 35S::RFP-FBW2 constructs. Bacteria were infiltrated at an OD of 0,1, pictures and tissues were sampled 3 days later. iFBW2 corresponds to the coding sequence of FBW2 with the intron.

A. Western blot of protein extracts from agroinfiltrated leaves. Expression of GUS serves as negative control. Coomassie blue staining was used as a loading control. "@" indicates hybridization with the corresponding antibody.

B. Subcellular localization of RFP-FBW2 by confocal microscopy. The RFP was excited at 561 nm. The emission signals were recovered between 594 and 634 nm. (Scale bars: 40 μm)

Currently, the results concerning these stable pFBW2:Venus-FBW2 transgenic lines remain inconclusive. As FBW2 mutants does not present any phenotype, we could not assess whether the pFBW2:Venus-FBW2 could complement the loss of FBW2. Quenching of the Venus is unlikely because the GateWay recombination sequence produces a linker that separates the Venus from FBW2. It is possible that the chemicals that we used were inefficient in stabilizing the fusion protein. Bortezomib, which is an improved version of MG132 (Goldberg, 2012), and other drugs blocking protein degradation, could still be used in the future. More results on the turnover of the FBW2 protein will be presented in another section of the Thesis manuscript.

- Importance of the intron

As we encoutered these problems when expressing the coding sequence of FBW2, we next considered cloning of the genomic sequence of FBW2, including the intron, as was also done in the previous work by Scott Poethig. Indeed, as observed for some genes, introns can contain regulatory elements improving their expression (Emami et al., 2013; Gallegos and Rose, 2015). We transiently expressed in *Nicotiana benthamiana* the FBW2 sequence, with or without the intron, fused to the Red Fluorescent Protein (RFP) under the control of the 35S promoter. Because these assays can show variations in transient gene expression depending on the age of the plants or the developmental stage of the leaf, all constructs were expressed side by side on the same leaf for optimal comparison.

As with the YFP fusions, the RFP-FBW2 signal was detectable in the cytoplasm and nucleus of transformed cells. The expression of the fusion protein was also confirmed by Western blot. (Figure 23A). The fluorescence appeared reproducibly stronger in cells transformed with the *FBW2* version containing the intron compared to the one transformed with only the coding sequence (Figure 23B). The intron seems thus likely to play a regulatory function for *FBW2* expression. Stable Arabidopsis lines have now been produced in order to study the intron effect in a more robust way, but have not yet been analysed.
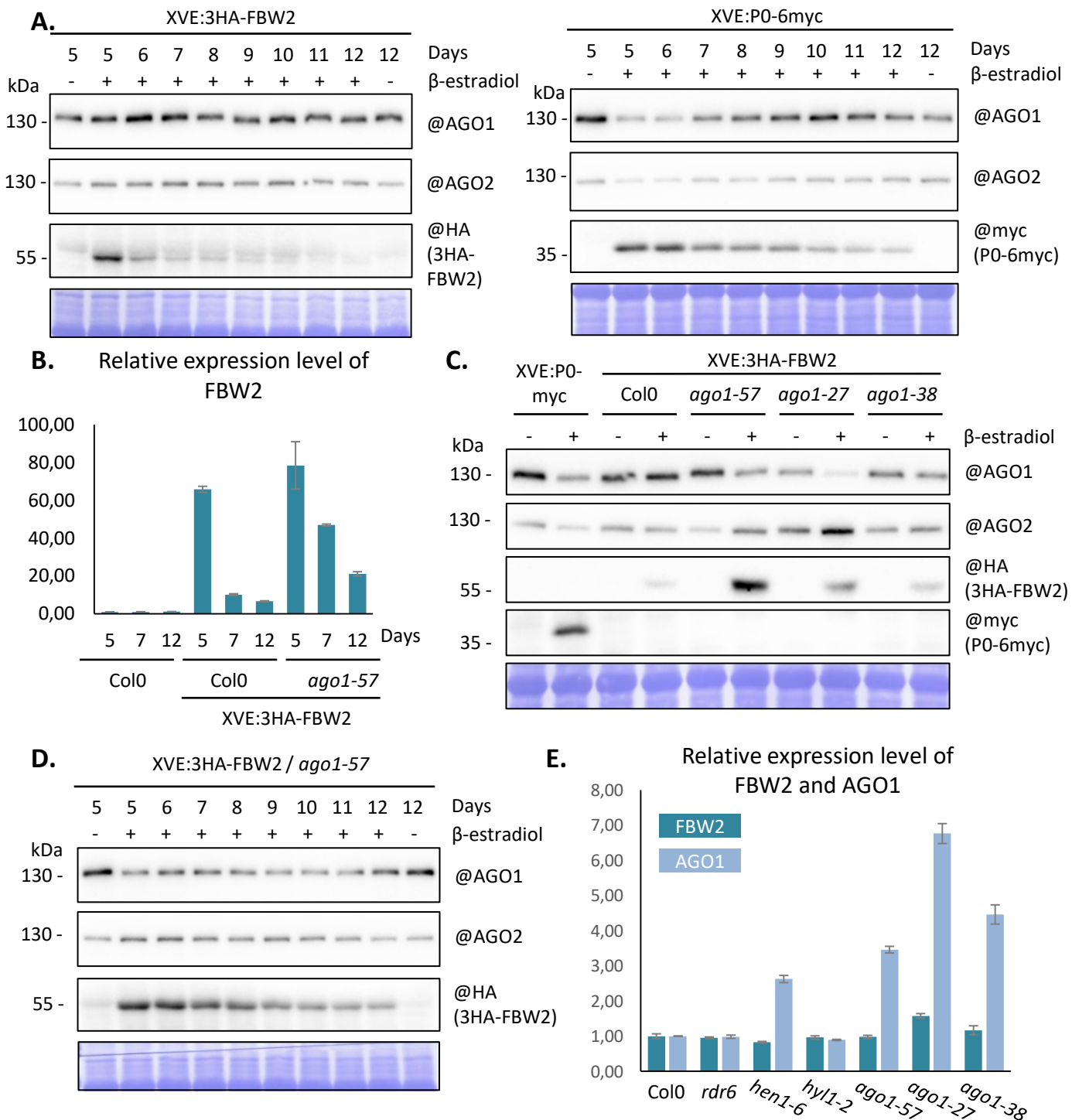
Figure 24 : Kinetic induction of FBW2

Induction of 3HA-FBW2 construct under the control of the β-estradiol inducible promoter XVE (Zuo et al., 2000). For all western blot Coomassie blue staining was used as a loading control and "@" indicates hybridization with antibody. The XVE:P0-myc line was established in Derrien et al., 2012.

A. and D. Western blots of protein extracts from 5 to 12 day-old seedlings of the specified transgenic plants grown on MS medium supplemented with DMSO (-) or β-estradiol (10 µM) (+).

B. RT-qPCR analysis of *FBW2* expression level, relative to the 5 day-old Col-0, in seedlings grown on MS medium supplemented with β-estradiol (10 µM).

C. Western blot of protein extracts from 7 day-old seedlings XVE-P0-myc and XVE::3HA-FBW2 crossed with the specified AGO1 mutants and grown on MS medium supplemented with DMSO (-) or β-estradiol (10 µM) (+).

E. RT-qPCR analysis of *FBW2* expression level relative Col-0 in seedlings of the specified mutants grown on MS medium.

2.1.2 Silencing of the FBW2 transgene

As shown above, we were unsuccessful in properly expressing *FBW2* in stable lines with the endogenous promoter, and we thus tried several attempts to obtain transgenic Arabidopsis lines expressing a robust amount of FBW2 protein. Most of these lines did not include the intron sequence, as we were not aware of its regulatory function when they were generated. Thus, we first generated transgenic Arabidopsis lines containing the *FBW2* coding sequence fused at its N-terminus to a (3x) Human influenza Hemagglutinin (HA) tag under the control a β-estradiol-inducible 35S minimal promoter (XVE:3HA-FBW2). This system was already successfully used in the laboratory to express the viral F-box protein P0, which also targets AGO1 for degradation (Derrien et al., 2012, 2018). In total, 65 stable lines harbouring this construct (XVE:3HA-FBW2) were generated. Among them, seven lines were further selected for high expression upon β-estradiol induction without leakage (Supplementary Figure 4).

To test the functionality of this line (XVE:3HA-FBW2), we monitored the activity of FBW2 on AGO1 protein level in a kinetic experiment where FBW2 was induced over time. The plants harbouring the inducible construct were grown for 12 days on medium containing β-estradiol (Figure 24A). The Western blot of protein extracts shows that FBW2 was nicely induced at the start of the kinetic but, surprisingly, quickly disappeared over time. The AGO1 protein level is not affected in this experiment, but in others AGO1 show a weak decrease (Supplementary Figure 5). As a control, we performed a similar kinetic experiment with the XVE:P0-6myc line (Derrien et al., 2012), which showed a constant expression over time of P0-myc and reproducible degradation of AGO1 and AGO2. The expression system is thus suitable to generate the line we aim, but it is unclear why the FBW2 protein level is decreasing after the initial accumulation.

To explain such a transient expression of FBW2, we first checked its transcript level at different time points by qRT-PCR. Hence, the *FBW2* transcript level quickly dropped after β-estradiol induction (Figure 24B), suggesting that it is silenced. Notably, this was not the case for the XVE:P0-6myc line.

If silencing of the transgene limits *FBW2* expression in our system, we reasoned that introgressing the construct in *ago1* mutants or other mutants affected in PTGS would counteract this effect. Thus, the XVE:3HA-FBW2 line was crossed with *ago1-27* (Brodersen et al., 2008), *ago1-38* (Brodersen et al., 2012) and *ago1-57* (Derrien et al., 2018). Interestingly, in most of these lines the expression level of *FBW2* was increased, confirming the hypothesis that the *FBW2* was silenced. Moreover, in these mutant backgrounds, a significant decay of AGO1 was observed upon induction of the FBW2 expression (Figure 24C). To further explore this in more detail, we conducted a kinetic experiment inducing *FBW2* in the *ago1-57* background. This showed that FBW2 protein accumulates for a longer period of time and AGO1 destabilization was clearer in this genetic background (Figure 24D). Consistent with this observation, qPCR analysis of *FBW2* expression showed that, in contrast to the Col-0 background, the transcript level of *FBW2* decreased less over time in *ago1-57* (Figure 24B). Based on these experiments, we conclude that the *FBW2* transgene can be subjected to silencing, and that expressing it in a *ago1* mutant background provides a good tool for studying FBW2 in relation to AGO1 protein degradation.

Finally, we wondered whether the endogenous *FBW2* gene is also subjected to such a regulation. We analysed its expression level in different silencing mutant backgrounds, but none of them showed a significant increase in *FBW2* expression (Figure 24E). Thus, the reduction of *FBW2* expression is most likely due to silencing of the transgene but not of endogenous *FBW2* transcripts.

A. 35S:3HA-FBW2

	10.3	7.10	8.6	21.5
kDa				

130 - @ AGO1

55 - @ HA (3HA-FBW2)

B.

C.

GUS P0 FBW2 3HA-FBW2

kDa
130 - @AGO1
100 -
55 - @HA (3HA-FBW2)
40 -
35 -

Relative expression level of FBW2
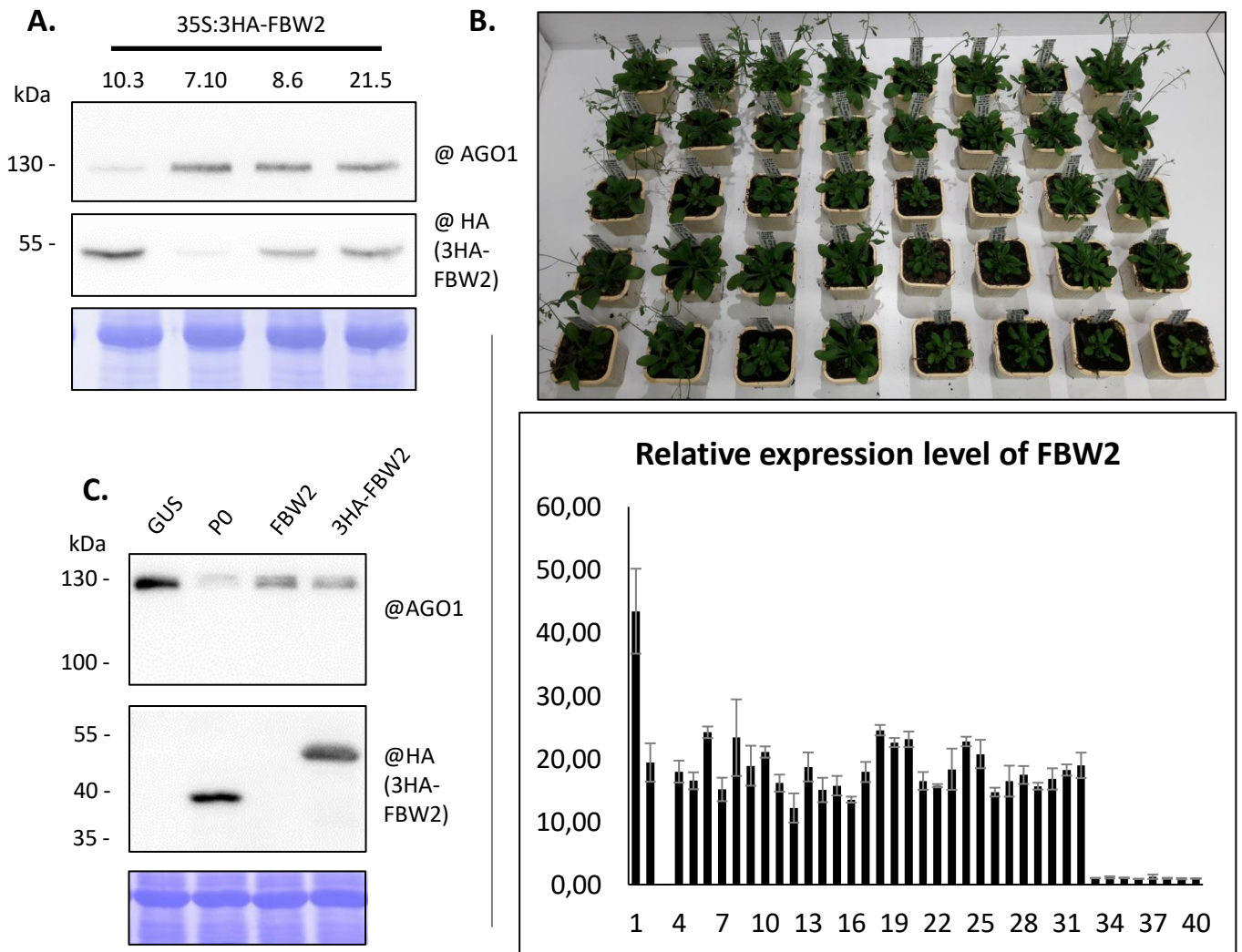
Figure 25 : Constitutive overexpression of FBW2

Analysis of 35S:3HA-FBW2 and 35S:FBW2 constructs.

A. Western blot of protein extracts from 7 day-old seedlings grown on MS medium. Four independent homozygous and single insertion 35S:3HA-FBW2 transgenic lines are presented. Coomassie blue staining was used as a loading control. "@" indicates hybridization with the corresponding antibody.

B. Top : Picture of 40 days old 35S:FBW2 transformants selected on MS medium supplemented with Basta and transferred in soil. The plants are ordered from the healthiest to the sickest from left to right and top to bottom.
Bottom : RT-qPCR analysis of FBW2 expression in these plants. The measures are relative to the plant #40.

C. Western blot of protein extracts from four week-old *Nicotiana benthamiana* agroinfiltrated leaves. Agrobacteria harbouring the indicated constructs were infiltrated at an OD of 0,3 and tissues were sampled 3 days later. Expression of GUS serves as control. Coomassie blue staining was used as a loading control. "@" indicates hybridization with the corresponding antibody.

2.1.3 FBW2 is an unstable F-box protein that is degraded by the proteasome

In order to further study the FBW2 protein while circumventing the silencing problems caused by the inducible system, we subsequently engineered plants constitutively overexpressing *FBW2*. The same 3HA-FBW2 construct was put under the control of the Cauliflower mosaic virus (CaMV) 35S promoter and transformed in Arabidopsis (Col-0). At first, 60 stable lines harbouring this construct (35S:3HA-FBW2) were generated, out of which nine lines were further selected for single insertion and only four of them showed robust expression of the transgene (Figure 25A). Surprisingly, these plants did not exhibit the published strong developmental defects, described earlier for strong expression of *FBW2* (Earley et al., 2010). In this publication, the construct used for FBW2 protein overexpression was untagged. To rule out a possible hindrance caused by the 3HA tag, we also generated transgenic Arabidopsis lines using the untagged FBW2 CDS (35S:FBW2). Around 40 stable lines harbouring the 35S:FBW2 construct were generated and the transgene expression was analyzed in T1 by qPCR (Figure 25B). However, none of these lines, even the ones highly expressing *FBW2*, showed important developmental defects. It should also be noted that both 35S:3HA-FBW2 and 35S:FBW2 constructs were verified in transient expression in *Nicotiana benthamiana*, and showed similar effects on AGO1 levels (Figure 25C). Thus, the presence of the 3HA-tag was not the cause of the absence of strong phenotype and the discrepancy with the results of Earley et al. (2010) still remain unclear. As both lines are likely functionally equivalent, all further described analyses were performed on the line with the tagged version of FBW2, as it offers more advantages for molecular characterization of the FBW2 protein.

In our kinetic assays, the quick disappearance of the FBW2 protein cannot only be explained by silencing of the transgene, but instead also suggests a short half-life of the protein. To investigate the FBW2 protein stability, the 35S:3HA-FBW2 line (line 10) was treated with cycloheximide (CHX), which blocks the translation of proteins, and the FBW2 protein level was monitored over time. FBW2 quickly disappeared upon CHX treatment (Figure 26A), while the AGO1 protein did not seem
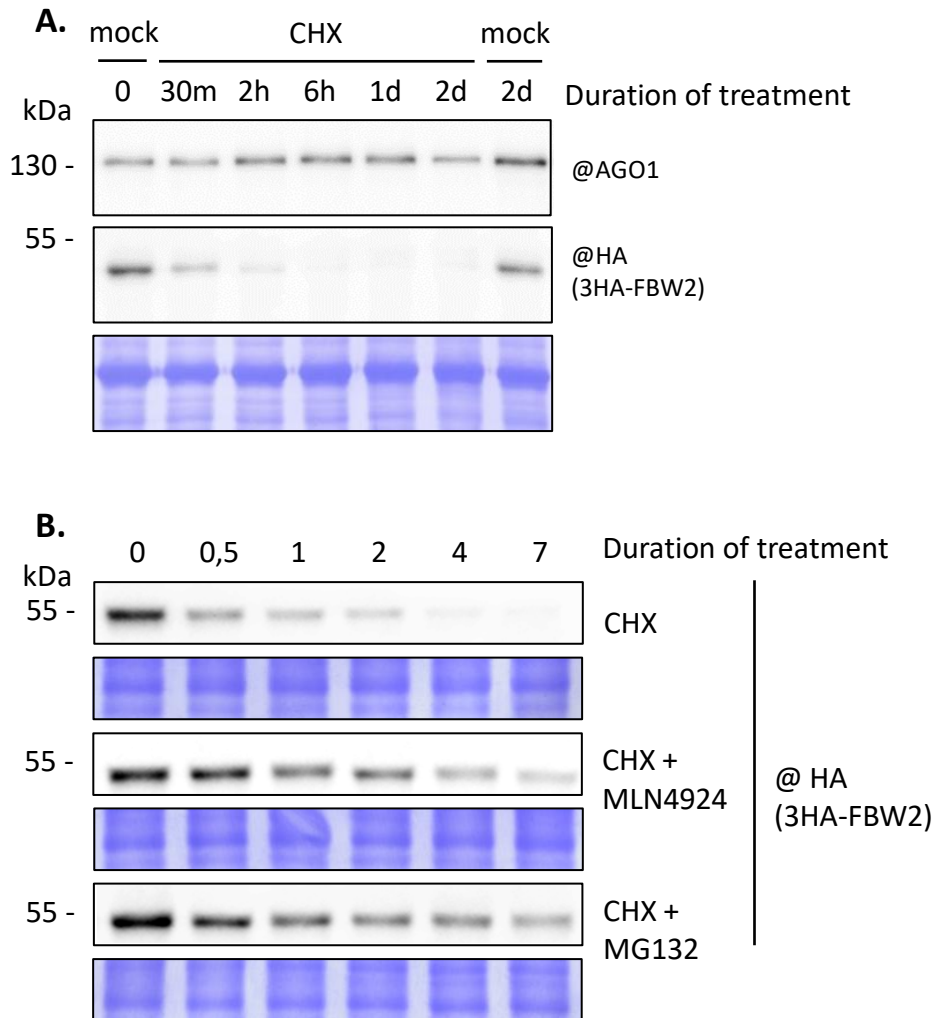
Figure 26 : FBW2 protein stability

Half-life measurements of FBW2 in 35S:3HA-FBW2 seedlings treated with cycloheximide (CHX). CHX blocks the translation of proteins.

A. Western blot of protein extracts from 10 day-old seedlings either mock (DMSO) or cycloheximide (100 µM) treated. Coomassie blue staining was used as a loading control. "@" indicates hybridization with the corresponding antibody

B. Western blot of protein extracts from 10 days old seedlings treated with cycloheximide (100 µM) plus MLN4924 (25 µM) or MG132 (100 µM). MNL4924 blocks the activity of CRL-based E3 ubiquitin ligases. MG132 inhibits proteasomal degradation. Coomassie blue staining was used as a loading control. "@" indicates hybridization with the corresponding antibody

affected, even after two days of treatment, which is consistent with published data (Csorba et al., 2010). This and further experiments allowed us to estimate the half-life of the FBW2 proteins to be less than 30 minutes. It has previously been shown that several F-box proteins are unstable and often regulated by the ubiquitin-proteasome system (Galan and Peter, 1999; Petroski and Deshaies, 2005). We therefore repeated these experiments by combining CHX with MNL4924 or Mg132. Both drugs efficiently reduced FBW2 protein decay in this assay, indicating that the FBW2 protein is itself a target of the ubiquitin-proteasome machinery (Figure 26B).
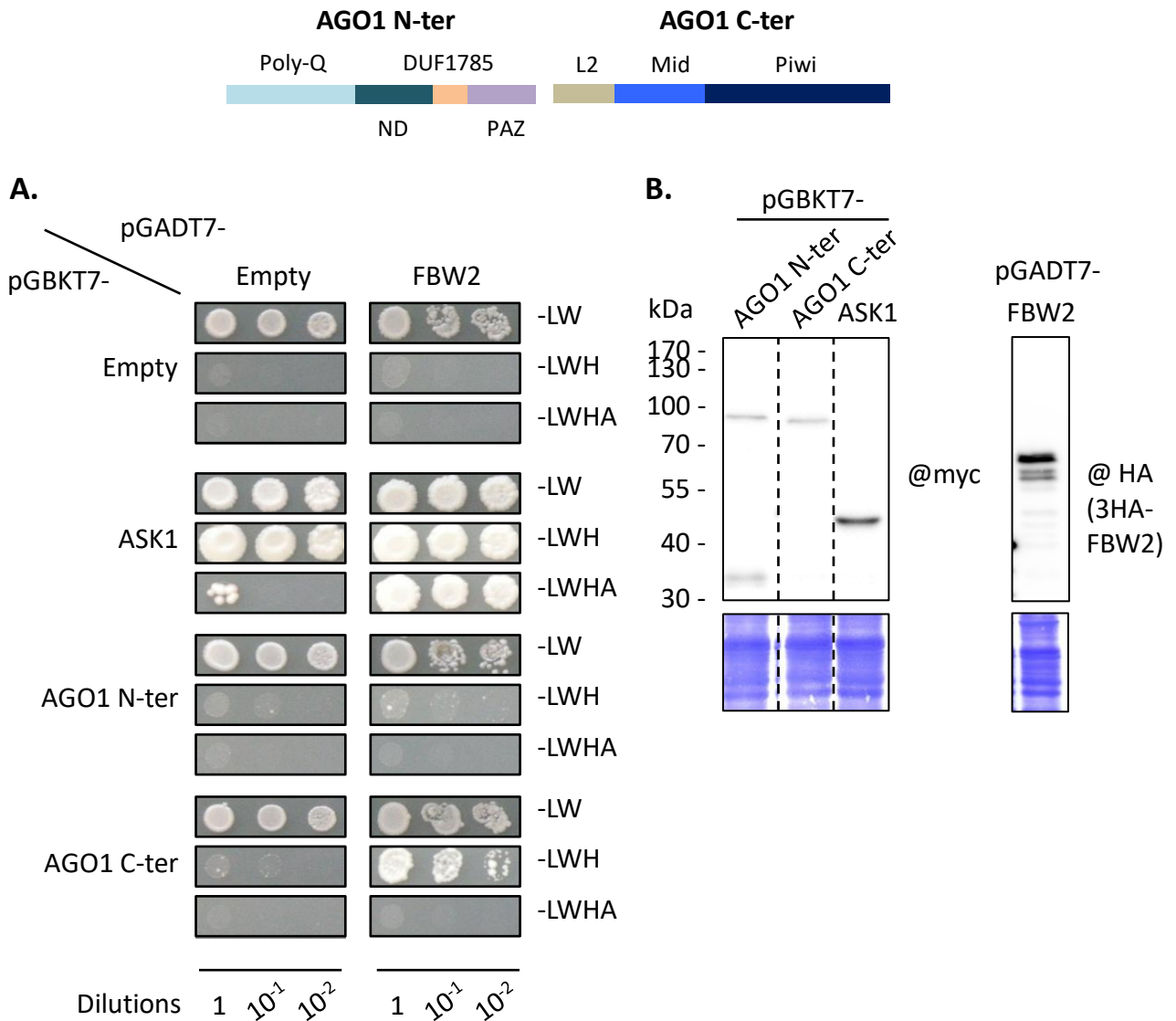
Figure 27 : FBW2 Yeast Two-Hybrid interactions

Yeast two-hybrid interaction assays between FBW2 and AGO1 fragments (schematic representation shown on the top. ASK1 serves as positive control. Yeast cells were grown for 15 days at 28°C on selective plates lacking leucine and tryptophan (-L-W) or also lacking histidine and adenine (-H-A).

A. Pictures of yeast colonies growing on the selective media.
B. Western blot of protein extracts from yeast parental lines. Coomassie blue staining was used as a loading control. "@" indicates hybridization with the corresponding antibody. Expected sizes for the proteins are 77 kDa for AGO1 N-ter, 83 kDa for AGO1 C-ter, 40 kDa for ASK1 and 56 kDa for FBW2.

2.1.4 FBW2 is part of an SCF complex and physically interacts with AGO1

As an F-box protein, FBW2 is supposed to directly interact with an Arabidopsis SKP1-like (ASK1) protein, acting as an adaptor, and to be part of an SCF complex containing also CULLIN1 and RBX1. Moreover, if AGO1 would be a direct substrate of FBW2, one may also expect to see both proteins interacting. These putative protein interactions were investigated by yeast two hybrid and co-immunoprecipitation assays.

- Yeast two hybrid interactions

A classical experiment to test the interaction between two proteins is the yeast-two-hybrid assay. To perform these assays, FBW2 was fused at its N-terminus with the GAL4 activation domain (AD) and the coding sequence of putative interactors were fused at their N-terminus with the GAL4 binding domain (BD). Yeast cells transformed with these constructs were mixed to form mating groups and tested on selective media (Figure 27A). Unfortunately, the AGO1 full-length protein was only very poorly expressed in this system, and therefore we decided to express the N-terminal (AGO1 N-ter) and C-terminal (AGO1 C-ter) halves of AGO1 separately. All constructs were correctly expressed in yeast cells, as shown by Western blot (Figure 27B). Yeast colonies grew efficiently on the most selective media (-LWHA) when AD-FBW2 transformed cells are mated with BD-ASK1, as previously published (Risseeuw et al., 2003). In contrast to the strong interaction with ASK1, FBW2 was able to interact only with the AGO1 C-terminal domain on the –LWH medium. This interaction was clearly visible after 15 days of incubation and absent in the control condition, it can therefore be considered as real, but weak. From these assays in yeast, we could confirm that FBW2 interacts strongly with ASK1 and that FBW2 also interacts with the C-terminal part of AGO1.
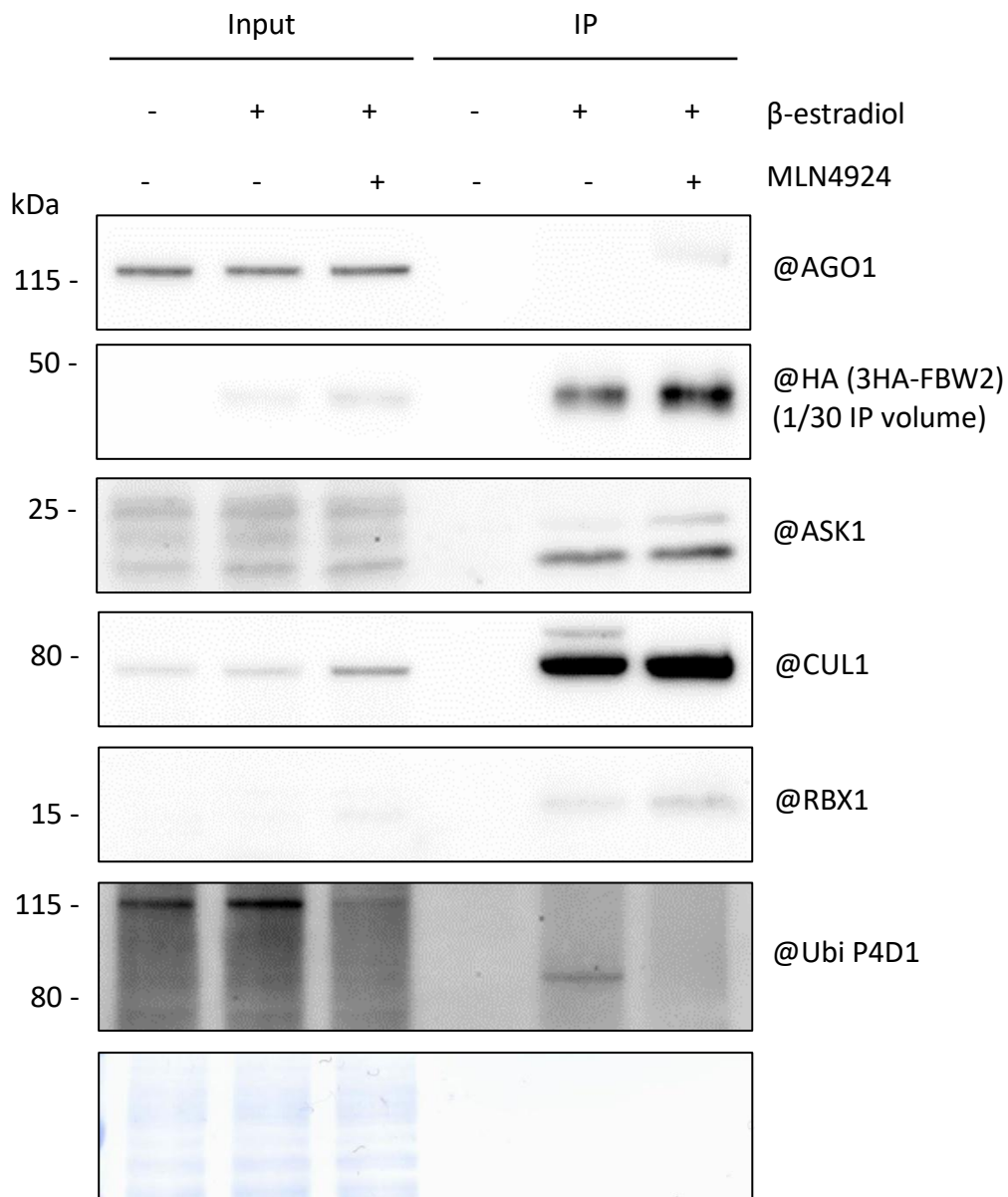
Figure 28 : Immunoprecipitation of FBW2

Western blot of protein extracts from 10 day-old seedlings. 3HA-FBW2 was immunoprecipitated with anti-HA antibodies after an overnight induction of expression in liquid MS medium supplemented with DMSO (-) or β-estradiol (10 µM) (+). 3HA-FBW2 co-immunoprecipitates with the SCF components ASK1, CUL1 and RBX1. Blocking the SCF activity with the drug MLN4924 further allows co-immunoprecipitation of AGO1. Reduced overall ubiquitination by MLN4924 is visible with the antibody P4D1 directed against ubiquitin. Coomassie blue staining was used as a loading control. "@" indicates hybridization with the corresponding antibody.

- Co-immunoprecipitation

In order to study the identified interactions with FBW2 *in planta*, we used the XVE:3HA-FBW2 transgenic line previously reported. Upon β-estradiol induction, FBW2 was induced and could be efficiently immunoprecipitated using anti-HA beads (Figure 28). We could also show that ASK1 nicely co-immunoprecipitated with 3HA-FBW2, as well CUL1 and to a lesser extent RBX1. These proteins constitute the complete SCF complex and clearly confirm *in vivo* that FBW2 is part of it.

Next, we further aimed to confirmed the possible interaction between FBW2 and AGO1. Under standard condition, AGO1 could not be recovered in these FBW2 immunoprecipitation assays. Since F-box proteins trigger the degradation of their target proteins, MLN4924, a drug that inhibits CULLIN neddylation and thus SCF activity, was added in our assay (Figure 28). Indeed, preventing ubiquitination allowed us to co-immunoprecipitate AGO1 with FBW2, but less efficiently than with ASK1 or CUL1, suggesting here again that the interaction is weak or transient. It is also possible that FBW2 can only interact with a pool of AGO1 that might not be very abundant, a hypothesis that will be discussed later.
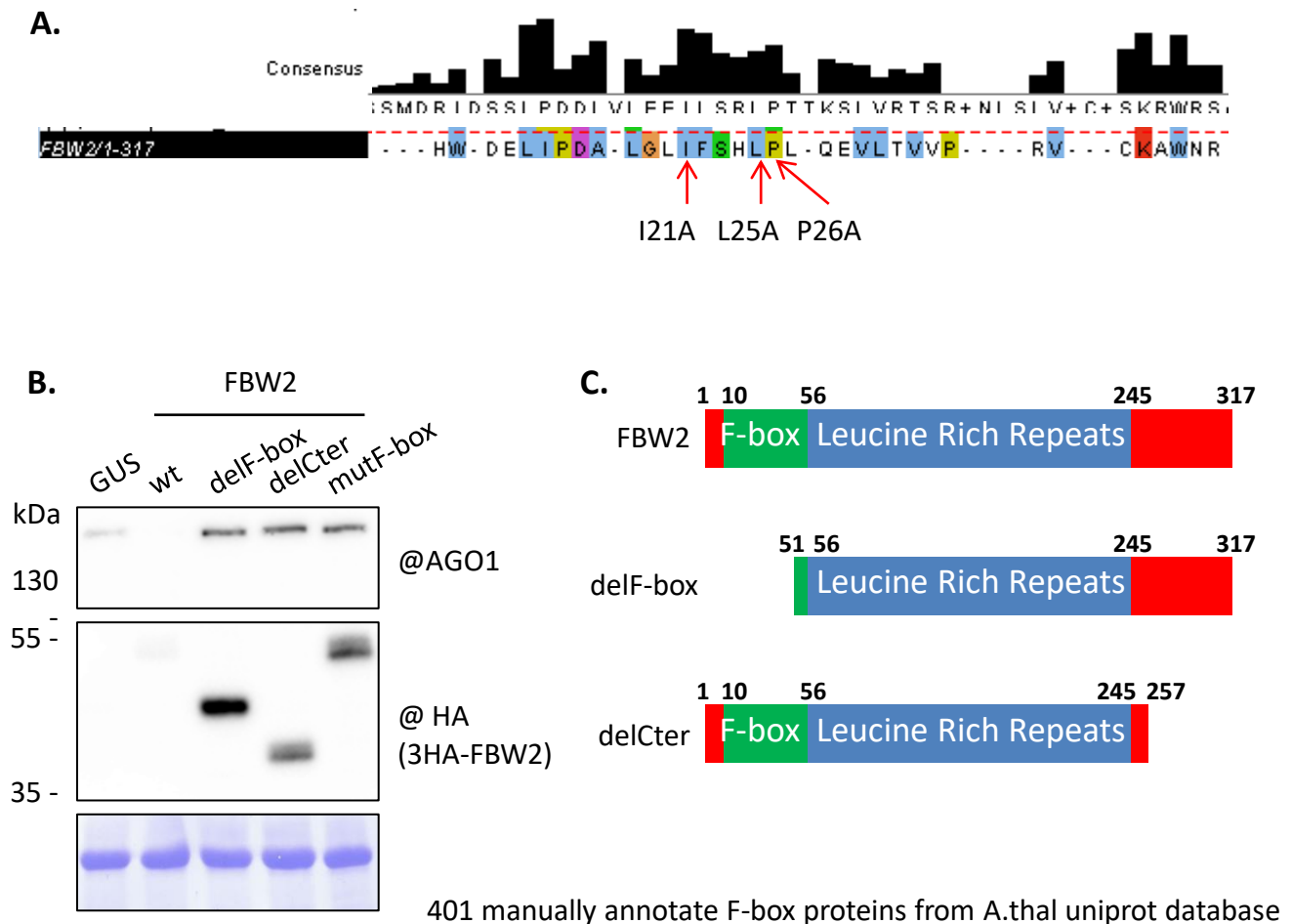
Figure 29 : FBW2 F-box mutagenesis and deletions

A. Consensus sequence of the Clustal Omega alignment of FBW2 with 401 manually annotated Arabidopsis F-box proteins from the UniProt database. Mutated amino acids in the mutF-box version of FBW2 are indicated by red arrows. Conserved amino acids with hydrophobic side chains are in blue, positively charged in red, negatively charged in magenta, polar in green, aromatic in cyan, cysteines are in pink, prolines in yellow and glycines in orange.

B. Western blot of protein extracts from four week-old *Nicotiana benthamiana* agroinfiltrated leaves. Agrobacteria harbouring a 35S:CFP-AGO1 and a 35S:3HA-FWB2 (wild type, mutant and deletions) constructs were infiltrated at an OD of 0,3 and tissues were sampled 3 days later. Expression of GUS serves as control. Coomassie blue staining was used as a loading control. "@" indicates hybridization with the corresponding antibody.

C. Scheme of the deleted version of FBW2 (see Figure 18).

- F-box mutagenesis and deletion

We next aimed to demonstrate that the FBW2 association to the SCF through its F-box is important for AGO1 degradation. Therefore, FBW2 F-box mutant and deletion constructs were engineered (Figure 29A). These FBW2 variants were fused to a 3HA tag and expressed in *Nicotinana benthamiana*. Infiltration of a construct expressing the GUS protein serves as a negative control.

Analysis of protein extracts from agro-infiltrated areas revealed that transient overexpression of AGO1 and native FBW2 produced a clear and reproducible destabilization of AGO1 (Figure 29B). Although deletion or mutation of the F-box motif resulted in higher expression levels of the FBW2 variants, compared to the native 3HA-FBW2, these proteins were unable to degrade AGO1. Therefore, interfering with the ability of FBW2 to interact with the SCF complex completely abolishes AGO1 degradation. In our assay, we also deleted the unstructured C-terminal part of FBW2 (Figure 29C). Interestingly, this domain appeared to be essential for the function of FBW2 and might be needed for the interaction with AGO1. This will be developed further in a later section of the thesis manuscript.
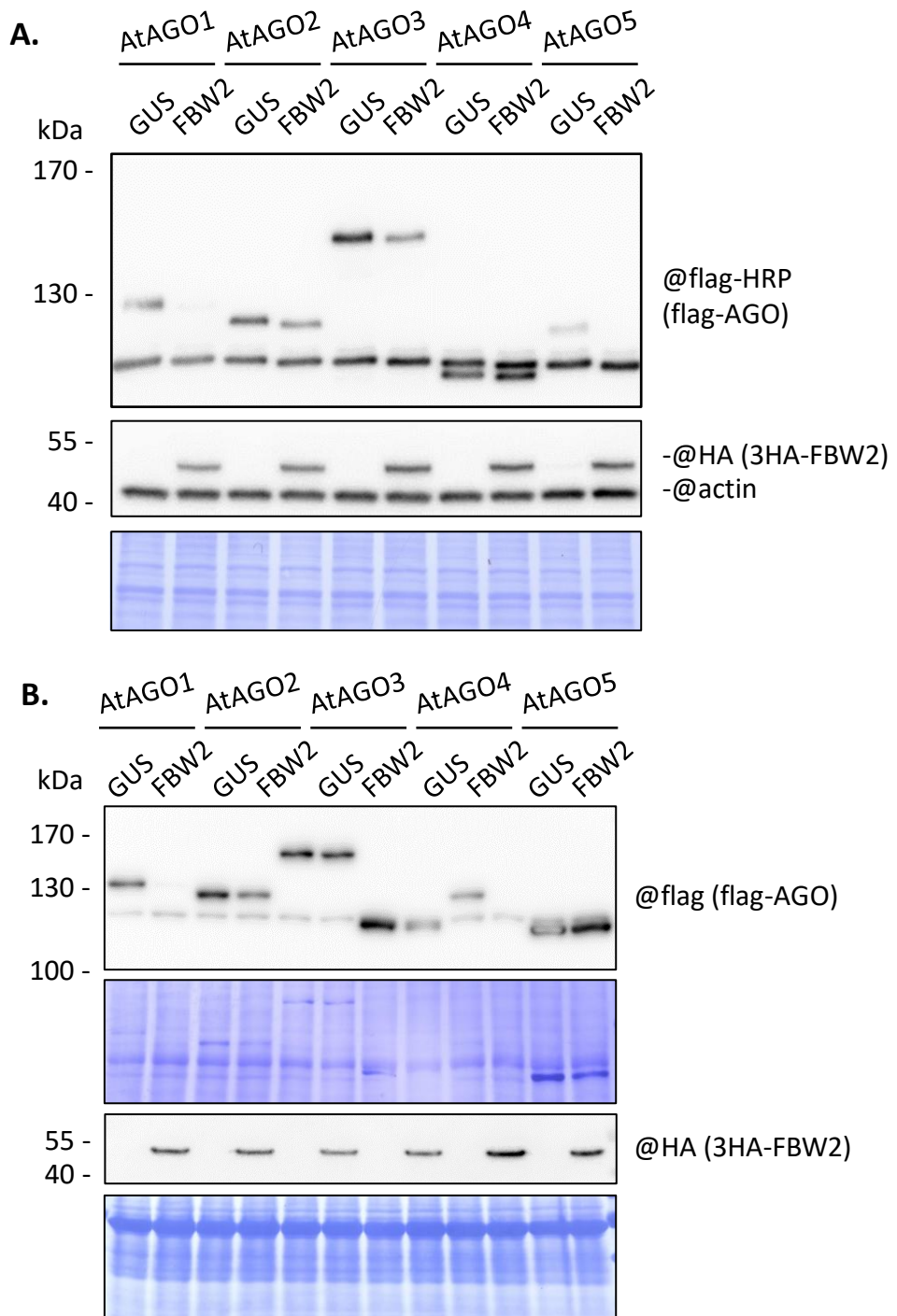
Figure 30 : Susceptibility of several Arabidopsis AGO proteins towards FBW2

A. and B. Western blot of protein extracts from four week old *Nicotiana benthamiana* agroinfiltrated leaves. Agrobacteria harbouring 35S:Flag-AGO and a 35S:3HA-FWB2 constructs were infiltrated at an OD of 0,3 and tissues were sampled 3 days later. Expression of GUS serves as control. Coomassie blue staining and actin protein level were used as loading controls. "@" indicates hybridization with the corresponding antibody.

2.2 AGO1 degradation

2.2.1 Degradation by FBW2 of AGO1 and other AGO proteins

F-box proteins are known to efficiently trigger the degradation of their targets. As shown by the above-mentioned experiments, AGO1 is presumably the target of FBW2, but since AGO proteins are well-conserved, we next wondered whether other AGOs might also be targeted.

- In *Nicotiana benthamiana*

N-terminally flag-tagged Arabidopsis AGO1, AGO2, AGO3, AGO4, AGO5 and AGO9 were agro-infiltrated in *Nicotiana benthamiana* in the absence or presence of FBW2 (or GUS as a control) and the level of each AGO protein was monitored with the FLAG antibody (Figure 30A). As expected, AGO1 was degraded by FBW2. Additionally, also AGO5 and AGO9 proteins were significantly affected. AGO2 and AGO3 were degraded to a lesser extent and AGO4 was even insensitive towards FBW2. However, these transient degradation assays showed some variations, as in another experiment AGO3 was insensitive to FBW2, whereas AGO4 showed some partial degradation (Figure 30B).

Even though the susceptibility of some AGO proteins toward FBW2 is still unclear, this experiment suggests that FBW2 is not only specific to AGO1 but has the capacity to interact with and trigger the degradation of some other AGO proteins. In particular, AGO5 belongs to the same phylogenetic clade as AGO1, suggesting that members of this clade are good substrates for FBW2. Results obtained by transient expression assays need, however, to be validated in stable transgenic Arabidopsis lines.

- In stable Arabidopsis lines

As presented previously, β-estradiol induction of *FBW2*, leads to significant decrease of AGO1 protein levels (Figure 24C). However, we noticed that under these conditions AGO2 protein level did not seem to decrease (Figure 24A and C), but instead rather slightly increased. These results were surprising, as they are in
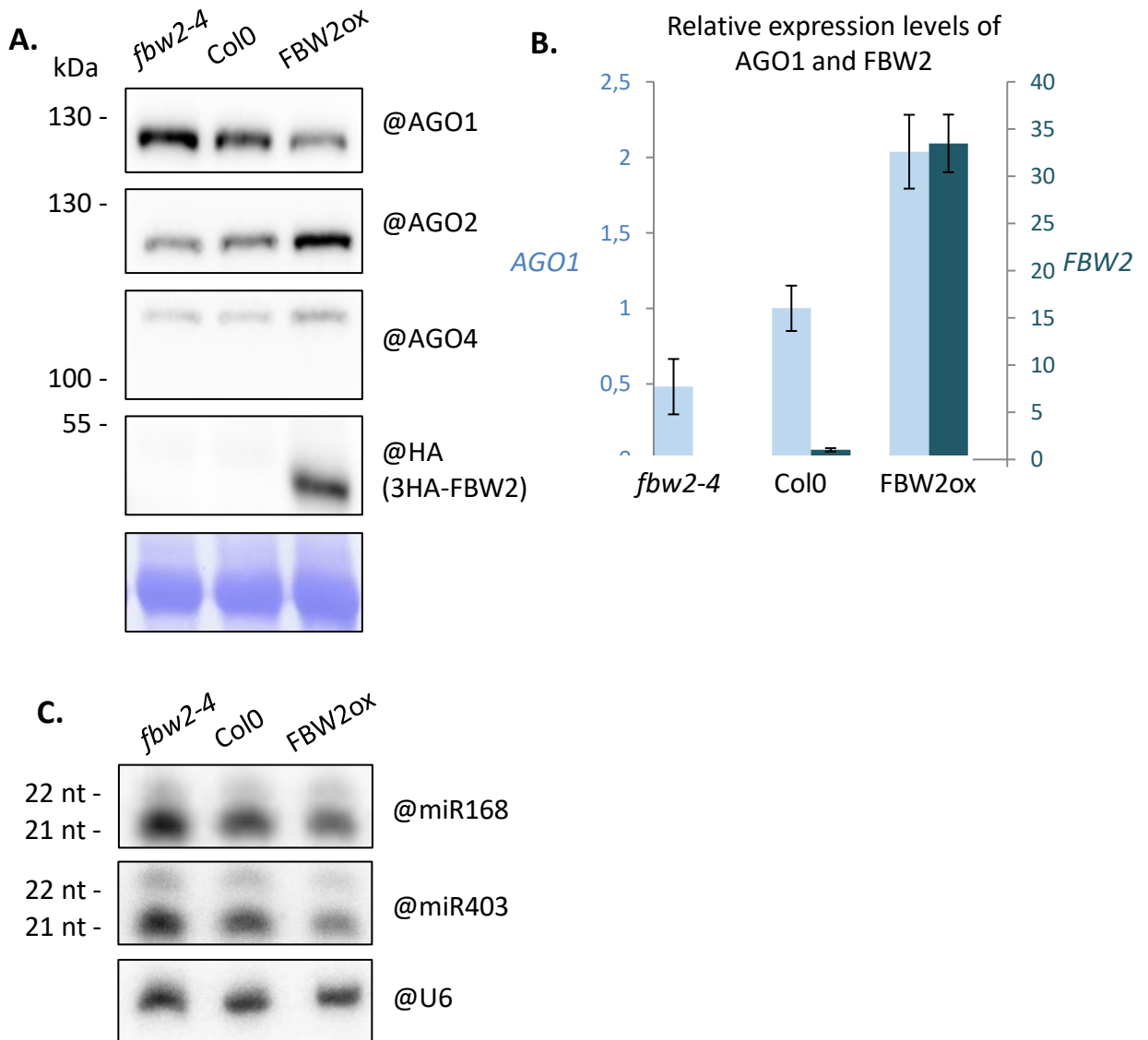
Figure 31 : AGO1 protein level in wild type, null mutant and FBW2 ox seedlings

A. Western blot of protein extracts from 8 day-old seedlings (col-0, *fbw2-4* and 35S:3HA-FBW2 line 10) grown on MS medium. Coomassie blue staining was used as a loading control. "@" indicates hybridization with the corresponding antibody.
B. RT-qPCR analysis of *AGO1* and *FBW2* expression in *fbw2-4* and 35S:3HA-FBW2 (line 10) relative to Col0.
C. Northern blot of small RNA extracted from the same seedlings. "@" indicates hybridization with a probe. U6 RNA level was used as a loading control.

contradiction with the transient assays and this was not observed after P0 induction (Derrien et al., 2018 and Figure 24A), where both AGO1 and AGO2 protein decayed. To further analyse this inconsistency, we repeated this experiment with the *FBW2* overexpressor (35S:3HA-FBW2) line (Figure 31A). As already observed previously, AGO1 is partially degraded in FBW2-overexpressing seedlings, but not AGO2. Also the AGO4 protein level is not significantly affected.

In order to exclude that these observations on the AGOs protein levels are caused by the artificial overexpression of the F-box protein, we also included a null mutant of FBW2, *fbw2-4*, in this experiment. In the *fbw2-4* mutant, the AGO1 steady state level is slightly increased, indicating that FBW2 contributes to maintain AGO1 protein homeostasis under normal growing conditions. As introduced previously, AGO1 levels are also regulated at transcription and posttranscriptional levels, and we thus also verified the AGO1 transcript and miR168 amounts in this experiment. A qRT-PCR analysis revealed that *AGO1* expression rises alongside with *FBW2* overexpression, an effect most probably linked to the AGO1 self-regulation feedback loop (reviewed in Mallory and Vaucheret, 2010) (Figure 31B). Indeed, a Northern blot of small RNAs points out an increase of miR168 level in *fbw2-4* and a decrease in the FBW2-overexpressing plants (Figure 31C). The same is apparent for the miR403, which is used by AGO1 but in this case to regulate *AGO2* messenger.

This experiment puts forward another important aspect of AGO1 regulation by the miR168. Before being subjected to post-translational regulation, AGO1 level is already controlled and maintained by PTGS (reviewed in Mallory and Vaucheret, 2010). This effect complicates our interpretation regarding the FBW2 activity on AGOs, and might also explain the less visible degradation of AGO1 in Arabidopsis as compared to in *Nicotiana benthamiana*. As regarding AGO2, which higher accumulation was at a first glance unexpected and contradicting transient assays, the alleviation of regulation by the miR403 is probably the cause of this accumulation, and illustrates the crosstalk between AGO proteins.

Finally, we wondered whether the expression level of *FBW2* was determinant for the effect on AGO1. We thus measured the *FBW2* transcripts in the β-estradiol-inducible *FBW2* line (that did not show clear AGO1 degradation), and in the

constitutive *FBW2* overexpression line (that showed AGO1 degradation). Remarkably, *FBW2* overexpression reached 30 times its endogenous expression level when constitutively expressed under the 35S promoter, while it reached an increase of 80-fold with the inducible promoter, before silencing kicked in (Figure 24B). Thus, a 30-fold increase in *FBW2* level yielded a visible degradation of AGO1, while a transient 80-fold increase did not. One can thus wonder whether the amount of expressed *FBW2* is really key for AGO1 degradation. Again, we can speculate here that FBW2 might only be able to degrade a subpool of AGO1 and that another pool of it would be resistant to this degradation, independently of the level of FBW2.

2.2.2 Discrimination of AGO1 pools by FBW2

Although both FBW2 and P0 are F-box proteins that target AGO1, their effectiveness in degrading AGO1 is not comparable in stably transformed Arabidopsis plants, whereas they destabilize AGO1 in a similar manner in transient expression assays in *Nicotiana benthamiana leaves*.

- In *Nicotiana benthamiana*

One possible explanation for the difference in FBW2-mediated AGO1 degradation efficiency between stable FBW2-overexpression in Arabidopsis and transient expression in *Nicotiana benthamiana* could be the presence of the viral suppressors of silencing P19 (Lakatos et al., 2004; Scholthof, 2006). P19 is commonly used in transient expression assays to repress silencing, which is quickly induced by artificial overexpression. Since P19 specifically binds 19- to 21-nucleotide double-stranded small RNAs, its expression may result in more unloaded form of AGO1. At the mean time, P19 may also sequester the miRNA168 and thus increase *AGO1* expression. One opposite condition, where sRNAs are more abundant, could be artificially produced by expressing an inverse repeat of the *GFP* gene (*gffg*), which is known to produce functional small siRNAs (Himber et al., 2003). To test the effect of P19 and *gffg* expression on FBW2-mediated AGO1 decay, transient overexpression of CFP-AGO1 with or without 3HA-FBW2 was performed in *Nicotiana benthamiana* and protein extracts were analyzed by Western blot.
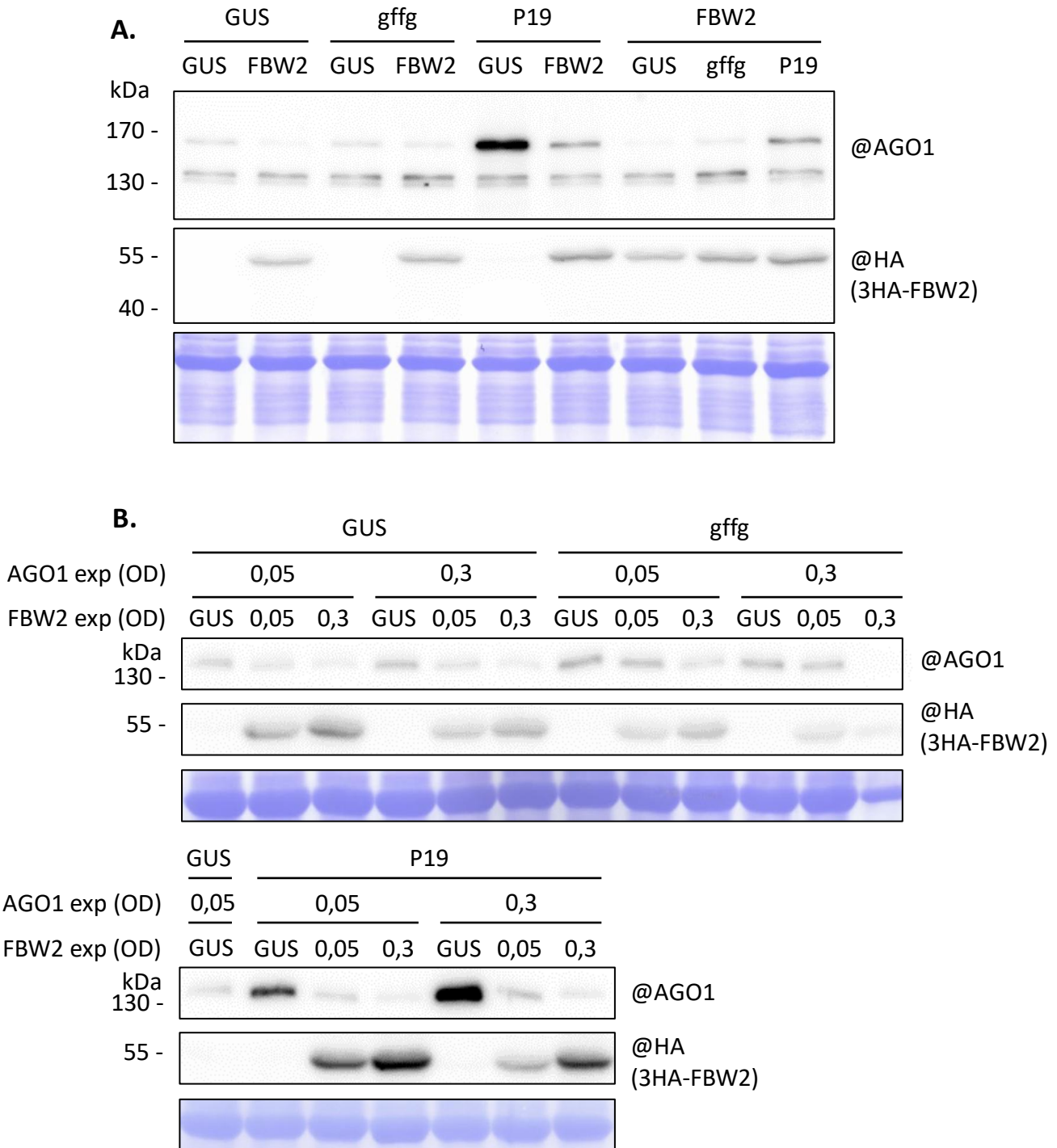
Figure 32 : P19 expression influences AGO1 destabilization by FBW2 in *Nicotiana benthamiana*

Western blots of protein extracts from four week-old *Nicotiana benthamiana* agroinfiltrated leaves with *Agrobacteria* harbouring binary vectors for the expression of 35S:CFP-AGO1, 35S:3HA-FWB2, 35S:GUS (expression control), 35S:*gffg* and 35S:P19 constructs. Tissues for protein analysis were sampled 3 days later. Coomassie blue staining was used as loading control. "@" indicates hybridization with the corresponding antibody.

A. All constructs were infiltrated at an OD of 0,3.
B. AGO1 and FBW2 were infiltrated at various OD as indicated. The rest of the constructs were infiltrated at an OD of 0,3 in every conditions.

First, we observed a difference of AGO1 protein level, which was found far more expressed in presence of P19, as expected (Figure 32A). Second, AGO1 destabilization by FBW2 is much clearer and efficient in presence of P19 than without. Without P19, AGO1 degradation by FBW2 is visible but seems attenuated, in a way reminiscent to its degradation in stable Arabidopsis lines. Co-expression of the *gffg* construct with FBW2 did not dramatically change the destabilization of AGO1, but slightly weakened it (Figure 32A). The availability of small RNAs is known to control the steady state level of AGO proteins in plants and metazoans (Derrien et al., 2012; Smibert et al., 2013; Martinez and Gregory, 2013). However, it was shown that miRNAs and not siRNAS contribute to to this effect, at least in animal cells (Smibert et al., 2013; Martinez and Gregory, 2013). Therefore, it would be interesting in the future to co-express in our assays a miRNA-generating construct and investigate whether it would have a stronger effect on AGO1 than the siRNA generating *gffg* construct.

To assess the contribution of *AGO1* and *FBW2* expression levels on AGO1 destabilization in transient assays, the same experiment was repeated with different quantities of CFP-AGO1 and 3HA-FBW2 infiltrated Agrobacteria (Figure 32B). A 6-fold change in *AGO1* expression has no strong impact on AGO1 protein level without P19, but more FBW2 protein was produced, possibly indicating that FBW2 is also rapidly silenced in this system (Figure 32B). Without P19, increasing *FBW2* expression levels reduced AGO1 protein level without fully degrading it. Interestingly, AGO1 seems more resistant towards low FBW2 level when *gffg* was co-expressed, further supporting the idea that loaded AGO1 is less prone to degradation by FBW2. In presence of P19, a higher *FBW2* expression level only slightly improved AGO1 degradation, as even at the lowest concentration FBW2 was already very efficient. Note also that even with P19, FBW2-mediated AGO1 degradation was never complete, suggesting that there is a portion of AGO1 proteins that is resistant to degradation. Overall, these experiments support that FBW2 more efficiently targets the unloaded pool of AGO1, but additional experiment will be required to clearly prove it.
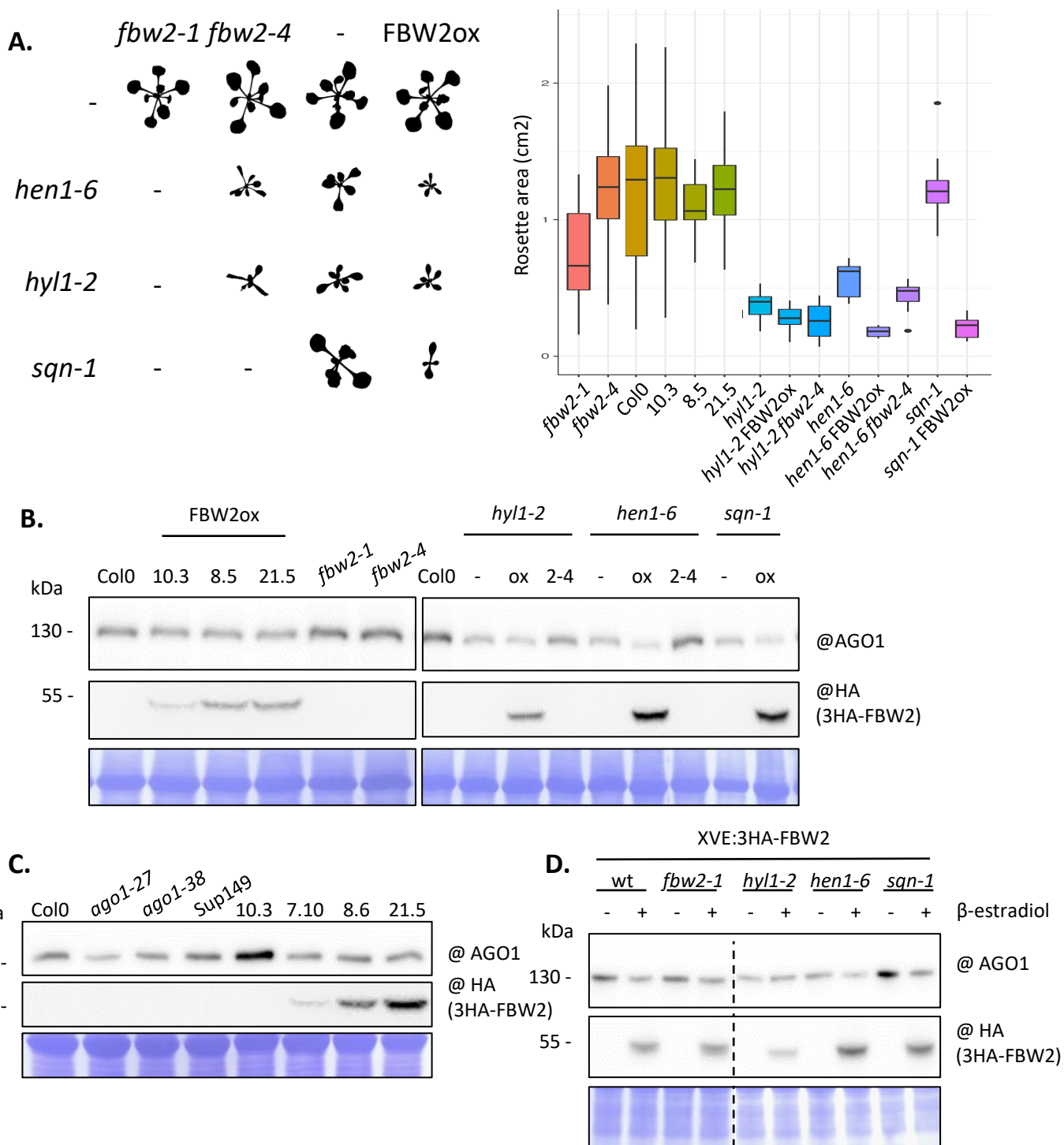
Figure 33 : FBW2 induction in *hen1-6* and *hyl1-2* mutants further destabilizes AGO1

A. Left: Shape imprint of 17 day-old seedlings *hen1-6*, *hyl1-2* and *sqn-1*, and the corresponding crosses to *fbw2-4* and 35S:3HA-FBW2 (FBW2ox) line 10 as indicated. Right: Measurements of the rosette area of the same seedlings. 10.3, 8.5 and 21.5 correspond to independent 35S:3HA-FBW2 lines. A third experiment is underway to statistically assess these data.

B. Western blot of protein extracts from the same seedlings. ox corresponds to the crossing with the overexpressor line 10.3, 2-4 with the mutant *fbw2-4* and – to the simple mutant.

C. Western blot of protein extracts from 4 week-old plant leaves. In the 35S:3HA-FBW2 line 10 FBW2 is not expressed anymore and AGO1 is stabilized.

D. Western blot of protein extracts from the indicated mutants crossed with the inducible XVE:3HA-FBW2 line and grown on MS medium supplemented with DMSO (-) or β-estradiol (10 μM) (+). Coomassie blue staining was used as loading control and "@" indicates hybridization with the corresponding antibodies for all Western blot.

- In stable Arabidopsis lines

To further explore the link between loaded versus unloaded forms of AGO1 on FBW2-mediated decay, we took advantage of Arabidopsis mutants affecting the production or stability of small RNAs. Both the *fbw2-4* mutant and the 35S:3HA-FBW2 overexpressor were crossed with *hyl1-2* and *hen1-6*. The first mutant is affected in the double stranded RNA-binding protein DRB1/HYL1 that mediates the processing of most miRNA precursors (Kurihara et al., 2006; Dong et al., 2008), and the second one is mutated in the RNA methyltransferase HEN1, critical for small RNA stability (Li et al., 2005; Ren et al., 2014). Both are null T-DNA mutants from the Salk collection (Alonso et al., 2003) and must be studied with care as their respective T-DNA insertions contain a 35S promoter which could interfere with the expression of the 35S:3HA-FBW2 construct. We also crossed the 35S:3HA-FBW2 overexpressor to the *sqn-1* EMS mutant generated in the Scott Poethig laboratory (Berardini et al., 2001). SQUINT (SQN) acts together with HSP90 and facilitates small RNA loading (Iki et al., 2011; Earley and Poethig, 2011).

The analysis of these mutant plants revealed interesting genetic interactions. Both the absence or overexpression of *FBW2* worsened the phenotype of the *hen1-6* mutant (Figure 33A). In the case of *hyl1-2*, overexpression of *FBW2* affected less the plant development than the loss of *FBW2* function. On the opposite, overexpression of *FBW2* greatly hinders the *sqn-1* mutant plant growth. The cross between *sqn-1* and *fbw2-4* mutant was not done, but should restore a wild type phenotype as published with the *fbw2-1* mutant allele (Earley et al., 2010). On the molecular level, the analysis of protein extracts by Western blot showed a clear stabilization of AGO1 in *hyl1-2 fbw2-4* and *hen1-6 fbw2-4* double mutants compared to the single *hyl1-2* and *hen1-6* mutants (Figure 33B and Supplementary Figure 9). Overexpressing *FBW2* in *hen1-6* and *sqn-1* produced a clear destabilization of AGO1, which is less apparent in the *hyl1-2* mutant. Notably, in all these double mutant lines, the FBW2 protein level is also higher than in the mother overexpressor line, likely because the transgene is less silenced. Note that experiments carried out afterwards revealed that *FBW2* expression disappeared as the plant gets older (Figure 33C).
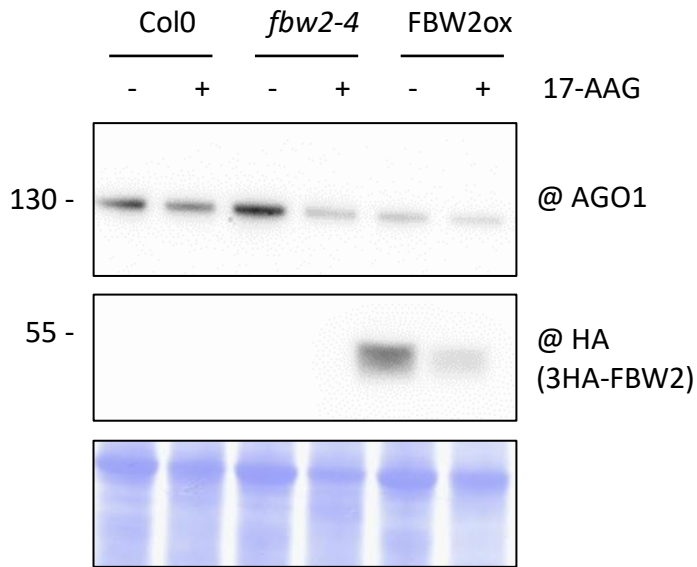
Figure 34: AGO1 destabilization upon HSP90 inhibition

Western blot of protein extracts from 10 day-old seedling grown on MS medium and treated with DMSO (-) or with 17-AAG (50 µM) (+) for 24 hours in liquid MS medium. The 17-AAG inhibits the activity of HSP90, a chaperone known to be required for the loading of small RNAs in AGO1.

The destabilization of AGO1 by overexpressing *FBW2* nicely correlates with the impaired development of the double mutants. In particular, the increased degradation rate of AGO1 in *hen1-6* further supports that it is the unloaded pool of AGO1, which is degraded. Hence, in this mutant most of the small RNAs would be degraded suggesting that most AGO1 is unloaded. This is not exactly the same situation in the *hyl1-2* mutant background, as not all miRNAs require HYL1 for their maturation (Szarzynska et al., 2009; see RNA seq data later) and endogenous siRNAs are still present. Thus the AGO1 partial resistance towards *FBW2* overexpression in *hyl1-2* seems coherent. Moreover, the same results were reproduced with less variations in FBW2 protein level by crossing the XVE:3HA-FBW2 line 13 with *hyl1-2, hen1-6* and *sqn-1* (Figure 33D). Even more interesting are the results obtained with the crosses with the *fbw2-4* null mutant. One might speculate that an opposite effect (more healthy plants) would have been expected in *hyl1-2 fbw2-4*, *hen1-6 fbw2-4* and *sqn1 fbw2-4* mutants as the level of AGO1 was partially restored. This was however not the case as the phenotype of the double mutants was stronger, suggesting that the stabilized AGO1 protein became somehow toxic. This issue will be further investigated and discussed in a following section of the Thesis manuscript.

As the AGO1 loading step with small RNA requires the chaperone protein HSP90, FBW2 action was also assessed when HSP90 activity is inhibited. Thus, both *fbw2-4* and the 35S:3HA-FBW2 line were treated with Tanespimycin (17-N-allylamino-17-demethoxygeldanamycin, 17-AAG), a recently generated and improved version of the geldanamycin. Protein extracts of 24 hours mock or 17-AAG-treated seedlings were analysed by Western blot (Figure 34). As in animals (Iwasaki et al., 2010; Johnston et al., 2010), inhibition of HSP90 triggered the destabilization of AGO1 in Col-0 plants. Presumably, it is the unloaded form of AGO1 that is degraded upon HSP90 inhibition, and we thus expected that the *fbw2-4* mutation would counteract this effect. This was however not the case, indicating as HSP90-mediated regulation of AGO1 is independent of FBW2. This suggests that more than one endogenous AGO1 decay pathway may exist in plants and/or that the drug could act at other levels.
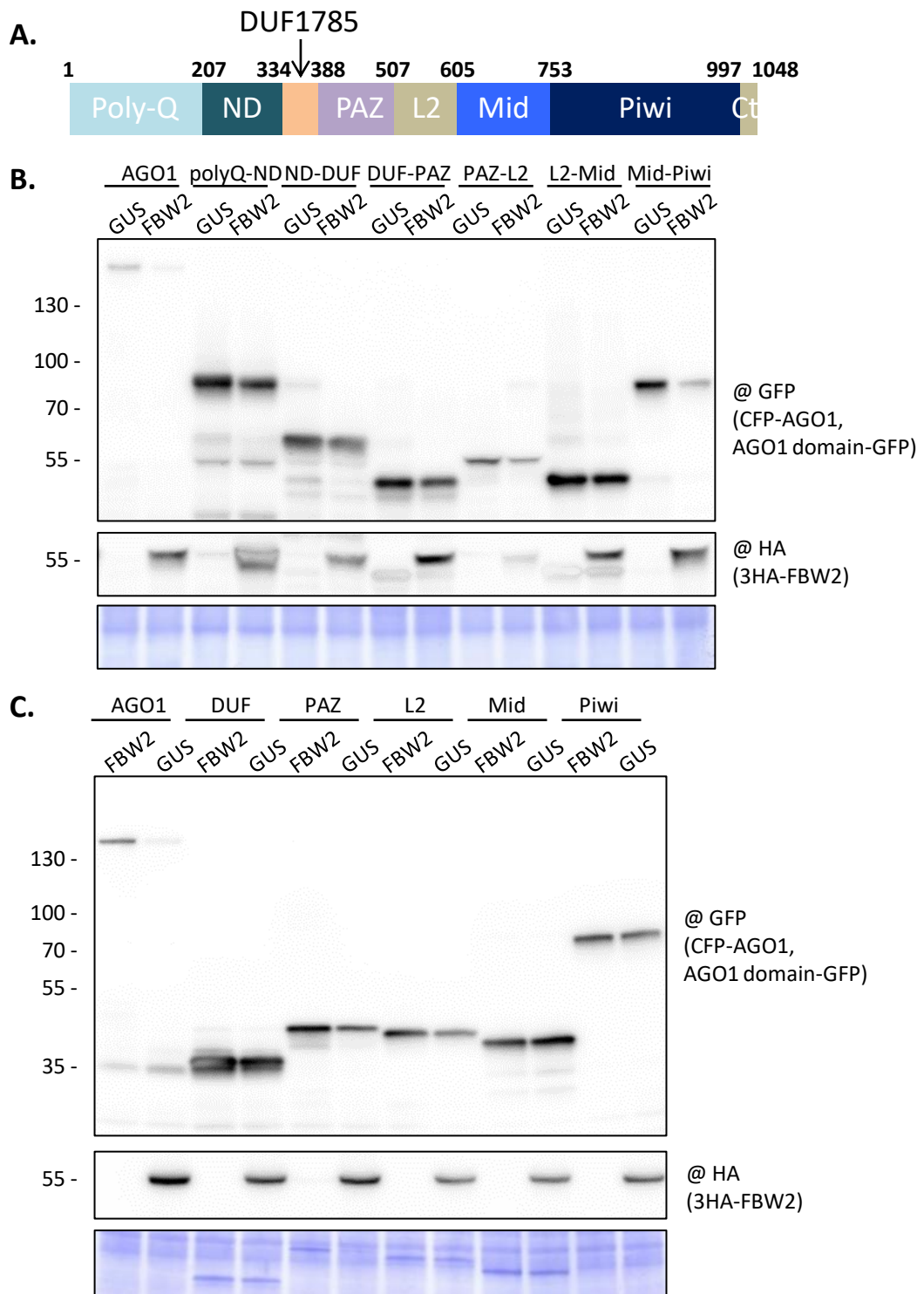
Figure 35 : The PAZ and the Mid-Piwi domains are targeted by FBW2

A. Scheme of the AGO1 domains repartition along the amino acids sequence.

B. and C. Western blot of protein extracts from four week old *Nicotiana benthamiana* agroinfiltrated leaves. Agrobacteria harbouring full length CFP-AGO1 or AGO1 protein domains, as specified and C-terminally fused to the GFP, and a 35S:3HA-FWB2 constructs were infiltrated at an OD of 0,3 and tissues were sampled 3 days later. Expression of GUS serves as control. Coomassie blue staining was used as a loading control. "@" indicates hybridization with the corresponding antibody.

2.2.3 Mechanism of AGO1 recognition by FBW2

Studying the interaction between two proteins often brings valuable information concerning their mode of action. For example, the viral F-box P0 targets the DUF1785 of AGO1 and allowed us to functionally characterize this domain (see Derrien et al, 2018). As FBW2 and P0 are both F-box proteins that destabilize AGO1, one can wonder whether they interact with AGO1 in a similar way.

- Defining the degron

We first aimed to determine the degron required for FBW2 degradation. To do so, the protein sequence of AGO1 was split according to its structural domains (Figure 35A) and the resulting fragments were fused to the GFP at their C-terminini. They were then transiently expressed in *Nicotiana benthamiana* leaves, with or without 3HA-FBW2.

The combination of successive domains in AGO1 were first tested in order to avoid missing a possible degron in between (Figure 35B and supplementary Figure 6A). Several combinations of domains showed some sensitivity regarding FBW2-mediated decay, including the DUF-PAZ, the PAZ-L2 and MID-PIWI. The MID-PIWI domain showed, however, the most pronounced degradation, which was equally-well degraded by FBW2 as the full length AGO1. Next, these domains were individually expressed in this system to further define the degron sequence (Figure 35C and supplementary Figure 6A). From these assays, only the PAZ domain is partially destabilized by FBW2 while the MID and the PIWI domains taken individually were resistant. Notably, the DUF1785, which is recognized by the viral F-box P0 (Derrien et al., 2018), is not targeted by FBW2, indicating that P0 and FBW2 do not recognize AGO1 in the same way.

From these assays, we concluded that the degron in AGO1 recognized by FBW2 is likely a structural motif requiring both the MID and PIWI domains, and that an additional motif may exist in the PAZ. These degradation assays are also consistent with the yeast-two-hybrid assays showing that FBW2 prefers the C-terminal part of AGO1 and, in particular, the combination of the MID-PIWI domains (Supplementary Figure 6B). Interestingly, the MID and PIWI domains are necessary

for anchoring of the 5' end of the small RNA, while the PAZ is required for the 3' end binding. Since these 3 domains are specifically targeted by FBW2, one can wonder if FBW2 is able to differentiate the small RNA loaded from the non-loaded form of AGO1. Also, at the structural level, FBW2 is a much smaller protein than AGO1 (36 kDa versus 116 kDa), and one may ask how FBW2 can recognize the distant PAZ and the MID-PIWI domains.

- A phospho-degron in AGO1?

Many F-box proteins are known to recognize their target only when they are post-translationally modified, most commonly by phosphorylation (Skowyra et al., 1997). If such a modification is necessary for FBW2 to interact with AGO1, this could explain the weak interaction between both proteins that we observed in yeast-two-hybrid assays. Notably, several phosphorylation residues have already been identified on human AGO2 (Kim et al., 2013, unpublished data). We collaborated with Esther Izquierdo (BPMP, Montpellier), to identify phosphorylated residues in Arabidopsis AGO1. To do so, AGO1 was analysed in plant samples after digestion by trypsin, and loaded on a TiO2 resin in order to enrich phosphopetides. The resulting samples were analysed by LC-MS on a Q Exactive Mass spectrometer. By this approach, we only identified one phosphorylated peptide on AGO1 corresponding to FYMEPET(pS)DSGSMASGSMAR (phosphorylation on S1001). This phosphorylated S1001 is followed by other serine residues. Interestingly, this stretch of serine is also conserved in human AGO2 and is known as highly phosphorylated (Figure 14). Hence, two recent reports indicate that human AGO2 phosphorylation by CSNK1A1 (CASEIN KINASE 1) on a cluster of conserved residues (S824-S834) impairs mRNA target association (Golden et al., 2017; Quévillon Huberdeau et al., 2017). The negatively charged phosphates would remove the mRNA from AGO2, and the mRNA target is released. Thus, after dephosphorylation, AGO2 could be recycled and guided to a new target mRNA, or would be degraded.

In order to investigate if the identified Arabidopsis AGO1 phosphorylation is important for FBW2-mediated degradation, AGO1 was site-directed mutagenized on the serine residues 1001, 1003 and 1005 to generate phosphodead and
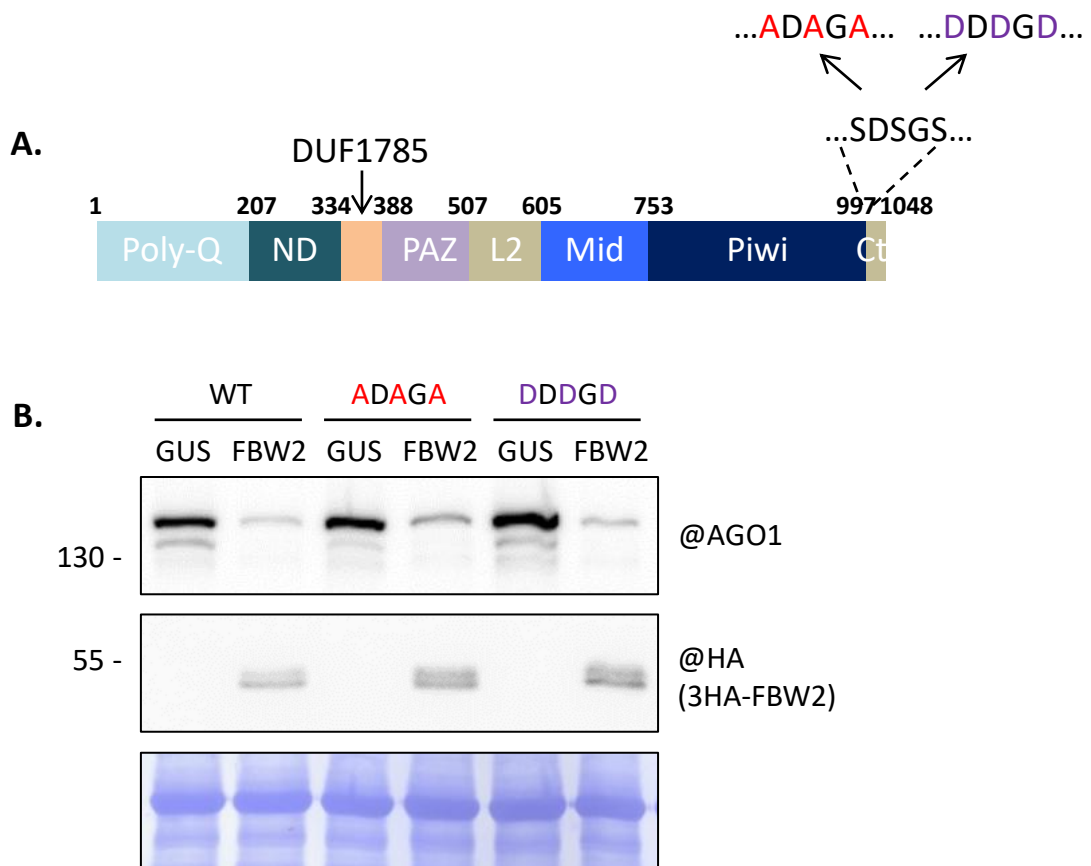
Figure 36: C-terminal phosphorylation of AGO1 does not affect FBW2-mediated decay

A. Schematic representation of the localization of the putative phosphorylated serine residues (1001, 1003 and 1005) and their mutant counterparts.
B. Western blot of protein extracts from four week-old *Nicotiana benthamiana* agroinfiltrated leaves. Agrobacteria harbouring CFP-AGO1 wild type (WT) or mutated as specified and a 35S:3HA-FWB2 constructs were infiltrated at an OD of 0,3 and tissues were sampled 3 days later. Expression of GUS serves as control. Coomassie blue staining was used as a loading control. "@" indicates hybridization with the corresponding antibody.

phosphomimic mutants (Figure 36). These constructs were then assayed by transient expression in *Nicotiana benthamiana* with or without 3HA-FBW2 and protein extracts were analyzed by Western blot. These experiments showed that both the phosphodead and the phosphomimic AGO1 mutant proteins were destabilized by FBW2, as is the wild type protein. Thus, phosphorylation at the C-terminal end of Arabidopsis AGO1 does not influence FBW2-mediated AGO1 degradation.

In the future, it would be of particular interest to identify a phosphorylation site that could affect the binding of small RNA, as this may affect the stability of AGO proteins. In human, a tyrosine residue within the 5' phosphate-binding pocket of the MID domain has been highlighted as a potential phosphorylation site (Figure 14) (Rüdel et al., 2011). The negative charge upon phosphorylation of this residue has been proposed to inhibit access of the 5' phosphate of the miRNA and thus blocks miRNA binding. Interestingly, this site is conserved in Arabidopsis AGO1. Attempts to identify this site and others by phosphoproteomics are currently under way.

- An AGO-hook motif in FBW2?

Since FBW2 principally targets the MID-PIWI domains, which contain the binding pocket necessary for the interaction with GW proteins (Till et al., 2007; Elkayam et al., 2017), we wondered whether FBW2 contains an AGO-hook motif. FBW2 amino acid sequence was first analyzed using a prediction tool recognizing such a motif (Karlowski et al., 2010; Zielezinski and Karlowski, 2011). However, only a single GW motif was predicted with low confidentiality, at residues 287-299 (Figure 37A). The tryptophan in this stretch is well-conserved among FBW2 homologs but the glycine can be replaced by other amino acids such as methionine, valine or isoleucine (Supplementary Figure 7). Interestingly, a closer examination of the FBW2 protein sequence indicates that tryptophan residues are not evenly distributed, but are either part of the F-box domain or at the C-terminal end of the protein. Thus, other tryptophan residues than the W295 from the putative GW motif were also found conserved in the C-terminal part of the protein and are spaced by around 20 amino acids. As the glycine residue flanking the tryptophan is not mandatory for the AGO-hook motif and the C-terminal region of FBW2 is most likely unstructured, the presence of an AGO-hook motif is still credible. To assess this hypothesis, FBW2

A. Results

Data info:

id:	FBW2
description:	
length:	317 aa
WG/GW no:	1

WG/GW domains:

no.	start	end	length	motifs	dos	p-value	ics
1	287	299	13	1	-2.65	5.01E-01	25.93

B.
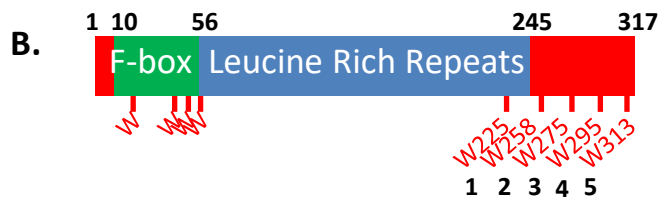
C.
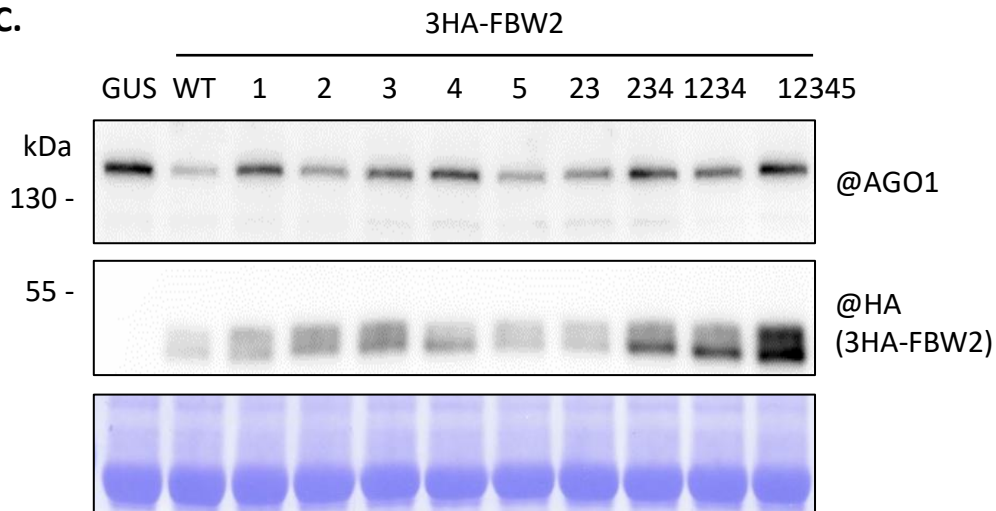
Figure 37 : FBW2 contains a putative GW motif

A. GW motif prediction from http://www.combio.pl/agos/help/ (Karlowski et al., 2010; Zielezinski and Karlowski, 2011). The FBW2 protein sequence from residue 287 to 299 may contain an ago hook motif.

B. Scheme of FBW2 tryptophan (W) residue repartition, which are either part of the F-box motif or localized in the C-terminal part of the protein.

C. Western blot of protein extracts from four week-old *Nicotiana benthamiana* agroinfiltrated leaves. Agrobacteria harbouring CFP-AGO1 and a 35S:3HA-FWB2, wild type (WT) or mutated as specified, constructs were infiltrated at an OD of 0,3 and tissues were sampled 3 days later. Expression of GUS serves as control. Coomassie blue staining was used as a loading control. "@" indicates hybridization with the corresponding antibody.

was site-directed mutagenized to generate mutants where the tryptophan residues were replaced by alanine residues (Figure 37B). These constructs were then assayed in transient expression in *Nicotiana benthamiana* with CFP-AGO1 . Strikingly, mutation of the tryptophan residues in FBW2 reduced AGO1 destabilization but the individual contribution of each tryptophan is not equal (Figure 37C). For example, mutation of W225, W275 or W295 impaced more strongly FBW2 activity. Combining these mutations further impaired AGO1 degradation until a stage where no degradation occurred anymore was reached (Figure 37C).

It should also be noticed that the deletion of the region covering these W-residues abolished AGO1 degradation, indicating that the LRR repeats alone were not sufficient to trigger AGO1 degradation (see Figure 29B). Even though these results tend to validate the presence of an AGO-hook motif in FBW2, more experiments are required to demonstrate it. In particular, interaction assays between native and mutated forms of FBW2 are necessary to confirm this hypothesis, for example by GST pull down assays. One could also imagine to generate a minimal F-box-GW motif protein to investigate if the AGO-hook motif alone is sufficient to target and trigger AGO1 degradation.

2.2.4 Degradation pathways involved in AGO1 destabilization

To decipher the degradation pathway involved in the destabilization of a protein, it is possible to use selective chemical inhibitors or mutants affected in the degradation pathway. We first used drugs to inhibit FBW2-mediated AGO1 degradation, as this strategy had been successfully used with P0 (Derrien et al., 2012). Experiments were carried out with the MLN4924, MG132, Bortzeomib, E-64d, Wortmannin, 3-Methyladenine (3-MA) and Concanamycin A (ConA). The MLN4924 inhibits the rubylation of CRL-based E3 ligases, which impairs their activity. MG132 and Bortezomib inhibit the chymotrypsin-like proteases contained in the proteasome. The drug E-64d targets cysteine proteases blocking autophagy and more globally vacuolar protein degradation. Wortmannin and the 3-MA prevent autophagosome formation via the inhibition of class III PI3K. Finally, ConA blocks vacuolar proton

A.

XVE:3HA-FBW2 / *ago1-57*

| - | + | β-estradiol |

mock MLN4924 MG132 E-64d | mock MLN4924 MG132 E-64d

kDa
130 -
100 -
@AGO1

55 -
40 -
@ HA (3HA-FBW2)
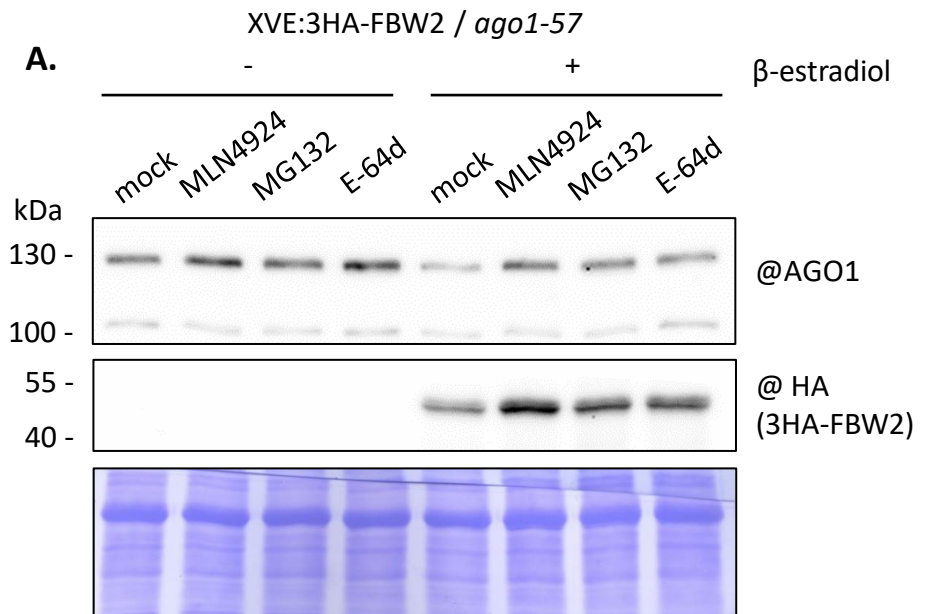
Figure 38 : Investigation of FBW2-mediated AGO1 decay pathway

Western blot of protein extracts from 10 day-old seedlings grown on MS medium and treated in liquid MS with the indicated chemicals overnight. MNL4924 (25 µM) blocks the activity of CULLIN-based E3 ubiquitin ligases. MG132 (50 µM) inhibits proteasomal degradation. E-64d (100 µM) blocks cysteine proteases involved in autophagy and vacuolar degradation. Concanamycin A (ConA, 1 µM) blocks vacuolar proton pumps raising the pH of the vacuole and hindering degradation processes inside the vacuole. Wortmannin (Wort, 20 µM) prevents autophagosome formation via the inhibition of class III PI3K. Coomassie blue staining was used as a loading control. "@" indicates hybridization with corresponding antibody.

A. XVE:3HA-FBW2 in the *ago1-57* mutant background induced with β-oestradiol (+) or DMSO (-) simultaneously with the pharmacological treatments.

B. and C 35S:3HA-FBW2 line compared to AGO1 steady state protein level in Col-0. MG/E means combined treatment with MG132 and E-64d. FBW2ox corresponds to the 35S:3HA-FBW2 line 10.

B.

mock MLN4924 MG132 ConA Wort

Col0 FBW2ox Col0 FBW2ox Col0 FBW2ox Col0 FBW2ox Col0 FBW2ox

kDa
130 -
@ AGO1

55 -
@ HA (3HA-FBW2)

C.

Col0 | 35S:3HA-FBW2

mock MLN4924 MG132 E-64d Mg/E | mock MLN4924 MG132 E-64d MG/E

kDa
170 -
130 -
@AGO1

100 -
55 -
40 -
@HA (3HA-FBW2)

55 -
40 -
@Actin
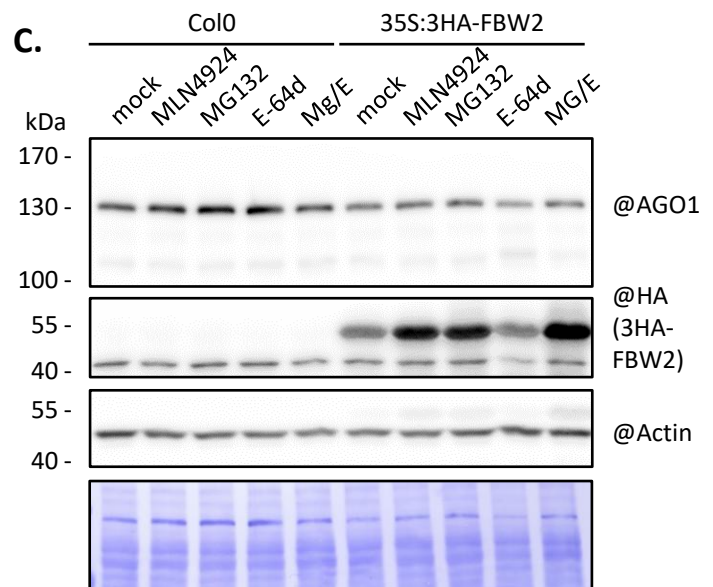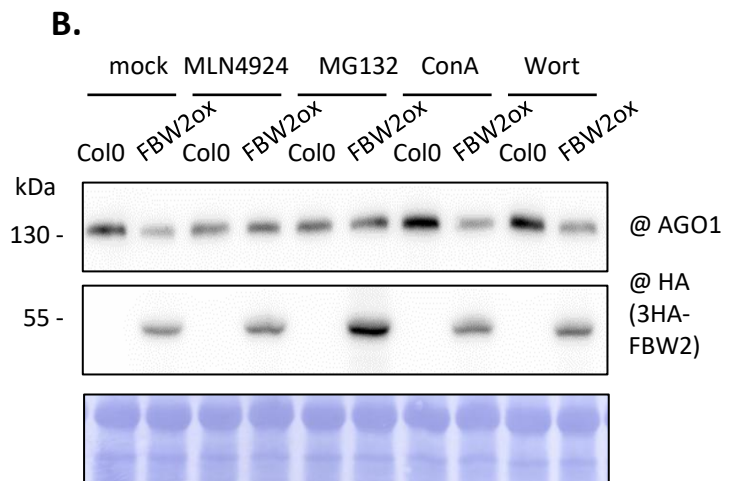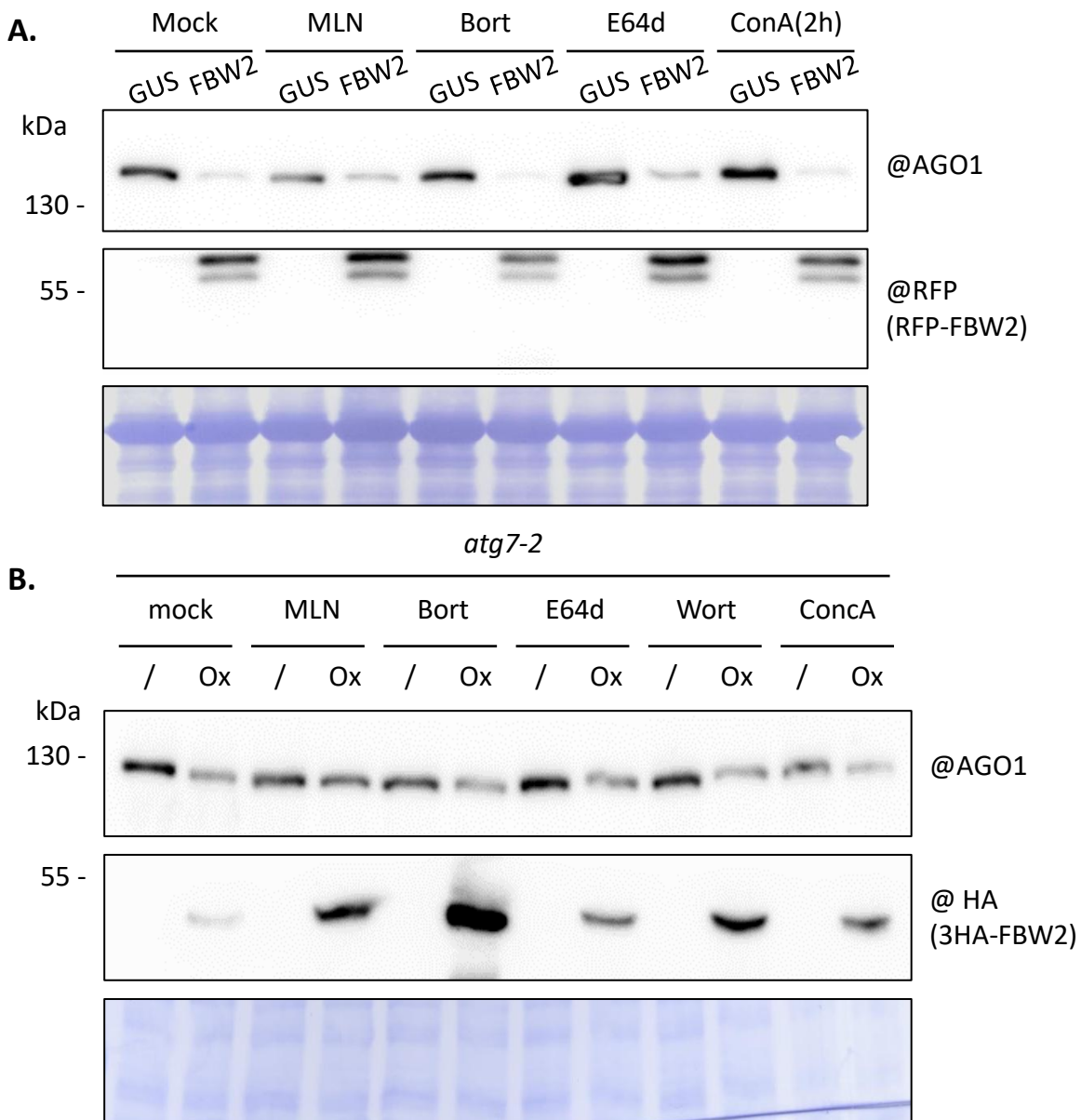
Figure 39 : FBW2-mediated AGO1 decay does not seem to use either the 26S proteasome or autophagy degradation pathways

Pharmacological treatment of plant tissues with the indicated chemicals. MNL4924 (25 µM) blocks the activity of CULLIN-based E3 ubiquitin ligases. Bortezomib (50 µM) inhibits proteasomal degradation. The E-64d (100 µM) blocks the cysteine proteases involved in the autophagy and vacuolar degradation. Concanamycin A (ConA, 1 µM) blocks vacuolar proton pumps raising the pH of the vacuole and hindering degradation processes inside the vacuole. Wortmannin (Wort, 20 µM) prevents autophagosome formation via the inhibition of class III PI3K. Coomassie blue staining was used as a loading control. "@" indicates hybridization with the corresponding antibody.

A. Western blot of protein extracts from four week-old *Nicotiana benthamiana* agroinfiltrated leaves. Agrobacteria harbouring CFP-AGO1 and a 35S:RFP-FBW2 constructs were infiltrated at an OD of 0,3 and tissues were treated 3 days later. GUS expression serves as control. The chemicals were infiltrated in leaves and tissues were sampled 15 hours later unless otherwise specified.

B. Western blot of protein extracts from 10 day-old seedlings from the *atg7-2* mutant or 35S:3HA-FBW2 in the *atg7-2* mutant background. Seedlings were grown on MS medium, acclimated for 48 hours in liquid MS and treated over night with the indicated chemicals.

pumps raising the pH of the vacuole and hindering degradation processes inside the vacuole. Since the proteasome and the autophagy may also act together as redundant degradation pathways for ubiquitinated proteins, MG132 and the E-64d were also combined.

Using these chemicals, we performed many attempts to stabilize AGO1 when *FBW2* is expressed in different Arabidopsis lines. The XVE:3HA-FBW2 line in Col-0 background was not suitable for these experiments as FBW2 was only transiently accumulating and AGO1 decay was not always visible (see above). Therefore, we used the XVE:3HA-FBW2/*ago1-57* line showing a clearer degradation of AGO1 (Figure 38A). With this line, we observed a significant restoration of AGO1 protein amount in presence of FBW2 when MLN4924 was used. We also observed that MG132 and E64-d could block AGO1 degradation, but this was not reproduced in all experiments (data not shown). We next used the 35S:3HA-FBW2 overexpressor line, in which AGO1 protein level is durably diminished. However, this did not enable us to draw strong conclusions neither. As can be seen in Figure 38B, FBW2-mediated decay of AGO1 was blocked with both MLN4924 and MG132, while in another experiment (Figure 38C), this was not the case anymore. Notably, we also tried to chemically block the FBW2-mediated degradation pathway of AGO1 in *Nicotiana benthamiana* transient expression assays (Figure 39A), but these experiments we not more successful. Overall, no stabilization of AGO1 could be reproducibly observed in any of our assays and with any of the drugs, except for MLN4924.

We next tried to combine the pharmacological approach with genetics. The 35S:3HA-FBW2 overexpressor line was crossed with the knockout *atg7-2* mutant, in which the macroautophagy pathway is genetically disrupted (Thompson, 2005; Li and Vierstra, 2012). ATG7 encodes an E1-like activating enzyme for the ubiquitin-like proteins ATG12 and ATG8 and is essential for autophagosome assembly. Nevertheless, *3HA-FBW2* overexpression in the *atg7-2* mutant background was still able to degrade AGO1 (Figure 39B). Thus, we speculated that both autophagy and the proteasome could simultaneously contribute to the FBW2-mediated AGO1 decay. We therefore treated the 35S:3HA-FBW2/*atg7-2* line with Bortezomib and found that, although the drug efficiently increased the 3HA-FBW2 protein level, this was not the case for AG01. From these results we conclude that FBW2-mediated AGO1 decay
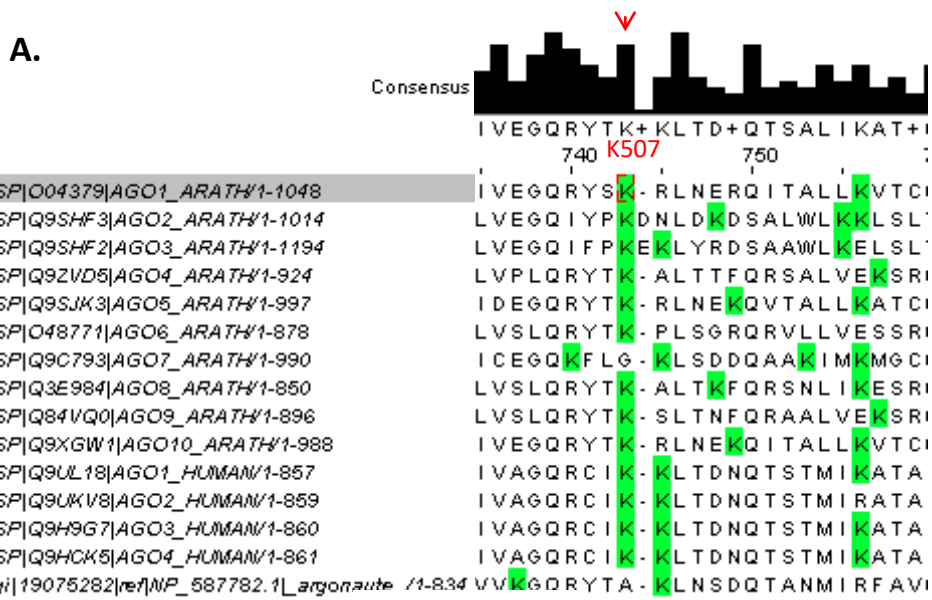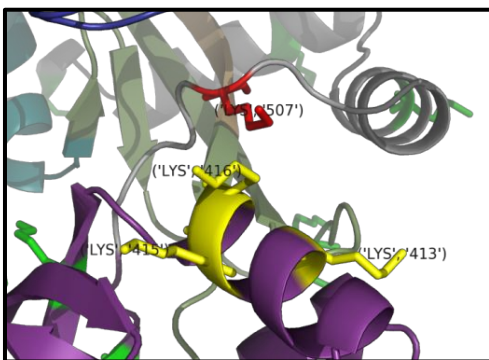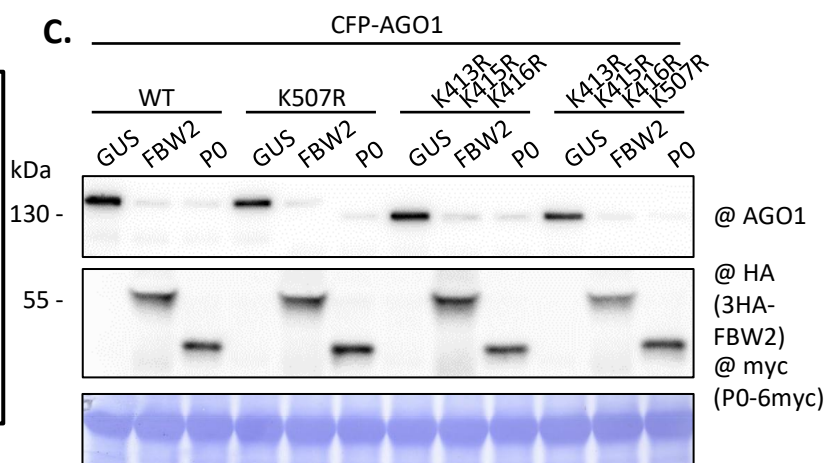
Figure 40 : Site-directed mutagenesis of putative ubiquitination sites on AGO1

A. Clustal Omega alignment of AGO proteins from Arabidopsis, human and *Schizosaccharomyces pombe*. Lysines are coloured in green. The alignment consensus sequence is shown on top. The red arrow indicates the AtAGO2 ubiquitinated lysine residue, which corresponds to lysine residue 507 on AGO1.

B. 3D representation of the putative structural context of the lysine 507. Three other lysine residues are located nearby on residues 413, 415 and 416.

C. Western blot of protein extracts from four week-old *Nicotiana benthamiana* agroinfiltrated leaves. Agrobacteria harbouring CFP-AGO1, wild type (WT) or mutated as indicated, and a 35S:3HA-FWB2 or 35S:P0-6myc constructs were infiltrated at an OD of 0,3. Tissues were sampled 3 days later. GUS expression serves as control. Modifying the lysine residue to arginine abolishes ubiquitination but conserves the steric properties of the amino acid. Coomassie blue staining was used as a loading control. "@" indicates hybridization with the corresponding antibody.

likely employs a proteasome- and autophagy-independent route for degradation, which still remains to be characterized.

Because MLN4924 was the only drug that reproducibly blocked FBW2-mediated AGO1 decay, we can conclude that SCF-dependent ubiquitination of AGO1 is determinant for this decay pathway, which is in accordance with the previously described results. Interestingly, AGO1 was found enriched in mass spectrometry analysis of purified ubiquitinated proteins when the proteasome is blocked by MG132 (Kim et al., 2013). In this analysis, AGO2 could also be recovered and the ubiquitination site has been mapped (unpublished data from Dr R. Vierstra, University of Wisconsin, Madison, USA). As the modified lysine residue is well-conserved among AGO proteins (Figure 40A), AGO1 was site-directed mutagenized to generate a mutant variant that cannot be ubiquitinated on this lysine residue (K507R). Other lysine residues at positions close to the 507 amino acid on our 3D model of AGO1 were also mutagenized to prevent alternative ubiquitination, often happening when the primary ubiquitination site is not available (Figure 40B). Western blot analysis of protein extract from *Nicotiana benthamiana* leaves agro-infiltrated with these constructs did, however, not prevent the destabilization of AGO1 by FBW2 nor by P0 (Figure 40C). Note that the lysine residue 507 is localized at the end of the PAZ domain. Even though this lysine could play a role on AGO1 regulation, FBW2 mainly targets the C-terminal part of AGO1, which is supposed to be ubiquitinated. However, no ubiquitination sites have been described so far in this region of AGO1.

2.3 Physiological role of FBW2

Since *FBW2* overexpression moderately impacts AGO1 protein level and loss of FBW2 does not produce a visible phenotype (Earley et al., 2010 and our work, data not shown), one can wonder why is FBW2 conserved in flowering plants and what could be its function. To answer these questions, we first looked at the effect of FBW2 on AGO1 activity in PTGS, and then searched for conditions in which AGO1 destabilization occurs.
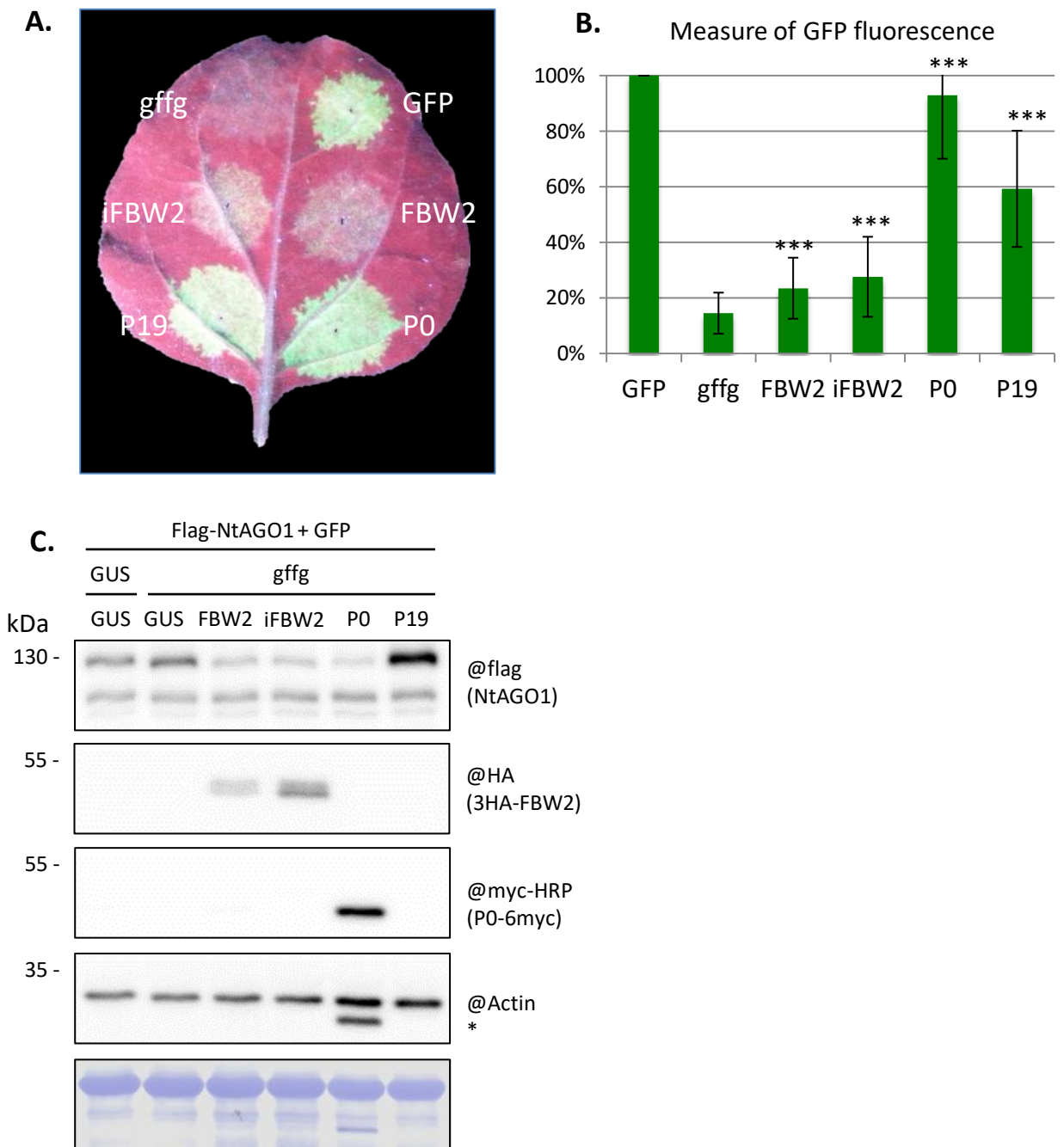
Figure 41: FBW2 is a weak suppressor of silencing

A. Picture of a *Nicotiana benthamiana* leaf 72 hours after infiltration with agrobacteria harbouring a 35S:Flag-NtAGO1 and a 35S:GFP construct plus either a 35S:GUS, 35S:*gffg* (GFP mRNA hairpin; Himber et al., 2003), 35S:3HA-AtFBW2, 35S:3HA-FBW2 (CDS + intron), 35S:P0-6myc or 35S:P19.

B. Intensity of GFP signal in the infiltration area was measured with an Ettan DIGE imager (GE healthcare) and normalized to the GFP control condition. *** p < 0,001 as compared to *gffg* (T-test).

C. Western blot of protein extracts from tissues sampled 72 hours after agro-infiltration. Coomassie blue staining and actin protein level were used as a loading control. "@" indicates hybridization with the corresponding antibodies. * Remaining signal of P0-6myc.

2.3.1 FBW2 is a weak suppressor of silencing

Because FBW2 antagonizes AGO1 by destabilizing it, we first investigated its activity in suppressing silencing. A common way to validate suppressors of silencing is the patch assay on GFP-expressing plants. In this experiment, a GFP transgene is transiently expressed in *Nicotiana benthamiana* and RNA silencing is triggered against it with *gffg*-construct described above (Chapter 2.2.2) (Himber et al., 2003). The GFP fluorescence allows a fast and visible assessment of its expression level. If a suppressor of silencing is co-expressed, GFP silencing is impaired and the fluorescence is restored, regardless of *gffg* expression. We conducted these patch assays with FBW2 (without or with the putative regulatory intron) and used P0 and P19 as positive controls.

In comparison to P0 or P19, co-expression of *FBW2* had only a weak impact on the silencing triggered by the *gffg* (Figure 41A). Quantification of the GFP-fluorescence showed around 10% more fluorescence of the silenced GFP when *FBW2* is co-expressed (Figure 41B). We thought that in contrast to P0, FBW2 may not target the degradation of the endogenous tobacco AGO1 and that this could in part explain the weak suppressor activity of FBW2. Therefore, we also co-expressed *Nicotiana tabacum* AGO1 N-terminally fused to a flag-tag and checked its sensitivity towards FBW2 by Western blot. Similarly to Arabidopsis AGO1, tobacco AGO1 is at least partially destabilized by FBW2 and its expression is further increased in presence of P19 (Figure 41C). This experiment suggests that there is a non-degradable pool of AGO1 that is functional and sufficient to mediate RNA silencing in this system. FBW2 may even not target at all AGO1 when the latter is incorporated into an active RISC.

To further investigate this possibility, another silencing reporter system was used. The pSUC:SUL Arabidopsis transgenic line was previously engineered to constitutively silence an endogenous gene (Himber et al., 2003). These plants express an inverted repeat of the *SULPHUR* gene (At4g18480) under the control of the phloem-companion cell-specific promoter SUC2, generating a leaf chlorotic phenotype that expands 10-15 cells beyond the vasculature. The XVE:3HA-FBW2 line was crossed with the SUC:SUL and continuously induced by growing plantlets
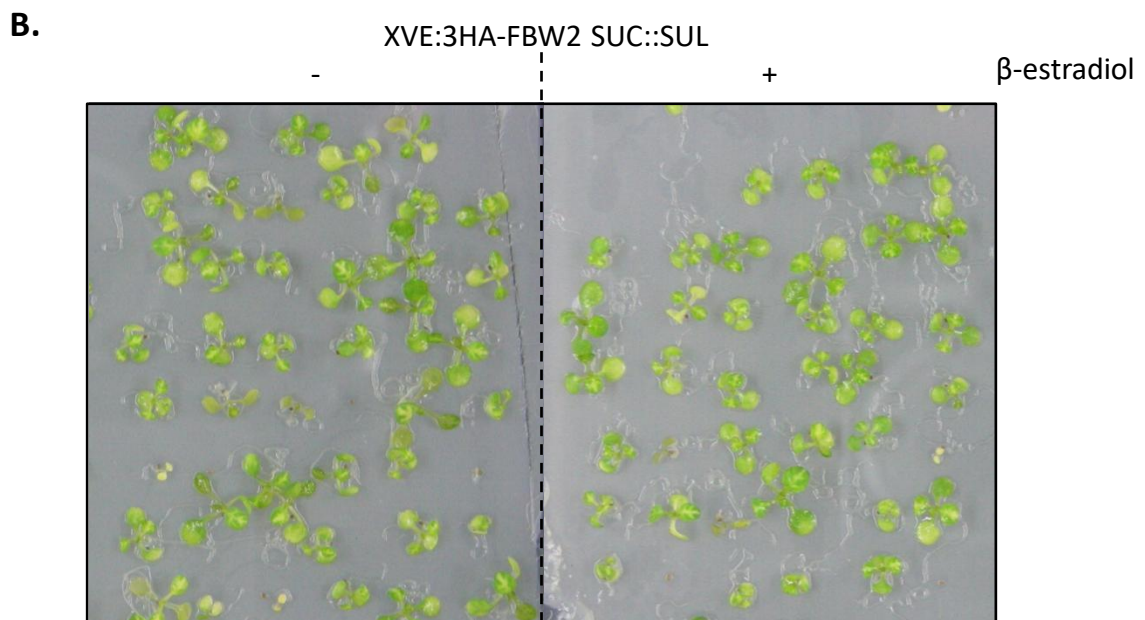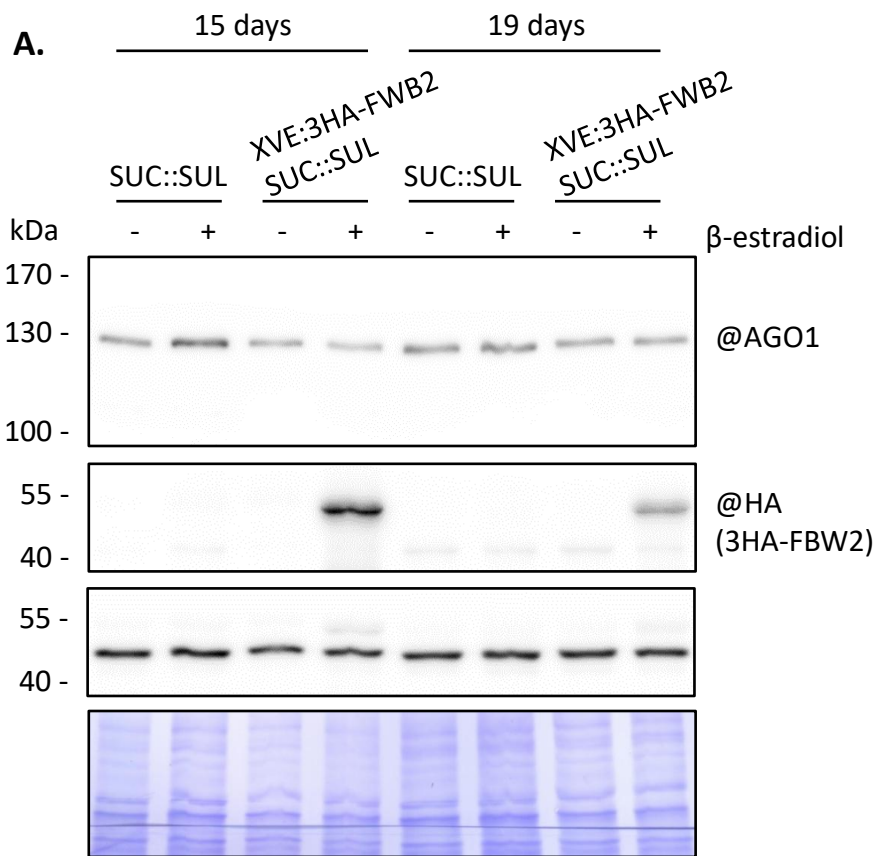
Figure 42 : FBW2 does not prevent the silencing of the *SULPHUR* gene

The XVE:3HA-FBW2 line 13 was crossed with plants harbouring the silencing reporter SUC::SUL.
A. Western blot of protein extracts from seedlings grown on MS medium supplemented with DMSO (-) or β-estradiol (10 µM) (+). Coomassie blue staining was used as a loading control. "@" indicates hybridization with the corresponding antibody.
B. Picture of 15 day-old seedlings grown on MS medium supplemented with DMSO (-) or β-estradiol (10 µM) (+). Both show similar pattern of *SULPHUR* silencing.
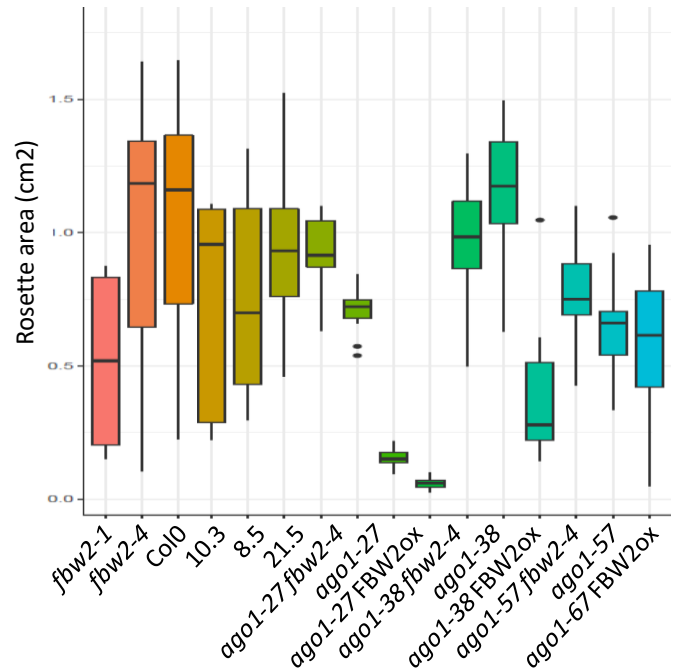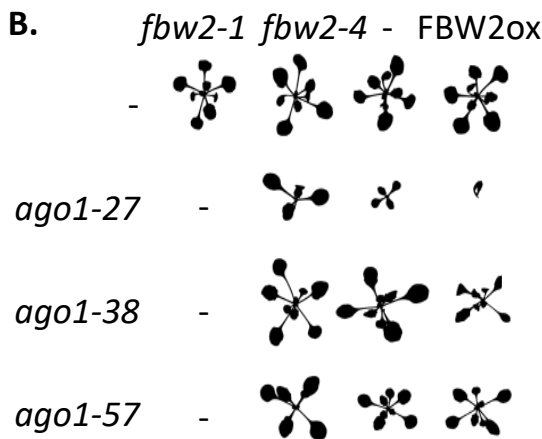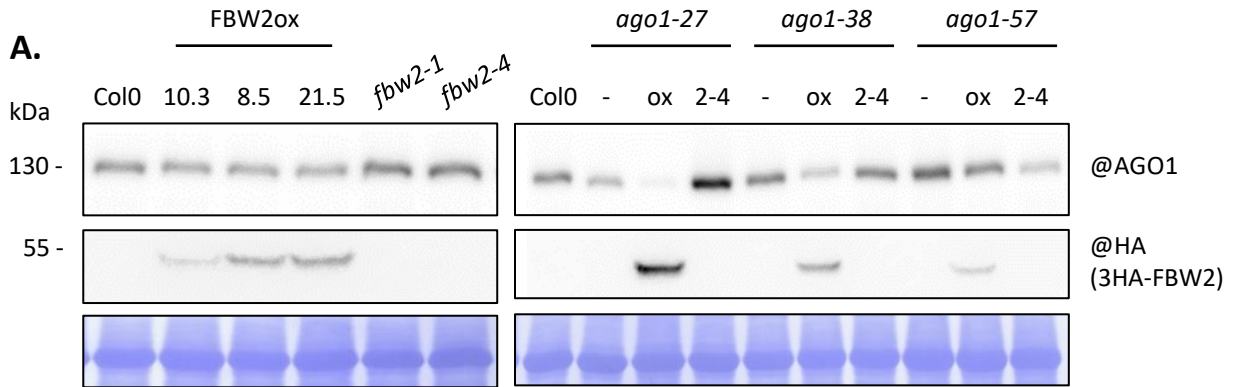
Figure 43 : Presence or absence of FBW2 affects *ago1* mutants

A. Western blot of protein extracts from 17 day-old seedlings of *ago1-27*, *ago1-38* and *ago1-57*, also crossed with *fbw2-4* or 35S:3HA-FBW2 (FBW2ox) line 10 as indicated. 10.3, 8.5 and 21.5 correspond to independent 35S:3HA-FBW2 lines. ox corresponds to the crossing with the overexpressor line 10.3, 2-4 with the mutant *fbw2-4* and – to the simple mutant. Coomassie blue staining was used as loading control and "@" indicates hybridization with the corresponding antibodies for all Western blots. The low level of AGO1 observed in *ago1-57 fbw2-4* is most probably due to a technical error as other Western blots showed stabilization of the protein.

B. Left: shape imprint of the same seedlings. Right: Measurements of the rosette area of the same seedlings. A third experiment is underway to statistically assess these data.

on nylon mesh and transferring them on fresh β-estradiol medium. In this system, AGO1 was only weakly destabilized by FBW2 and the chlorotic phenotype was not suppressed (Figure 42). This result is in line with the observations made in *Nicotiana benthamiana* transient assays and further indicates that FBW2 does not distinctly prevent AGO1 activity. In the future, the more robust silencing reporter lines L1 and Hc1 (Elmayan et al., 1998) will be tested and double transgenic lines await to be analysed.

2.3.2 FBW2 mutation restores AGO1 protein level in *ago1* mutants

As shown in Chapter 2.1.2 (Figure 24C), *FBW2* overexpression in *ago1-27* (Morel et al., 2002; Brodersen et al., 2008), *ago1-38* (Gregory et al., 2008; Brodersen et al., 2012) and *ago1-57* (Derrien et al., 2018) mutants allows a better degradation of the mutated AGO1 proteins, possibly because of higher *FBW2* expression due to impaired silencing. We next wondered whether crossing the *ago1* mutants with the null mutation of *fbw2-4* would restore AGO1 protein level in these mutants. Notably, *ago1-27* is strongly impaired in post-transcriptional RNA silencing (Morel et al., 2002) and is presumably inapt to perform translational repression (Brodersen et al., 2008). This mutant also accumulates a lower level of AGO1 protein. Interestingly, the cross of *ago1-27* with *fbw2-4* restored the AGO1 protein level and, consistently, alleviated the mutant phenotype (Figure 43B). The *fbw2-4* mutation also improved the phenotype of *ago1-38* and *ago1-57* mutants, though the quantification of this effect is still underway. Note that the weak AGO1 protein level in the double mutant *ago1-57 fbw2-4* is likely a technical problem of transfer on this particular Western blot, but this will need to be repeated. Finally, as already indicated earlier, *FBW2* overexpression in *ago1* mutants led to significant decay of AGO1 protein (Figure 43; Supp Figure 8), consequently exacerbating the growth and developmental phenotype of these mutants (Figure 43; Supp Figure 8),

Interestingly, taken together these results demonstrated that mutated alleles of AGO1 are targetted by FBW2 for degradation, and that blocking this degradation rescues partially the mutant phenotype. One possible explanation for this could be that FBW2 degrades the unloaded pool of AGO1. The disruption of its function may increase the accumulation of the AGO1 protein in *ago1-27*, allowing the assembly of
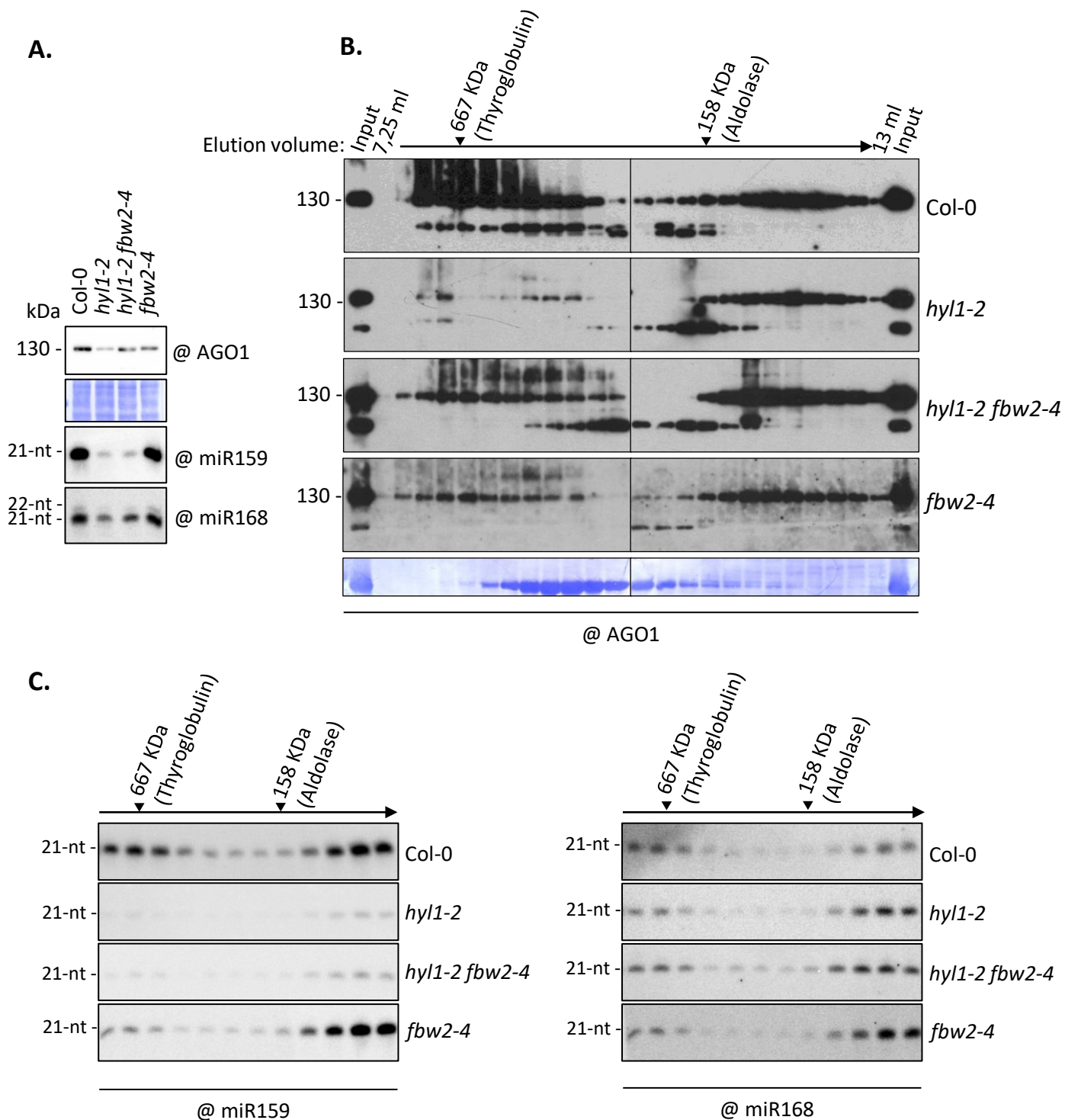
Figure 44 : Loss of *FBW2* restores high molecular weight AGO1 complexes in *hyl1-2*

Gel filtration analysis of AGO1-based RISC complexes in Col-0, *hyl1-2*, *fbw2-4* and *hy1-2 fbw2-4* 13 day-old seedlings using a superdex 200 10/300 increase column on an AKTA Pure system . Proteins of known molecular weight are shown on top of the blot. Coomassie blue staining was used as loading control and "@" indicates hybridization with the corresponding antibody or oligonucleotide probe.

A. Protein and small RNA analysis of the input fraction prior to gel filtration. Equal amounts of starting material was used for the protein blot and for the column run, as quantified by the amido black method. For analysis of the RNA, 10µg per lane was loaded.

B. AGO1 elution profile from all 24 fractions recovered, spanning 7,25 ml to 13 ml of the column. AGO1 corresponds to the signal at 130 kDa

C. Small RNA analysis from even fractions (one out of two fractions), spanning the same range.

more RISC complexes. The miR168 would, however, counteract this effect and maintain AGO1 protein homeostasis. Our results also suggest that the phenotype observed in *ago1-27* mainly results from a lower expression level of AGO1 rather than from an impaired activity due to its mutation "per se". Probably other interpretations are also possible and one may even wonder whether FBW2 has the capacity to regulate specifically aberrant activities of AGO1, as its mutation at least partially suppressed the phenotype of several alleles of *ago1*.

2.3.3 Stabilized AGO1 in mutants impaired in miRNA accumulation becomes toxic

Overall, our results indicate that FBW2 degrades the unloaded form of AGO1. However, it still remains striking and even strange that, although the *fbw2-4* mutation restored AGO1 protein level in *hyl1-2* and *hen1-6*, it worsened their phenotype. In this last results section, we aimed to understand this seeming discrepancy. As *hen1-6* and *hen1-6 fbw2-4* mutants are nearly sterile, we chose to continue only with *hyl1-2* and *hyl1-2 fbw2-4*.

- Protein complexes around AGO1 in *hyl1-2 (fbw2-4)* mutants

We first questioned if the AGO1 proteins, of which the level is restored in *hyl1-2 fbw2-4*, are functional. RISC complexes are present in high and a low molecular weight complexes (Baumberger and Baulcombe, 2005; Pantaleo et al., 2007; Csorba et al., 2010), but only the low molecular weight complex presents the slicing activity, as in animals (Nykänen et al., 2001). We thus examined the molecular weight of AGO1-based RISCs in the *hyl1-2 fbw2-4* by gel filtration, and the elution fractions were analyzed by Western blot (Figure 44). As expected, Col-0 exhibits both high and low molecular weight AGO1-based RISCs in comparable amounts. The *fbw2-4* single mutant behaves similar to Col-0 showing both types of complexes but at a lesser level of protein accumulation. As this difference could be caused by variations in transfer efficiency between the two Western blots, we decided not to take it into account. In contrast, the *hyl1-2* single mutant mainly presents low molecular weight RISCs. Thus, the loss of high molecular weight AGO1 complexes in this mutant likely results from its reduced level of miRNAs accumulation and the still present AGO1-
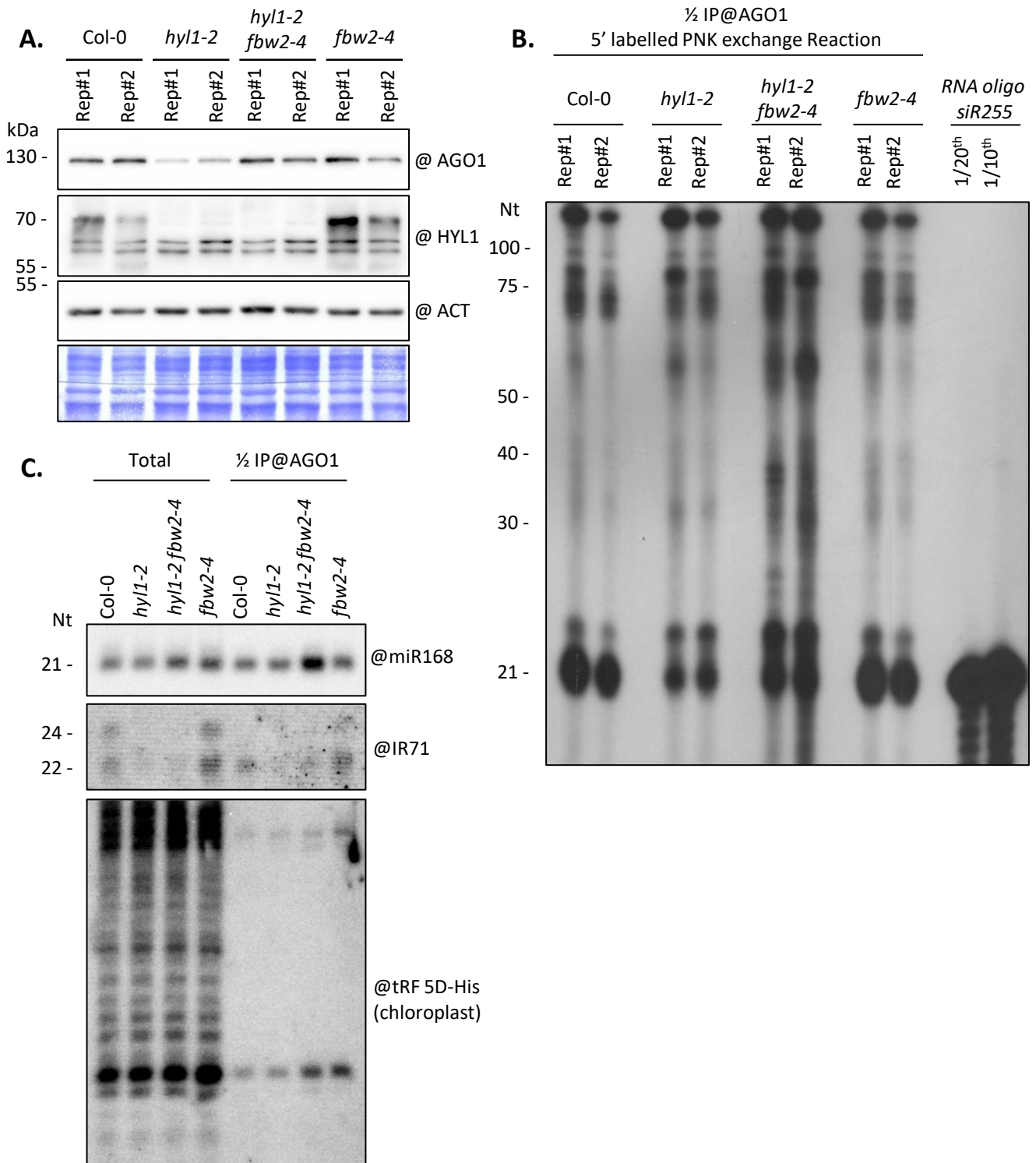
Figure 45 : Loss of *FBW2* modifies AGO1 loading in *hyl1-2*

Immunoprecipitation of AGO1 in Col0, *hyl1-2*, *fbw2-4* and *hy1-2 fbw2-4* mutants. Two biological replicates (Rep#1 and Rep#2) were made.

A. Western blot of protein crude extracts from two week-old seedlings. Coomassie blue staining was used as loading control and "@" indicates hybridization with the corresponding antibodies.

B. Denaturing polyacrylamide gel of small RNAs from immunoprecipitated AGO1. RNAs were indiscriminately labelled by replacing their 5' phosphate with a radioactive one using Polynucleotide Kinase (PNK). An oligo corresponding to the siR255 serves as control for small RNA size.

C. Northern blot of small RNAs from input and immunoprecipitated AGO1 fractions from the second replicate. "@" indicates hybridization with corresponding probes.

based RISCs are mostly involved in slicing. Interestingly, in the *hyl1-2 fbw2-4* double mutant, at least a fraction of the high molecular weight AGO1 complexes were re-established. From these results, we can speculate that the remaining AGO1 pool in *hyl1-2* consists mainly of the low molecular weight slicer complexes and that in conditions of lower content of miRNAs, a considerable amount of AGO1 is degraded by FBW2.

Based on these observations, we hypothesized that when miRNA availability is compromised and AGO1 degradation is impaired, as in the *hyl1-2 fbw2-4* double mutant, stabilized AGO1 might associate with some 'aberrant' RNAs, that would not exist under normal conditions. This unconventional AGO1-bound RNA may still be incorporated in RISCs, as supported by our gel filtration assay. However, it could ultimately become toxic for the plant, as supported by the more severe phenotype in *hyl1-2 fbw2-4* and *hen1-6 fbw2-4* (Figure 33).

- Global analysis of AGO1-incorporated sRNAs in *hyl1-2 (fbw2-4)*

To identify these putative unconventional AGO1-bound RNA, we first assayed the global RNA-binding activity of AGO1 in *hyl1-2* and *hyl1-2 fbw2-4*. To do so, we immunoprecipitated AGO1 from the different genetic backgrounds and indiscriminately labelled the incorporated RNAs by replacing their 5' phosphate with a radioactive one, using a Polynucleotide Kinase (PNK) (Figure 45A). As expected, the *hyl1-2* mutant showed a reduced amount of miRNA loaded in AGO1 while the pattern of RNA associated to AGO1 in *fbw2-4* was similar to the Col-0. Remarkably, the amount of 21/22 nt long small RNAs bound to AGO1 is re-established in the *hyl1-2 fbw2-4* double mutant and, in addition, another class of longer RNAs (going up to 75 nt) also appeared associated to AGO1 in this mutant.

In order to get more insights regarding the identity of small RNAs bound to AGO1 in the *hyl1-2 fbw2-4* double mutant, we performed deep-sequencing analyses on total sRNAs and AGO1-associated sRNAs in our different mutants. AGO1 protein level in the different mutants was beforehand verified by Western blot (Figure 45B). As expected, AGO1 protein amount was low in the two replicates of *hyl1-2*, but re-established in the *hyl1-2 fbw2-4* double mutant. An antibody against HYL1 also
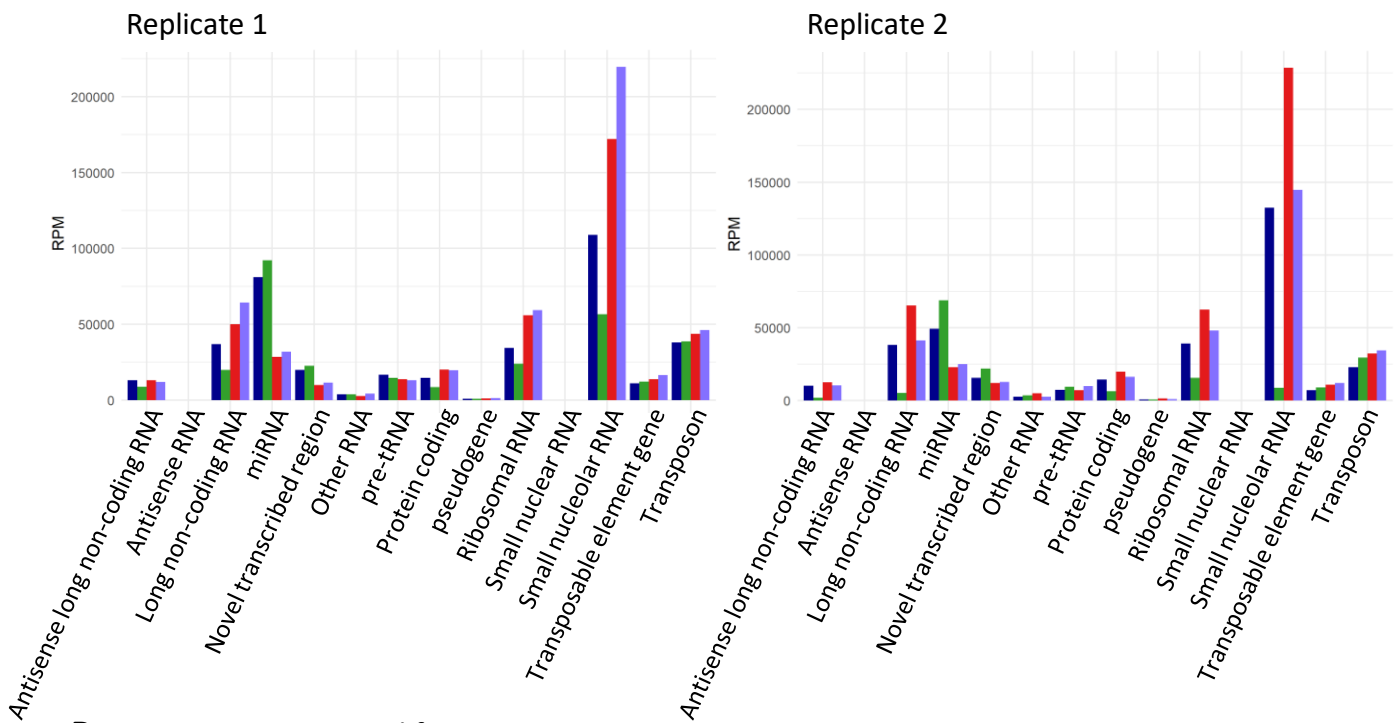
A. Total fractions
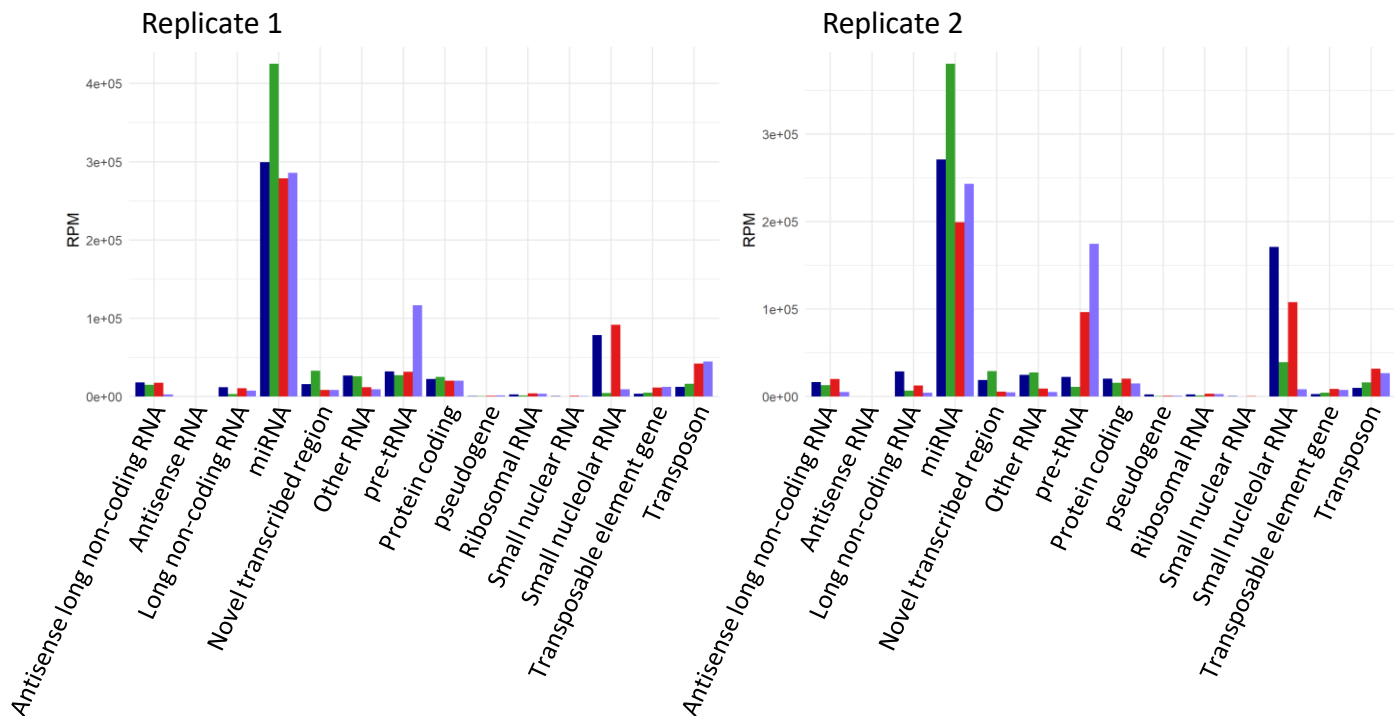
Figure 46: Quantification of the mapped reads from the RNA seq libraries

Abundance of normalized reads (RPM, read per million) mapped against the 14 annotation categories of Araport11 in the different RNA-seq libraries (- intergenic). Col0 is shown in dark blue, *fbw2-4* in green, *hyl1-2* in red and *hyl1-2 fbw2-4* in light blue.

A. Analysis of the total RNA.
B. Analysis of the AGO1 associated RNA.

Color code
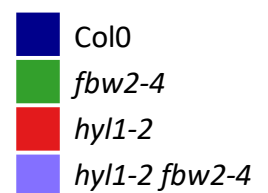
- ■ Col0
- ■ *fbw2-4*
- ■ *hyl1-2*
- ■ *hyl1-2 fbw2-4*
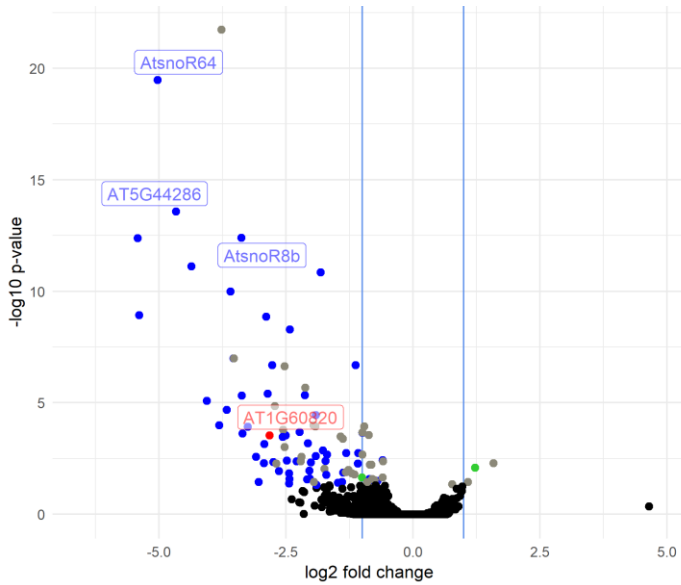
Figure 47:

Differential analysis of the mapped reads from the RNA seq libraries

Volcano plots of the differentially represented loci in the indicated libraries compared to Col0. The blue bars indicate a log2 fold change inferior or superior to 2. Black dots correspond to reads with a p-value superior or equal to 0.05, gray or colored dots correspond to reads with a p-value inferior to 0.05. Green indicates miRNAs genes, red pre-tRNAs genes and blue small nucleolar RNAs genes.
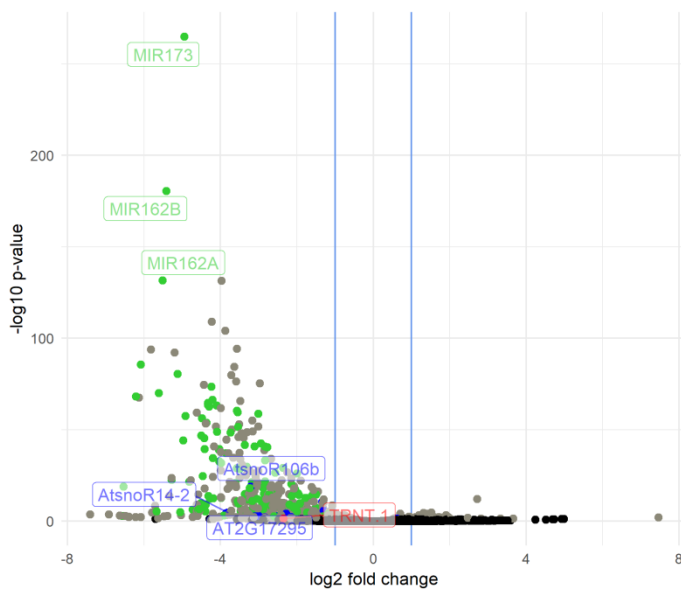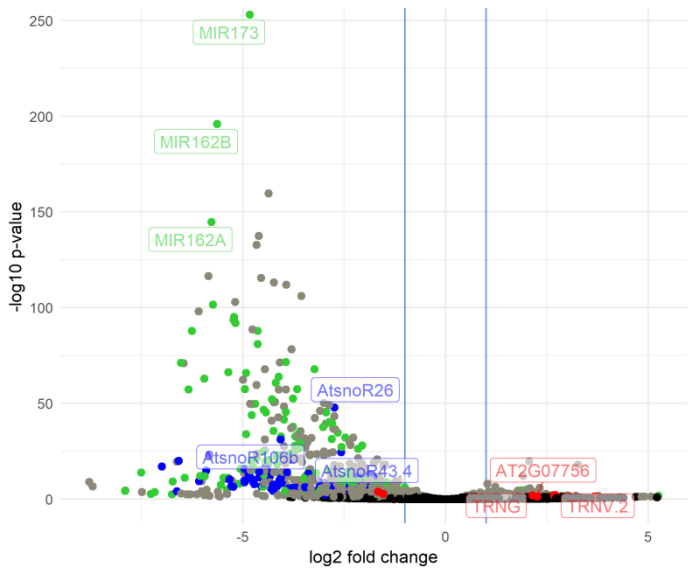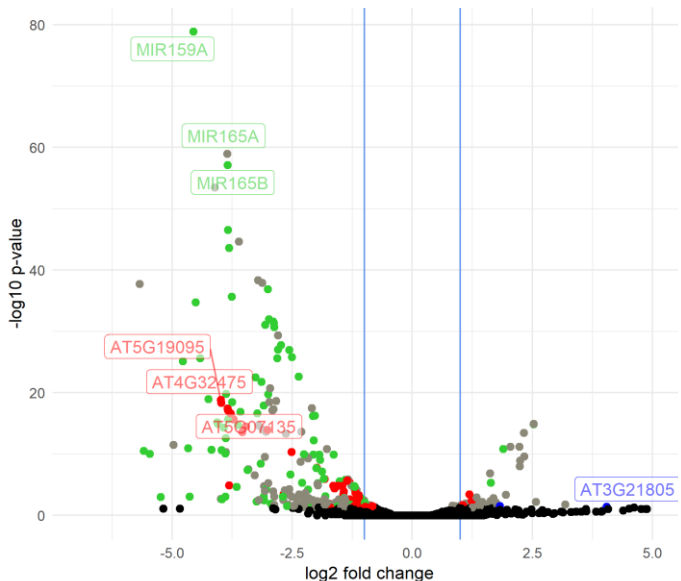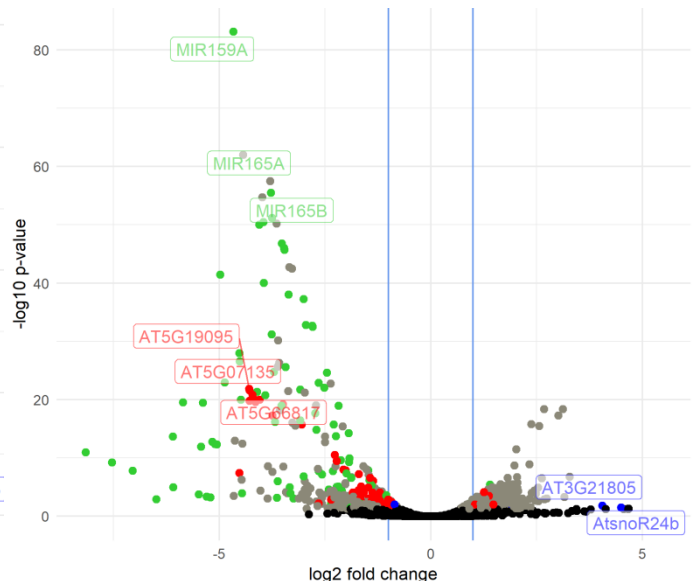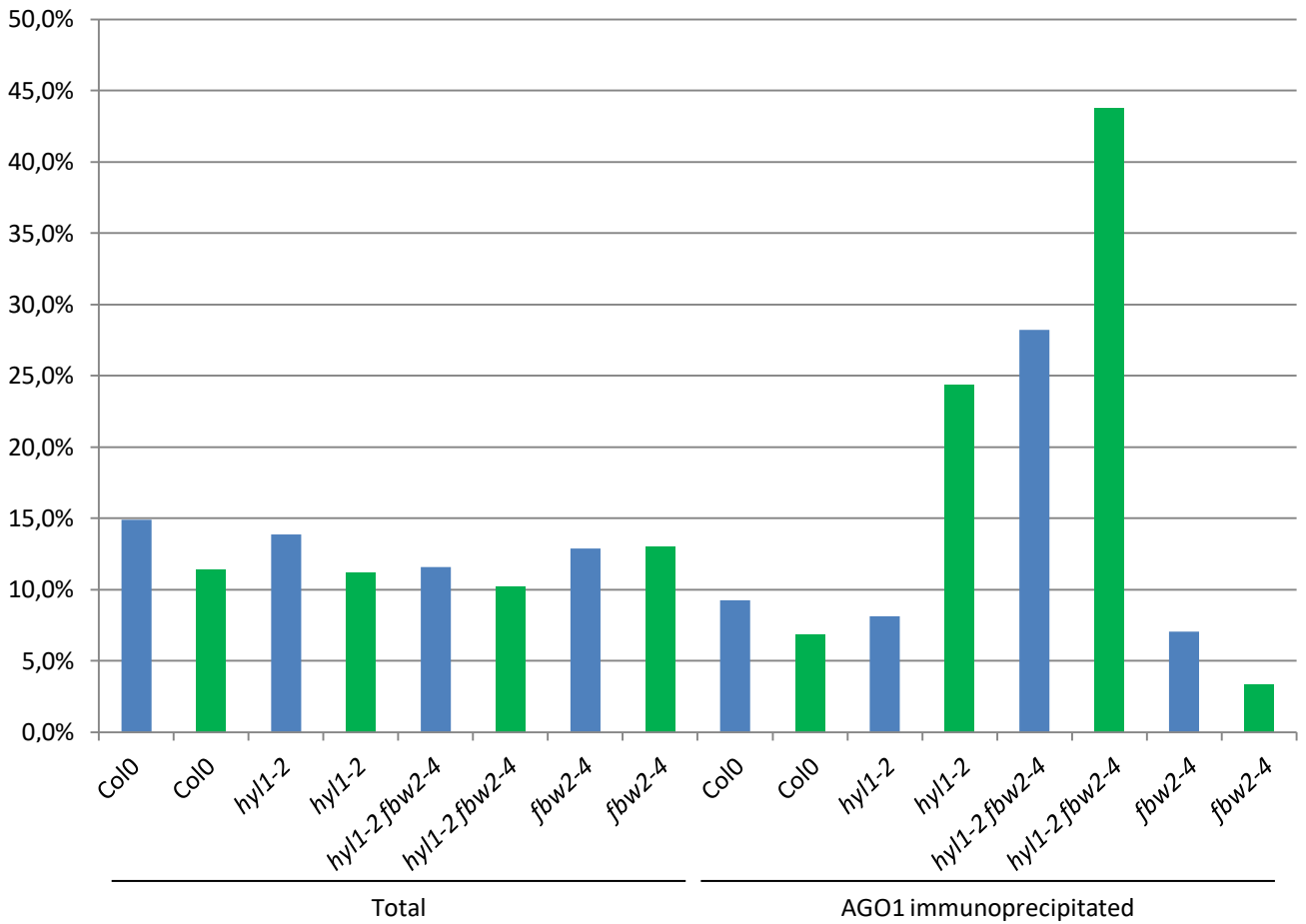
Figure 48 : tRFs associated with AGO1 are enriched in the *hyl1-2 fbw2-4* double mutant

Bar plot showing the percentage of reads mapping to tRFs in the RNA-seq libraries. Replicate one is indicated in blue, replicate two in green. Total RNA fractions are on the left, AGO1 immunoprecipitated fractions are on the right.

confirmed the absence of the protein in these mutants. Interestingly, analysis of the miR168 amount by Northern blot shows that it is enriched in the AGO1 IP fraction of the double mutant (Figure 45C). This observation suggests that although AGO1 is more prone to repress its own expression in *hyl1-2 fbw2-4*, its protein level still remains high.

The RNA sequencing analysis was performed on small RNAs whose size is comprised between 15- and 75-nucleotides. The reads were aligned on the 69 355 genomic loci annotated in Araport11 (without allowing mismatches) and counted by the shortstack program (Johnson et al., 2016). The differential analysis was carried out on the summed reads per loci with the R DESeq package (Anders and Huber, 2010). The full analysis of these results is still underway.

Overall, our analysis showed that in total small-RNA fractions of the *hyl1-2* mutant, the number of reads mapping miRNAs is, as expected, reduced at least twice (Figure 46A). However this number is comparable to Col-0 when considering only the AGO1-bound fractions (Figure 46B and Supplementary Figure 10). Moreover, the differential analysis revealed that the majority of the differential reads comparing *hyl1-2* to Col-0 corresponds to miRNAs both in the total and the IPs fractions (Figure 47). The same miRNAs are similarly misregulated in the *hyl1-2 fbw2-4* double mutant. These results further indicate that loss of FBW2 does not rescue the *hyl1-2* mutation on the molecular level.

Interestingly, reads mapping pre-tRNA are enriched to a level approaching the miRNAs in the IPs of *hyl1-2* and even further in the IPs of *hyl1-2 fbw2-4* (Figure 46B). However, the reads corresponding to the pre-tRNA were not present in the differential analysis with a P-value threshold set to 5 %, probably caused by the variability in the replicates. Because the shortstack analysis did not take into account mismatches in pre-tRNA, we carried out additional analyses on the raw reads with homemade tools (Cognat et al., 2017). These analyses have confirmed that the reads mapping pre-tRNAs correspond to tRNA-derived RNA fragments (tRFs) and are enriched in *hyl1-2* in one library and even further in *hyl1-2 fbw2-4* in both libraries (Figure 48). tRFs have been previously found loaded in AGO1 and are thought to target TE transcripts (Loss-Morais et al., 2013; Martinez, 2018). Their relation to the

phenotype of *hyl1-2* and *hyl1-2 fbw2-4* is however not yet understood and will require further investigations. In particular, the link between the simple *hyl1-2* and tRFs needs to be further verified as it was only observed in one replicate out of two.

Notably, a high number of reads corresponding to 75-nt fragments of small nucleolar RNAs (snoRNAs) are found in the AGO1 IPs (Figure 46 and Supplementary Figure 10). This class of RNA is probably underrepresented as the deep sequencing analysis stopped at 75 nt RNA size.

Discussion and outlooks

Post-translational regulation of ARGONAUTE proteins has remained a complex topic since their discovery (Johnston and Hutvagner, 2011; Jee and Lai, 2014). Both the proteasome and the autophagy have been shown to participate in their degradation (Johnston et al., 2010; Gibbings et al., 2012; Smibert et al., 2013; Martinez and Gregory, 2013; Chinen and Lei, 2017). In plants, the F-box protein FBW2 has been shown to regulate AGO1 activity and stability in a proteasome-independent manner (Earley et al., 2010) reminiscent of the viral suppressor of silencing P0, well studied in the laboratory (Derrien et al., 2012). The objectives of my thesis were to investigate the mode of action of FBW2 and its consequences, if any, on RNA silencing. During my thesis, I demonstrated that FBW2 is a *bona fide* F-box that interacts with and trigger the degradation of AGO1. I could also show that FBW2 does not targets AGO1 indiscriminately and only weakly interferes with its activity. In this last chapter, I will discuss the results obtained so far and present some perspectives.

1 FBW2 expression, stability and AGO1 decay

One major challenge encountered during this study has been to achieve both stable expression of the *FBW2* mRNA as well as stable FBW2 protein amount, possibly for different reasons.

One of the encountered problems seems to be pervasive silencing of FBW2 transgenic copies in stable plant lines, and more particularly of the inducible XVE:3HA-FBW2 construct (Figure 24B), a phenomenon that is not observed when P0 is expressed with the same system. If indeed FBW2 acts like P0 and efficiently shuts down the effector phase of silencing in virtue of degrading AGO proteins, then it is surprising that the transgene would in turn be silenced. One explanation would be that PTGS of the FBW2 transgene is achieved before requirements have been met for FBW2 to efficiently degrade AGO1 (see Discussion part 3).

No change of *FBW2* transcript levels can be observed in the RNA silencing mutants tested (Figure 24E). Also, in the earliest time point of the kinetic experiments, 3HA-FBW2 is expressed 60 times more than the endogenous copy while the tagged protein is clearly visible (Figure 24A and B) attesting that primary expression is not at fault. Yet no destabilisation of the AGO1 protein is observed at

this time point, which would suggest that strong expression of FBW2 is not the sole determinant of AGO1 degradation. To assess the full impact of sense-PTGS on this inducible system, the XVE:3HA-FBW2 line has been crossed to a *rdr6* (*sgs2-1)* mutant (Elmayan et al., 1998), in which production of putative secondary siRNA from the transgene is expected to be absent.

In contrast to the inducible lines, partial AGO1 destabilization could be robustly achieved with constitutive overexpression of FBW2. These plants express 30 times more FBW2 (Figure 31 B). Despite several attempts, plants expressing even higher amount of FBW2 were not obtained (Figure 25B and data not shown). Still, a 30-fold increase in expression affects AGO1 protein in a reproducible manner while a 60-fold increase does not in the kinetic experiments (Figure 24B). This suggests that, when FBW2 is expressed at medium but constant rates, its action is more effective to destabilize AGO1, than when an initial higher amount of FBW2 is followed by quick disappearance. However, previous findings show that the presence of a 35S:FBW2 transgene leads to a majority of plants with *ago1*-like phenotypes and a strong decrease of AGO1 protein levels (Earley et al., 2010). This is in partial disagreement with our findings and with the fact that in our hands overexpressing plants had no noticeable phenotypes. In the study of Earley et al., a genomic construct from the ATG to the stop of FBW2 was used. Unfortunately, no information regarding FBW2 transcript levels is included in that study, precluding any comparison with the lines used in this thesis. Presence of an intron in the cloned YFP-FBW2 (iFBW2) seems to enhance expression, as shown in Figure 23. Indeed, introns can contain regulatory elements improving their expression (Emami et al., 2013; Gallegos and Rose, 2015). Thus, constructs carrying genomic FBW2 will be employed in future studies.

The discrepancy between the results obtained by using either the 35s driven or the inducible XVE driven FBW2 could further be explained by the second encountered challenge: the fact that FBW2 is an unstable protein, with a half-life of approximately 30 minutes only (Figure 26). This could partly explain the fast disappearance of the FBW2 protein in the kinetic experiments, in which expression is not sustained overtime. Thus, in order to be detectable, AGO1 decay might require a constant action of FBW2. As FBW2 is regulated by the ubiquitin-proteasome system, it would be interesting to engineer a non-ubiquitinable version of FBW2 by mutating
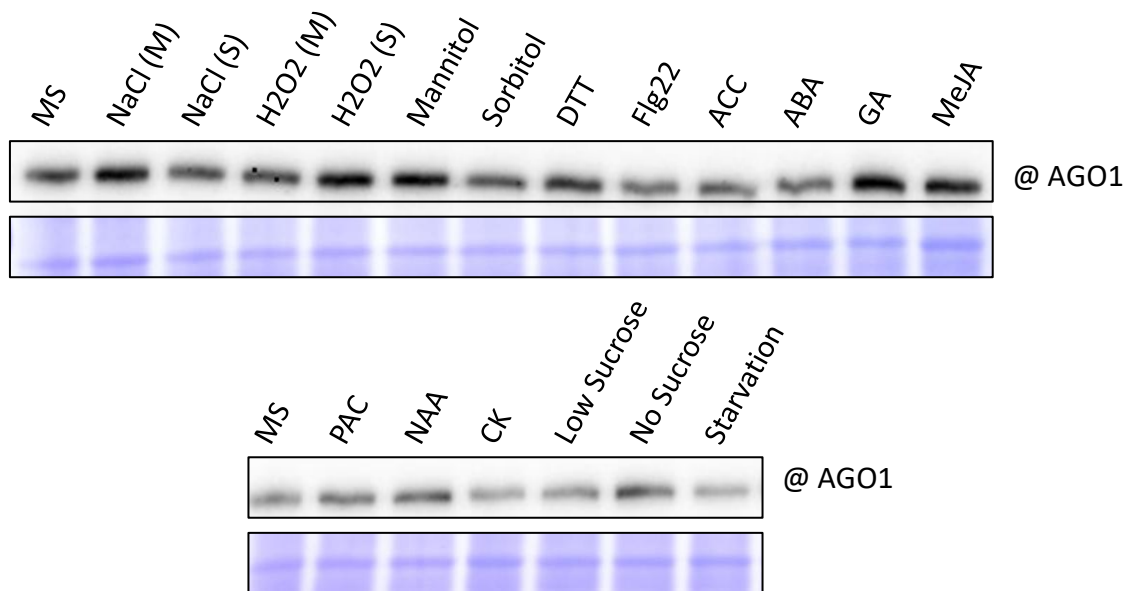
Figure 49 : AGO1 steady state protein level varies depending on growth conditions

Western blots of proteins extracts from 7 day-old seedlings grown on MS medium and subjected to the indicated stresses for 24 hours. Respectively ; 50 mM NaCl (M), 100 mM NaCl (S), 1 mM H2O2 (M), 1.5 mM H2O2 (S), 100 mM Mannitol, 50 mM Sorbitol, 1 mM dithiothréitol (DTT), 1 µM flagellin (flg22), 5 µM 1-Aminocyclopropane-1-carboxylic acid (ACC), 50 µM abscisic acid (ABA), 10 µM gibberellic acid (GA), 10 µM methyl jasmonate (MeJA), 0.5 µM naphthaleneacetic acid (NAA), 0.5 µM cytokinin (CK), 2 g/L sucrose instead of 10 g/L (Low sucrose), 0 g/L sucrose (No sucrose), 0 g/L sucrose and obscurity (Starvation). Coomassie blue staining was used as loading control and "@" indicates hybridization with the AGO1 antibody.

its lysine residues. Would this non-degradable FBW2 be more efficient at destabilizing AGO1?

Is FBW2 overall abundance important for AGO1 regulation? Infiltration of very different quantities of FBW2-coding plasmid in *Nicotiana benthamiana* has little effect on AGO1 decay, which was of similar efficiency yet always incomplete (Figure 32). Strikingly, suppression of silencing by FBW2 was only minimal as displayed by patch assay, despite degradation of a Flag-NtAGO1 to a similar level to that observed for P0-myc in the same experiment (Figure 41). These observations suggest that only a subset of AGO1 is susceptible to FBW2, regardless whether AGO1 from *N. tabacum* or Arabidopsis was used. Finally, it is noteworthy to mention that endogenous expression level seems to be far from being sufficient to overcome FBW2 instability. This is illustrated by the Venus-FBW2 construct under the control of the FBW2 promoter, that only allows poor detection of the fusion protein in few cells (Figure 22). Therefore, unless some element greatly improves its promoter activity, FBW2 function *in planta* might simply not be to destabilize AGO1 at any given time and location. With respect to the notion that degradation of AGO1 might be required in certain conditions, we have found that AGO1 protein level is markedly reduced in various stress conditions (Figure 49). In turn these experiments suggest that at least one other degradation process might exist besides FBW2, as destabilization of AGO1 was still achieved in the *fbw2-4* mutant.

2 FBW2 interaction with AGO1

Although the non-genomic construct of FBW2 only mildly affected AGO1 protein level, an interaction could be observed by co-immunoprecipitation *in planta*, and further confirmed by yeast two-hybrid experiments (Figures 27 and 28). In both cases, the interaction was weak, mirroring AGO1 decay. The *in vivo* interaction could only be detected when MLN4924 was added, a drug that inhibits neddylation of the CULLIN1 and therefore restricts the complete cycle of target association and ubiquitination. This suggests that the interaction is transient and/or scarce enough to not be detected unless AGO1 and SCF^{FBW2} are artificially stacked together.

Therefore, it would be interesting to see if this interaction can be improved by additional means. Since FBW2 is subjected to regulation through the ubiquitin-26S

proteasome system (Figure 26) and that increased stability is observed when its F-box domain is mutated or deleted (Figure 29), it is likely that FBW2 catalyses its own ubiquitination, like it is the case for other F-box proteins (Li et al., 2004; Zhou and Howley, 1998; Galan and Peter, 1999). Can the interaction between AGO1 and FBW2 be improved by using these stable mutant versions, thereby establishing that both the F-box and the target form a complex before entry into the SCF and are likely co-degraded even if through separate pathways? This hypothesis will soon be tested, as transgenic plants expressing these constructs are close to be established.

Alternatively, the interaction could possibly be improved by rendering the target more susceptible to FBW2, perhaps by using missense mutants of AGO1, that display increase turnover in the presence of FBW2 compared to the wild type allele (Figure 43 and Supplementaty Figure 8). This would also help clarify whether AGO1 mutants appear more unstable because of increased FBW2 expression or rather because they are more targeted by FBW2 (see Discussion part 3 and 4)

The search for the FBW2 degron of AGO1, *i.e.* the minimal element within a protein that is sufficient for recognition and degradation (Varshavsky, 1991), by expressing separate AGO1 domains in presence of FBW2 led to the identification of both the PAZ and the MID-PIWI regions (Figure 35 and Supplementary Figure 6), two modules that are on separate lobes of the AGO1 protein (Poulsen et al., 2013). It is noteworthy that both these modules participate in a basic requirement of AGO proteins: anchoring of the mature small RNA. Indeed the 5' monophosphate extremity of the small RNA is bound to a composite pocket located at the interface of the MID and PIWI domains (Frank et al., 2010; Nakanishi, 2016), while the PAZ domains anchors the 3' end through its sugar-phosphate backbone (Elkayam et al., 2012; Nakanishi et al., 2012; Schirle and MacRae, 2012). It is therefore tempting to postulate that FBW2 recognises a specific conformation of AGO1 that is intimately linked to its ability to bind small RNA. This is in agreement with the fact that FBW2 seems to interact directly with the C-terminal half of AGO1 that contains the MID-PIWI module, but not with the fact that the PAZ domain on its own is degraded by FBW2 in a transient expression system while the N-terminal part of the protein did not interact with FBW2 in Y2H.

The degradation of the MID-PIWI domains was the strongest and comparable to that of AGO1 full length. Interestingly, the hydrophobic GW-binding pocket, that can accommodate two tryptophan residues (Till et al., 2007; Schirle and MacRae, 2012; Elkayam et al., 2017), is also found within this region. A putative ago hook motif was predicted at the C-terminal end of FBW2 (Karlowski et al., 2010; Zielezinski and Karlowski, 2011). This region is required for FBW2-mediated AGO1 decay (Figure 29) and mutation of the tryptophan residues within reduces AGO1 degradation (Figure 37). This suggests that FBW2 interacts with AGO1 through an ago hook motif. While only one GW motif was predicted, four other tryptophan residues can be found in this portion of the protein (residues 225, 258, 275, 295, 313) (Supplementary Figure 7). Except for W313, all are flanked by amino acids that have proved to provide a context good enough for the hook motif of TNRC6B to bind hAGO2 (Pfaff et al., 2013). Moreover, the tryptophan residues are spaced by approximately 20 amino acids in an unstructured region, a characteristic also found in mammalian GW proteins (Pfaff et al., 2013; Elkayam et al., 2017). Taken together, these observations suggest that the presence of an ago hook motif in the C-terminal region of FBW2 is required for recruitment of ARGONAUTES to the E3 ubiquitin-ligase. Further interaction assays will be done to validate this hypothesis, both *in vitro* and *in vivo*. If this proves true, FBW2 would embody a novel targeting strategy employed by a F-box to bind its target in a selective manner, as well as a classical example of the modular nature of protein organization.

3 Targeting of unloaded AGO1

The stability AGO proteins has been extensively linked to their loading state. *Drosophila* AGO1 and mouse AGO2 homeostasis depend on small RNA availability (Smibert et al., 2013). The incorporation of small RNAs in AGO proteins is an energy consuming, active process that requires chaperoning, that for fly AGO2 is performed in a manner reminiscent of mammalian steroid hormone receptors binding to their ligand (Iwasaki et al., 2015). Requirement for the HSC70/HSP90 chaperone machinery to load AGO proteins seems conserved across eukaryotes, as analogous mechanisms have been described in mammals (Iwasaki et al., 2010), ciliates (Woehrer et al., 2015) and plants (Iki et al., 2010). Accordingly, inhibition of HSP90

activity destabilizes human AGO1 and AGO2 proteins (Johnston et al., 2010). Plant AGO1 seems to share these characteristics: mutants impaired in small RNA synthesis present reduced levels of AGO1 protein (Derrien et al., 2012 ; Figure 33; Supplementary Figure 8) and inhibition of HSP90 activity also impacts AGO1 stability (Figure 34).

Several observations suggest that FBW2 activity depends on the loading state of AGO1. 1), FBW2 specifically destabilize the domains responsible for the anchoring of the small RNAs (Figure 35 and Supplementary Figure 6). 2) Although *fbw2* mutants or FBW2 overexpressing plants have no obvious phenotype, they strongly worsen the developmental defects of the mutants *hyl1-2* and *hen1-6*, which are knock-outs for components of small RNA biogenesis (Boutet et al., 2003; Han et al., 2004; Vazquez et al., 2004a; Yu et al., 2005; Dong et al., 2008; Szarzynska et al., 2009; Ren et al., 2014), while clearly affecting the overall amount of the AGO1 protein (Figure 33), something that was hard to achieve in a wild type background. This suggests that in small RNA depleted conditions, maintenance of the proper homeostasis of AGO1 is important, and that it is at least partly achieved through the degradation mediated by FBW2. Likewise, P0 has been shown to target unloaded AGO proteins (Csorba et al., 2010) and this mode of action is consistent with its role as a suppressor of silencing. If FBW2 also targets the unloaded form of AGO1, why does it not display the same activity as P0? A likely hypothesis could be that, before loading can occur, AGO1 is protected from FBW2 by an unknown element, like a post-translational modification or a protein interactor.

In this regard, it is noteworthy to mention that *fbw2-1* was originally identified in a genetic screen for suppressors of the *sqn-1* mutant phenotype (Earley et al., 2010). SQUINT (SQN) is a co-chaperone protein that acts with HSP90 in the loading process of small RNAs in AGO1 (Smith et al., 2009; Earley and Poethig, 2011). Interestingly, SQN is not strictly required but facilitates AGO1 loading in a semi *in vitro* system (Iki et al., 2011), while *in planta*, loss of SQN partially impairs miRNA activity and consequent mRNA target gene expression (Smith et al., 2009). Overexpression of FBW2 in *sqn-1* shows an enhanced destabilization of AGO1 and severe alteration of the phenotype (Figure 33). Here again, the genetic interaction between FBW2 and SQN indicates the loading step as a key element for FBW2-

mediated AGO1 decay. It is therefore possible that it is in fact the association of SQN to AGO1 that inhibits recognition by FBW2, and prevents AGO1 degradation. To test this hypothesis, it would be interesting to see if the interaction between FBW2 and AGO1 is improved in the *sqn-1* genetic background by co-immunoprecipitation. Also, what would be the impact of SQN overexpression on FBW2 activity? Could the *sqn-1* phenotype be caused by an improved activity of FBW2?

To this day, little is known about precise amino acid modifications of AGO1 (see Introduction part 3.3.1), except for the phosphorylation of the serine residue 1001, that has been recovered from AGO1 immunoprecipitates (see Results part 2.2.3). Phosphomutant versions of AGO1 were designed to assess the importance of this phosphorylation in FBW2-mediated AGO1 decay. Transient expression experiments in *Nicotiana benthamiana* clearly showed that both constructs were degraded as well as the wild type protein (Figure 36), demonstrating the irrelevance of this modification for FBW2 activity. Other phosphorylation sites have been identified on human AGO2 and some are linked to the loading state of AGO2. For example, phosphorylation of the tyrosine residue 529 prevents the binding of small RNAs (Rüdel et al., 2011). Is this modification conserved on Arabidopsis AGO1? Could it affect AGO1 susceptibility towards FBW2? This residue is well conserved among AGO proteins (Data not shown, but see Figure 14) and a site-directed mutagenesis could be done to generate the relevant phosphomutant versions of AGO1.

In striking contrast to FBW2, GW proteins have been shown to favour interaction with the loaded form of AGO proteins. It was recently demonstrated that binding of the GW protein hGW182 to the PIWI domain favours the guide-loaded over the RNA-free form of hAGO1, which suggests that GW182 only engages with productive AGO molecules in order to form a functional silencing complex (Elkayam et al., 2017). In *Schizosaccharomyces pombe*, the GW protein TAS3 interacts exclusively with the loaded form of AGO1 (Holoch and Moazed, 2015). In this study, the authors propose a model in which GW proteins reject the unloaded form of AGO proteins that could otherwise act as sponges for the GW proteins and downstream factors required for silencing, and would result in unproductive RISCs. If AGO co-factors are limiting, what would occur in the case of an excess of AGO proteins?

AGO1 homeostasis is already maintained by the miR168 self-regulation loop, and its importance in achieving proper silencing activity is evidenced by the aberrant development of 4m-AGO1 plants that lack this regulation (Vaucheret et al., 2004). It is possible that FBW2 is also implicated in the maintenance of a certain homeostasis of the AGO1 protein, at the post-translational level. This activity would be primarily to avoid titration of RISC components by unloaded and therefore unproductive AGO1 moieties. Could then FBW2 modulate the 4m-AGO1 phenotype? The *fbw2-1* mutant and FBW2 overexpressor lines have been crossed with this AGO1 mutant and the progeny is about to be characterized. The hypothesis of deleterious inactive AGO1 proteins is further supported by the observation that stabilization of AGO1 in the *hyl1-2* and *hen1-6* single mutants in absence of FBW2 worsens their phenotypes (Figure 33A). Investigations regarding the understanding of this phenomenon are discussed in part 6. .

Finally, since FBW2 harbours an ago hook motif, one could imagine that it would compete with GW proteins for interaction with AGO1. Hence, it is possible that small RNA loaded AGO1 proteins are in fact protected from FBW2 degradation by their competitive binding to GW proteins. A GW protein named SUO has been identified in plants and proposed to play the same role as animal GW182 (Yang et al., 2012). While the *suo-2* mutation does not produce striking developmental defects, combination of the *suo-2* mutation with mutants impaired in miRNA biogenesis produces severely affected plants, reminiscent of the *hen1-6* mutant overexpressing FBW2 (Supplementary Figure 11). FBW2 could then be responsible for the observed phenotype of the *suo-2* plants that would lack the protective effect of SUO bound to AGO1, and would lead to spurious degradation of AGO1 RISC. It would then be interesting to study the genetic interaction between SUO and FBW2 by crossing the *suo-2* mutant with our diverse FBW2 lines.

4 FBW2 weakly affects AGO1 silencing activities

Despite the weak effect of FBW2 on the steady state level of the AGO1 protein, we could observe an effect on the efficiency of RNA silencing. Indeed, FBW2 overexpression led to fewer amount of the two tested microRNAs: miR168 and

miR403, while loss of FBW2 had the opposite effect. This is consistent with the fact that the level of AGO1 is decreased, which would in turn lead to destabilisation of the loaded miRNAs. In turn, downstream action of mir403-RISC seems to be perturbed, since the level of the AGO2 protein is clearly increased in the FBW2 overexpressor (Figure 31). This is reminiscent of the *ago1-27* mutant, in which RISC action is impaired and both *AGO2* mRNA and AGO2 protein levels are increased (Derrien et al., 2018). *AGO1* mRNA levels are also increased in FBW2 overexpressing plants, which also suggests impairment of the miR168-RISC activity. This is an effect that is also observed upon P0-myc induction in which *AGO1* level can rise 6-fold (Derrien et al., 2018), and in diverse miRNA deficient mutants (Derrien et al., 2012).

Patch assay experiments in *Nicotiana benthamiana,* where the fluorescence of the GFP acts as reporter for the silencing activity, were conducted to assess FBW2 silencing suppressor activity (Figure 41A). Quantification of the GFP signal shows that FBW2 overexpression alleviates around 10 % of the silencing directed against the GFP while P0 reached 90 % of silencing suppression (Figure 41B). As such, we qualified FBW2 as a weak suppressor of silencing.

On the other hand, the effect of FBW2 is much stronger in missense *ago1* mutants. We observed a general tendency to rescue the *ago1* phenotype by the removal of FBW2, while its addition led to increased severity of the phenotype (Figure 43B). This was particularly striking for the *ago1-27* mutant, which is the most affected mutant of the three alleles we tested. This suggests that FBW2 can strongly influence AGO1-mediated silencing if the latter is already partly crippled. While the precise effect of most of the missense mutations found in AGO1 are not known, many alleles seem to share a certain degree of small RNA loading defect, as evidenced by the overaccumulation of unloaded small RNA duplexes in the total RNA fraction in these mutants (Arribas-Hernández et al., 2016; Derrien et al., 2018). Once again, these observations strongly suggest that FBW2 exhibits a strong preference for unloaded AGO1 molecules (see Discussion part 3).

5 Degradation pathways

The mechanism controlling the stability of AGO proteins seems to be linked to the ubiquitin mediated proteolysis. Animal AGO2 has been shown to be subjected to proteasomal degradation (Johnston et al., 2010; Chinen and Lei, 2017) but also to degradation in the lysosome (Martinez and Gregory, 2013; Gibbings et al., 2012). As such, E3 ubiquitin ligases have been proposed to control AGO stability, although few have been formally identified. The E3 ubiquitin ligase mLin41/Trim71 has been shown to interacts with mouse AGO2 to promote its ubiquitination and control its stability (Rybak et al., 2009), but more recent studies have demonstrated that it is dispensable for AGO2 ubiquitination and rather acts in downstream post-transcriptional gene repression in embryonic stem cells (Chang et al., 2012; Chen et al., 2012). In plants, only FBW2 has been proposed to play a role in AGO1 ubiquitination so far. We consequently tried to decipher the proteolysis pathway involved in FBW2-mediated AGO1 decay.

Having identified reproducible conditions where AGO1 degradation is visible in Arabidopsis, we undertook a pharmacological approach to block known degradations pathways. Except for the MLN4924, which blocks the activity of CULLIN-based E3 ubiquitin ligases, none of the chemicals tested led to reproducible stabilization of the AGO1 protein (Figure 38). This was partly caused by the difficulty to use the chemicals and to control for their efficiency *in planta*. Having clearly established that FBW2 is degraded by the proteasome, its increased protein abundance was used as a control for successful MG132 treatment. In later experiments Bortezomib, an improved version of the MG132 (Goldberg, 2012), was added to the roster of drugs. Although further experiments have to be carried out with Bortezomib, the experiments performed so far strongly suggest that the proteasome is not responsible for AGO1 decay.

Concerning the autophagy pathway, we rather chose to make use of the *atg7-2* mutant background. ATG7 is a central protein of the autophagy pathway, that acts as an E1 activating enzyme towards ATG8 and ATG12 (Taherbhoy et al., 2011; Noda et al., 2011) and loss of ATG7 results in an inability to deliver autophagosomes to the vacuole (Marshall and Vierstra, 2018), thus providing a genetic tool in which

macroautophagy is not functioning. Intriguingly, combining genetic inactivation of macroautophagy with blockage of the proteasome with Bortezomib still failed to stabilize AGO1 but not FBW2 (Figure 39B), indicating that neither of these two pathways are in charge of AGO1 decay. In light of this result, what could then be the employed degradation pathway?

The macroautophagy is only one of several ways to direct a protein to the lytic compartment, and evidences for additional trafficking routes have been described in animal systems. Of particular interest is a process resembling autophagy that operates in late endosomal multi vesicular bodies (MVBs), transporting cytosolic proteins to the lysosomes. This proteolysis was thus termed endosomal microautophagy, and involves HSP70 for selection of cargo proteins (Sahu et al., 2011). Interestingly, HSP70 is part of the AGO loading complex in many eukaryotes (see Discussion part 3), and might provide the basis for AGO1 degradation by a related process in plants.

An Alternative possibility would be that AGO1 is degraded from a particular sub-cellular location. Indeed, AGO1 is associated to the Endoplasmic reticulum, where it appears to fulfil at least some of its PTGS functions (Li et al., 2013, 2016), and an additional degradation pathway emerge from this organelle. Misfolded proteins are known to be degraded by the Endoplasmic reticulum (ER)-associated protein degradation (ERAD) (Vembar and Brodsky, 2008). In this case also, HSP70 chaperone can play a role at the substrate recognition step (Park et al., 2007) while targeted proteins are degraded by the ubiquitin-proteasome system.

As mentioned in the first chapter of this discussion, several degradation processes are probably regulating AGO1 homeostasis. Moreover, AGO1 steady state protein level is elevated in the mutant *atg7-2* (Supplementary Figure 9), suggesting that at least part of AGO1 is degraded by autophagy. Could the aforementioned degradation processes contribute to AGO1 homeostasis? Could redundancy between several overlapping pathways explain the difficulties encountered in destabilizing AGO1 with FBW2? At least one of such process is currently the subject of investigation in the laboratory but its link with FBW2 is currently unknown.

6 Physiological role

If FBW2 has such a limited impact on AGO1 activity, what would be its role in plants? As loss of FBW2 clearly has an impact on the plant development when small RNA biogenesis and/or stability are impaired (Figure 33), we tried to understand why stabilization of AGO1 is deleterious (Figure 44A).

RISCs are known to form complexes of varying weight and with variable activity (Baumberger and Baulcombe, 2005; Rivas et al., 2005; Pantaleo et al., 2007; Kawamata et al., 2009; Csorba et al., 2010). In plants, although it is clear that a low molecular weight complex, presumably AGO1 and a small RNA only, can perform target slicing, much less is known about the activity and identity of higher order complexes. Aiming to assess the impact of FBW2 on the repartition of AGO1 in these complexes, we performed size exclusion chromatography on the double mutant *hyl1-2 fbw2-4*. While *fbw2-4* mutants do not show any particular phenotype compared to Col0, *hyl1-2* presents a reduced content of high molecular weight AGO1-containing complexes (Figure 44B), suggesting that they are reliant on proper miRNA biogenesis. Interestingly these complexes reappear in *hyl1-2 fbw2-4*, suggesting that FBW2 was actively degrading them in *hyl1-2*. Accordingly, miR159 co-fractionates with both the low and high molecular weight AGO1-containing complexes in Col0, while in *hyl1-2* and *hyl1-2 fbw2-4* the miR159 is barely detected in any fraction (Figure 44C) probably because of its impaired synthesis (Figure 44A). This observation does not hold true for a microRNA whose abundance is only marginally affected by the loss of HYL1 (Szarzynska et al., 2009), like miR168, that is found in all mutants in high and low molecular weight complexes (Figure 44C). This shows that the reassembled high molecular weight complex present in the double mutant is available for loading with the small RNA species present in the cell. But then, with what are the *hyl1-2 fbw2-4* high molecular weight RISCs loaded with? It is noteworthy to mention that GW proteins co-localize with the high molecular weight RISCs in animals (Baillat and Shiekhattar, 2009). Here again, it would make sense that loss of interaction with GW proteins, because of absence of loading, renders the high molecular weight RISCs susceptible to FBW2 (see Discussion part 3).

In order to identify the loaded RNA species present in the stabilized AGO1 (Figure 45) we immunoprecipitated AGO1 and performed deep sequencing of the recovered RNA fraction.

One major difference between the RNA-seq libraries comes from the reads mapping to tRNAs in the AGO1 immunoprecipitated fractions (Figure 46 and Supplementary Figure 10). These are more abundant in the *hyl1-2 fbw2-4* double mutant than in the single mutants *hyl1-2* or *fbw2-4*. Further analyses performed with collaborators experts in the field, have shown that these reads actually correspond to tRNA-derived RNA fragments (tRFs) (Figure 48). tRFs have been shown to be loaded in AGO proteins and to target the transcripts of some classes of transposable elements (Loss-Morais et al., 2013; Alves et al., 2017; Martinez et al., 2017). Accordingly, tRFs are also present in the corresponding Col0 library but to a lesser extent (Figure 46B and Supplementary Figure 10). It is therefore possible that in a miRNA-depleted condition, here mimicked by the *hyl1-2* background, degradation of unloaded AGO1 by FBW2 is used as a failsafe mechanism to avoid entry of unwanted and potentially harmful RNA molecules into the RISC. In absence of the SCF^{FBW2}, AGO1 protein level would rise enough to allow incorporation of these unwanted RNA species, in this case identified as the tRF category (Figure 46A), although we cannot exclude that other RNA species could also fulfil this criterion, they have not been identified in the RNA-seq experiment (Figure 45B). In this scenario, the strong developmental phenotype observed in the *hyl1-2 fbw2-4* and *hen1-6 fbw2-4* would be caused be spurious targeting of cellular RNAs by the reprogrammed RISC. It would thus be enlightening to identify novel tRFs targets and monitor their stability in our conditions. As some tRF-5D have been reported to direct slicing of a target when loaded into AGO1 (Martinez et al., 2017)), this could be achieved by a PARE-seq analysis of the transcripts in this double mutant, although in mammalian systems, tRFs have also been reported as regulating translation (Sobala and Hutvagner, 2013; Kuscu et al., 2018).

Another striking difference between the RNA-seq libraries comes from the reads mapping to miR genes in the AGO1 immunoprecipitated fractions. AGO1-purified samples from *fbw2-4* present markedly more reads that map to miRNAs producing loci (Figure 46B). This suggests an improved capability of AGO1 to load

small RNAs in this mutant. Unfortunately preliminary differential analysis did not allow identification of particular loci corresponding to both pre-tRNAs and miRNAs as they were discarded because of insufficient statistical support (Figure 47). This could perhaps be explained if unloaded AGO1 in absence of FBW2 is made available for the loading of small RNAs, irrespective of their provenance, which would hinder detection of particular loci. Perhaps, combining these mutants of interest with stress situations were both tRFs (Hsieh et al., 2008; Cognat et al., 2017) and maybe other small RNA "bursts" would be recreated and would enable full display of the deficiency exhibited by the lack of FBW2.

Material and methods

1 Material

1.1 Bacterial strains

1.1.1 Escherichia coli

E.coli, TOP10 (Invitrogen) were used for plasmid amplification. This strain carries a mutated *recA* recombinase to minimize recombination events between plasmids and bacterial DNA.

Genotype: *F- mcrA Δ(mrr-hsdRMS-mcrBC) Φ80lacZΔM15 ΔlacX74 recA1 araD139 Δ(araleu)7697 galU galK rpsL (StrR) endA1 nupG*

E.coli, DB3.1 (Invitrogen) were used for propagating empty Gateway vectors containing the *ccdB* gene. *ccdB* gene encodes a protein that interferes with the bacterial gyrase. DB3.1 strain carries the gyrA462 allele that confers the resistance to the *ccdB* gene.

Genotype: *gyrA462 endA1 Δ(sr1-recA) mcrB mrr hsdS20 glnV44 (=supE44) ara14 galK2 lacY1 proA2 rpsL20 xyl5 leuB6 mtl1*

1.1.2 Agrobacterium tumefaciens

A.tumefaciens, GV3101 (PMP90) were used for Arabidopsis transformation. It carries chromosomal resistance to rifampicin. Gentamycin resistance is conferred by the disarmed Ti (Tumor inducing) plasmid PMP90 that encodes *vir* genes required for T-DNA transfer.

1.2 Yeast Strains

Saccharomyces cerevisiae, PJ69-4A were used for yeast-two-hybrid assays.

Genotype: MATa, trp1-901, leu2-3, -112, ura3-52, his3-200, gal4Δ, gal80Δ, LYS2::GAL1-HIS3, GAL2-ADE2, Met2::GAL7-lacZ

1.3 Plant material

1.3.1 Arabidopsis thaliana

All *Arabidopsis thaliana* plants used in this study are in Columbia-0 genetic background (Col-0). The mutants and transgenic lines used are either EMS or T-DNA insertion mutants and are listed in the table 1.

Table 1: Mutants and transgenic lines used in this study

Mutants and transgenic lines	Ecotype	Mutagenesis	Mutation	Resistance	Origin
ago1-27	Col-0	EMS	A994V		Morel et al., 2002
ago1-38	Col-0	EMS	G186R		0Gregory et al., 2008
ago1-57	Col-0	EMS	G371D		Derrien et al., 2018
atg7-2	Col-0	T-DNA	Exon	sulfadiazine	GK-655B06
fbw2-1	Col-0	EMS	P48L		Earley et al., 2010
fbw2-4	Col-0	T-DNA		kanamycine	SALK_144548
sqn-1	Col-0	EMS			Berardini et al., 2001
hyl1-2	Col-0	T-DNA		kanamycine	SALK_064863
hen1-6	Col-0	T-DNA		kanamycine	SALK_090960
GFP-AGO1 / *ago1-27*	Col-0	T-DNA	promAGO1::GFP-AGO1	Basta	Derrien et al., 2012
P0-myc	Col-0	T-DNA	XVE::P0-6myc	hygromycine	Derrien et al., 2012
SUC::SUL	Col-0	T-DNA	pSUC2:SUL-LUS	Basta	Himber et al., 2003

1.3.2 Nicotiana benthamiana

Wild type *Nicotiana benthamiana* were used for all transient expression experiments.

1.4 Vectors and binary constructs

1.4.1 pENTRY vectors

- pDONR207, pDONR221, pDONRZeo based constructs

These three pDONOR (pDONR) are relatively similar except for the different antibiotic resistance genes they carry. pDONR207 (5508 base pairs) carries a gentamycin resistance gene, pDONR221 (4762 base pairs) carries a kanamycin resistance gene and pDONRZeo (4291 base pairs) a zeocin resistance gene. All plasmids contain the *att*P1 and *att*P2 recombination sites in which a *ccd*B gene and the chloramphenicol resistance gene lie. The full sequences of these plasmids are available on www.invitrogen.com. To create ENTRY clones, the pDONR plasmids were recombined with PCR fragments (corresponding to the gene of interest) flanked by *att*B1 and *att*B2 recombination sites. All the Entry clones, based on pDONR207, pDONR221 and pDONRZeo, used in this study are described in the table 3 hereafter with the according coupled primers and DNA matrices used for the PCR amplification. The pDONR207-AGO1 and pSP-flag-NtAGO1 have been used as DNA matrices to amplify by PCR the coding sequence of AGO1 and have been provided by Benoît Derrien (previous post-doc in the laboratory). The sequences of the primers are listed in table 2. The Gateway technology is described in the methods part.

AGO1-1f	ggggacaagtttgtacaaaaaagcaggctccatggtgagaaagagaagaacg
AGO1-2f	ggggacaagtttgtacaaaaaagcaggctccatggttgaacaaggagctccc
AGO1-3f	ggggacaagtttgtacaaaaaagcaggctccatgattccggtgggccggtcc
AGO1-4f	ggggacaagtttgtacaaaaaagcaggctccatgcctgtgattcagtttgtc
AGO1-5f	ggggacaagtttgtacaaaaaagcaggctccatgggccagcggtattccaaaag
AGO1-6f	ggggacaagtttgtacaaaaaagcaggctccatgggaacggtgaataattgg
AGO1-7f	ggggacaagtttgtacaaaaaagcaggctccatggatctgcttattgtcattc
AGO1-8f	ggggacaagtttgtacaaagaaagcaggctccatgccagagacatcagacagtg
AGO1-1r	ggggaccactttgtacaagaaagctgggtcagagagttgttcaaattgctg
AGO1-2r	ggggaccactttgtacaagaaagctgggtcatacctgattctagaggtcgg
AGO1-3r	ggggaccactttgtacaagaaagctgggtcgtttgcctctatgaaggc
AGO1-4r	ggggaccactttgtacaagaaagctgggtcttcaacaatcttgcatacctc
AGO1-5r	ggggaccactttgtacaagaaagctgggtcaccattgatcattttcttattcat
AGO1-6r	ggggaccactttgtacaagaaagctgggtcaatttcttttccttgggagag
AGO1-7r	ggggaccactttgtacaagaaagctgggtcctccatgtagaatcgagccc
AGO1-8r	ggggaccactttgtacaagaaagctgggtcgcagtagaacatgacacg
ago1-4r-stop	ggggaccactttgtacaagaaagctgggtcattcaacaatcttgcatacctc
ago1-stop-attb2-r	accactttgtacaagaaagctgggtatcagcagtagaac
gwb1-ntago1-f	ggggacaagtttgtacaaaaaagcaggctccatggactacaaggatgacgatg
gwb2-ntago1-r	ggggaccactttgtacaagaaagctgggtctctaacaataaaacataaccctc
cds-fbw2-gw-b1	ggggacaagtttgtacaaaaaagcaggctggatggaagaagattgcgagtttcg
cds-fbw2stop-gw-b2	ggggaccactttgtacaagaaagctgggtgtcatggagatggtggccaaatatg
gwb1-fbw2geno-f	ggggacaagtttgtacaaaaaagcaggctggatggaagaagattgcgag
gwb2-fbw2geno-r	ggggaccactttgtacaagaaagctgggttcatggagatggtggccaaa
fbw2_f-box-r	ggggaccactttgtacaagaaagctgggtcaatgtcaatctcttgcc
fbw2_hook-f	ggggacaagtttgtacaaaaaagcaggcttaggtccacgcgtgatcgg
fbw2-BamHI-fwd	cccccggatccatggaagaagattgcgagtttcg
fbw2-NotI-rev	gtttgcggccgctggagatggtggccaaatatg
pfbw2-gw_b4-par	gtatagaaaagttgggcggaaccctagtctgaccc
pfbw2-gw_b1r-par	tttgtacaaacttggctaacaaatatctgtttcacaaaaacc
attb4-pfbw2	ggggacaactttgtatagaaaagttgggcgg
attb1r-pfbw2	ggggactgctttttttgtacaaacttggctaac
cds-fbw2-gw-b2r	ggggacagctttcttgtacaaagtggggatggaagaagattgcgagtttcg
cds-fbw2-gw-b3	ggggacaactttgtataataaagttggtcatggagatggtggccaaatatg
degronAGO1_HindIIIF	aaacaaagcttgggggatggcttgg
degronAGO1_ClaIR	tttgcatcgatgaaggctgtcgatgac
degronAGO2_HindIIIF	gctcaagctttcgtttcgggggttatagc
degronAGO2_ClaIR	attgcatcgatgaacgccaacaccgag
degronAGO4_HindIIIF	ctcaagctttggtggtaacatcttagg
degronAGO4_ClaIR	ctggaccaggatcgatgatcatggtgg
fbw2_mutw225a-f	ggaacttagaggctgtgcggacgtgcaacttg
fbw2_mutw258a-f	gatatgataaatgatgcggaggattgctgc
fbw2_mutw275a-f	ctgattacttggctgcggagttttttgaag
fbw2_mutw295a-f	gagtttgagcatggtgcggacgataattttttatgc
fbw2_mutw313a-f	ggaaccgcatattgcgccaccatctccatg
fbw2_mutw225a-r	caagttgcacgtccgcacagcctctaagttcc
fbw2_mutw258a-r	gcagcaatcctccgcatcatttatcatatc
fbw2_mutw275a-r	cttcaaaaaactccgcagccaagtaatcag
fbw2_mutw295a-r	gcataaaaattatcgtccgcaccatgctcaaactc
fbw2_mutw313a-r	catggagatggtggcgcaatatgcggttcc
fbw2_mutfbox-f	ccagatgctcttggtttagcctttagccacgcagctcttcaagaagtactaacag
fbw2_mutfbox-r	ctgttagtacttcttgaagagctgcgtggctaaaggctaaaccaagagcatctgg
ago1_mut_s1001d-s1003d-s1005d-f	ggagccagagacagacgacgatggcgacatggctagtggg
ago1_mut_s1001d-s1003d-s1005d-r	cccactagccatgtcgccatcgtcgtctgtctctggctcc
ago1_mut_s1001a-s1003a-s1005a-f	ggagccagagacagcagacgctggcgcaatggctagtggg
ago1_mut_s1001a-s1003a-s1005a-r	cccactagccattgcgccagcgtctgctgtctctggctcc
ago1_mutk507r-f	ggccagcggtattccagaagattgaatgagagacag
ago1_mutk507r-r	ctgtctctcattcaatcttctggaataccgctggcc
ago1_mutk413-415-416r-f	ctgatgctgatcgtgttaggataagaagggctcttagaggtgtc
ago1_mutk413-415-416r-r	gacacctctaagagcccttcttatcctaacacgatcagcatcag

Table 2: Primers used for cloning

Table 3: pENTRY clones generated

Gene	DNA matrix	Primers	pDONR used for BP reaction	Resulting ENTRY clone
polyQ (AGO1)	pDONR207-AGO1	AGO1-1F AGO1-1R	pDONR221	pENTRY(221)-polyQ
polyQ-ND (AGO1)	pDONR207-AGO1	AGO1-1F AGO1-2R	pDONR221	pENTRY(221)-polyQ-ND
ND (AGO1)	pDONR207-AGO1	AGO1-2F AGO1-2R	pDONR221	pENTRY(221)-ND
ND-DUF (AGO1)	pDONR207-AGO1	AGO1-2F AGO1-3R	pDONR221	pENTRY(221)- ND-DUF
ND-PAZ (AGO1)	pDONR207-AGO1	AGO1-2F AGO1-4R	pDONR221	pENTRY(221)-ND-PAZ
DUF (AGO1)	pDONR207-AGO1	AGO1-3F AGO1-3R	pDONR221	pENTRY(221)-DUF
DUF-PAZ (AGO1)	pDONR207-AGO1	AGO1-3F AGO1-4R	pDONR221	pENTRY(221)-DUF-PAZ
PAZ (AGO1)	pDONR207-AGO1	AGO1-4F AGO1-4R	pDONR221	pENTRY(221)-PAZ
PAZ-L2 (AGO1)	pDONR207-AGO1	AGO1-4F AGO1-5R	pDONR221	pENTRY(221)-PAZ-L2
L2 (AGO1)	pDONR207-AGO1	AGO1-5F AGO1-5R	pDONR221	pENTRY(221)-L2
L2-MID (AGO1)	pDONR207-AGO1	AGO1-5F AGO1-6R	pDONR221	pENTRY(221)-L2-MID

L2-PIWI (AGO1)	pDONR207-AGO1	AGO1-5F AGO1-7R	pDONR221	pENTRY(221)-L2-PIWI
MID (AGO1)	pDONR207-AGO1	AGO1-6F AGO1-6R	pDONR221	pENTRY(221)-MID
MID-PIWI (AGO1)	pDONR207-AGO1	AGO1-6F AGO1-7R	pDONR221	pENTRY(221)-MID-PIWI
MID-PIWI-Ct (AGO1)	pDONR207-AGO1	AGO1-6F AGO1-8R	pDONR221	pENTRY(221)-MID-PIWI-Ct
PIWI (AGO1)	pDONR207-AGO1	AGO1-7F AGO1-7R	pDONR221	pENTRY(221)-PIWI
PIWI-Ct (AGO1)	pDONR207-AGO1	AGO1-7R AGO1-8R	pDONR221	pENTRY(221)-PIWI-Ct
Ct (AGO1)	pDONR207-AGO1	AGO1-8F AGO1-8R	pDONR221	pENTRY(221)-Ct
polyQ-PAZ (AGO1)	pDONR207-AGO1	AGO1-1F ago1-4r-stop	pDONRZeo	pDONRZeo- polyQ-PAZ (AGO1)
L2-Ct (AGO1)	pDONR207-AGO1	AGO1-5F ago1-stop-attb2r	pDONRZeo	pDONRZeo- L2-Ct (AGO1)
AGO1 (CDS)	pDONR207-AGO1	md30-ago1-f ago1-stop-attb2r	pDONRZeo	pDONRZeo-AGO1
flag-NtAGO1	pSP-flag-NtAGO1	gwb1-ntago1-f gwb2-ntago1-r	pDONR221	pENTRY(221)-flag-NtAGO1
FBW2 (CDS)	pE2N-FBW2 (described below)	cds-fbw2-gw-b1 cds-fbw2stop-gw-b2	pDONR221	pENTRY(221)-FBW2

99

iFBW2 (genomic atg to stop)	pEG104-FBW2 (described below)	gwb1-fbw2geno-f gwb2-fbw2geno-r	pDONR221	pENTRY(221)-iFBW2
delF-box (FBW2)	pE2N-FBW2 (described below)	cds-fbw2-gw-b1 fbw2_f-box-r	pDONR221	pENTRY(221)-delF-box (FBW2)
delCter (FBW2)	pE2N-FBW2 (described below)	fbw2_hook-f cds-fbw2stop-gw-b2	pDONR221	pENTRY(221)-delCter (FBW2)

- pE2N-FBW2

The pE2N-FBW2 was created by inserting the coding sequence of FBW2 in the pE2N plasmid. The pE2N plasmid contains the *att*P1 and *att*P2 recombination sites (Dubin et al., 2010). A (3)HA tag followed by the BamH1 and the Not1 endoribonucleases sites is located between the *att*P1 and *att*P2 recombination sites. FBW2 coding sequence was amplified with the primers fbw2-BamHI-fwd and fbw2-NotI-rev listed in table 2 then digested with BamH1 and a Not1 restriction enzymes and further ligated in the corresponding sites of pE2N.

- pENTRY(221)-promFBW2

The pENTRY(221)-promFBW2 was created by Gateway recombination using the pDONR221 and a PCR product corresponding to the promoter of FBW2 gene flanked by the *att*B4 and *att*B1r recombination sites. The primers pfbw2-gw_b1-par and pfbw2-gw_b2-par used for FBW2 promoter amplification encompassed 2 kb sequence upstream of the FBW2 gene. This PCR product was further amplified with the primers attb1-pfbw2 and attb2-fbw2 to add the full *att*B1 and *att*B2 recombination sites. The primer sequences are listed in table 2.

- pENTRY(P4-P1R)-promFBW2

The pENTRY(P4-P1R)-promFBW2 was created by Gateway recombination using the pDONR221 P4-P1R and a PCR product corresponding to the promoter of FBW2 gene flanked by the *att*B4 and *att*B1r recombination sites. The pDONR221 P4-P1R differs from pDONR221 by the presence of the *att*P4 and *att*P1r recombination sites (www.invitrogen.com, see manual MultiSite Gateway ® Three-Fragment Vector Construction). The primers pfbw2-gw_b4-par and pfbw2-gw_b1r-par used for FBW2 promoter amplification encompassed 2 kb sequence upstream of the FBW2 gene. This PCR product was further amplified with the primers attb4-pfbw2 and attb1r-fbw2 to add the full *att*B4 and *att*B1r recombination sites. The primer sequences are listed in table 2.

- pENTRY(221)-FBW2

The pENTRY(221)-FBW2 was created by Gateway recombination using the pDONR221 and a PCR product corresponding to the coding sequence of FBW2 gene flanked by the *att*B2r and *att*B3 recombination sites. The primers cds-fbw2-gw-b1 and cds-fbw2stop-gw-b2 were used for FBW2 coding sequence amplification and are listed in table 2.

- pENTRY(P2R-P3)-FBW2

The pENTRY(P2R-P3)-FBW2 was created by Gateway recombination using the pDONR221 P2R-P3 and a PCR product corresponding to the coding sequence of FBW2 gene flanked by the *att*B2r and *att*B3 recombination sites. The pDONR221 P2R-P3 differs from pDONR221 by the presence of the *att*P2 and *att*P3 recombination sites (www.invitrogen.com, see manual MultiSite Gateway ® Three-Fragment Vector Construction). The primers cds-fbw2-gw-b2r and cds-fbw2-gw-b3 were used for FBW2 coding sequence amplification and are listed in table 2.

- pENTRY(Zeo)-AGO1

The pENTRY(Zeo)-AGO1 was created by Gateway recombination using the pDONR221 and a PCR product corresponding to the coding sequence of AGO1 gene flanked by the *att*B2r and *att*B3 recombination sites. The primers AGO1-1F and ago1-stop-attb2-r were used for AGO1 coding sequence amplification and are listed in table 2.

- pENTRY207-AGO1(HC), pENTRY207-AGO1(degAGO2) and pENTRY207-AGO1(degAGO4)

In order to replace the P0 degron of AGO1 by the homologous sequences of AGO2 or AGO4, two silent mutations were introduced in the pENTRY207-AGO1 by site-directed mutagenesis using the primers degronAGO1_HindIIIF and degronAGO1_ClaIR. This mutagenesis allowed to create two restriction sites (HindIII and ClaI) on either sides of the P0 degron of AGO1, generating the pENTRY207-AGO1(HC). The restriction HindIII and ClaI restriction sites were added on the corresponding sequences from AGO2 and AGO4 by PCR amplification with the following primers ; degronAGO2_HindIIIF, degronAGO2_ClaIR, degronAGO4_HindIIIF and degronAGO4_ClaIR. These sequences were then digested with the HindIII and ClaI restriction enzymes and ligated in the mutagenized AGO1(HC) to generate the pENTRY207-AGO1(degAGO2) and the pENTRY(207)-AGO1(degAGO4). The sequences of the primers are listed in table 2.

1.4.2 FBW2 mutagenized constructs

We generated a serie of plasmids in which FBW2 was mutagenized either in the F-box domain or in the putative GW motif. The mutagenesis was conducted using pENTRY(221)-FBW2 as a PCR matrix and with the primers listed in the following table 4. The sequences of the primers are listed in table 2.

Table 4: pENTRY-FBW2 mutagenized clones

DNA matrix	Primers	Resulting entry clone
pENTRY(221)-FBW2	fbw2_mutfbox-f fbw2_mutfbox-r	pENTRY(221)-FBW2(mutF-box)
pENTRY(221)-FBW2	fbw2_mutw225a-f fbw2_mutw225a-r	pENTRY(221)-FBW2(W225A)
pENTRY(221)-FBW2	fbw2_mutw258a-f	pENTRY(221)-FBW2(W258A)

	fbw2_mutw258a-r	
pENTRY(221)-FBW2	fbw2_mutw275a-f fbw2_mutw275a-r	pENTRY(221)-FBW2(W275A)
pENTRY(221)-FBW2	fbw2_mutw295a-f fbw2_mutw295a-r	pENTRY(221)-FBW2(W295A)
pENTRY(221)-FBW2	fbw2_mutw313a-f fbw2_mutw313a-r	pENTRY(221)-FBW2(W313A)
pENTRY(221)-FBW2(W258A)	fbw2_mutw275a-f fbw2_mutw275a-r	pENTRY(221)-FBW2(W258A, W275A)
pENTRY(221)-FBW2(W258A, W275A)	fbw2_mutw295a-f fbw2_mutw295a-r	pENTRY(221)-FBW2(W258A,W275A, W295A)
pENTRY(221)-FBW2(W258A,W275A, W295A	fbw2_mutw225a-f fbw2_mutw225a-r	pENTRY(221)-FBW2(W225A,W258A, W275A, W295A)
pENTRY(221)-FBW2(W225A,W258A, W275A, W295A)	fbw2_mutw313a-f fbw2_mutw313a-r	pENTRY(221)-FBW2(W225A,W258A, W275A, W295A, W313A)

1.4.3 AGO1 mutagenized constructs

We generated a serie of constructs in which AGO1 was mutated either in the putative phosphorylation sites or in the putative ubiquination site. The mutagenesis was conducted using pENTRY(Zeo)-AGO1 as a PCR matrix and with the primers listed in the following table 5. The sequences of the primers are listed in table 2.

Table 5: pENTRY-AGO1 mutagenized clones

DNA matrix	Primers	Resulting entry clone
pENTRY(Zeo)-AGO1	ago1_mut_s1001a-s1003a-s1005a-f	pENTRY(Zeo)-AGO1(ADAGA)

	ago1_mut_s1001a-s1003a-s1005a-r	
pENTRY(Zeo)-AGO1	ago1_mut_s1001d-s1003d-s1005d-f ago1_mut_s1001d-s1003d-s1005d-r	pENTRY(Zeo)-AGO1(DDDGD)
pENTRY(Zeo)-AGO1	ago1_mutk507r-f ago1_mutk507r-r	pENTRY(Zeo)-AGO1(K507R)
pENTRY(Zeo)-AGO1	ago1_mutk413-415-416r-f ago1_mutk413-415-416r-r	pENTRY(Zeo)-AGO1(K413R, K415R, K416R)
pENTRY(Zeo)-AGO1(K413R, K415R, K416R)	ago1_mutk507r-f ago1_mutk507r-r	pENTRY(Zeo)-AGO1(K507R, K413R, K415R, K416R)

- Yeast-two-hybrid vectors

pGADT7 and pGBKT7 (Clontech) were converted into Gateway destination plasmids previously in the lab and named pGADT7GW and pGBKT7GW. pGADT7-FBW2, pGBKT7-polyQ-PAZ and pGBKT7-L2-Ct were created by LR recombination with the indicated pENTRY clones and one of the two yeast-two-hybrid destination vectors.

Table 6: Yeast-two-hybrid vectors

Entry clone	Destination vector	Resulting destination vector
pENTRY(Zeo)-FBW2	pGADT7GW	pGADT7-FBW2
pENTRY(Zeo)-polyQ-PAZ	pGBKT7GW	pGBKT7-polyQ-PAZ
pENTRY(Zeo)-L2-Ct	pGBKT7GW	pGBKT7-L2-Ct

The pGBKT7-ASK1 was previously generated in the laboratory.

1.4.4 Binary vectors

- pMDC7-3HA-FBW2

The pMDC7 correspond to the pER8 plasmids converted into in a Gateway destination vector (Zuo et al., 2000; Curtis, 2003). This vector allows β-estradiol induced expression of the gene of interest. The pMDC7-3HA-FBW2 was created by LR recombination with the pE2N-FBW2 and the pMDC7.

- pB2GW7-3HA-FBW2 and pB2GW7-flag-NtAGO1

The pB2GW7 vector was engineered by Plant Systems Biology, VIB, Ghent, Belgium. This vector is spectinomycin resistant in bacteria and carries the Basta resistance gene for plant selection. It is used to express ectopically constructs under the control of the 35S promoter and the 35S terminator. The detailed map of this vector is available on the web site https://gateway.psb.ugent.be/. pB2GW7-flag-NtAGO1 and pB2GW7-3HA-FBW2 were created by LR recombination with the indicated pENTRY clones and the pB2GW7 vector.

Table 7: Destination vectors for constitutive ectopic expression

Entry clone	Destination vector	Resulting destination vector
pENTRY(221)-flag-NtAGO1	pB2GW7	pB2GW7-flag-NtAGO1
pE2N-FBW2	pB2GW7	pB2GW7-3HA-FBW2

- pK7FWG2, pH7WGR2 and pB7WGC2 based constructs

These vectors were engineered by Plant Systems Biology, VIB, Ghent, Belgium. All vectors are spectinomycin resistant in bacteria and carry different resistance genes for plant selection (pK7WGF2 : kanamycin, pH7WGR2 : hygromycin, pB7WGC2 : Basta). They are used to create fluorescent tags either as N-terminal fusion with the RFP (pH7WGR2), CFP (pB7WGC2) or C-terminal fusion with the GFP (pK7WGF2) of the construct of interest under the control of the 35S promoter and the 35S terminator. The detailed map of these vectors is available on the web site https://gateway.psb.ugent.be/. The following plasmids were created by LR

recombination with the indicated pENTRY clones and the pK7FWG2, pH7WGR2 or pB7WGC2.

Table 8: Destination vectors for fluorescent-tagged constructs

Entry clone	Destination vector	Resulting destination vector
pENTRY(221)-polyQ-PAZ	pK7FWG2	pK7FWG2-polyQ-PAZ
pENTRY(221)-polyQ-ND	pK7FWG2	pK7FWG2-polyQ-ND
pENTRY(221)-polyQ--PAZ	pK7FWG2	pK7FWG2-polyQ--PAZ
pENTRY(221)-ND	pK7FWG2	pK7FWG2-ND
pENTRY(221)-ND-DUF	pK7FWG2	pK7FWG2-ND-DUF
pENTRY(221)-ND-PAZ	pK7FWG2	pK7FWG2-ND-PAZ
pENTRY(221)-DUF	pK7FWG2	pK7FWG2-DUF
pENTRY(221)-DUF-PAZ	pK7FWG2	pK7FWG2-DUF-PAZ
pENTRY(221)-PAZ	pK7FWG2	pK7FWG2-PAZ
pENTRY(221)- PAZ-L2	pK7FWG2	pK7FWG2-PAZ-L2
pENTRY(221)- L2	pK7FWG2	pK7FWG2-L2
pENTRY(221)-L2-MID	pK7FWG2	pK7FWG2-L2-MID
pENTRY(221)-L2-PIWI	pK7FWG2	pK7FWG2-L2-PIWI
pENTRY(221)-MID	pK7FWG2	pK7FWG2-MID
pENTRY(221)-MID-PIWI	pK7FWG2	pK7FWG2-MID-PIWI
pENTRY(221)-MID-PIWI-Ct	pK7FWG2	pK7FWG2-MID-PIWI-Ct
pENTRY(221)-PIWI	pK7FWG2	pK7FWG2-PIWI
pENTRY(221)-PIWI-Ct	pK7FWG2	pK7FWG2-PIWI-Ct
pENTRY(221)-Ct	pK7FWG2	pK7FWG2-Ct

pENTRY(207)-FBW2	pH7WGR2	pH7WGR2-FBW2
pENTRY(207)-iFBW2	pH7WGR2	pH7WGR2-iFBW2
pENTRY(Zeo)-AGO1	pB7WGC2	pB7WGC2-AGO1
pENTRY(Zeo)-AGO1(ADAGA)	pB7WGC2	pB7WGC2-AGO1(ADAGA)
pENTRY(Zeo)-AGO1(DDDGD)	pB7WGC2	pB7WGC2-AGO1(DDDGD)
pENTRY(Zeo)-AGO1(K507R)	pB7WGC2	pB7WGC2-AGO1(K507R)
pENTRY(Zeo)-AGO1(K413R, K415R, K416R)	pB7WGC2	pB7WGC2-AGO1(K413R, K415R, K416R)
pENTRY(Zeo)-AGO1(K507R, K413R, K415R, K416R)	pB7WGC2	pB7WGC2-AGO1(K507R, K413R, K415R, K416R)

- pGWB415-FBW2, deletions and mutagenized FBW2

The pGWB415 plasmid is used to create an N-terminal fusion of the construct of interest with a 3HA tag under the control of the 35S promoter and the Nopalin Synthase Gene Terminator terminator (Nakagawa et al., 2007). The following plasmids were created by LR recombination with the indicated pENTRY clones and the pGWB415.

Table 9: HA-tagged FBW2 mutagenized or deleted constructs

Entry clone	Destination vector	Resulting destination vector
pENTRY(221)-FBW2	pGWB415	pGWB415-FBW2
pENTRY(221)-delF-box (FBW2)	pGWB415	pGWB415-FBW2(delF-box)
pENTRY(221)-delCter (FBW2)	pGWB415	pGWB415-FBW2(delCter)
pENTRY(221)-FBW2(mutF-box)	pGWB415	pGWB415-FBW2(mutF-box)

pENTRY(221)-FBW2(W225A)	pGWB415	pGWB415-FBW2(W225A)
pENTRY(221)-FBW2(W258A)	pGWB415	pGWB415-FBW2(W258A)
pENTRY(221)-FBW2(W275A)	pGWB415	pGWB415-FBW2(W275A)
pENTRY(221)-FBW2(W295A)	pGWB415	pGWB415-FBW2(W295A)
pENTRY(221)-FBW2(W313A)	pGWB415	pGWB415-FBW2(W313A)
pENTRY(221)-FBW2(W258A, W275A)	pGWB415	pGWB415-FBW2(W258A, W275A)
pENTRY(221)-FBW2(W258A,W275A, W295A)	pGWB415	pGWB415-FBW2(W258A,W275A, W295A)
pENTRY(221)-FBW2(W225A,W258A, W275A, W295A)	pGWB415	pGWB415-FBW2(W225A,W258A, W275A, W295A)
pENTRY(221)-FBW2(W225A,W258A, W275A, W295A, W313A)	pGWB415	pGWB415-FBW2(W225A,W258A, W275A, W295A, W313A)

- pEG101-FBW2 and pEG104-FBW2

These plasmids were kindly provided by Scott Poethig (University of Pennsylvania, USA). They are respectively based on the pEarlyGate101 and pEarlyGate104 vectors (Earley et al., 2006) and contain the genomic (ATG to stop, including intron) sequence of FBW2 C-terminally (pEarleyGate101) or N-terminally (pEarleyGate104) fused to the YFP under the control of the 35S promoter and the Octopine Synthase Gene Terminator.

- promFBW2:Venus-FBW2

The promFBW2:Venus-FBW2 plasmid is generated by the triple LR recombination of the pENTRY(P4-P1R)-promFBW2, the pENTRY-Venus (generated in the lab with the Venus sequence from the ATG to the stop) and the pENTRY(P2R-P3)-FBW2 with the pH7m34GW vector. The pH7m34GW was engineered by Plant Systems Biology,

VIB, Ghent, Belgium and its detailed map is available on the web site https://gateway.psb.ugent.be/. The transcription of the inserted construct is stopped by the 35S terminator.

- pGREENII pAGO1: GFP-AGO1

The pGREENII pAGO1: GFP-AGO1 construct is described in Derrien et al., 2012. This binary vector encodes a functional GFP-AGO1 protein that complements *ago1-11* and *ago1-27* arabidopsis mutants. Promoter and 5'UTR sequences were amplified from 1654 bp upstream the ATG and AGO1 cDNA (including the 3'UTR) was fused in 5' to eGFP coding sequence. pGREENII confers resistance to Basta for plant selection.

1.5 Antibodies used for Western blots

The antibodies used in this study are listed in the following table with their working concentration and their origin.

Table 10: Antibodies used for Western blots

Antibody directed against	Dilution	HRP-coupled secondary antibody	Supplier
AGO1	1 / 10 000	Goat Anti Rabbit	www.agrisera.com
AGO2	1 / 10 000	Goat Anti Rabbit	www.agrisera.com
AGO4	1 / 1 000	Goat Anti Rabbit	www.agrisera.com
HYL1	1 / 2 000	Goat Anti Rabbit	www.agrisera.com
Actin3	1 / 10 000	Goat Anti Rabbit	www.agrisera.com
ASK1	1 / 2 000	Goat Anti Rabbit	Generated in the laboratory
CUL1	1 / 10 000	Goat Anti Rabbit	Generated in the laboratory
RBX1 (ROC1)	1 / 2 000	Goat Anti Rabbit	www.mybiosource.com
Ubi P4D1	1 / 1 000	Goat Anti Mouse	www.scbt.com

HA H9658	1 / 10 000	Goat Anti Mouse	www.sigmaaldrich.com
c-myc-HRP	1 / 10 000		www.miltenyibiotec.com
Flag M2	1 / 10 000	Goat Anti Mouse	www.sigmaaldrich.com
flag-M2-HRP	1 / 5 000		www.sigmaaldrich.com
GFP-HRP	1 / 5 000		www.miltenyibiotec.com
RFP 6G6	1 / 2 000	Goat Anti Mouse	www.chromotek.com

1.6 Chemicals and antibiotics

1.6.1 Antibiotics and herbicides used for plant and bacterial selection

Chemicals and antibiotics used for bacterial and plant selection are listed below with their corresponding working concentrations:

Table 11: Chemicals and antibiotics used for bacterial and plant selection

	Soluble in	Stock solution (mg/ml)	Final concentration (µg/ml) Bacteria	Plants
Cefotaxime	Water	250	500	
Carbenicillin	Water	200	100-500	
Kanamycin	Water	100	50	50
Tetracyclin	Ethanol	12,5	12,5	
Gentamycin	Water	100	50	
Spectinomycin	Water	100	100	
Streptomycin	Water	30	30	
Chloroamphenicol	Ethanol	30	30	
Rifampicin	DMSO	100	50	
Hygromycin	Water	500		30
Basta/glufosinate	Water	10		10

Note that cefotaxime and carbenicillin have been used at a concentration of 500 µg/ml to kill Agrobacteria after Arabidopsis transformation.

1.6.2 Chemicals / drugs applied to plants

The following chemicals have been applied directly on Arabidopsis seedlings or in *Nicotiana benthamiana* leaves by infiltration. The details of the treatments are specified for each experiments in the legend of the figures of the result part.

Table 12: Chemicals applied to plants

Name	Solvent	Stock solution concentration	Dilution	Origin
MLN4924	DMSO	25 mM	25 µM	www.activebiochem.com
MG132	DMSO	50 mM	100 µM	www.sigmaaldrich.com
Bortezomib (PS-341)	DMSO	50 mM	50 µM	www.selleckchem.com
E64-d	DMSO	50 mM	50 µM	www.euromedex.com
Wortmannin	DMSO	20 mM	20 µM	www.enzolifesciences.com
Concanamycin A	DMSO	1 mM	1 µM	www.sigmaaldrich.com

2 Methods

2.1 Protocols related to cloning and bacterial transformation

2.1.1 DNA amplification by PCR

Polymerase chain reaction (PCR) is performed for DNA amplification for cloning purpose or bacterial colony screening or plant genotyping. Phusion High-Fidelity DNA Polymerase (ThermoFisher Scientific) is used for high-fidelity DNA amplification while Phire2 DNA polymerase (ThermoFisher Scientific) was used for other applications. PCR conditions are listed below:

	Phusion 2X mix	Phire 2
Total volume	50 µl	20 µl
Froward primer (10µM)	1 µl	1 µl
Reverse primer (10µM)	1 µl	1 µl
dNTP (10mM)		0,4 µl
Buffer		5X: 4 µl
DNA polymerase		0,1 µl
Master mix	2X: 25 µl	
DNA matrix	10 ng vector/up to 200 ng genomic DNA	

PCR programs are listed below:

	Phusion	Phire 2
Initial Denaturation	2 min 98 °C	30 sec 98°C
Denaturation	15 sec	5 sec 98°C
Priming	15-30 sec	5 sec
Elongation	30 sec/kb 72°C	15 sec/kb 72°C
Final elongation	5 min 72°C	1 min 72°C

The number of PCR cycle is generally comprised between 30 and 35.

2.1.2 DNA analysis

Amplified PCR fragment and vectors are analyzed by agarose gel electrophoresis on 1X TAE agarose gel (0.8% to 2% Agarose). DNA is stained with ethidium bromide and revealed on a UV transilluminator.

2.1.3 Purification of PCR products

In order to recover and purify DNA fragment from agarose gels, specific Ultrafree-da centrifugal filter unit (Millipore) were used. The kit consists of a pre-assembled filter device with an agarose gel nebulizer, a microcentrifuge vial, and modified TAE gel extraction buffer Agarose gel slices are placed in the filter unit followed by in a single 10-minute centrifugation at 13 000 rpm. The device utilizes gel compression to extract DNA from the agarose. Centrifugal force collapses the gel structure, drives the agarose through a small orifice in the gel nebulizer and the resultant gel slurry is sprayed into the sample filter cup. Prepared DNA requires no further purification and can be directly used for cloning.

2.1.4 The Gateway™ technology

The Gateway™ technology is based on the bacteriophage lambda site-specific recombination system that facilitates the integration of lambda into the *E.coli* chromosome. Lambda recombination occurs between site-specific *att*achment (*att*) sites *att*B on the *E.coli* chromosome and *att*P on the lambda chromosome to give rise to *att*L and *att*R sites.

The Gateway™ technology uses the lambda recombination system to facilitate the transfer of heterologous DNA sequences (flanked by modified *att* sites) between vectors. Two recombination reactions constitute the basis of the Gateway™ technology: BP reaction which facilitates the recombination of an *att*B substrate (*att*B PCR product) with an *att*P substrate (pDONOR vector) to create an *att*L containing entry clone; and the LR reaction which facilitates recombination of an *att*L substrate (ENTRY clone) with an *att*R containing expression vector (destination vector). Further detail of Gateway cloning protocol is available in the www.invitrogen.com. BP clonase and LR clonase reaction are incubated overnight at 25°C. Reaction conditions are listed below:

BP clonase reaction		LR clonase reaction		Triple LR reaction	
Purified PCR product	5 µl	Entry vector	150 ng	Entry vectors	75 ng each
pDONR221	150 ng	Destination vector	150 ng	Destination vector	100 ng
BP clonase	1 µl	LR clonase	1 µl	LR clonase	1 µl
TE buffer	up to 10 µl	TE buffer	up to 10µl	TE buffer	up to 10µl

BP clonase and LR clonase reactions are treated with 1µl Proteinase K (Invitrogen) for 10 minutes at 37°C prior to bacterial transformation using TOP10.

2.1.5 Plasmid purification and sequencing

Plasmids are purified using the Macherey Nagel® kit (NucleoSpin Plasmid QuickPure) according to the manufacturers' recommendations or lysis by alkaly (Sambrook et al., 1989 (book))

GTE buffer: 50 mM glucose, 25 mM Tris HCl pH8, 10 mM EDTA, 0.1 mg/ml RNase A (stored at 4°C)

Lysis buffer: 0.2 N NaOH, 2% SDS (freshly prepared)

Neutralization buffer: 3 M CH_3CO_2K pH 5.2

CAI solution : Chloroform : 24 volumes, Isoamyl alcohol : 1volume

2.5 ml of overnight *E. coli* culture is pelleted by centrifugation at 3500 rpm for 10 minutes and resuspended in 250 µl of GTE buffer. 250 µl of lysis buffer are added, tubes are gently mixed by hand and incubated at room temperature for 5 minutes maximum. Lysis is immediately stopped by adding 250 µl of neutralization buffer and gently mixing tubes again. Debris are pelleted at maximum speed for 10 minutes and the supernatant is mixed with 1 volume of CAI solution. Phases are separated by centrifugation at maximum speed for 15 minutes and aqueous phase is precipitated at -20°C with 1 volume of cold isopropanol for 20 minutes. Plasmid DNA is then pelleted by centrifugation at maximum speed for 20 minutes and washed 2 times with 70% ethanol. Pellets are air dried and resuspended in 50 µl bidistilled water.

Nucleic acid dosage is performed using NanoDrop spectrophotometer (ThermoFisher Scientific). Amplified vectors are sequenced at the IBMP sequencing platform by the Sanger method.

2.1.6 Site-directed mutagenesis

pENTRY clones were site-directed mutagenized according to Edelheit et al., (2009). This method consists of two parallel single primer reactions that synthesize each one strand of the plasmid with primers containing the mutation. The aim is to prevent amplification of unwanted mutation events that could occur with standard PCR. The two single primer reactions are then hybridized together and digested with the DpnI

enzyme to discard the methylated original plasmids. The resulting plasmids are then transformed in *E. coli* and screened by sequencing to recover the wanted mutations.

This method has been used to generate all pENTRY-FBW2 and pENTRY-AGO1 mutagenized vectros listed in table 4 and 5.

2.1.7 Bacterial transformation

LB (Luria Bertini) medium: 10 g/L bacto-tryptone, 5 g/L yeast extract, 5 g/L NaCL, pH 7.2

- Preparation of thermocompetent *E. coli* cells

A 5 ml preculture is inoculated with *E. coli* cells and grown overnight at 37°C in liquid LB medium. 250 ml of LB medium in one-liter Erlenmeyer is then inoculated with the entire preculture and grown at 37°C until the optical density at 600 nm reaches 0.7. The following steps are then done at 4°C in sterile conditions. Cells are centrifuged at 5000xg for 15 minutes and washed two times with cold 0.1 M $CaCl_2$. They are resuspended in 50ml of 0.1 M $CaCl_2$ and incubated at 4°C overnight. Cells are then centrifuged as previously and resuspended in 3 ml of cold 0.1 M $CaCl_2$, 15% glycerol solution before being divided in 50 µl aliquots. Aliquots can be directly used for high efficiency transformation or are frozen in liquid nitrogen and stored at -80°C.

- Preparation of electrocompetent *A.tumefaciens* cells

10 ml of LB supplemented with necessary antibiotics are inoculated with GV3101 (PMP90) strain and grown overnight at 28°C in dark on a shaker (180 rpm). 250 ml of LB medium supplemented with antibiotics in one-liter Erlenmeyer are inoculated with the preculture and grown at 28°C until the optical density at 600 nm reaches 0.6. The following steps are then done at 4°C in sterile conditions. Cells are centrifuged at 5000xg for 15 minutes and washed 3 times with cold sterile water and resuspended in 10% glycerol before being divided in 50µl aliquots. Aliquots can be directly used for high efficiency transformation or are frozen in liquid nitrogen and stored at -80°C.

- *E.coli* heat shock transformation

Competent *E.coli* cells, stored at -80°C, are thawed on ice. DNA that needs to be amplified (10 ng of vector or 5 µl of BP/LR clonase reaction) is gently mixed with the cells and incubated on ice for 20 minutes. Cells are then transferred to a heated bath at 42°C for 45 seconds and immediately chilled on ice for 2 minutes. 500 µl of LB medium are added and cells are incubated 20 minutes at 37°C. 250 µl of cells are finally plated on solid LB medium (1,5 % agar) supplemented with the appropriate antibiotics and incubated for overnight at 37°C. List of used antibiotics and concentration for bacterial selection is described above in material section.

- *A.tumefaciens* transformation by electroporation

Competent *A.tumefaciens* cells, stored at -80°C, are thawed on ice. 10 ng of vector are gently mixed in a microtube and then transferred in an ice-chilled electroporation cuvette and electroporated at 2500 V, 400 Ohm resistance, 0.25 µF, τ±3.8 ms on a Gene pulser (BioRad) apparatus. Cells are transferred in 500 µl of LB medium and incubated for 1 hour at 28°C. Finally, 250 µl of cells are plated on solid LB medium with antibiotics and incubated at 28°C for 36 to 48 hours. List of used antibiotics and concentration for bacterial selection is described in table 11.

2.1.8 Protocols related to yeast

Yeast Two-Hybrid assays were performed following Matchmaker GAL4 Yeast Two-Hybrid handbook (Clontech). Matchmaker systems use the transcription activating and DNA-binding domains of GAL4, a well-characterized yeast transcription factor (Zhu and Hannon, 2000) that are present in pGADT7 and pGBKT7 vectors (Clonetch)

Yeast strain PJ69-4A were transformed using LiAc–PEG transformation methods following Matchmaker handbook recommendations.

Transformed yeasts were selected on the basis of leucine and tryptophan auxotophy provided respectively by the presence of pGADT7 and pGBKT7 vectors. Protein interaction assays were scored on selective medium deprived of Histidine and /or Adenine.

2.1.9 Protocols related to plants

2.1.9.1 Arabidopsis growing conditions

<u>In soil</u>

Plants were cultivated in growth chambers with a 16 hours light and 8 hours dark photoperiod, temperature of 21/18°C and 80% humidity.

<u>*In vitro*</u>

Prioir to *in vitro* culture, seeds are sterilized in a 70% Ethanol, 0.05% TWEEN 20 (Sigma-Aldrich) solution during 30 minutes, followed by two washing steps of 5 minutes in Ethanol 96%. Seeds are then air dried under the sterile hood until sowing. Sterilized seeds are sawn of MS medium 0.8% and stratified 2 days at 4°C in dark conditions. Seeds are then germinated in growth chambers with a 16 hours light and 8 hours dark photoperiod, temperature of 21/18°C and 80% humidity.

Murashige and Skoog (MS) medium: MS with micro and macro elements M0255 (KALYS), 10 g/L sucrose, pH 5.8

2.1.9.2 Agro-transformation of Arabidopsis plants

T-DNA plant transformation are performed with "floral dip" method as described in Clough and Bent, 1998. Two days before floral dip, a 3 mL culture of transformed *A. tumefaciens* is started. An aliquot of the culture (1 mL) is added to 10 mL LB supplemented with the appropriate antibiotics and grown at 28 °C until the OD is superior to 2. Cells are then harvested by centrifugation (10 min, 3500 rpm, RT) and resuspended in 20 mL of a 10 mM $MgSO_4$ solution supplemented with 50 µM acetosyringone. Cells are then added to 1 L of infiltration medium (5 % sucrose, 400 µL Silwet,). Plants with young multiple secondary bolts are then transformed by submerging their bolts for 3 min in the bacteria solution. They are then uncovered and transferred to the greenhouse. When siliques on plants are dry, seeds can be taken for selection of transformants. About 40 heterozygous T1 transformants were selected on soil using appropriate selection. Mono-insertion homozygous lines (representing 75% resistance in T2, 100% resistance in T3) were selected *in vitro* and used for analyses.

2.1.9.3 Gus staining

The preparation of the material and GUS staining was done based on Donelly PM et al. (1999) which can be described as the following: the plant materials were fixed with 90% cold acetone for 20 minutes on ice. The acetone was then drained and the plant material was washed in phosphate buffer (0.1M $NaPO_4$ pH7.0) followed by a 1 hours incubation in the X-gluc buffer (0.1M $NaPO_4$ pH7.0, 0,5mM $K4Fe(CN)_6$, 0,5mM $K3Fe(CN)_6$, 0.2% TritonX100, 2mM X-gluc) at 37°C. Further rinsing the material in 70% ethanol bleached the chlorophyll of the tissues. Visualization and images were taken by using a normal bright field macroscope (Leica).

2.1.9.4 Confocal Microscopy

Confocal microscopy was performed on a LEICA TCS SP8 laser scanning microscope (Leica Microsystem) using the objective HCX APO CS 20X magnification with a numeric aperture of 0,7 without immersion. The microscopy settings for imaging *Arabidopsis thaliana* and *Nicotiana benthamiana* leaves are listed below:

Protein	CFP-tagged proteins	YFP/Venus-tagged proteins	RFP-tagged proteins
Laser	Argon	Argon	DPSS 561
Excitation	458 nm, 5 % intensity	514 nm, 5 % intensity	561 nm, 1 % intensity
Emission	465-510 nm	600-630 nm	594-634 nm
Pinhole	1	1	1
Gain	PMT - 1000 %	HYD - 100%	HYD - 200 %

Microscopy images are processed using the ImageJ software.

2.1.9.5 Transient expression in *Nicotiana benthamiana* leaves

Agrobacterium cells harboring the constructs of interest were grown overnight at 28 °C in 10 mL LB medium supplemented with antibiotics, resuspended in 10 mM MgCl2 supplemented with 200mM acetosyringone at an OD of 0.3 per construct (unless otherwise specified), and incubated for 1 hour at room temperature before being pressure infiltrated into leaves of 4 weeks old plants. Unless otherwise specified, all agro-infiltration were conducted in presence of P19. Plants were maintained in growth chambers under a 16 hours light and 8 hours dark photoperiod

with a constant temperature of 22 °C. Sampling and observations were performed 72 hours after agro-infiltration. When treatments were applied (as specified in the legend of the figures of the result part), drugs were redissolved in 10 mM MgCl2 and pressure infiltrated into leaves 12–16 h before observation.

2.1.9.6 GFP fluorescence quantification

GFP fluorescence emitted from the *Nicotiana benthamiana* agro-infiltrated leaves was quantified with a Ettan DIGE image (GE healthcare) with the parameters set for the SYPRO Ruby 1 dye (excitation filter 480/30 and emission filter 595/25) with 0.017 second exposure time.

2.1.9.7 DNA extraction for genotyping purpose

Edwards Buffer: (200 mM Tris-HCl pH 7.5, 250 mM NaCl, 25 mM EDTA and 0.5% SDS)

About 100 mg of plant tissue are collected and grinded with 2 mm metal beads and 500 µl Edwards buffer by using the Tissue Lyser (QIAGEN) (setting: 2x 1 min at 25 fpm). Samples are clarified by centrifugation at 4000rpm for 25 minutes. 400 µl of supernatant is collected and mixed with 1 volume of isopropanol and incubated at room temperature for 10 minutes. DNA is pelleted by centrifugation at maximum speed for 15 minutes. Pellets are washed with 70% Ethanol and air dried until pellets became colorless. They are finally redissolved in 100 µl of PCR-grade water.

2.2 Protocols related to protein analysis

2.2.1 Protein extraction from Arabidopsis

- Protein extraction

Laemmli buffer: 62 mM Tris HCl pH 6.8, 3% SDS, 40% glycerol, 0,1% bromophenol blue, DTT100mM (freshly added)

Approximately 100 mg of frozen plant tissue are grinded with 1.7-2.1 mm glass beads using a Silamat grinding apparatus (Ivoclar Vivadent) and resuspended in 250

µl of Laemmli buffer preheated at 95°C. Samples are then denatured at 95°C for 2 minutes. Debris are eliminated by centrifugation at maximum speed for 15 minutes.

- Protein quantification (Popov et al., 1975)

Amidoblack solution: 10% acetic acid, 90% methanol, 0.05% Naphthol Blue Black (Sigma-Aldrich)

Washing solution: 10% acetic acid, 90% ethanol

190 µl of sterile water are added to 10µl of total protein extracts and mixed 1 ml of Amidoblack solution is then added and mixed by hand. Tubes are centrifuged at maximum speed for 15 minutes and the supernatant is discarded. Pellets are rinsed with washing solution and centrifuged again at maximum speed for 15 minutes. When the supernatant has been removed and the pellets are dry, they are resuspended in 1 ml of 0,2 N Sodium hydroxide solution (NaOH). 200 µl are used for measuring optical density at 630 nm. Protein concentration is calculated according to a BSA (bovine serum albumin) standard curve.

2.2.2 Immunodetection by Western blot

Tris-Glycine electrophoresis buffer: 25 mM Tris Base, 250 mM glycine, 0.1% SDS

Transfer buffer: 25 mM Tris base, 192 mM glycine, 15% ethanol

TBST-T (Tris-buffered saline-Tween) buffer: 20 mM Tris base, 150 mM NaCl, 0.1% Tween20 (Sigma-Aldrich) pH 7.4

Coomassie blue staining solution: 90% ethanol, 10% acetic acid, 0.05% Brilliant blue R250 (Sigma-Aldrich)

Destaining solution: 30% ethanol, 10% acetic acid

Total protein extract and immunoprecipitated proteins were separated by SDS-PAGE. Acrylamide gels are prepared as described in Sambrook et al., 1989 (book) using Mini-Protean III (BioRad) casting system. Frozen protein samples are thawed at 56°C for 2 minutes and loaded on 7-12% Tris-glycine gels or gradient NuPAGE 4-12% Bis-Tris Protein Gels (Thermo Fischer). Protein are first migrated at 50 V until

the migration front reaches the resolving gel and are then migrated at 100 V. Proteins separated on gel are then transferred on previously activated Immobilon-P PVDF membrane (GE Healthcare-Life Sciences) at 400 mA for 1 hour. Transferred membranes are rinsed with TBS-T and incubated with 5% milk TBS-T for 20 minutes at room temperature. Membranes are incubated in 5% milk TBS-T with primary antibody for 2 hours at room temperature or overnight at 4°C. Membranes are rinsed 3 times with TBS-T, 5 minutes each and incubated for 1 hour in 5% milk TBS-T with secondary antibody at room temperature. Membrane is washed 3 times, as done previously and revealed using Clarity chemoluminescent substrate (BIORA. Chemiluminescence signal is detected by Fusion FX imager (Vilber). Total proteins can be stained with Coomassie blue solution. To enhance contrast, membrane are washed with destaining solution. The antibodies and their dilutions are listed in the material part.

2.2.3 Immunoprecipitation

IP Extraction buffer: 25 mM Tris HCl, pH 7.5, 150 mM NaCl, 10% glycerol, 5 mM MgCl$_2$, 0.1% Tween20, 15 mM EGTA, 10 µM MG132, and 1×Complete protease inhibitors cocktail [Roche]).

For immunoprecipitation of HA-FBW2, 1g of frozen plant material was ground to a fine powder with a mortar and pestle, resuspended in 3 volumes (3 ml) of IP Extraction buffer and incubated for 30 min at 8 rpm in the cold room. Insoluble material was removed by centrifugation (twice 15 min, 16 000g, 4°C). Identical amounts of crude extracts were incubated with 25µl anti-HA magnetic beads (Pierce) (pre-washed three times in IP Extraction buffer) for 3 hours at 7 rpm at room temperature. Immune complexes were washed three times in the IP Extraction buffer. Elution of the immunoprecipitated proteins was performed by adding 30 µl of Glycine 0,2M pH3 to the magnetic beads and immediately transferring the eluate to a new tube containing 10 µl Tris HCl 1M pH 11. Before analyzing the immunoprecipitated proteins on Acrylamide Gels, 4X loading buffer was added to a final concentration of 1X to the samples and then denatured for 5 minutes at 95°C.

In parallel, 150 µl of input fraction and unbound fraction are kept as control and denatured 2 minutes at 95°C with 50 µl of 4X loading buffer.

2.3 Protocols related to RNA analysis

2.3.1 RNA extraction

100 mg of plant material frozen in liquid nitrogen are first grinded with 1.7-2.1 mm glass beads using a Silamat grinding apparatus (Ivoclar Vivadent) and resuspended in 800 µl of Tri-reagent (Sigma-Aldrich). Microtubes are incubated 3 minutes under strong agitation. 200 µl of Chloroform (Sigma-Aldrich) are added and microtubes are again vortexed for 3 minutes. Phases are separated by centrifugation at maximum speed for 15 minutes. Aqueous phase is recovered and incubated for 1 hour at -20°C with 1 volume of cold Isopropanol. RNA is then precipitated by centrifugation at maximum speed for 20 minutes at 4°C. Pellet are washed twice with 1 ml of 70% ethanol and air dried until they became colorless. RNA pellets are finally resuspended in 50 µl of RNase-free water and dosed using Nanodrop spectrophotometer (ThermoFisher Scientific).

2.3.2 Northern blot for small RNA detection

Loading buffer: deionized formamide, 0.01% bromophenol blue (Sigma-Aldrich), 0.05% Xylene Cyanol blue (Sigma-Aldrich)

10X TBE buffer (Tris Borate EDTA): 89 mM Tris, 89 mM boric acid, 2 mM EDTA, pH 7.5

20X SSC buffer (Saline sodium citrate): 3M NaCl, 300mM $C_6H_5Na_3O$; $2H_20$, pH 7.2

EDC crosslinking buffer: 0.16 M l-ethyl-3-(3-dimethylaminopropyl) carbodiimide (EDC) (Sigma-Aldrich), 0.13 M 1-methylimidazole, pH 8

Methylene blue staining buffer: 0.04% methylene blue (Sigma-Aldrich), 0.5 M CH_3COONa pH 5.2

Mild stringency washing buffer: 2X SSC, 2% SDS

High stringency washing buffer: 1X SSC 1% SDS

- Sample preparation

20 µg of total RNA are first standardized to identical volumes to minimize migration variation. Loading buffer is then added to reach a final concentration of 60% formamide. Samples are denatured at 95°C for 5 minutes and immediately chilled on ice before loading on gel.

- Electrophoresis and transfer of RNA

RNA samples are separated on a 15% acrylamide, 0.5X TBE, 8 M urea gel prior samples loading, acrylamide gels are preheated for 30 minutes at 15 W. Gel is then run at 3 W for 30 minutes followed by approximately 4 hours at 15 W in 0.5X TBE. After electrophoresis, RNA loading is checked by ethidium bromide coloration. Separated RNAs are transferred on Amersham Hybond-NX nylon membrane (GE Healthcare-Life Sciences) for 1h30 at 400 mA in 0.5X TBE.

- Chemical crosslinking (see Pall et al., 2007)

Membranes are put on a Whatman paper imbibed with freshly prepared EDC-crosslinking buffer, sealed in a bag (the transferred face must be upside) and incubated 1 hour at 60°C. membranes can be rinsed with demineralized water and RNA quality can be verified with methylene blue staining buffer.

- 5' radio-labelling of oligonucleotides

DNA oligonucleotides complementary to miR403, miR168 and U6 RNA were 5' end-labeled with [γ-32P]ATP using T4 polynucleotide kinase (PNK) (Promega). Reaction conditions are listed below:

Total volume	20 µl
Buffer A	2 µl
DNA oligonucleotide (10µM)	1 µl
[γ-P32]ATP	25 µCi (2,5 µl)

T4 PNK	1,5 µl
H$_2$0	13 µl

PNK reaction is incubated at 37°C for 1 hour.

Radio-labeled probes were then purified from non-incorporated γ-32P using Microspin G-25 column (GE Healthcare-Life Sciences).

The primer sequences are the following :

 ath-miR168 : TTCCCGACCTGCACCAAGCGA

ath-miR403 : CGACTTTGTGCGTGAATCTAA

ath-U6 : AGGGGCCATGCTAATCTTCTC

tRF-5D_5D-His_chloro   TCCACTTGGCTACATCCGC

- Labeling of PCR product

PCR product corresponding to the IR71 sequence (IR71-fwd AAATGACCGCTACACTGCTTATCT, IR71-rev TCTCTCGTCAATGGACAATGAATC) was used as a probe. 100ng of purified PCR product was used to obtain a [α-32P]CTP–labeled Klenow product (Prime-a-gene, Promega) following the manufacturers' protocol. Radio-labeled probes were then purified from non-incorporated α-32P using Microspin G-50 column (GE Healthcare-Life Sciences).

- Hybridization

Crosslinked membranes are incubated 2 hours in 15ml of PerfectHyb hybridization buffer (Sigma-Aldrich) at 42°C and then incubated overnight with the radio-labeled probes. Membranes are finally washed 2 times with mild stringency buffer and high stringency buffer for 15 minutes at 50°C before exposure.

The signals were detected using BAS-IIIS imaging plate (FUJIFILM) and a Typhoon phosphorimager (Amersham).

2.3.3 Quantitative real-time PCR (qRT-PCR)

1 µg of total RNAs samples are first treated with DNase I (ThermoFisher Scientific). cDNAs are reverse transcribed using High-capacity cDNA Reverse Transcription Kit (Applied Bioscience). cDNAs are further diluted 3 times prior to qRT-PCR. qRT-PCR is performed using LigthCycler 480 SYBR Green I Master mix (Roche) on a LigthCycler 480 apparatus (Roche) following constructor recommendations. The mean value of three replicates was normalized using the EXP (AT4G26410), and TIP4.1 (AT4G34270) genes as internal controls. All primers used in quantitative qRT-PCR are listed below.

Gene	Forward primer (5'->3')	Reverse primer (5'->3')	Type
EXP (*At2g25810*)	GAGCTGAAGTGGCTTCAATGAC	GGTCCGACATACCCATGATCC	Reference
Tip41 (*At4g26410*)	GTGAAAACTGTTGGAGAGAAGCAA	TCAACTGGATACCCTTTCGCA	Reference
YFP	GCACAAGCTGGAGTACAACTA	TGTTGTGGCGGATCTTGAA	Target
FBW2	CTTCTCCTTCATTGCACAACATGC	TCAGACCACTTCTTGGCACCTTC	Target
AGO1	CGGTGGACAGAAGTGGGAAT	GGTCGAGAAGTGCCCTGAAT	Target

2.3.4 RNA immunoprecipitation of AGO1-associated small RNAs

Extraction buffer : 50 mM Tris, pH 7.5, 150 mM NaCl, 10% glycerol, 5 mM MgCl2, 0.1% Igepal, 5 mM DTT, 10 µM MG132, and 1×Complete protease inhibitors cocktail [Roche]

For immunoprecipitation of endogenous AGO1, frozen tissues were ground to a fine powder with a mortar and pestle, resuspended in 3 volumes of extraction buffer, and incubated for 20 min at 8 rpm in the cold room. Insoluble material was removed by centrifugation (twice 15 min, 16 000g, 4°C). Identical amounts of crude extracts were incubated with prebound @AGO1 (5 µg) PureProteome Protein A magnetic beads (30 µL; Millipore) for 1 h at 7 rpm in the cold room. Immune complexes were washed three times in the extraction buffer. AGO1-loaded sRNAs were then extracted by

adding directly 800 μl of Tri-reagent (Sigma- Aldrich) to 30 μl of magnetic beads. Extraction of RNA was then performed according to the manufacturer's instructions Extracted small RNA was precipitated in 2 volumes of isopropanol and 40 μg of glycogen overnight at −20°C. Pellets were resuspended in 60% formamide and analyzed by RNA gel blot as described above.

2.3.5 Libraries preparation and high-throughput sequencing

Total-RNA samples were extracted from 2-week-old seedlings grown on MS-agar plates using Tri-Reagent according to the manufacturer's instruction.

For AGO1-loaded sRNA samples, IPs were performed as described above from 300 mg of 2-week-old arabidopis seedlings grown on MS-agar plates. AGO1-loaded sRNAs were then extracted by adding Tri-Reagent directly on the magnetic beads and extraction of RNA was then performed according to the manufacturer's instructions.

RNA samples were sent to Fasteris (http://www.fasteris.com) for library preparation and sRNA sequencing on an Illumina HiSeq sequencer. For total-RNA library preparation, 3 μg of total RNA from each sample was sent to Fasteris and for AGO1 loaded sRNA the total amount of RNA recovered from each IP were used. For each condition, two biological replicates were processed. FASTQ file generation, demultiplexing, and adapter removal were done by Fasteris.

2.3.6 Bioinformatic analysis

Sequencing data quality was assed using FastQC (www.bioinformatics.babraham.ac.uk/projects/fastqc/). The reads were then mapped against the 69355 genomic loci annotated in the *Arabidopsis thaliana* Col0 genome version 11 (www.araport.org/data/araport11) using the Shortstack program (Johnson et al., 2016) with the following parameters :

--dicermin 15 --dicermax 75: reads from 15 to 75 nts are processed.

--nohp: novel miRNA search is disabled

--mismatches 0: reads are aligned without allowing mismatches

--pad 75: Clusters of reads within 75 nts of each other are merged.

--mincov: 0.5rpm: Clusters of reads must at least contain 0,5 reads per million.

--show_secondaries: secondary alignments of multi-mapping reads are kept in the alignment file

--bowtie_m all: multi-mapping reads are mapped at every possible location

--mmap f: multi-mapping reads are counted evenly on their mapping site

--ranmax none: no multi-mapping reads are discarded

 The total number of reads per locus was then differentially analyzed against the Col0 libraries with the R DEseq2 package (Love et al., 2014).

Bibliography

Adams, B.D., Claffey, K.P., and White, B.A. (2009). Argonaute-2 expression is regulated by epidermal growth factor receptor and mitogen-activated protein kinase signaling and correlates with a transformed phenotype in breast cancer cells. Endocrinology **150**: 14–23.

Addo-Quaye, C., Eshoo, T.W., Bartel, D.P., and Axtell, M.J. (2008). Endogenous siRNA and miRNA targets identified by sequencing of the Arabidopsis degradome. Curr. Biol. **18**: 758–62.

Alcaide-Loridan, C. and Jupin, I. (2012). Ubiquitin and Plant Viruses, Let's Play Together! Plant Physiol. **160**: 72–82.

Allen, E., Xie, Z., Gustafson, A.M., and Carrington, J.C. (2005). microRNA-directed phasing during trans-acting siRNA biogenesis in plants. Cell **121**: 207–221.

Alonso, J.M. et al. (2003). Genome-wide insertional mutagenesis of Arabidopsis thaliana. Science (80-.). **301**: 653–657.

Alves, C.S., Vicentini, R., Duarte, G.T., Pinoti, V.F., Vincentz, M., and Nogueira, F.T.S. (2017). Genome-wide identification and characterization of tRNA-derived RNA fragments in land plants. Plant Mol. Biol. **93**: 35–48.

Anders, S. and Huber, W. (2010). Differential expression analysis for sequence count data. Genome Biol. **11**: R106.

Andersen, P., Kragelund, B.B., Olsen, A.N., Larsen, F.H., Chua, N.H., Poulsen, F.M., and Skriver, K. (2004). Structure and biochemical function of a prototypical Arabidopsis U-box domain. J. Biol. Chem. **279**: 40053–40061.

Anderson, P. and Kedersha, N. (2008). Stress granules: the Tao of RNA triage. Trends Biochem. Sci. **33**: 141–150.

Angot, A., Peeters, N., Lechner, E., Vailleau, F., Baud, C., Gentzbittel, L., Sartorel, E., Genschik, P., Boucher, C., and Genin, S. (2006). Ralstonia solanacearum requires F-box-like domain-containing type III effectors to promote disease on several host plants. Proc. Natl. Acad. Sci. **103**: 14620–14625.

Aravind, L. and Koonin, E. V. (2000). The U box is a modified RING finger - A common domain in ubiquitination [1]. Curr. Biol. **10**: 132–134.

Arribas-Hernández, L., Kielpinski, L.J., and Brodersen, P. (2016). mRNA decay of most Arabidopsis miRNA targets requires slicer activity of AGO1. Plant Physiol.: pp.00231.2016.

Asher, G., Reuven, N., and Shaul, Y. (2006). 20S proteasomes and protein degradation "by default." BioEssays **28**: 844–849.

Axtell, M.J. (2013). Classification and Comparison of Small RNAs from Plants. Annu. Rev. Plant Biol. **64**: 137–159.

Azevedo, J., Garcia, D., Pontier, D., Ohnesorge, S., Yu, A., Garcia, S., Braun, L., Bergdoll, M., Hakimi, M.A., Lagrange, T., and Voinnet, O. (2010). Argonaute quenching and global changes in Dicer homeostasis caused by a pathogen-encoded GW repeat protein. Genes Dev. **24**: 904–915.

Baboshina, O. V. and Haas, A.L. (1996). Novel multiubiquitin chain linkages catalyzed by the conjugating enzymes E2EPFand RAD6 are recognized by 26 S proteasome subunit 5. J. Biol. Chem. **271**: 2823–2831.

Baillat, D. and Shiekhattar, R. (2009). Functional Dissection of the Human TNRC6 (GW182-Related) Family of Proteins. Mol. Cell. Biol. **29**: 4144–4155.

Bartel, D.P. (2004). MicroRNAs: Genomics, Biogenesis, Mechanism, and Function. Cell **116**: 281–297.

Bassham, D.C., Laporte, M., Marty, F., Moriyasu, Y., Ohsumi, Y., Olsen, L.J., and

Yoshimoto, K. (2006). Autophagy in development and stress responses of plants. Autophagy **2**: 2–11.

Baulcombe, D. (2004). RNA silencing in plants. Nature **431**: 356–63.

Baumberger, N. and Baulcombe, D.C. (2005). Arabidopsis ARGONAUTE1 is an RNA Slicer that selectively recruits microRNAs and short interfering RNAs. Proc. Natl. Acad. Sci. U. S. A. **102**: 11928–33.

Baumberger, N., Tsai, C., Lie, M., Havecker, E., and Baulcombe, D.C. (2007). The Polerovirus silencing suppressor P0 targets ARGONAUTE proteins for degradation. Curr. Biol. **17**: 1609–14.

Behm-Ansmant, I., Rehwinkel, J., Doerks, T., Stark, A., Bork, P., and Izaurralde, E. (2006). mRNA degradation by miRNAs and GW182 requires both CCR4 : NOT deadenylase and DCP1 : DCP2 decapping complexes. Genes Dev. **20**: 1885–1898 ST–MRNA degradation by miRNAs and GW1.

Berardini, T.Z., Bollman, K., Sun, H., and Poethig, R.S. (2001). Regulation of vegetative phase change in Arabidopsis thaliana by cyclophilin 40. Sci. (New York, NY) **291**: 2405–2407.

Bernhardt, A., Lechner, E., Hano, P., Schade, V., Dieterle, M., Anders, M., Dubin, M.J., Benvenuto, G., Bowler, C., Genschik, P., and Hellmann, H. (2006). CUL4 associates with DDB1 and DET1 and its downregulation affects diverse aspects of development in Arabidopsis thaliana. Plant J. **47**: 591–603.

Bernstein, E., Caudy, A.A., Hammond, S.M., and Hannon, G.J. (2001). Role for a bidentate ribonuclease in the initiation step of RNA interference. Nature **409**: 363–6.

Bies-Etheve, N., Pontier, D., Lahmy, S., Picart, C., Vega, D., Cooke, R., and Lagrange, T. (2009). RNA-directed DNA methylation requires an AGO4-interacting member of the SPT5 elongation factor family. EMBO Rep. **10**: 649–654.

Blevins, T., Rajeswaran, R., Shivaprasad, P. V., Beknazariants, D., Si-Ammour, A., Park, H.S., Vazquez, F., Robertson, D., Meins, F., Hohn, T., and Pooggin, M.M. (2006). Four plant Dicers mediate viral small RNA biogenesis and DNA virus induced silencing. Nucleic Acids Res. **34**: 6233–6246.

Bohmert, K., Camus, I., Bellini, C., Bouchez, D., Caboche, M., and Benning, C. (1998). AGO1 defines a novel locus of Arabidopsis controlling leaf development. EMBO J. **17**: 170–80.

Bologna, N.G., Iselin, R., Abriata, L.A., Sarazin, A., Pumplin, N., Jay, F., Grentzinger, T., Dal Peraro, M., and Voinnet, O. (2018). Nucleo-cytosolic Shuttling of ARGONAUTE1 Prompts a Revised Model of the Plant MicroRNA Pathway. Mol. Cell **69**: 1–11.

Borges, F. and Martienssen, R.A. (2015). The expanding world of small RNAs in plants. Nat. Rev. Mol. Cell Biol. **16**: 727–741.

Borsani, O., Zhu, J., Verslues, P.E., Sunkar, R., and Zhu, J.K. (2005). Endogenous siRNAs derived from a pair of natural cis-antisense transcripts regulate salt tolerance in Arabidopsis. Cell **123**: 1279–1291.

Bortolamiol, D., Pazhouhandeh, M., Marrocco, K., Genschik, P., and Ziegler-Graff, V. (2007). The Polerovirus F box protein P0 targets ARGONAUTE1 to suppress RNA silencing. Curr. Biol. **17**: 1615–21.

Bossi, F., Fan, J., Xiao, J., Chandra, L., Shen, M., Dorone, Y., Wagner, D., and Rhee, S.Y. (2017). Systematic discovery of novel eukaryotic transcriptional regulators using sequence homology independent prediction. BMC Genomics

18: 1–20.

Bourbousse, C., Ahmed, I., Roudier, F., Zabulon, G., Blondet, E., Balzergue, S., Colot, V., Bowler, C., and Barneche, F. (2012). Histone H2B monoubiquitination facilitates the rapid modulation of gene expression during arabidopsis photomorphogenesis. PLoS Genet. **8**.

Boutet, S., Vazquez, F., Liu, J., Béclin, C., Fagard, M., Gratias, A., Morel, J.B., Crété, P., Chen, X., and Vaucheret, H. (2003). Arabidopsis HEN1: a genetic link between endogenous miRNA controlling development and siRNA controlling transgene silencing and virus resistance. Curr. Biol. **13**: 843–8.

Brosseau, C. and Moffett, P. (2015). Functional and Genetic Analysis Identify a Role for Arabidopsis ARGONAUTE5 in Antiviral RNA Silencing. Plant Cell **27**: 1742–1754.

Callis, J. (2014). The Ubiquitination Machinery of the Ubiquitin System. Arab. B. **12**: e0174.

Callis, J., Carpenter, T., Sun, C.W., and Vierstra, R.D. (1995). Structure and evolution of genes encoding polyubiquitin and ubiquitin-like proteins in Arabidopsis thaliana ecotype Columbia. Genetics **139**: 921–939.

Callis, J., Raasch, J.A., and Vierstra, R.D. (1990). Ubiquitin Extension Proteins of Arabidopsis thaliana. J. Biol. Chem. **265**: 12486–12493.

Cao, X., Aufsatz, W., Zilberman, D., Mette, M.F., Huang, M.S., Matzke, M., and Jacobsen, S.E. (2003). Role of the DRM and CMT3 Methyltransferases in RNA-Directed DNA Methylation. Curr. Biol. **13**: 2212–2217.

Cerutti, L., Mian, N., and Bateman, A. (2000). Domains in gene silencing and cell differentiation proteins: tTe novel PAZ domain and redefinition of the Piwi domain. Trends Biochem. Sci. **25**: 481–482.

Chang, B., Partha, S., Hofmann, K., Lei, M., Goebl, M., Harper, J.W., and Elledge, S.J. (1996). SKP1 connects cell cycle regulators to the ubiquitin proteolysis machinery through a novel motif, the F-box. Cell **86**: 263–274.

Chang, H.M., Martinez, N.J., Thornton, J.E., Hagan, J.P., Nguyen, K.D., and Gregory, R.I. (2012). Trim71 cooperates with microRNAs to repress Cdkn1a expression and promote embryonic stem cell proliferation. Nat. Commun. **3**: 910–923.

Chau, V., Tobias, J., Bachmair, A., Marriott, D., Ecker, D., Gonda, D., and Varshavsky, A. (1989). A multiubiquitin chain is confined to specific lysine in a targeted short-lived protein. Science (80-.). **243**: 1576–1583.

Chen, H.-M., Chen, L.-T., Patel, K., Li, Y.-H., Baulcombe, D.C., and Wu, S.-H. (2010). 22-nucleotide RNAs trigger secondary siRNA biogenesis in plants. Proc. Natl. Acad. Sci. **107**: 15269–15274.

Chen, H.Y., Yang, J., Lin, C., and Yuan, Y.A. (2008). Structural basis for RNA-silencing suppression by Tomato aspermy virus protein 2b. EMBO Rep. **9**: 754–760.

Chen, J., Lai, F., and Niswander, L. (2012). The ubiquitin ligase mLin41 temporally promotes neural progenitor cell maintenance through FGF signaling. Genes Dev. **26**: 803–815.

Chen, L. and Hellmann, H. (2013). Plant E3 ligases: flexible enzymes in a sessile world. Mol. Plant **6**: 1388–404.

Chenon, M., Camborde, L., Cheminant, S., and Jupin, I. (2012). A viral deubiquitylating enzyme targets viral RNA-dependent RNA polymerase and affects viral infectivity. EMBO J. **31**: 741–753.

Chinen, M. and Lei, E.P. (2017). Drosophila Argonaute2 turnover is regulated by the ubiquitin proteasome pathway. Biochem. Biophys. Res. Commun. **483**: 951–957.

Chiu, M.-H., Chen, I.-H., Baulcombe, D.C., and Tsai, C. (2010). The silencing suppressor P25 of Potato virus X interacts with Argonaute1 and mediates its degradation through the proteasome pathway. Mol. Plant Pathol. **11**: 641–9.

Christensen, D.E., Brzovic, P.S., and Klevit, R.E. (2007). E2-BRCA1 RING interactions dictate synthesis of mono- or specific polyubiquitin chain linkages. Nat. Struct. Mol. Biol. **14**: 941–948.

Ciechanover, A. and Ben-Saadon, R. (2004). N-terminal ubiquitination: More protein substrates join in. Trends Cell Biol. **14**: 103–106.

Clough, S.J. and Bent, A.F. (1998). Floral dip : a simplified method for Agrobacterium-mediated transformation of Arabidopsis thaliana. Plant J. **16**: 735–743.

Cognat, V., Morelle, G., Megel, C., Lalande, S., Molinier, J., Vincent, T., Small, I., Duchêne, A.-M., and Maréchal-Drouard, L. (2017). The nuclear and organellar tRNA-derived RNA fragment population in Arabidopsis thaliana is highly dynamic. Nucleic Acids Res. **45**: 3460–3472.

Csorba, T., Kontra, L., and Burgyán, J. (2015). Viral silencing suppressors: Tools forged to fine-tune host-pathogen coexistence. Virology **479–480**: 85–103.

Csorba, T., Lózsa, R., Hutvágner, G., and Burgyán, J. (2010). Polerovirus protein P0 prevents the assembly of small RNA-containing RISC complexes and leads to degradation of ARGONAUTE1. Plant J. **62**: 463–72.

Curtis, M.D. (2003). A Gateway Cloning Vector Set for High-Throughput Functional Analysis of Genes in Planta. PLANT Physiol. **133**: 462–469.

D'Andréa, A. and Pellman, D. (1998). Deubiquitinating enzymes: A new class of biological regulators. Crit. Rev. Biochem. Mol. Biol. **33**: 337–352.

DeBeauchamp, J.L., Moses, A., Noffsinger, V.J.P., Ulrich, D.L., Job, G., Kosinski, A.M., and Partridge, J.F. (2008). Chp1-Tas3 Interaction Is Required To Recruit RITS to Fission Yeast Centromeres and for Maintenance of Centromeric Heterochromatin. Mol. Cell. Biol. **28**: 2154–2166.

Deleris, A., Gallago-Bartolome, J., Bao, J., Kasschau, K.D., Carrington, J.C., and Voinnet, O. (2006). Hierarchical action and inhibition of plant dicer-like proteins in antiviral defense. Science (80-.). **313**: 68–71.

Derrien, B., Baumberger, N., Schepetilnikov, M., Viotti, C., De Cillia, J., Ziegler-Graff, V., Isono, E., Schumacher, K., and Genschik, P. (2012). Degradation of the antiviral component ARGONAUTE1 by the autophagy pathway. Proc. Natl. Acad. Sci. U. S. A. **109**: 15942–6.

Derrien, B., Clavel, M., Baumberger, N., Iki, T., Sarazin, A., Hacquard, T., Ponce, M.R., Ziegler-Graff, V., Vaucheret, H., Micol, J.L., Voinnet, O., and Genschik, P. (2018). A Suppressor Screen for AGO1 Degradation by the Viral F-Box P0 Protein Uncovers a Role for AGO DUF1785 in sRNA Duplex Unwinding. Plant Cell **30**: 1353–1374.

Deshaies, R.J. and Joazeiro, C.A.P. (2009). RING Domain E3 Ubiquitin Ligases. Annu. Rev. Biochem. **78**: 399–434.

Dezfulian, M.H., Soulliere, D.M., Dhaliwal, R.K., Sareen, M., and Crosby, W.L. (2012). The SKP1-Like Gene Family of Arabidopsis Exhibits a High Degree of Differential Gene Expression and Gene Product Interaction during Development. PLoS One **7**: 18–20.

Dhahbi, J.M. (2015). 5' tRNA halves: The next generation of immune signaling

molecules. Front. Immunol. **6**: 1–5.

Díaz-Pendón, J.A. and Ding, S.-W. (2008). Direct and Indirect Roles of Viral Suppressors of RNA Silencing in Pathogenesis. Annu. Rev. Phytopathol. **46**: 303–326.

Diaz-Pendon, J.A., Li, F., Li, W.-X., and Ding, S.-W. (2007). Suppression of antiviral silencing by cucumber mosaic virus 2b protein in Arabidopsis is associated with drastically reduced accumulation of three classes of viral small interfering RNAs. Plant Cell **19**: 2053–63.

Dieterle, M., Thomann, A., Renou, J.-P., Parmentier, Y., Cognat, V., Lemonnier, G., Müller, R., Shen, W.-H., Kretsch, T., and Genschik, P. (2005). Molecular and functional characterization of Arabidopsis Cullin 3A. Plant J. **41**: 386–99.

Ding, L. and Han, M. (2007). GW182 family proteins are crucial for microRNA-mediated gene silencing. Trends Cell Biol. **17**: 411–416.

Dobrenel, T., Caldana, C., Hanson, J., Robaglia, C., Vincentz, M., Veit, B., and Meyer, C. (2016). TOR Signaling and Nutrient Sensing. Annu. Rev. Plant Biol. **67**: 261–285.

Dong, Z., Han, M.-H., and Fedoroff, N. (2008). The RNA-binding proteins HYL1 and SE promote accurate in vitro processing of pri-miRNA by DCL1. Proc. Natl. Acad. Sci. U. S. A. **105**: 9970–5.

Downes, B.P., Stupar, R.M., Gingerich, D.J., and Vierstra, R.D. (2003). The HECT ubiquitin-protein ligase (UPL) family in Arabidopsis: UPL3 has a specific role in trichome development. Plant J. **35**: 729–742.

Dubin, M.J., Bowler, C., and Benvenuto, G. (2010). Overexpressing tagged proteins in plants using a modified gateway cloning strategy. Cold Spring Harb. Protoc. **5**: 1–11.

Earley, K., Smith, M., Weber, R., Gregory, B., and Poethig, R. (2010). An endogenous F-box protein regulates ARGONAUTE1 in Arabidopsis thaliana. Silence **1**: 15.

Earley, K.W., Haag, J.R., Pontes, O., Opper, K., Juehne, T., Song, K., and Pikaard, C.S. (2006). Gateway-compatible vectors for plant functional genomics and proteomics. Plant J. **45**: 616–29.

Earley, K.W. and Poethig, R.S. (2011). Binding of the cyclophilin 40 ortholog SQUINT to Hsp90 protein is required for SQUINT function in Arabidopsis. J. Biol. Chem. **286**: 38184–38189.

Edelheit, O., Hanukoglu, A., and Hanukoglu, I. (2009). Simple and efficient site-directed mutagenesis using two single-primer reactions in parallel to generate mutants for protein structure-function studies. BMC Biotechnol. **9**: 61.

El-shami, M., Pontier, D., Lahmy, S., Braun, L., Picart, C., Vega, D., Hakimi, M., Jacobsen, S.E., Cooke, R., and Lagrange, T. (2007). Reiterated WG / GW motifs form functionally and evolutionarily conserved ARGONAUTE-binding platforms in RNAi-related components service Reiterated WG / GW motifs form functionally and evolutionarily conserved platforms in RNAi-related components. Genes Dev.: 2539–2544.

Elkayam, E., Faehnle, C.R., Morales, M., Sun, J., Li, H., and Joshua-Tor, L. (2017). Multivalent Recruitment of Human Argonaute by GW182. Mol. Cell **67**: 646–658.e3.

Elkayam, E., Kuhn, C.D., Tocilj, A., Haase, A.D., Greene, E.M., Hannon, G.J., and Joshua-Tor, L. (2012). The structure of human argonaute-2 in complex with miR-20a. Cell **150**: 100–110.

Elmayan, T., Balzergue, S., Béon, F., Bourdon, V., Daubremet, J., Guénet, Y., Mourrain, P., Palauqui, J.C., Vernhettes, S., Vialle, T., Wostrikoff, K., and Vaucheret, H. (1998). Arabidopsis mutants impaired in cosuppression. Plant Cell **10**: 1747–1758.

Elsasser, S., Gali, R.R., Schwikart, M., Larsen, C.N., Leggett, D.S., Müller, B., Feng, M.T., Tübing, F., Dittmar, G.A.G., and Finley, D. (2002). Proteasome subunit Rpn1 binds ubiquitin-like protein domains. Nat. Cell Biol. **4**: 725–730.

Emami, S., Arumainayagam, D., Korf, I., and Rose, A.B. (2013). The effects of a stimulating intron on the expression of heterologous genes in Arabidopsis thaliana. Plant Biotechnol. J. **11**: 555–563.

Erpapazoglou, Z., Walker, O., and Haguenauer-Tsapis, R. (2014). Versatile Roles of K63-Linked Ubiquitin Chains in Trafficking. Cells **3**: 1027–1088.

Eystathioy, T., Chan, E.K.L., Tenenbaum, S.A., Keene, J.D., Griffith, K., and Fritzler, M.J. (2002). A phosphorylated cytoplasmic autoantigen, GW182, associates with a unique population of human mRNAs within novel cytoplasmic speckles. Mol. Biol. Cell **13**: 1338–51.

Fabian, M.R. et al. (2009). Mammalian miRNA RISC Recruits CAF1 and PABP to Affect PABP-Dependent Deadenylation. Mol. Cell **35**: 868–880.

Fagard, M., Boutet, S., Morel, J.B., Bellini, C., and Vaucheret, H. (2000). AGO1, QDE-2, and RDE-1 are related proteins required for post-transcriptional gene silencing in plants, quelling in fungi, and RNA interference in animals. Proc. Natl. Acad. Sci. U. S. A. **97**: 11650–11654.

Finley, D. (2009). Recognition and Processing of Ubiquitin-Protein Conjugates by the Proteasome. Annu. Rev. Biochem. **78**: 477–513.

Floyd, B.E., Morriss, S.C., MacIntosh, G.C., and Bassham, D.C. (2015). Evidence for autophagy-dependent pathways of rRNA turnover in Arabidopsis. Autophagy **11**: 2199–2212.

Frank, F., Hauver, J., Sonenberg, N., and Nagar, B. (2012). Arabidopsis Argonaute MID domains use their nucleotide specificity loop to sort small RNAs. EMBO J. **31**: 3588–3595.

Frank, F., Sonenberg, N., and Nagar, B. (2010). Structural basis for 5′-nucleotide base-specific recognition of guide RNA by human AGO2. Nature **465**: 818–822.

Freemont, P.S., Hanson, I.M., and Trowsdale, J. (1991). A novel cysteine-rich sequence motif. Cell **64**: 483–4.

Friedman, R.C., Farh, K.K.-H., Burge, C.B., and Bartel, D.P. (2009). Most mammalian mRNAs are conserved targets of microRNAs. Genome Res. **19**: 92–105.

Fu, H., Sadis, S., Rubin, D.M., Glickman, M., Van Nocker, S., Finley, D., and Vierstra, R.D. (1998). Multiubiquitin chain binding and protein degradation are mediated by distinct domains within the 26 S proteasome subunit Mcb1. J. Biol. Chem. **273**: 1970–1981.

Fultz, D., Choudury, S.G., and Slotkin, R.K. (2015). Silencing of active transposable elements in plants. Curr. Opin. Plant Biol. **27**: 67–76.

Fusaro, A.F., Correa, R.L., Nakasugi, K., Jackson, C., Kawchuk, L., Vaslin, M.F.S., and Waterhouse, P.M. (2012). The Enamovirus P0 protein is a silencing suppressor which inhibits local and systemic RNA silencing through AGO1 degradation. Virology **426**: 178–187.

Gagne, J.M., Downes, B.P., Shiu, S.-H., Durski, A.M., and Vierstra, R.D. (2002). The F-box subunit of the SCF E3 complex is encoded by a diverse superfamily

of genes in Arabidopsis. Proc. Natl. Acad. Sci. **99**: 11519–11524.

Galan, J.-M. and Peter, M. (1999). Ubiquitin-dependent degradation of multiple F-box proteins by an autocatalytic mechanism. Proc. Natl. Acad. Sci. **96**: 9124–9129.

Gallegos, J.E. and Rose, A.B. (2015). The enduring mystery of intron-mediated enhancement. Plant Sci. **237**: 8–15.

Gasciolli, V., Mallory, A.C., Bartel, D.P., and Vaucheret, H. (2005). Partially redundant functions of arabidopsis DICER-like enzymes and a role for DCL4 in producing trans-Acting siRNAs. Curr. Biol. **15**: 1494–1500.

Genschik, P., Sumara, I., and Lechner, E. (2013). The emerging family of CULLIN3-RING ubiquitin ligases (CRL3s): Cellular functions and disease implications. EMBO J. **32**: 2307–2320.

German, M.A. et al. (2008). Global identification of microRNA-target RNA pairs by parallel analysis of RNA ends. Nat. Biotechnol. **26**: 941–946.

Ghag, S.B., Shekhawat, U.K.S., and Ganapathi, T.R. (2014). Host-induced post-transcriptional hairpin RNA-mediated gene silencing of vital fungal genes confers efficient resistance against Fusarium wilt in banana. Plant Biotechnol. J. **12**: 541–553.

Gibbings, D., Mostowy, S., Jay, F., Schwab, Y., Cossart, P., and Voinnet, O. (2012). Selective autophagy degrades DICER and AGO2 and regulates miRNA activity. Nat. Cell Biol. **14**: 1314–21.

Gieffers, C., Dube, P., Harris, J.R., Stark, H., and Peters, J.M. (2001). Three-dimensional structure of the anaphase-promoting complex. Mol. Cell **7**: 907–13.

Gingerich, D.J., Gagne, J.M., Salter, D.W., Hellmann, H., Estelle, M., Ma, L., and Vierstra, R.D. (2005). Cullins 3a and 3b assemble with members of the broad complex/tramtrack/ bric-a-brac (BTB) protein family to form essential ubiquitin-protein ligases (E3s) in arabidopsis. J. Biol. Chem. **280**: 18810–18821.

Goldberg, A.L. (2012). Development of proteasome inhibitors as research tools and cancer drugs. J. Cell Biol. **199**: 583–588.

Golden, R.J. et al. (2017). An Argonaute phosphorylation cycle promotes microRNA-mediated silencing. Nature **542**: 197–202.

Goto, K., Kobori, T., Kosaka, Y., Natsuaki, T., and Masuta, C. (2007). Characterization of silencing suppressor 2b of cucumber mosaic virus based on examination of its small RNA-binding abilities. Plant Cell Physiol. **48**: 1050–1060.

Graciet, E. and Wellmer, F. (2010). The plant N-end rule pathway: Structure and functions. Trends Plant Sci. **15**: 447–453.

Grumati, P. and Dikic, I. (2018). Ubiquitin signaling and autophagy. J. Biol. Chem. **293**: 5404–5413.

Guo, H.S. and Ding, S.W. (2002). A viral protein inhibits the long range signaling activity of the gene silencing signal. EMBO J. **21**: 398–407.

Haas, A.L. and Rose, I.A. (1982). The mechanism of ubiquitin activating enzyme. A kinetic and equilibrium analysis. J. Biol. Chem. **257**: 10329–10337.

Haas, A.L., Warms, J. V, Hershko, A., and Rose, I.A. (1982). Ubiquitin-activating enzyme. Mechanism and role in protein-ubiquitin conjugation. J. Biol. Chem. **257**: 2543–8.

Han, M.-H., Goud, S., Song, L., and Fedoroff, N. (2004). The Arabidopsis double-stranded RNA-binding protein HYL1 plays a role in microRNA-mediated gene regulation. Proc. Natl. Acad. Sci. **101**: 1093–1098.

Harvey, J.J.W., Lewsey, M.G., Patel, K., Westwood, J., Heimstädt, S., Carr, J.P., and Baulcombe, D.C. (2011). An antiviral defense role of AGO2 in plants. PLoS One **6**: 1–6.

Hatfield, P.M., Gosink, M.M., Carpenter, T.B., and Vierstra, R.D. (1997). The ubiquitin-activating enzyme (E1) gene family in Arabidopsis thaliana. Plant J. **11**: 213–226.

Havecker, E.R., Wallbridge, L.M., Hardcastle, T.J., Bush, M.S., Kelly, K.A., Dunn, R.M., Schwach, F., Doonan, J.H., and Baulcombe, D.C. (2010). The Arabidopsis RNA-Directed DNA Methylation Argonautes Functionally Diverge Based on Their Expression and Interaction with Target Loci. Plant Cell **22**: 321–334.

Herr, A.J., Jensen, M.B., Dalmay, T., and Baulcombe, D.C. (2005). RNA polymerase IV directs silencing of endogenous DNA. Science (80-.). **308**: 118–120.

Hershko, A. (1998). The Ubiquitin System. In Ubiquitin and the Biology of the Cell (Springer US: Boston, MA), pp. 1–17.

Hershko, A. (1983). Ubiquitin: Roles in protein modification and breakdown. Cell **34**: 11–12.

Hershko, A. and Ciechanover, A. (1992). The Ubiquitin System for Protein Degradation. Annu. Rev. Biochem. **61**: 761–807.

Hicke, L. and Dunn, R. (2003). Regulation of Membrane Protein Transport by Ubiquitin and Ubiquitin-Binding Proteins. Annu. Rev. Cell Dev. Biol. **19**: 141–172.

Higa, L. and Zhang, H. (2007). Stealing the spotlight: CUL4-DDB1 ubiquitin ligase docks WD40-repeat proteins to destroy. Cell Div. **2**: 1–9.

Himanen, K., Woloszynska, M., Boccardi, T.M., De Groeve, S., Nelissen, H., Bruno, L., Vuylsteke, M., and Van Lijsebettens, M. (2012). Histone H2B monoubiquitination is required to reach maximal transcript levels of circadian clock genes in Arabidopsis. Plant J. **72**: 249–260.

Himber, C., Dunoyer, P., Moissiard, G., Ritzenthaler, C., and Voinnet, O. (2003). Transitivity-dependent and -independent cell-to-cell movement of RNA silencing. EMBO J. **22**: 4523–33.

Höck, J. and Meister, G. (2008). The Argonaute protein family. Genome Biol. **9**.

Höck, J., Weinmann, L., Ender, C., Rüdel, S., Kremmer, E., Raabe, M., Urlaub, H., and Meister, G. (2007). Proteomic and functional analysis of Argonaute-containing mRNA-protein complexes in human cells. EMBO Rep. **8**: 1052–1060.

Holoch, D. and Moazed, D. (2015). Small-RNA loading licenses Argonaute for assembly into a transcriptional silencing complex. Nat. Struct. Mol. Biol. **22**: 328–35.

Hoppe, T. (2005). Multiubiquitylation by E4 enzymes: "One size" doesn't fit all. Trends Biochem. Sci. **30**: 183–187.

Horman, S.R. et al. (2013). Akt-mediated phosphorylation of argonaute 2 downregulates cleavage and upregulates translational repression of MicroRNA targets. Mol. Cell **50**: 356–367.

Hotton, S.K. and Callis, J. (2008). Regulation of Cullin RING Ligases. Annu. Rev. Plant Biol. **59**: 467–489.

Hsieh, J., Walker, S.C., Fierke, C.A., and Engelke, D.R. (2008). Pre-tRNA turnover catalyzed by the yeast nuclear RNase P holoenzyme is limited by product release Pre-tRNA turnover catalyzed by the yeast nuclear RNase P holoenzyme

is limited by product release.: 224–234.

Hua, Z. and Vierstra, R.D. (2011). The cullin-RING ubiquitin-protein ligases. Annu. Rev. Plant Biol. **62**: 299–334.

Huang, Y., Minaker, S., Roth, C., Huang, S., Hieter, P., Lipka, V., Wiermer, M., and Li, X. (2014). An E4 Ligase Facilitates Polyubiquitination of Plant Immune Receptor Resistance Proteins in Arabidopsis. Plant Cell **26**: 485–496.

Huibregtse, J.M., Scheffner, M., Beaudenon, S., and Howley, P.M. (1995). A family of proteins structurally and functionally related to the E6-AP ubiquitin-protein ligase. Proc. Natl. Acad. Sci. **92**: 2563–2567.

Hutvágner, G., McLachlan, J., Pasquinelli, A.E., Bálint, E., Tuschl, T., and Zamore, P.D. (2001). A cellular function for the RNA-interference enzyme Dicer in the maturation of the let-7 small temporal RNA. Science **293**: 834–8.

Ikeda, F. and Dikic, I. (2008). Atypical ubiquitin chains: new molecular signals. 'Protein Modifications: Beyond the Usual Suspects' Review Series. EMBO Rep. **9**: 536–542.

Iki, T., Yoshikawa, M., Meshi, T., and Ishikawa, M. (2011). Cyclophilin 40 facilitates HSP90-mediated RISC assembly in plants. EMBO J. **31**: 267–278.

Iki, T., Yoshikawa, M., Nishikiori, M., Jaudal, M.C., Matsumoto-Yokoyama, E., Mitsuhara, I., Meshi, T., and Ishikawa, M. (2010). In vitro assembly of plant RNA-induced silencing complexes facilitated by molecular chaperone HSP90. Mol. Cell **39**: 282–291.

Isono, E., Katsiarimpa, A., Müller, I.K., Anzenberger, F., Stierhof, Y.-D., Geldner, N., Chory, J., and Schwechheimer, C. (2010). The Deubiquitinating Enzyme AMSH3 Is Required for Intracellular Trafficking and Vacuole Biogenesis in *Arabidopsis thaliana*. Plant Cell **22**: 1826–1837.

Iwasaki, S., Kobayashi, M., Yoda, M., Sakaguchi, Y., Katsuma, S., Suzuki, T., and Tomari, Y. (2010). Hsc70/Hsp90 chaperone machinery mediates ATP-dependent RISC loading of small RNA duplexes. Mol. Cell **39**: 292–299.

Iwasaki, S., Sasaki, H.M., Sakaguchi, Y., Suzuki, T., Tadakuma, H., and Tomari, Y. (2015). Defining fundamental steps in the assembly of the Drosophila RNAi enzyme complex. Nature **521**: 533–536.

Izumi, M., Ishida, H., Nakamura, S., and Hidema, J. (2017). Entire Photodamaged Chloroplasts Are Transported to the Central Vacuole by Autophagy. Plant Cell **29**: 377–394.

Jakymiw, A., Lian, S., Eystathioy, T., Li, S., Satoh, M., Hamel, J.C., Fritzler, M.J., and Chan, E.K.L. (2005). Disruption of GW bodies impairs mammalian RNA interference. Nat. Cell Biol. **7**: 1167–1174.

Jaubert, M., Bhattacharjee, S., Mello, A.F.S., Perry, K.L., and Moffett, P. (2011). ARGONAUTE2 Mediates RNA-Silencing Antiviral Defenses against Potato virus X in Arabidopsis. Plant Physiol. **156**: 1556–1564.

Jee, D. and Lai, E.C. (2014). Alteration of miRNA activity via context-specific modifications of Argonaute proteins. Trends Cell Biol. **24**: 546–553.

Johnson, N.R., Yeoh, J.M., Coruh, C., and Axtell, M.J. (2016). Improved Placement of Multi-mapping Small RNAs. G3&#58; Genes|Genomes|Genetics **6**: 2103–2111.

Johnston, M., Geoffroy, M.C., Sobala, A., Hay, R., and Hutvagner, G. (2010). HSP90 Protein Stabilizes Unloaded Argonaute Complexes and Microscopic P-bodies in Human Cells. Mol. Biol. Cell **21**: 1462–1469.

Johnston, M. and Hutvagner, G. (2011). Posttranslational modification of

Argonautes and their role in small RNA-mediated gene regulation. Silence **2**: 5.

Jones-Rhoades, M.W., Bartel, D.P., and Bartel, B. (2006). MicroRNAS and their regulatory roles in plants. Annu. Rev. Plant Biol. **57**: 19–53.

Josa-Prado, F., Henley, J.M., and Wilkinson, K.A. (2015). SUMOylation of Argonaute-2 regulates RNA interference activity. Biochem. Biophys. Res. Commun. **464**: 1066–1071.

Ju, D., Wang, L., Mao, X., and Xie, Y. (2004). Homeostatic regulation of the proteasome via an Rpn4-dependent feedback circuit. Biochem. Biophys. Res. Commun. **321**: 51–57.

Kalantidis, K., Tsagris, M., and Tabler, M. (2006). Spontaneous short-range silencing of a GFP transgene in Nicotiana benthamiana is possibly mediated by small quantities of siRNA that do not trigger systemic silencing. Plant J. **45**: 1006–1016.

Kalde, M., Barth, M., Somssich, I.E., and Lippok, B. (2003). Members of the Arabidopsis WRKY group III transcription factors are part of different plant defense signaling pathways. Mol. Plant-Microbe Interact. **16**: 295–305.

Kane, L.A., Lazarou, M., Fogel, A.I., Li, Y., Yamano, K., Sarraf, S.A., Banerjee, S., and Youle, R.J. (2014). PINK1 phosphorylates ubiquitin to activate parkin E3 ubiquitin ligase activity. J. Cell Biol. **205**: 143–153.

Kanno, T., Huettel, B., Mette, M.F., Aufsatz, W., Jaligot, E., Daxinger, L., Kreil, D.P., Matzke, M., and Matzke, A.J.M. (2005). Atypical RNA polymerase subunits required for RNA-directed DNA methylation. Nat. Genet. **37**: 761–765.

Karlowski, W.M., Zielezinski, A., Carrère, J., Pontier, D., Lagrange, T., and Cooke, R. (2010). Genome-wide computational identification of WG/GW Argonaute-binding proteins in Arabidopsis. Nucleic Acids Res. **38**: 4231–4245.

Kawamata, T., Seitz, H., and Tomari, Y. (2009). Structural determinants of miRNAs for RISC loading and slicer-independent unwinding. Nat. Struct. Mol. Biol. **16**: 953–960.

Kelly, L.A., Mezulis, S., Yates, C., Wass, M., and Sternberg, M. (2015). The Phyre2 web portal for protein modelling, prediction, and analysis. Nat. Protoc. **10**: 845–858.

Khaminets, A., Behl, C., and Dikic, I. (2016). Ubiquitin-Dependent And Independent Signals In Selective Autophagy. Trends Cell Biol. **26**: 6–16.

Kim, D.-Y., Scalf, M., Smith, L.M., and Vierstra, R.D. (2013). Advanced proteomic analyses yield a deep catalog of ubiquitylation targets in Arabidopsis. Plant Cell **25**: 1523–1540.

Kipreos, E.T. and Pagano, M. (2000). The F-box protein family. Genome Biol. **1**: REVIEWS3002.

Knip, M., Constantin, M.E., and Thordal-Christensen, H. (2014). Trans-kingdom Cross-Talk: Small RNAs on the Move. PLoS Genet. **10**.

Kobayashi, K. and Zambryski, P. (2007). RNA silencing and its cell-to-cell spread during Arabidopsis embryogenesis. Plant J. **50**: 597–604.

Koch, A., Kumar, N., Weber, L., Keller, H., Imani, J., and Kogel, K.-H. (2013). Host-induced gene silencing of cytochrome P450 lanosterol C14 -demethylase-encoding genes confers strong resistance to Fusarium species. Proc. Natl. Acad. Sci. **110**: 19324–19329.

Koegl, M., Hoppe, T., Schlenker, S., Ulrich, H.D., Mayer, T.U., and Jentsch, S. (1999). A novel ubiquitination factor, E4, is involved in multiubiquitin chain assembly. Cell **96**: 635–644.

Komander, D. and Rape, M. (2012). The Ubiquitin Code. Annu. Rev. Biochem. **81**: 203–229.

Korolchuk, V.I., Menzies, F.M., and Rubinsztein, D.C. (2010). Mechanisms of cross-talk between the ubiquitin-proteasome and autophagy-lysosome systems. FEBS Lett. **584**: 1393–1398.

Kraft, C., Deplazes, A., Sohrmann, M., and Peter, M. (2008). Mature ribosomes are selectively degraded upon starvation by an autophagy pathway requiring the Ubp3p/Bre5p ubiquitin protease. Nat. Cell Biol. **10**: 602–610.

Krol, J., Loedige, I., and Filipowicz, W. (2010). The widespread regulation of microRNA biogenesis, function and decay. Nat. Rev. Genet. **11**: 597–610.

Krüger, E. and Kloetzel, P.M. (2012). Immunoproteasomes at the interface of innate and adaptive immune responses: Two faces of one enzyme. Curr. Opin. Immunol. **24**: 77–83.

Kumar, S., Kao, W.H., and Howley, P.M. (1997). Physical interaction between specific E2 and hect E3 enzymes determines functional cooperativity. J. Biol. Chem. **272**: 13548–13554.

Kurepa, J. and Smalle, J.A. (2008). Structure, function and regulation of plant proteasomes. Biochimie **90**: 324–335.

Kurihara, Y., Takashi, Y., and Watanabe, Y. (2006). The interaction between DCL1 and HYL1 is important for efficient and precise processing of pri-miRNA in plant microRNA biogenesis. Rna **12**: 206–212.

Kurihara, Y. and Watanabe, Y. (2004). From The Cover: Arabidopsis micro-RNA biogenesis through Dicer-like 1 protein functions. Proc. Natl. Acad. Sci. **101**: 12753–12758.

Kuscu, C., Kumar, P., Kiran, M., Su, Z., Malik, A., and Dutta, A. (2018). tRNA fragments (tRFs) guide Ago to regulate gene expression post-transcriptionally in a Dicer-independent manner. RNA **24**: 1093–1105.

Kwak, P.B. and Tomari, Y. (2012). The N domain of Argonaute drives duplex unwinding during RISC assembly. Nat. Struct. Mol. Biol. **19**: 145–151.

Kwon, Y.T. and Ciechanover, A. (2017). The Ubiquitin Code in the Ubiquitin-Proteasome System and Autophagy. Trends Biochem. Sci. **42**: 873–886.

Lageix, S., Catrice, O., Deragon, J.-M., Gronenborn, B., Pelissier, T., and Ramirez, B.C. (2007). The Nanovirus-Encoded Clink Protein Affects Plant Cell Cycle Regulation through Interaction with the Retinoblastoma-Related Protein. J. Virol. **81**: 4177–4185.

Lahmy, S., Pontier, D., Bies-Etheve, N., Laudié, M., Feng, S., Jobet, E., Hale, C.J., Cooke, R., Hakimi, M., Angelov, D., Jacobsen, S.E., and Lagrange, T. (2016). Evidence for ARGONAUTE4 – DNA interactions in RNA- directed DNA methylation in plants. Genes Dev.: 1–6.

Lahmy, S., Pontier, D., Cavel, E., Vega, D., El-Shami, M., Kanno, T., and Lagrange, T. (2009). PolV(PolIVb) function in RNA-directed DNA methylation requires the conserved active site and an additional plant-specific subunit. Proc. Natl. Acad. Sci. **106**: 941–946.

Lakatos, L., Szittya, G., Silhavy, D., and Burgyán, J. (2004). Molecular mechanism of RNA silencing suppression mediated by p19 protein of tombusviruses. EMBO J. **23**: 876–884.

Lamark, T. and Johansen, T. (2012). Aggrephagy: Selective disposal of protein aggregates by macroautophagy. Int. J. Cell Biol. **2012**.

Lechner, E., Achard, P., Vansiri, A., Potuschak, T., and Genschik, P. (2006). F-

box proteins everywhere. Curr. Opin. Plant Biol. **9**: 631–638.

Lechner, E., Leonhardt, N., Eisler, H., Parmentier, Y., Alioua, M., Jacquet, H., Leung, J., and Genschik, P. (2011). MATH/BTB CRL3 receptors target the homeodomain-leucine zipper ATHB6 to modulate abscisic acid signaling. Dev. Cell **21**: 1116–1128.

Lechner, E., Xie, D., Grava, S., Pigaglio, E., Planchais, S., Murray, J.A.H., Parmentier, Y., Mutterer, J., Dubreucq, B., Shen, W.H., and Genschik, P. (2002). The AtRbx1 protein is part of plant SCF complexes, and its down-regulation causes severe growth and developmental defects. J. Biol. Chem. **277**: 50069–50080.

Lee, I. and Schindelin, H. (2008). Structural Insights into E1-Catalyzed Ubiquitin Activation and Transfer to Conjugating Enzymes. Cell **134**: 268–278.

Lee, J.-H., Terzaghi, W., Gusmaroli, G., Charron, J.-B.F., Yoon, H.-J., Chen, H., He, Y.J., Xiong, Y., and Deng, X.W. (2008). Characterization of Arabidopsis and Rice DWD Proteins and Their Roles as Substrate Receptors for CUL4-RING E3 Ubiquitin Ligases. Plant Cell Online **20**: 152–167.

Lee, J. and Zhou, P. (2007). DCAFs, the Missing Link of the CUL4-DDB1 Ubiquitin Ligase. Mol. Cell **26**: 775–780.

Lee, Y., Ahn, C., Han, J., Choi, H., Kim, J., Yim, J., Lee, J., Provost, P., Rådmark, O., Kim, S., and Kim, V.N. (2003). The nuclear RNase III Drosha initiates microRNA processing. Nature **425**: 415–419.

Lee, Y., Kim, M., Han, J., Yeom, K.-H., Lee, S., Baek, S.H., and Kim, V.N. (2004). MicroRNA genes are transcribed by RNA polymerase II. EMBO J. **23**: 4051–4060.

Leung, A.K.L., Vyas, S., Rood, J.E., Bhutkar, A., Sharp, P.A., and Chang, P. (2011). Poly(ADP-Ribose) Regulates Stress Responses and MicroRNA Activity in the Cytoplasm. Mol. Cell **42**: 489–499.

Leverson, J.D., Joazeiro, C. a, Page, a M., Huang, H.K., Hieter, P., and Hunter, T. (2000). The APC11 RING-H2 finger mediates E2-dependent ubiquitination. Mol. Biol. Cell **11**: 2315–2325.

Li, F., Chung, T., and Vierstra, R.D. (2014). AUTOPHAGY-RELATED11 Plays a Critical Role in General Autophagy- and Senescence-Induced Mitophagy in Arabidopsis. Plant Cell **26**: 788–807.

Li, F., Pignatta, D., Bendix, C., Brunkard, J.O., Cohn, M.M., Tung, J., and Sun, H. (2011). MicroRNA regulation of plant innate immune receptors. Proc. Natl. Acad. Sci. U. S. A. **109**: 1790–1795.

Li, F. and Vierstra, R.D. (2012). Autophagy: a multifaceted intracellular system for bulk and selective recycling. Trends Plant Sci. **17**: 526–37.

Li, J., Yang, Z., Yu, B., Liu, J., and Chen, X. (2005). Methylation protects miRNAs and siRNAs from a 3′-end uridylation activity in Arabidopsis. Curr. Biol. **15**: 1501–1507.

Li, S. et al. (2016). Biogenesis of phased siRNAs on membrane-bound polysomes in Arabidopsis. Elife **5**: 1–24.

Li, S. et al. (2013). MicroRNAs inhibit the translation of target mRNAs on the endoplasmic reticulum in Arabidopsis. Cell **153**: 562–74.

Li, W., Tu, D., Brunger, A.T., and Ye, Y. (2007). A ubiquitin ligase transfers preformed polyubiquitin chains from a conjugating enzyme to a substrate. Nature **446**: 333–337.

Li, Y., Gazdoiu, S., Pan, Z.Q., and Fuchs, S.Y. (2004). Stability of Homologue of

Slimb F-box Protein Is Regulated by Availability of Its Substrate. J. Biol. Chem. **279**: 11074–11080.

Lingel, A., Simon, B., Izaurralde, E., and Sattler, M. (2004). Nucleic acid 3'-end recognition by the Argonaute2 PAZ domain. Nat. Struct. Mol. Biol. **11**: 576–7.

Lingel, A., Simon, B., Izaurralde, E., and Sattler, M. (2003). Structure and nucleic-acid binding of the Drosophila Argonaute 2 PAZ domain. Nature **426**: 465–469.

Lippman, Z., May, B., Yordan, C., Singer, T., and Martienssen, R. (2003). Distinct mechanisms determine transposon inheritance and methylation via small interfering RNA and histone modification. PLoS Biol. **1**.

Lorick, K.L., Jensen, J.P., Fang, S., Ong, a M., Hatakeyama, S., and Weissman, a M. (1999). RING fingers mediate ubiquitin-conjugating enzyme (E2)-dependent ubiquitination. Proc. Natl. Acad. Sci. U. S. A. **96**: 11364–11369.

Loss-Morais, G., Waterhouse, P.M., and Margis, R. (2013). Description of plant tRNA-derived RNA fragments (tRFs) associated with argonaute and identification of their putative targets. Biol. Direct **8**: 1–5.

Love, M.I., Huber, W., and Anders, S. (2014). Moderated estimation of fold change and dispersion for RNA-seq data with DESeq2. Genome Biol. **15**: 1–21.

Lovering, R., Hanson, I.M., Borden, K.L., Martin, S., O'Reilly, N.J., Evan, G.I., Rahman, D., Pappin, D.J., Trowsdale, J., and Freemont, P.S. (1993). Identification and preliminary characterization of a protein motif related to the zinc finger. Proc. Natl. Acad. Sci. U. S. A. **90**: 2112–2116.

Lozano-Duran, R., Rosas-Diaz, T., Gusmaroli, G., Luna, A.P., Taconnat, L., Deng, X.W., and Bejarano, E.R. (2011). Geminiviruses Subvert Ubiquitination by Altering CSN-Mediated Derubylation of SCF E3 Ligase Complexes and Inhibit Jasmonate Signaling in Arabidopsis thaliana. Plant Cell **23**: 1014–1032.

Lund, E., Güttinger, S., Calado, A., Dahlberg, J.E., and Kutay, U. (2004). Nuclear Export of MicroRNA Precursors. Science (80-.). **303**: 95–98.

Ma, J.B., Ye, K., and Patel, D.J. (2004). Structural basis for overhang-specific small interfering RNA recognition by the PAZ domain. Nature **429**: 318–322.

Ma, J.B., Yuan, Y.R., Meister, G., Pei, Y., Tuschl, T., and Patel, D.J. (2005). Structural basis for 5′ -end-specific recognition of guide RNA by the A. fulgidus Piwi protein. Nature **434**: 666–670.

Magori, S. and Citovsky, V. (2011). Hijacking of the Host SCF Ubiquitin Ligase Machinery by Plant Pathogens. Front. Plant Sci. **2**: 1–8.

Mallory, A. and Vaucheret, H. (2010). Form, function, and regulation of ARGONAUTE proteins. Plant Cell **22**: 3879–89.

Mallory, A.C., Hinze, A., Tucker, M.R., Bouché, N., Gasciolli, V., Elmayan, T., Lauressergues, D., Jauvion, V., Vaucheret, H., and Laux, T. (2009). Redundant and specific roles of the ARGONAUTE proteins AGO1 and ZLL in development and small RNA-directed gene silencing. PLoS Genet. **5**.

Mallory, A.C. and Vaucheret, H. (2009). ARGONAUTE 1 homeostasis invokes the coordinate action of the microRNA and siRNA pathways. EMBO Rep. **10**: 521–526.

Marrocco, K., Criqui, M.C., Zervudacki, J., Schott, G., Eisler, H., Parnet, A., Dunoyer, P., and Genschik, P. (2012). APC/C-mediated degradation of dsRNA-binding protein 4 (DRB4) involved in RNA silencing. PLoS One **7**: 1–10.

Marrocco, K., Lecureuil, A., Nicolas, P., and Guerche, P. (2003). The Arabidopsis SKP1-like genes present a spectrum of expression profiles. Plant Mol. Biol. **52**: 715–727.

Marshall, R.S., Li, F., Gemperline, D.C., Book, A.J., and Vierstra, R.D. (2015). Autophagic Degradation of the 26S Proteasome Is Mediated by the Dual ATG8/Ubiquitin Receptor RPN10 in Arabidopsis. Mol. Cell **58**: 1053–1066.

Marshall, R.S. and Vierstra, R.D. (2018). Autophagy: The Master of Bulk and Selective Recycling. Annu. Rev. Plant Biol. **69**: annurev-arplant-042817-040606.

Martinez, G. (2018). tRNA-derived small RNAs: New players in genome protection against retrotransposons. RNA Biol. **15**: 170–175.

Martinez, G., Choudury, S.G., and Slotkin, R.K. (2017). TRNA-derived small RNAs target transposable element transcripts. Nucleic Acids Res. **45**: 5142–5152.

Martinez, J. and Tuschl, T. (2004). RISC is a 5' phosphomonoester-producing RNA endonuclease. Genes Dev. **18**: 975–80.

Martinez, N.J. and Gregory, R.I. (2013). Argonaute2 expression is post-transcriptionally coupled to microRNA abundance. Rna **19**: 605–612.

Matzke, M.A., Kanno, T., and Matzke, A.J.M. (2015). RNA-Directed DNA Methylation: The Evolution of a Complex Epigenetic Pathway in Flowering Plants. Annu. Rev. Plant Biol. **66**: 243–267.

Maupin-Furlow, J.A. (2013). Ubiquitin-like proteins and their roles in archaea. Trends Microbiol. **21**: 31–38.

McCue, A.D., Nuthikattu, S., Reeder, S.H., and Slotkin, R.K. (2012). Gene expression and stress response mediated by the epigenetic regulation of a transposable element small RNA. PLoS Genet. **8**.

McCue, A.D., Panda, K., Nuthikattu, S., Choudury, S.G., Thomas, E.N., and Slotkin, R.K. (2015). ARGONAUTE 6 bridges transposable element mRNA-derived siRNAs to the establishment of DNA methylation. EMBO J. **34**: 20–35.

Meister, G. (2013). Argonaute proteins: Functional insights and emerging roles. Nat. Rev. Genet. **14**: 447–459.

Meister, G., Landthaler, M., Peters, L., Chen, P.Y., Urlaub, H., Lührmann, R., and Tuschl, T. (2005). Identification of novel argonaute-associated proteins. Curr. Biol. **15**: 2149–2155.

Meister, G. and Tuschl, T. (2004). Mechanisms of gene silencing by double-stranded RNA. Nature **431**: 343–9.

Melnyk, C.W., Molnar, A., and Baulcombe, D.C. (2011). Intercellular and systemic movement of RNA silencing signals. EMBO J. **30**: 3553–3563.

Mergner, J. and Schwechheimer, C. (2014). The NEDD8 modification pathway in plants. Front. Plant Sci. **5**: 1–15.

Mermigka, G., Verret, F., and Kalantidis, K. (2016). RNA silencing movement in plants. J. Integr. Plant Biol. **58**: 328–342.

Mi, S. et al. (2008). Sorting of small RNAs into Arabidopsis argonaute complexes is directed by the 5' terminal nucleotide. Cell **133**: 116–27.

Miao, Y. and Zentgraf, U. (2010). A HECT E3 ubiquitin ligase negatively regulates Arabidopsis leaf senescence through degradation of the transcription factor WRKY53. Plant J. **63**: 179–188.

Michaeli, S., Galili, G., Genschik, P., Fernie, A.R., and Avin-Wittenberg, T. (2016). Autophagy in Plants--What's New on the Menu? Trends Plant Sci. **21**: 134–144.

Michaeli, S., Honig, A., Levanony, H., Peled-Zehavi, H., and Galili, G. (2014). Arabidopsis ATG8-INTERACTING PROTEIN1 Is Involved in Autophagy-Dependent Vesicular Trafficking of Plastid Proteins to the Vacuole. Plant Cell **26**: 4084–4101.

Mlotshwa, S., Pruss, G.J., and Vance, V. (2008). Small RNAs in viral infection and host defense. Trends Plant Sci. **13**: 375–382.

Molnar, A., Csorba, T., Lakatos, L., Varallyay, E., Lacomme, C., and Burgyan, J. (2005). Plant Virus-Derived Small Interfering RNAs Originate Predominantly from Highly Structured Single-Stranded Viral RNAs. J. Virol. **79**: 7812–7818.

Montgomery, T.A., Howell, M.D., Cuperus, J.T., Li, D., Hansen, J.E., Alexander, A.L., Chapman, E.J., Fahlgren, N., Allen, E., and Carrington, J.C. (2008). Specificity of ARGONAUTE7-miR390 Interaction and Dual Functionality in TAS3 Trans-Acting siRNA Formation. Cell **133**: 128–141.

Morel, J.-B., Godon, C., Mourrain, P., Béclin, C., Boutet, S., Feuerbach, F., Proux, F., and Vaucheret, H. (2002). Fertile hypomorphic ARGONAUTE (ago1) mutants impaired in post-transcriptional gene silencing and virus resistance. Plant Cell **14**: 629–39.

Mourrain, P. et al. (2000). Arabidopsis SGS2 and SGS3 genes are required for posttranscriptional gene silencing and natural virus resistance. Cell **101**: 533–542.

Murphy, D., Dancis, B., and Brown, J.R. (2008). The evolution of core proteins involved in microRNA biogenesis. BMC Evol. Biol. **8**: 1–18.

Murray, A. (1995). Cyclin Ubiquitination: The destructive end of mitosis. Cell **81**: 149–152.

Nagai, T., Ibata, K., Park, E.S., Kubota, M., Mikoshiba, K., and Miyawaki, A. (2002). A variant of yellow fluorescent protein with fast and efficient maturation for cell-biological applications. Nat. Biotechnol. **20**: 87–90.

Nakagawa, T. et al. (2007). Improved Gateway binary vectors: high-performance vectors for creation of fusion constructs in transgenic analysis of plants. Biosci. Biotechnol. Biochem. **71**: 2095–100.

Nakamura, S., Mano, S., Tanaka, Y., Ohnishi, M., Nakamori, C., Araki, M., Niwa, T., Nishimura, M., Kaminaka, H., Nakagawa, T., Sato, Y., and Ishiguro, S. (2010). Gateway binary vectors with the bialaphos resistance gene, bar, as a selection marker for plant transformation. Biosci. Biotechnol. Biochem. **74**: 1315–1319.

Nakanishi, K. (2016). Anatomy of RISC: how do small RNAs and chaperones activate Argonaute proteins? Wiley Interdiscip. Rev. RNA.

Nakanishi, K., Weinberg, D.E., Bartel, D.P., and Patel, D.J. (2012). Structure of yeast Argonaute with guide RNA. Nature **486**: 368–74.

Napoli, C. (1990). Introduction of a Chimeric Chalcone Synthase Gene into Petunia Results in Reversible Co-Suppression of Homologous Genes in trans. PLANT CELL ONLINE **2**: 279–289.

Noda, N.N., Satoo, K., Fujioka, Y., Kumeta, H., Ogura, K., Nakatogawa, H., Ohsumi, Y., and Inagaki, F. (2011). Structural basis of Atg8 activation by a homodimeric E1, Atg7. Mol. Cell **44**: 462–475.

Nowara, D., Gay, A., Lacomme, C., Shaw, J., Ridout, C., Douchkov, D., Hensel, G., Kumlehn, J., and Schweizer, P. (2010). HIGS: Host-Induced Gene Silencing in the Obligate Biotrophic Fungal Pathogen *Blumeria graminis*. Plant Cell **22**: 3130–3141.

Nuthikattu, S., McCue, A.D., Panda, K., Fultz, D., DeFraia, C., Thomas, E.N., and Slotkin, R.K. (2013). The Initiation of Epigenetic Silencing of Active Transposable Elements Is Triggered by RDR6 and 21-22 Nucleotide Small Interfering RNAs. Plant Physiol. **162**: 116–131.

Nykänen, A., Haley, B., and Zamore, P.D. (2001). ATP requirements and small interfering RNA structure in the RNA interference pathway. Cell **107**: 309–21.

Ohsumi, Y. (2001). Molecular dissection of autophagy: two ubiquitin-like systems. Nat. Rev. Mol. Cell Biol. **2**: 211–216.

Olmedo-Monfil, V., Durán-Figueroa, N., Arteaga-Vázquez, M., Demesa-Arévalo, E., Autran, D., Grimanelli, D., Slotkin, R.K., Martienssen, R.A., and Vielle-Calzada, J.P. (2010). Control of female gamete formation by a small RNA pathway in Arabidopsis. Nature **464**: 628–632.

Onodera, Y., Haag, J.R., Ream, T., Nunes, P.C., Pontes, O., and Pikaard, C.S. (2005). Plant nuclear RNA polymerase IV mediates siRNA and DNA methylation- dependent heterochromatin formation. Cell **120**: 613–622.

Orban, T.I. and Izaurralde, E. (2005). Decay of mRNAs targeted by RISC requires XRN1, the Ski complex, and the exosome. RNA **11**: 459–69.

Pall, G.S., Codony-Servat, C., Byrne, J., Ritchie, L., and Hamilton, A. (2007). Carbodiimide-mediated cross-linking of RNA to nylon membranes improves the detection of siRNA, miRNA and piRNA by northern blot. Nucleic Acids Res. **35**: e60.

Pantaleo, V., Szittya, G., and Burgyan, J. (2007). Molecular Bases of Viral RNA Targeting by Viral Small Interfering RNA-Programmed RISC. J. Virol. **81**: 3797–3806.

Pao, K.-C., Wood, N.T., Knebel, A., Rafie, K., Stanley, M., Mabbitt, P.D., Sundaramoorthy, R., Hofmann, K., van Aalten, D.M.F., and Virdee, S. (2018). Activity-based E3 ligase profiling uncovers an E3 ligase with esterification activity. Nature **556**: 381–385.

Park, M.Y., Wu, G., Gonzalez-Sulser, A., Vaucheret, H., and Poethig, R.S. (2005). Nuclear processing and export of microRNAs in Arabidopsis. Proc. Natl. Acad. Sci. **102**: 3691–3696.

Park, S.-H., Bolender, N., Eisele, F., Kostova, Z., Takeuchi, J., Coffino, P., and Wolf, D.H. (2007). The cytoplasmic Hsp70 chaperone machinery subjects misfolded and endoplasmic reticulum import-incompetent proteins to degradation via the ubiquitin-proteasome system. Mol. Biol. Cell **18**: 153–65.

Parker, J.S., Roe, S.M., and Barford, D. (2004). Crystal structure of a PIWI protein suggests mechanisms for siRNA recognition and slicer activity. EMBO J. **23**: 4727–4737.

Parker, J.S., Roe, S.M., and Barford, D. (2005). Structural insights into mRNA recognition from a PIWI domain-siRNA guide complex. Nature **434**: 663–6.

Pazhouhandeh, M., Dieterle, M., Marrocco, K., Lechner, E., Berry, B., Brault, V., Hemmer, O., Kretsch, T., Richards, K.E., Genschik, P., and Ziegler-Graff, V. (2006). F-box-like domain in the polerovirus protein P0 is required for silencing suppressor function. Proc. Natl. Acad. Sci. U. S. A. **103**: 1994–9.

Peragine, A., Yoshikawa, M., Wu, G., Albrecht, H.L., and Poethig, R.S. (2004). SGS3 and SGS2/SDE1/RDR6 are required for juvenile development and the production of trans-acting siRNAs in Arabidopsis. Genes Dev. **18**: 2368–79.

Perazza, D., Herzog, M., Hülskamp, M., Brown, S., Dorne, A.M., and Bonneville, J.M. (1999). Trichome cell growth in Arabidopsis thaliana can be derepressed by mutations in at least five genes. Genetics **152**: 461–476.

Peters, J.M. (2006). The anaphase promoting complex/cyclosome: A machine designed to destroy. Nat. Rev. Mol. Cell Biol. **7**: 644–656.

Petroski, M.D. and Deshaies, R.J. (2005). Function and regulation of cullin-RING

ubiquitin ligases. Nat. Rev. Mol. Cell Biol. **6**: 9–20.

Pfaff, J., Hennig, J., Herzog, F., Aebersold, R., Sattler, M., Niessing, D., and Meister, G. (2013). Structural features of Argonaute – GW182 protein interactions. Proc. Natl. Acad. Sci. U. S. A. **110**: E3770–E3779.

Pfeffer, S., Dunoyer, P., Heim, F., Richards, K.E., Jonard, G., and Ziegler-Graff, V. (2002). P0 of beet Western yellows virus is a suppressor of posttranscriptional gene silencing. J. Virol. **76**: 6815–24.

Pickart, C.M. and Fushman, D. (2004). Polyubiquitin chains: polymeric protein signals. Curr. Opin. Chem. Biol. **8**: 610–6.

Pintard, L., Willems, A., and Peter, M. (2004). Cullin-based ubiquitin ligases: Cul3-BTB complexes join the family. EMBO J. **23**: 1681–1687.

Pinzón, N., Li, B., Martinez, L., Sergeeva, A., Presumey, J., Apparailly, F., and Seitz, H. (2017). microRNA target prediction programs predict many false positives. Genome Res. **27**: 234–245.

Pontes, O., Li, C.F., Nunes, P.C., Haag, J., Ream, T., Vitins, A., Jacobsen, S.E., and Pikaard, C.S. (2006). The Arabidopsis Chromatin-Modifying Nuclear siRNA Pathway Involves a Nucleolar RNA Processing Center. Cell **126**: 79–92.

Pontier, D. et al. (2012). NERD, a Plant-Specific GW Protein, Defines an Additional RNAi-Dependent Chromatin-Based Pathway in Arabidopsis. Mol. Cell **48**: 121–132.

Pontier, D., Yahubyan, G., Vega, D., Bulski, A., Saez-Vasquez, J., Hakimi, M.A., Lerbs-Mache, S., Colot, V., and Lagrange, T. (2005). Reinforcement of silencing at transposons and highly repeated sequences requires the concerted action of two distinct RNA polymerases IV in Arabidopsis. Genes Dev. **19**: 2030–2040.

Popov, N., Schmitt, M., Schulzeck, S., and Matthies, H. (1975). [Reliable micromethod for determination of the protein content in tissue homogenates]. Acta Biol. Med. Ger. **34**: 1441–6.

Poulsen, C., Vaucheret, H., and Brodersen, P. (2013). Lessons on RNA silencing mechanisms in plants from eukaryotic argonaute structures. Plant Cell **25**: 22–37.

Price, C.T.D. and Abu Kwaik, Y. (2010). Exploitation of host polyubiquitination machinery through molecular mimicry by eukaryotic-like bacterial F-box effectors. Front. Microbiol. **1**: 1–12.

Pulido, A. and Laufs, P. (2010). Co-ordination of developmental processes by small RNAs during leaf development. J. Exp. Bot. **61**: 1277–1291.

Pumplin, N. and Voinnet, O. (2013). RNA silencing suppression by plant pathogens: defence, counter-defence and counter-counter-defence. Nat. Rev. Microbiol. **11**: 745–60.

Qi, H.H., Ongusaha, P.P., Myllyharju, J., Cheng, D., Pakkanen, O., Shi, Y., Lee, S.W., Peng, J., and Shi, Y. (2008). Prolyl 4-hydroxylation regulates Argonaute 2 stability. Nature **455**: 421–424.

Qu, F. (2010). Antiviral Role of Plant-Encoded RNA-Dependent RNA Polymerases Revisited with Deep Sequencing of Small Interfering RNAs of Virus Origin. Mol. Plant-Microbe Interact. **23**: 1248–1252.

Qu, F., Ye, X., Hou, G., Sato, S., Clemente, T.E., and Morris, T.J. (2005). RDR6 has a broad-spectrum but temperature-dependent antiviral defense role in Nicotiana benthamiana. J. Virol. **79**: 15209–17.

Qu, F., Ye, X., and Morris, T.J. (2008). Arabidopsis DRB4, AGO1, AGO7, and

RDR6 participate in a DCL4-initiated antiviral RNA silencing pathway negatively regulated by DCL1. Proc. Natl. Acad. Sci. **105**: 14732–14737.

Quévillon Huberdeau, M. et al. (2017). Phosphorylation of Argonaute proteins affects mRNA binding and is essential for microRNA-guided gene silencing *in vivo*. EMBO J. **36**: 2088–2106.

Reinhart, B.J., Slack, F.J., Basson, M., Pasquienelll, A.E., Bettlnger, J.C., Rougvle, A.E., Horvitz, H.R., and Ruvkun, G. (2000). The 21-nucleotide let-7 RNA regulates developmental timing in Caenorhabditis elegans. Nature **403**: 901–906.

Ren, G., Xie, M., Zhang, S., Vinovskis, C., Chen, X., and Yu, B. (2014). Methylation protects microRNAs from an AGO1-associated activity that uridylates 5' RNA fragments generated by AGO1 cleavage. Proc. Natl. Acad. Sci. U. S. A. **111**: 6365–70.

Risseeuw, E.P., Daskalchuk, T.E., Banks, T.W., Liu, E., Cotelesage, J., Hellmann, H., Estelle, M., Somers, D.E., and Crosby, W.L. (2003). Protein interaction analysis of SCF ubiquitin E3 ligase subunits from Arabidopsis. Plant J. **34**: 753–67.

Rivas, F. V., Tolia, N.H., Song, J.J., Aragon, J.P., Liu, J., Hannon, G.J., and Joshua-Tor, L. (2005). Purified Argonaute2 and an siRNA form recombinant human RISC. Nat. Struct. Mol. Biol. **12**: 340–349.

Rüdel, S., Wang, Y., Lenobel, R., Körner, R., Hsiao, H.H., Urlaub, H., Patel, D., and Meister, G. (2011). Phosphorylation of human Argonaute proteins affects small RNA binding. Nucleic Acids Res. **39**: 2330–2343.

Rybak, A., Fuchs, H., Hadian, K., Smirnova, L., Wulczyn, E.A., Michel, G., Nitsch, R., Krappmann, D., and Wulczyn, F.G. (2009). The let-7 target gene mouse lin-41 is a stem cell specific E3 ubiquitin ligase for the miRNA pathway protein Ago2. Nat. Cell Biol. **11**: 1411–20.

Sahu, R., Kaushik, S., Clement, C.C., Cannizzo, E.S., Scharf, B., Follenzi, A., Potolicchio, I., Nieves, E., Cuervo, A.M., and Santambrogio, L. (2011). Microautophagy of Cytosolic Proteins by Late Endosomes. Dev. Cell **20**: 131–139.

Sarikas, A., Hartmann, T., and Pan, Z.Q. (2011). The cullin protein family. Genome Biol. **12**: 1–12.

Schalk, C., Cognat, V., Graindorge, S., Vincent, T., Voinnet, O., and Molinier, J. (2017). Small RNA-mediated repair of UV-induced DNA lesions by the DNA DAMAGE-BINDING PROTEIN 2 and ARGONAUTE 1. Proc. Natl. Acad. Sci. **114**: E2965–E2974.

Scheffner, M., Nuber, U., and Huibregtse, J.M. (1995). Protein ubiquitination involving an E1–E2–E3 enzyme ubiquitin thioester cascade. Nature **373**: 81–83.

Schimmel, P. (2018). RNA Processing and Modifications: The emerging complexity of the tRNA world: Mammalian tRNAs beyond protein synthesis. Nat. Rev. Mol. Cell Biol. **19**: 45–58.

Schirle, N.T. and MacRae, I.J. (2012). The crystal structure of human Argonaute2. Science **336**: 1037–40.

Scholthof, H.B. (2006). The Tombusvirus-encoded p19:from irrelevance to elegance. Nat. Rev. Microbiol. **4**: 405–411.

Schulman, B. a and Wade Harper, J. (2009). Ubiquitin-like protein activation by E1 enzymes: the apex for downstream signalling pathways. Nat. Rev. Mol. Cell Biol.

10: 319–331.

Schwab, R., Maizel, A., Ruiz-Ferrer, V., Garcia, D., Bayer, M., Crespi, M., Voinnet, O., and Martienssen, R.A. (2009). Endogenous TasiRNAs mediate non-cell autonomous effects on gene regulation in Arabidopsis thaliana. PLoS One **4**: 4–9.

Shen, W., Parmentier, Y., Hellmann, H., Lechner, E., Dong, A., Masson, J., Granier, F., Lepiniec, L., Estelle, M., and Genschik, P. (2002). Null Mutation of AtCUL1 Causes Arrest in Early Embryogenesis in Arabidopsis. Mol. Biol. Cell **13**: 1916–1928.

Shivaprasad, P. V., Chen, H.-M., Patel, K., Bond, D.M., Santos, B.A.C.M., and Baulcombe, D.C. (2012). A MicroRNA Superfamily Regulates Nucleotide Binding Site-Leucine-Rich Repeats and Other mRNAs. Plant Cell **24**: 859–874.

Si-Ammour, A., Windels, D., Arn-Bouldoires, E., Kutter, C., Ailhas, J., Meins, F., and Vazquez, F. (2011). miR393 and Secondary siRNAs Regulate Expression of the TIR1/AFB2 Auxin Receptor Clade and Auxin-Related Development of Arabidopsis Leaves. Plant Physiol. **157**: 683–691.

Sigismund, S., Polo, S., and Di Fiore, P.P. (2004). Signaling Through Monoubiquitination.: 149–185.

Silhavy, D., Molnár, A., Lucioli, A., Szittya, G., Hornyik, C., Tavazza, M., and Burgyán, J. (2002). A viral protein suppresses RNA silencing and binds silencing-generated, 21- to 25-nucleotide double-stranded RNAs. EMBO J. **21**: 3070–3080.

Skopelitis, D.S., Husbands, A.Y., and Timmermans, M.C.P. (2012). Plant small RNAs as morphogens. Curr. Opin. Cell Biol. **24**: 217–224.

Skowyra, D., Craig, K.L., Tyers, M., Elledge, S.J., and Harper, J.W. (1997). F-box proteins are receptors that recruit phosphorylated substrates to the SCF ubiquitin-ligase complex. Cell **91**: 209–219.

Smalle, J. and Vierstra, R.D. (2004). the Ubiquitin 26S Proteasome Proteolytic Pathway. Annu. Rev. Plant Biol. **55**: 555–590.

Smibert, P., Yang, J.-S., Azzam, G., Liu, J.-L., and Lai, E.C. (2013). Homeostatic control of Argonaute stability by microRNA availability. Nat. Struct. Mol. Biol. **20**: 789–795.

Smith, M.R., Willmann, M.R., Wu, G., Berardini, T.Z., Möller, B., Weijers, D., and Poethig, R.S. (2009). Cyclophilin 40 is required for microRNA activity in Arabidopsis. Proc. Natl. Acad. Sci. U. S. A. **106**: 5424–5429.

Sobala, A. and Hutvagner, G. (2013). Small RNAs derived from the 5′ end of tRNAs can inhibit protein translation in human cells. RNA Biol. **10**: 553–563.

Sobala, A. and Hutvagner, G. (2011). Transfer RNA-derived fragments: Origins, processing, and functions. Wiley Interdiscip. Rev. RNA **2**: 853–862.

Song, J.J., Liu, J., Tolia, N.H., Schneiderman, J., Smith, S.K., Martienssen, R.A., Hannon, G.J., and Joshua-Tor, L. (2003). The crystal structure of the Argonaute2 PAZ domain reveals an RNA binding motif in RNAi effector complexes. Nat. Struct. Biol. **10**: 1026–1032.

Sontheimer, E.J. (2005). Assembly and function of RNA silencing complexes. Nat. Rev. Mol. Cell Biol. **6**: 127–138.

Spence, J., Gali, R.R., Dittmar, G., Sherman, F., Karin, M., and Finley, D. (2000). Cell cycle-regulated modification of the ribosome by a variant multiubiquitin chain. Cell **102**: 67–76.

Stogios, P.J., Downs, G.S., Jauhal, J.J.S., Nandra, S.K., and Privé, G.G. (2005).

Sequence and structural analysis of BTB domain proteins. Genome Biol. **6**: R82.

Stone, S.L., Hauksdóttir, H., Troy, A., Herschleb, J., Kraft, E., and Callis, J. (2005). Functional analysis of the RING-type ubiquitin ligase family of Arabidopsis. Plant Physiol. **137**: 13–30.

Striebel, F., Imkamp, F., Sutter, M., Steiner, M., Mamedov, A., and Weber-Ban, E. (2009). Bacterial ubiquitin-like modifier Pup is deamidated and conjugated to substrates by distinct but homologous enzymes. Nat. Struct. Mol. Biol. **16**: 647–651.

Sun, C.W. and Callis, J. (1997). Independent modulation of Arabidopsis thaliana polyubiquitin mRNAs in different organs and in response to environmental changes. Plant J. **11**: 1017–1027.

Suttangkakul, A., Li, F., Chung, T., and Vierstra, R.D. (2011). The ATG1/ATG13 Protein Kinase Complex Is Both a Regulator and a Target of Autophagic Recycling in Arabidopsis. Plant Cell **23**: 3761–3779.

Swarts, D.C., Makarova, K., Wang, Y., Nakanishi, K., Ketting, R.F., Koonin, E. V., Patel, D.J., and Van Der Oost, J. (2014). The evolutionary journey of Argonaute proteins. Nat. Struct. Mol. Biol. **21**: 743–753.

Szarzynska, B., Sobkowiak, L., Pant, B.D., Balazadeh, S., Scheible, W.R., Mueller-Roeber, B., Jarmolowski, A., and Szweykowska-Kulinska, Z. (2009). Gene structures and processing of Arabidopsis thaliana HYL1-dependent pri-miRNAs. Nucleic Acids Res. **37**: 3083–3093.

Szittya, G. and Burgyán, J. (2013). RNA interference-mediated intrinsic antiviral immunity in plants. Curr. Top. Microbiol. Immunol. **371**: 153–81.

Taherbhoy, A.M., Tait, S.W., Kaiser, S.E., Williams, A.H., Deng, A., Nourse, A., Hammel, M., Kurinov, I., Rock, C.O., Green, D.R., and Schulman, B.A. (2011). Atg8 transfer from Atg7 to Atg3: A distinctive E1-E2 architecture and mechanism in the autophagy pathway. Mol. Cell **44**: 451–461.

Takeda, A., Iwasaki, S., Watanabe, T., Utsumi, M., and Watanabe, Y. (2008). The mechanism selecting the guide strand from small RNA duplexes is different among Argonaute proteins. Plant Cell Physiol. **49**: 493–500.

Tang, X., Wen, S., Zheng, D., Tucker, L., Cao, L., Pantazatos, D., Moss, S.F., and Ramratnam, B. (2013). Acetylation of Drosha on the N-Terminus Inhibits Its Degradation by Ubiquitination. PLoS One **8**.

Tang, Z., Li, B., Bharadwaj, R., Zhu, H., Ozkan, E., Hakala, K., Deisenhofer, J., and Yu, H. (2001). APC2 Cullin protein and APC11 RING protein comprise the minimal ubiquitin ligase module of the anaphase-promoting complex. Mol. Biol. Cell **12**: 3839–3851.

Thomann, A., Dieterle, M., and Genschik, P. (2005). Plant CULLIN-based E3s: Phytohormones come first. FEBS Lett. **579**: 3239–3245.

Thompson, A.R. (2005). Autophagic Nutrient Recycling in Arabidopsis Directed by the ATG8 and ATG12 Conjugation Pathways. Plant Physiol. **138**: 2097–2110.

Tijsterman, M., Ketting, R.F., and Plasterk, R.H.A. (2002). The Genetics of RNA Silencing. Annu. Rev. Genet. **36**: 489–519.

Till, S., Lejeune, E., Thermann, R., Bortfeld, M., Hothorn, M., Enderle, D., Heinrich, C., Hentze, M.W., and Ladurner, A.G. (2007). A conserved motif in Argonaute-interacting proteins mediates functional interactions through the Argonaute PIWI domain. Nat. Struct. Mol. Biol. **14**: 897–903.

Tournier, B., Tabler, M., and Kalantidis, K. (2006). Phloem flow strongly influences the systemic spread of silencing in GFP Nicotiana benthamiana plants. Plant J.

47: 383–394.

Trujillo, J.T., Beilstein, M.A., and Mosher, R.A. (2016). The Argonaute-binding platform of NRPE1 evolves through modulation of intrinsically disordered repeats. New Phytol. **212**: 1094–1105.

Tzfira, T., Vaidya, M., and Citovsky, V. (2004). Involvement of targeted proteolysis in plant genetic transformation by Agrobacterium. Nature **431**: 87–92.

Ulrich, H.D. (2002). Degradation or maintenance: Actions of the ubiquitin system on eukaryotic chromatin. Eukaryot. Cell **1**: 1–10.

Vargason, J.M., Szittya, G., Burgyán, J., and Tanaka Hall, T.M. (2003). Size Selective Recognition of siRNA by an RNA Silencing Suppressor. Cell **115**: 799–811.

Varshavsky, A. (1991). Naming a targeting signal. Cell **64**: 13–15.

Varshavsky, A. (1996). The N-end rule: functions, mysteries, uses. Proc. Natl. Acad. Sci. **93**: 12142–12149.

Vaucheret, H. (2008). Plant ARGONAUTES. Trends Plant Sci. **13**: 350–8.

Vaucheret, H., Mallory, A.C., and Bartel, D.P. (2006). AGO1 homeostasis entails coexpression of MIR168 and AGO1 and preferential stabilization of miR168 by AGO1. Mol. Cell **22**: 129–36.

Vaucheret, H., Vazquez, F., Crété, P., and Bartel, D.P. (2004). The action of ARGONAUTE1 in the miRNA pathway and its regulation by the miRNA pathway are crucial for plant development. Genes Dev. **18**: 1187–97.

Vazquez, F. (2006). Arabidopsis endogenous small RNAs: highways and byways. Trends Plant Sci. **11**: 460–468.

Vazquez, F., Gasciolli, V., Crété, P., and Vaucheret, H. (2004a). The nuclear dsRNA binding protein HYL1 is required for microRNA accumulation and plant development, but not posttranscriptional transgene silencing. Curr. Biol. **14**: 346–51.

Vazquez, F., Vaucheret, H., Rajagopalan, R., Lepers, C., Gasciolli, V., Mallory, A.C., Hilbert, J.L., Bartel, D.P., and Crété, P. (2004b). Endogenous trans-acting siRNAs regulate the accumulation of arabidopsis mRNAs. Mol. Cell **16**: 69–79.

van der Veen, A.G. and Ploegh, H.L. (2012). Ubiquitin-Like Proteins. Annu. Rev. Biochem. **81**: 323–357.

Vembar, S.S. and Brodsky, J.L. (2008). One step at a time: Endoplasmic reticulum-associated degradation. Nat. Rev. Mol. Cell Biol. **9**: 944–957.

Verdel, A., Jia, S., Gerber, S., Sugiyama, T., Gygi, S., Grewal, S.I.S., and Moazed, D. (2004). RNAi-Mediated Targeting of Heterochromatin by the RITS Complex. Science (80-.). **303**: 672–676.

Verma, R., Aravind, L., Oania, R., McDonald, W.H., Yates, J.R., Koonin, E. V., and Deshaies, R.J. (2002). Role of Rpn11 metalloprotease in deubiquitination and degradation by the 26S proteasome. Science (80-.). **298**: 611–615.

Vidal, E.A., Araus, V., Lu, C., Parry, G., Green, P.J., Coruzzi, G.M., and Gutierrez, R.A. (2010). Nitrate-responsive miR393/AFB3 regulatory module controls root system architecture in Arabidopsis thaliana. Proc. Natl. Acad. Sci. **107**: 4477–4482.

Vierstra, R.D. (2009). The ubiquitin–26S proteasome system at the nexus of plant biology. Nat. Rev. Mol. Cell Biol. **10**: 385–397.

Vijay-kumar, S., Bugg, C.E., and Cook, W.J. (1987). Structure of ubiquitin refined at 1.8 Å resolution. J. Mol. Biol. **194**: 531–544.

Voges, D., Zwickl, P., and Baumeister, W. (1999). The 26S Proteasome: A Molecular Machine Designed for Controlled Proteolysis. Annu. Rev. Biochem. **68**: 1015–1068.

Voinnet, O. (2009). Origin, Biogenesis, and Activity of Plant MicroRNAs. Cell **136**: 669–687.

Voinnet, O., Vain, P., Angell, S., and Baulcombe, D.C. (1998). Systemic spread of sequence-specific transgene RNA degradation in plants is initiated by localized introduction of ectopic promoterless DNA. Cell **95**: 177–187.

Voss, P. and Grune, T. (2007). The nuclear proteasome and the degradation of oxidatively damaged proteins. Amino Acids **32**: 527–534.

Wang, X.-B., Jovel, J., Udomporn, P., Wang, Y., Wu, Q., Li, W.-X., Gasciolli, V., Vaucheret, H., and Ding, S.-W. (2011). The 21-Nucleotide, but Not 22-Nucleotide, Viral Secondary Small Interfering RNAs Direct Potent Antiviral Defense by Two Cooperative Argonautes in Arabidopsis thaliana. Plant Cell **23**: 1625–1638.

Wang, X., Herr, R.A., and Hansen, T.H. (2012). Ubiquitination of substrates by esterification. Traffic **13**: 19–24.

Weber, H., Bernhardt, A., Dieterle, M., Hano, P., Mutlu, A., Estelle, M., Genschik, P., and Hellmann, H. (2005). Arabidopsis AtCUL3a and AtCUL3b form complexes with members of the BTB/POZ-MATH protein family. Plant Physiol. **137**: 83–93.

Wei, W., Ba, Z., Gao, M., Wu, Y., Ma, Y., Amiard, S., White, C.I., Danielsen, J.M.R., Yang, Y.G., and Qi, Y. (2012). A role for small RNAs in DNA double-strand break repair. Cell **149**: 101–112.

Weiberg, A., Wang, M., Bellinger, M., and Jin, H. (2014). Small RNAs: A New Paradigm in Plant-Microbe Interactions. Annu. Rev. Phytopathol. **52**: 495–516.

West, S.C., West, S.C., Louis, E., Louis, E., Mchugh, P., and Mchugh, P. (2003). Recognition of small interfering RNA by a viral suppressor ofRNAsilencing. Nature **426**: 0–4.

Wickliffe, K.E., Williamson, A., Meyer, H.J., Kelly, A., and Rape, M. (2011). K11-linked ubiquitin chains as novel regulators of cell division. Trends Cell Biol. **21**: 656–663.

Wierzbicki, A.T., Haag, J.R., and Pikaard, C.S. (2008). Noncoding Transcription by RNA Polymerase Pol IVb/Pol V Mediates Transcriptional Silencing of Overlapping and Adjacent Genes. Cell **135**: 635–648.

Wierzbicki, A.T., Ream, T.S., Haag, J.R., and Pikaard, C.S. (2009). RNA polymerase v transcription guides ARGONAUTE4 to chromatin. Nat. Genet. **41**: 630–634.

Wilkinson, K.D. (2000). Ubiquitination and deubiquitination: Targeting of proteins for degradation by the proteasome. Semin. Cell Dev. Biol. **11**: 141–148.

Wingard, S.A. (Virginina A.E.S. (1928). Hosts and symptoms of ring spot, a virus disease of plants. J. Agric. Res. **37**: 127–153.

Woehrer, S.L., Aronica, L., Suhren, J.H., Busch, C.J.-L., Noto, T., and Mochizuki, K. (2015). A Tetrahymena Hsp90 co-chaperone promotes siRNA loading by ATP-dependent and ATP-independent mechanisms. EMBO J. **34**: 559–77.

Wu, C., So, J., Davis-Dusenbery, B.N., Qi, H.H., Bloch, D.B., Shi, Y., Lagna, G., and Hata, A. (2011a). Hypoxia Potentiates MicroRNA-Mediated Gene Silencing through Posttranslational Modification of Argonaute2. Mol. Cell. Biol. **31**: 4760–4774.

Wu, X., Oh, M.-H., Schwarz, E.M., Larue, C.T., Sivaguru, M., Imai, B.S., Yau, P.M., Ort, D.R., and Huber, S.C. (2011b). Lysine Acetylation Is a Widespread Protein Modification for Diverse Proteins in Arabidopsis. Plant Physiol. **155**: 1769–1778.

Xie, Z., Allen, E., Fahlgren, N., Calamar, A., Givan, S.A., and Carrington, J.C. (2005a). Expression of Arabidopsis MIRNA genes. Plant Physiol. **138**: 2145–54.

Xie, Z., Allen, E., Wilken, A., and Carrington, J.C. (2005b). DICER-LIKE 4 functions in trans-acting small interfering RNA biogenesis and vegetative phase change in Arabidopsis thaliana. Proc. Natl. Acad. Sci. **102**: 12984–12989.

Xie, Z., Fan, B., Chen, C., and Chen, Z. (2001). An important role of an inducible RNA-dependent RNA polymerase in plant antiviral defense. Proc. Natl. Acad. Sci. U. S. A. **98**: 6516–6521.

Xu, P., Duong, D.M., Seyfried, N.T., Cheng, D., Xie, Y., Robert, J., Rush, J., Hochstrasser, M., Finley, D., and Peng, J. (2009). Quantitative Proteomics Reveals the Function of Unconventional Ubiquitin Chains in Proteasomal Degradation. Cell **137**: 133–145.

Yamano, K., Matsuda, N., and Tanaka, K. (2016). The ubiquitin signal and autophagy: an orchestrated dance leading to mitochondrial degradation. EMBO Rep. **17**: 300–316.

Yan, K.S., Yan, S., Farooq, A., Han, A., Zeng, L., and Zhou, M.M. (2004). Erratum: Structure and conserved RNA binding of the PAZ domain (Nature (2003) 426 (469-474)). Nature **427**: 265.

Yang, L., Liu, Z., Lu, F., Dong, A., and Huang, H. (2006). SERRATE is a novel nuclear regulator in primary microRNA processing in Arabidopsis. Plant J. **47**: 841–850.

Yang, L., Wu, G., and Poethig, R.S. (2012). Mutations in the GW-repeat protein SUO reveal a developmental function for microRNA-mediated translational repression in Arabidopsis. Proc. Natl. Acad. Sci. U. S. A. **109**: 315–20.

Yang, P., Fu, H., Walker, J., Papa, C.M., Smalle, J., Ju, Y.M., and Vierstra, R.D. (2004). Purification of the Arabidopsis 26 S proteasome: Biochemical and molecular analyses revealed the presence of multiple isoforms. J. Biol. Chem. **279**: 6401–6413.

Yee, D. and Goring, D.R. (2009). The diversity of plant U-box E3 ubiquitin ligases: From upstream activators to downstream target substrates. J. Exp. Bot. **60**: 1109–1121.

Yoo, B.-C., Kragler, F., Varkonyi-Gasic, E., Haywood, V., Archer-Evans, S., Lee, Y.M., Lough, T.J., and Lucas, W.J. (2004). A systemic small RNA signaling system in plants. Plant Cell **16**: 1979–2000.

Yoshikawa, M., Peragine, A., Park, M.Y., and Poethig, R.S. (2005). A pathway for the biogenesis of trans -acting siRNAs in Arabidopsis. Genes Dev.: 2164–2175.

Yu, B., Yang, Z., Li, J., Minakhina, S., Yang, M., Padgett, R.W., Steward, R., and Chen, X. (2005). Methylation as a crucial step in plant microRNA biogenesis. Science (80-.). **307**: 932–935.

Yuan, Y.R., Pei, Y., Ma, J.B., Kuryavyi, V., Zhadina, M., Meister, G., Chen, H.Y., Dauter, Z., Tuschl, T., and Patel, D.J. (2005). Crystal structure of A. aeolicus argonaute, a site-specific DNA-guided endoribonuclease, provides insights into RISC-mediated mRNA cleavage. Mol. Cell **19**: 405–419.

Zekri, L., Huntzinger, E., Heimstadt, S., and Izaurralde, E. (2009). The Silencing Domain of GW182 Interacts with PABPC1 To Promote Translational Repression and Degradation of MicroRNA Targets and Is Required for Target Release. Mol.

Cell. Biol. **29**: 6220–6231.

Zeng, Y., Sankala, H., Zhang, X., and Graves, P.R. (2008). Phosphorylation of Argonaute 2 at serine-387 facilitates its localization to processing bodies. Biochem. J. **413**: 429–436.

Zhai, J. et al. (2011). MicroRNAs as master regulators of the plant NB-LRR defense gene family via the production of phased, trans-acting siRNAs. Genes Dev. **25**: 2540–2553.

Zhang, X., Yuan, Y.-R., Pei, Y., Lin, S.-S., Tuschl, T., Patel, D.J., and Chua, N.-H. (2006). Cucumber mosaic virus-encoded 2b suppressor inhibits Arabidopsis Argonaute1 cleavage activity to counter plant defense. Genes Dev. **20**: 3255–3268.

Zhang, X., Zhang, X., Singh, J., Li, D., and Qu, F. (2012). Temperature-Dependent Survival of Turnip Crinkle Virus-Infected Arabidopsis Plants Relies on an RNA Silencing-Based Defense That Requires DCL2, AGO2, and HEN1. J. Virol. **86**: 6847–6854.

Zhang, Z., Liu, X., Guo, X., Wang, X.J., and Zhang, X. (2016). Arabidopsis AGO3 predominantly recruits 24-nt small RNAs to regulate epigenetic silencing. Nat. Plants **2**: 1–7.

Zheng, X., Zhu, J., Kapoor, A., and Zhu, J.K. (2007). Role of Arabidopsis AGO6 in siRNA accumulation, DNA methylation and transcriptional gene silencing. EMBO J. **26**: 1691–1701.

Zhong, X., Du, J., Hale, C.J., Gallego-Bartolome, J., Feng, S., Vashisht, A.A., Chory, J., Wohlschlegel, J.A., Patel, D.J., and Jacobsen, S.E. (2014). Molecular mechanism of action of plant DRM de novo DNA methyltransferases. Cell **157**: 1050–1060.

Zhou, J., Zhang, Y., Qi, J., Chi, Y., Fan, B., Yu, J.Q., and Chen, Z. (2014). E3 Ubiquitin Ligase CHIP and NBR1-Mediated Selective Autophagy Protect Additively against Proteotoxicity in Plant Stress Responses. PLoS Genet. **10**.

Zhou, P. and Howley, P.M. (1998). Ubiquitination and degradation of the substrate recognition subunits of SCF ubiquitin-protein ligases. Mol. Cell **2**: 571–580.

Zhu, H., Hu, F., Wang, R., Zhou, X., Sze, S.H., Liou, L.W., Barefoot, A., Dickman, M., and Zhang, X. (2011). Arabidopsis argonaute10 specifically sequesters miR166/165 to regulate shoot apical meristem development. Cell **145**: 242–256.

Zhu, L. and Hannon, G. (2000). Yeast hybrid technologies.

Zielezinski, A. and Karlowski, W.M. (2011). Agos-a universal web tool for GW Argonaute-binding domain prediction. Bioinformatics **27**: 1318–1319.

Zilberman, D., Cao, X., and Jacobsen, S.E. (2003). ARGONAUTE4 control of locus-specific siRNA accumulation and DNA and histone methylation. Science (80-.). **299**: 716–719.

Zuo, J., Niu, Q.W., and Chua, N.H. (2000). Technical advance: An estrogen receptor-based transactivator XVE mediates highly inducible gene expression in transgenic plants. Plant J. **24**: 265–73.
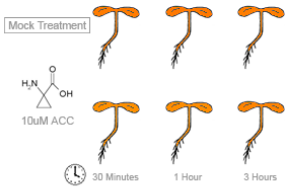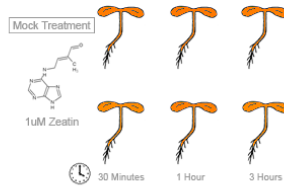
Supplementary files

At4g08980 255066_at FBW2
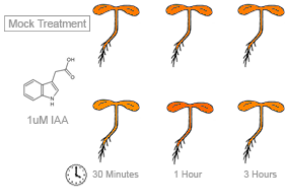
Arabidopsis eFP Browser at bar.utoronto.ca
Winter et al., 2007. PLoS One 2(8): e718

☐ = Control

Absolute
366.78
330.1
293.42
256.74
220.06
183.39
146.71
110.03
73.35
36.67
0.0
Masked

ACC
Mock Treatment
10uM ACC
30 Minutes 1 Hour 3 Hours

Zeatin
Mock Treatment
1uM Zeatin
30 Minutes 1 Hour 3 Hours

IAA
Mock Treatment
1uM IAA
30 Minutes 1 Hour 3 Hours

ABA
Mock Treatment
10uM ABA
30 Minutes 1 Hour 3 Hours

Methyl Jasmonate
Mock Treatment
10uM MJ
30 Minutes 1 Hour 3 Hours

GA-3
Mock Treatment (Wild-type)
1uM GA3 (Wild-type)
30 Minutes 1 Hour 3 Hours

Mock Treatment (ga1-5 Mutants)
1uM GA3 (ga1-5 Mutants)
30 Minutes 1 Hour 3 Hours
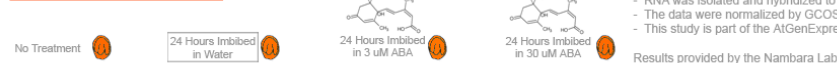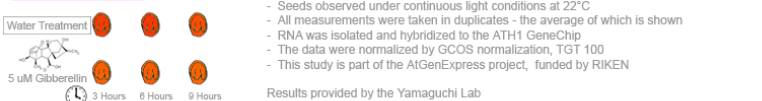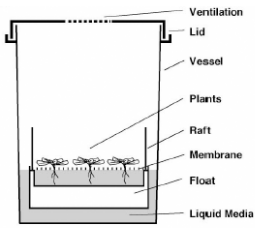
- Plant material from 7 day old wild-type or otherwise specified mutant *Arabidopsis thaliana* seedlings of Columbia-0 ecotype was analyzed
- Plants grown in liquid MS media under continuous light conditions at 23°C
- All measurements were taken in duplicates - the average of which is shown
- RNA was isolated and hybridized to the ATH1 GeneChip
- The data were normalized by GCOS normalization, TGT 100
- This study is part of the AtGenExpress project, funded by RIKEN

Results provided by the Shimada Lab

Brassinolide
Mock Treatment (Wild-type)
10nM BL (Wild-type)
30 Minutes 1 Hour 3 Hours

Mock Treatment (det-1 Mutants)
10nM BL (det-1 Mutants)
30 Minutes 1 Hour 3 Hours

Brassinosteroids
Mock Treatment for 3 Hours
10uM campestanol for 3 Hours
1uM 6-deoxo-cathasterone for 3 Hours
1uM cathasterone for 3 Hours
1uM 6-deoxo-teasterone for 3 Hours
1uM teasterone for 3 Hours
1uM 3-dehydro-6-deoxoteasterone for 3 Hours
1uM 3-dehydro-teasterone for 3 Hours
1uM 6-deoxo-typhasterol for 3 Hours
1uM typhasterol for 3 Hours
1uM 6-deoxo-castasterone for 3 Hours
100nM castasterone for 3 Hours
10nM brassinolide for 3 Hours

Cytokinin
No Treatment
20 uM t-zeatin for 3 Hours
Wild-Type (Col-0) ARR22 Overexpressing

- Plant material from 21 day old wild-type and ARR22 overexpressing mutant *Arabidopsis thaliana* seedlings of Columbia-0 ecotype was analyzed
- Plants grown on agar
- All measurements were taken in triplicates - the average of which is shown
- RNA was isolated and hybridized to the ATH1 GeneChip
- The data were normalized by GCOS normalization, TGT 100
- This study is part of the AtGenExpress project, funded by RIKEN

Results provided by the Mizuno Lab

ABA during Seed Imbibition
No Treatment
24 Hours Imbibed in Water
24 Hours Imbibed in 3 uM ABA
24 Hours Imbibed in 30 uM ABA

- Plant material from wild-type *Arabidopsis thaliana* seeds of Columbia-0 ecotype was analyzed
- Seeds observed under continuous light conditions at 22°C
- All measurements were taken in duplicates - the average of which is shown
- RNA was isolated and hybridized to the ATH1 GeneChip
- The data were normalized by GCOS normalization, TGT 100
- This study is part of the AtGenExpress project, funded by Riken

Results provided by the Nambara Lab

Basic Hormones
Water Treatment
5 uM Gibberellin
3 Hours 6 Hours 9 Hours

- Plant material from ga1-3 mutant *Arabidopsis thaliana* seeds of L*er* ecotype was analyzed
- Seeds observed under continuous light conditions at 22°C
- All measurements were taken in duplicates - the average of which is shown
- RNA was isolated and hybridized to the ATH1 GeneChip
- The data were normalized by GCOS normalization, TGT 100
- This study is part of the AtGenExpress project, funded by RIKEN

Results provided by the Yamaguchi Lab

eFP Browser Hormone Series by B. Vinegar and D. Winter. Data from AtGenExpress Hormone Series.

Supplementary Figure 1 : eFP browser view of FBW2 expression in response to hormones
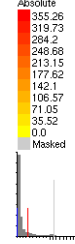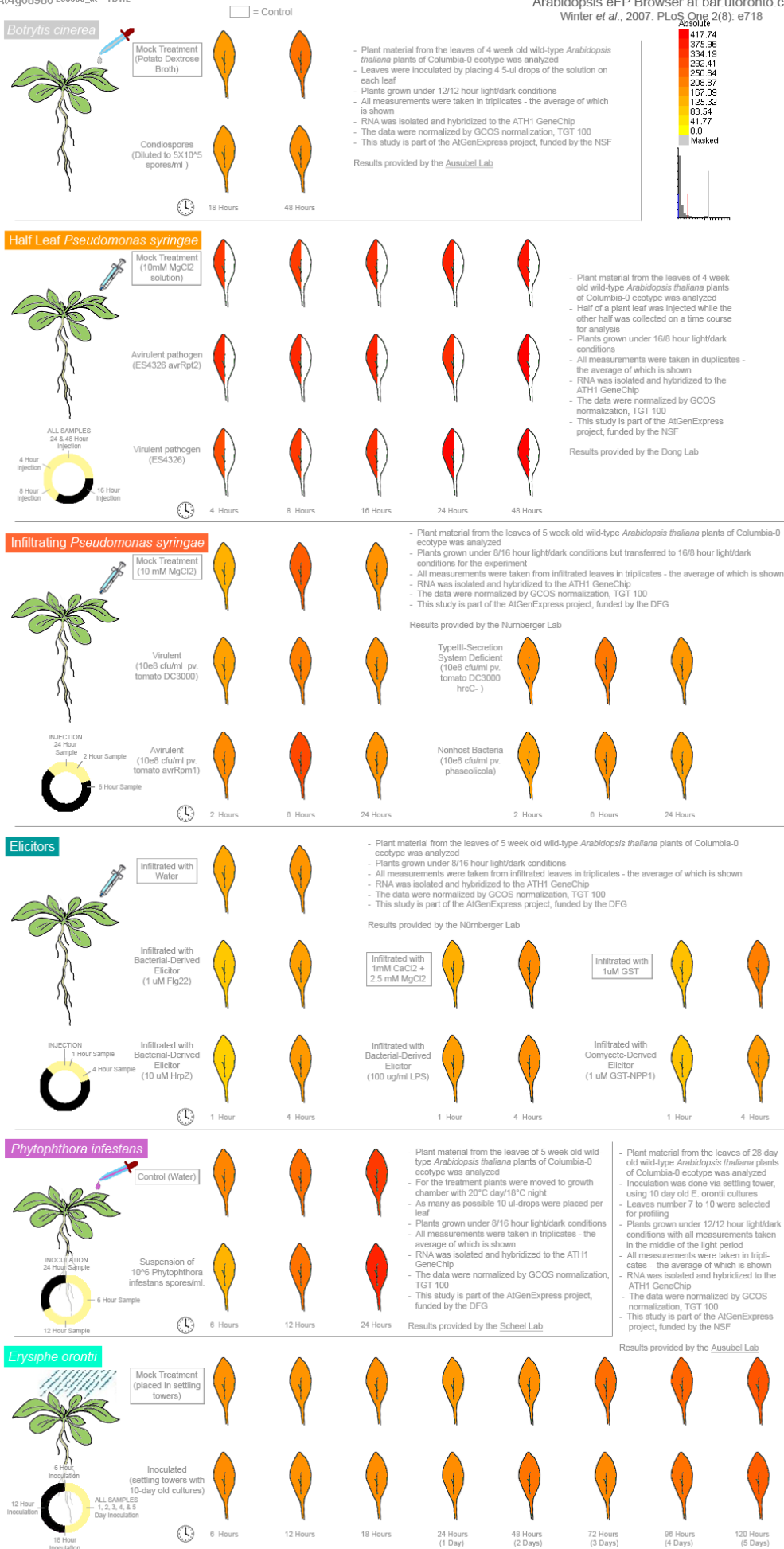
Transcriptomic data from the Arabidopsis eFP Browser (Winter et al., 2007). The expression level in seedlings was measured by the Shimada laboratory, in adult plants by the Mizuno laboratory, in seed with ABA treatment by Nambara laboratory and in seeds with Gibberellins (GAs) by Yamaguchi laboratory. The absolute level of expression is indicated by colors ranging from yellow (no expression) to red (strong expression) as indicated on the top right corner.

**Supplementary Figure 2 :
eFP browser view of FBW2 expression in response to abiotic stresses**

Transcriptomic data from the Arabidopsis eFP Browser (Winter et al., 2007). The expression level was measure by Kilian et al., 2007. The absolute level of expression is indicated by colors ranging from yellow (no expression) to red (strong expression) as indicated on the top right corner.

Supplementary Figure 3 : eFP browser view of FBW2 expression in response to biotic stresses

Transcriptomic data from the Arabidopsis eFP Browser (Winter et al., 2007). The expression level following elicitation or infection with *Botrytis cinerea* was measured by the Nürnberger laboratory, with *Pseudomonas syringae* by the Dong laboratory and the Nürnberger laboratory, with *Phytophtora infestans* by the Scheel laboratory, by *Erysiphe orontii* by the Ausubel laboratory. The absolute level of expression is indicated by colors ranging from yellow (no expression) to red (strong expression) as indicated on the top right corner.
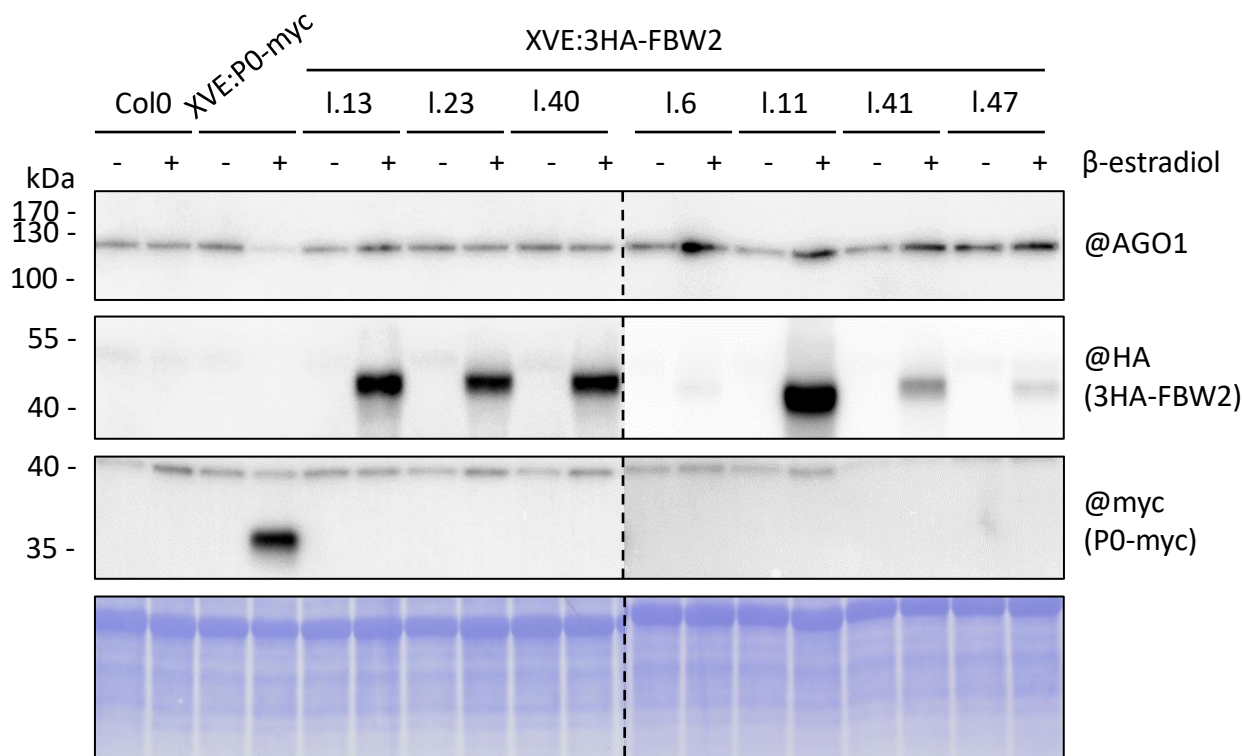
Supplementary Figure 4 : Comparison of the inducible P0 line with lines expressing FBW2

Western blot of protein extracts from 7 day-old seedlings grown on MS medium supplemented with DMSO (-) or β-estradiol (+). The XVE is a promoter inducible with β-estradiol (Zuo et al., 2000). The XVE:P0-myc line was established previously (Derrien et al., 2012). A 3HA tag was N-terminally fused to FBW2 put under the control of the XVE promoter and transformed in Arabidopsis to generate the independent homozygous, simple insertion lines presented here. Coomassie blue staining was used as a loading control. "@" indicates hybridization with the corresponding antibody.
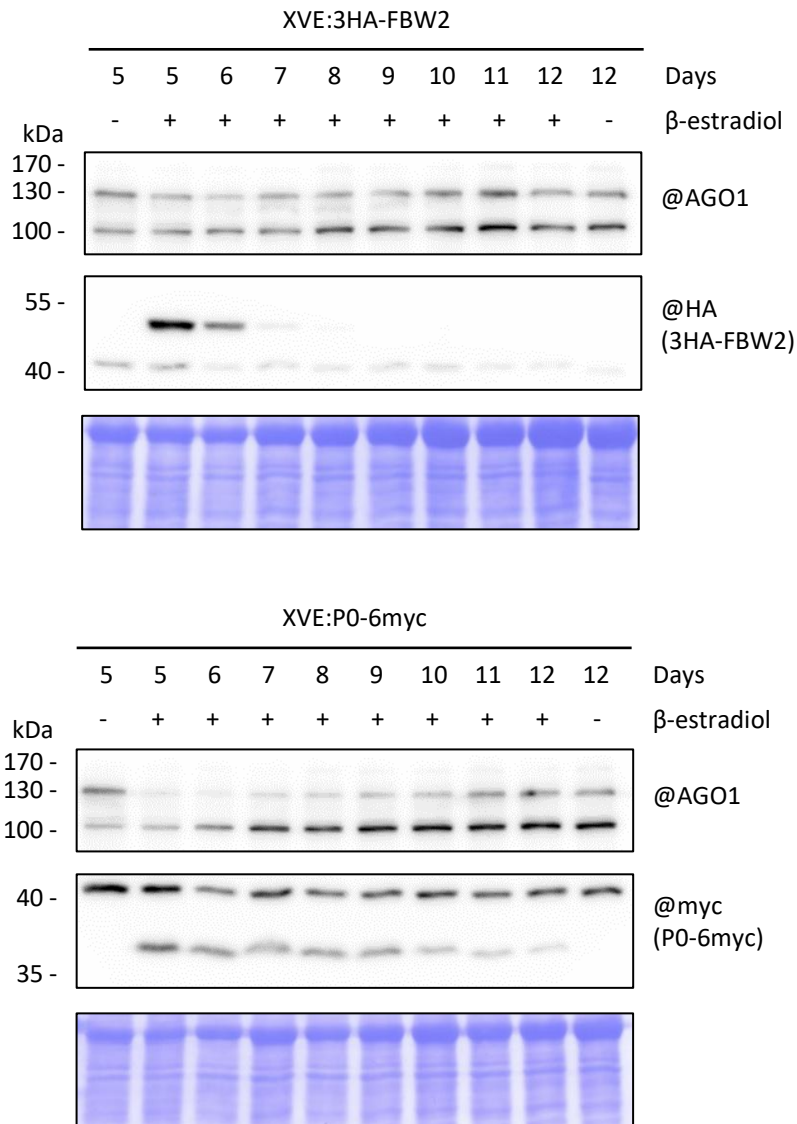
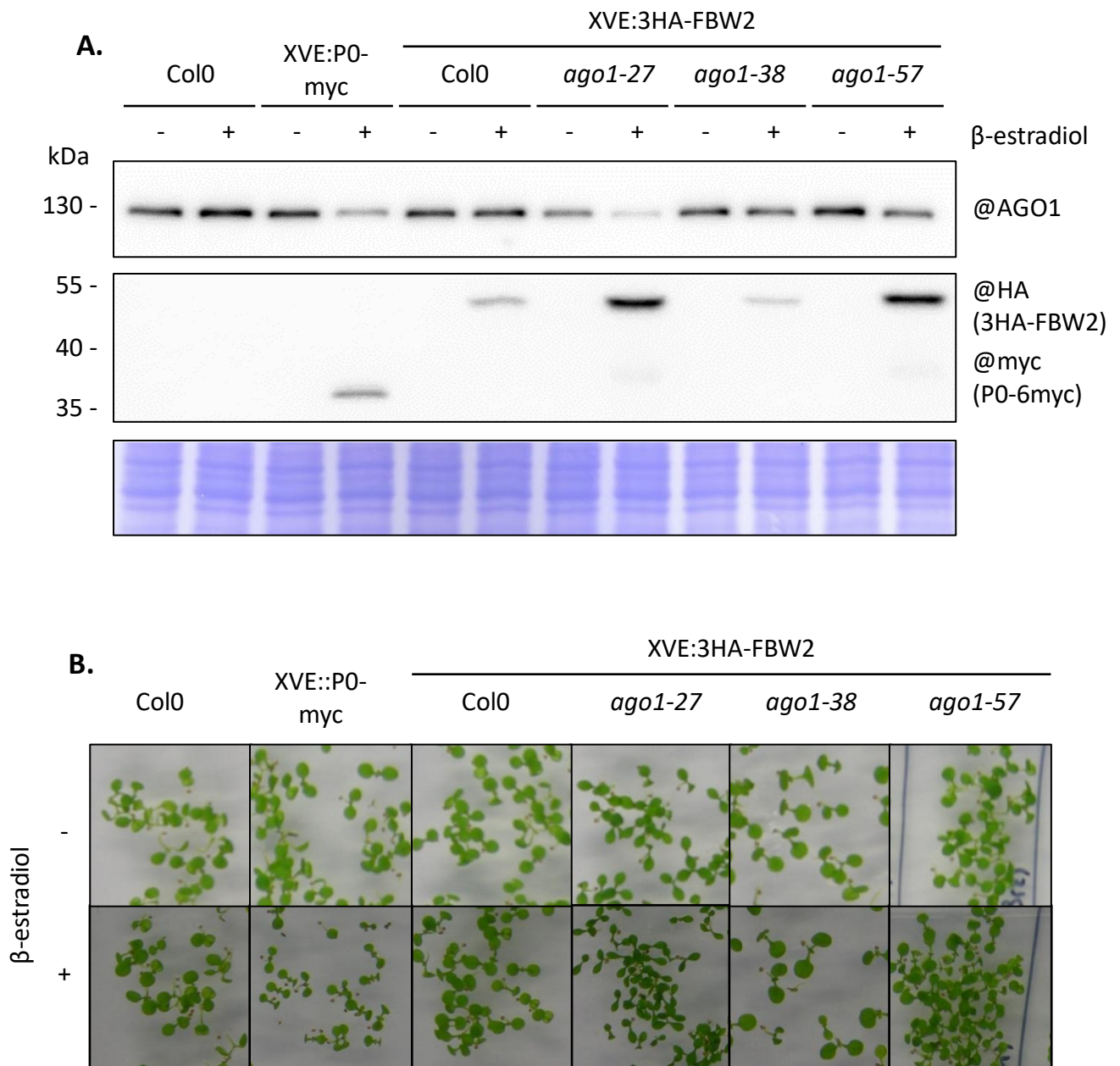**Supplementary Figure 5 : Kinetic induction of FBW2 expression**

Western blots of protein extracts from 5 to 12 day-old seedlings grown on MS medium supplemented with DMSO (-) or β-estradiol (10 μM) (+). The XVE is a promoter inducible with β-estradiol (Zuo et al., 2000) that controls the expression of the 3HA-FBW2 construct. The XVE:P0-myc line was established previously (Derrien et al., 2012). Coomassie blue staining was used as a loading control and "@" indicates hybridization with the corresponding antibody.
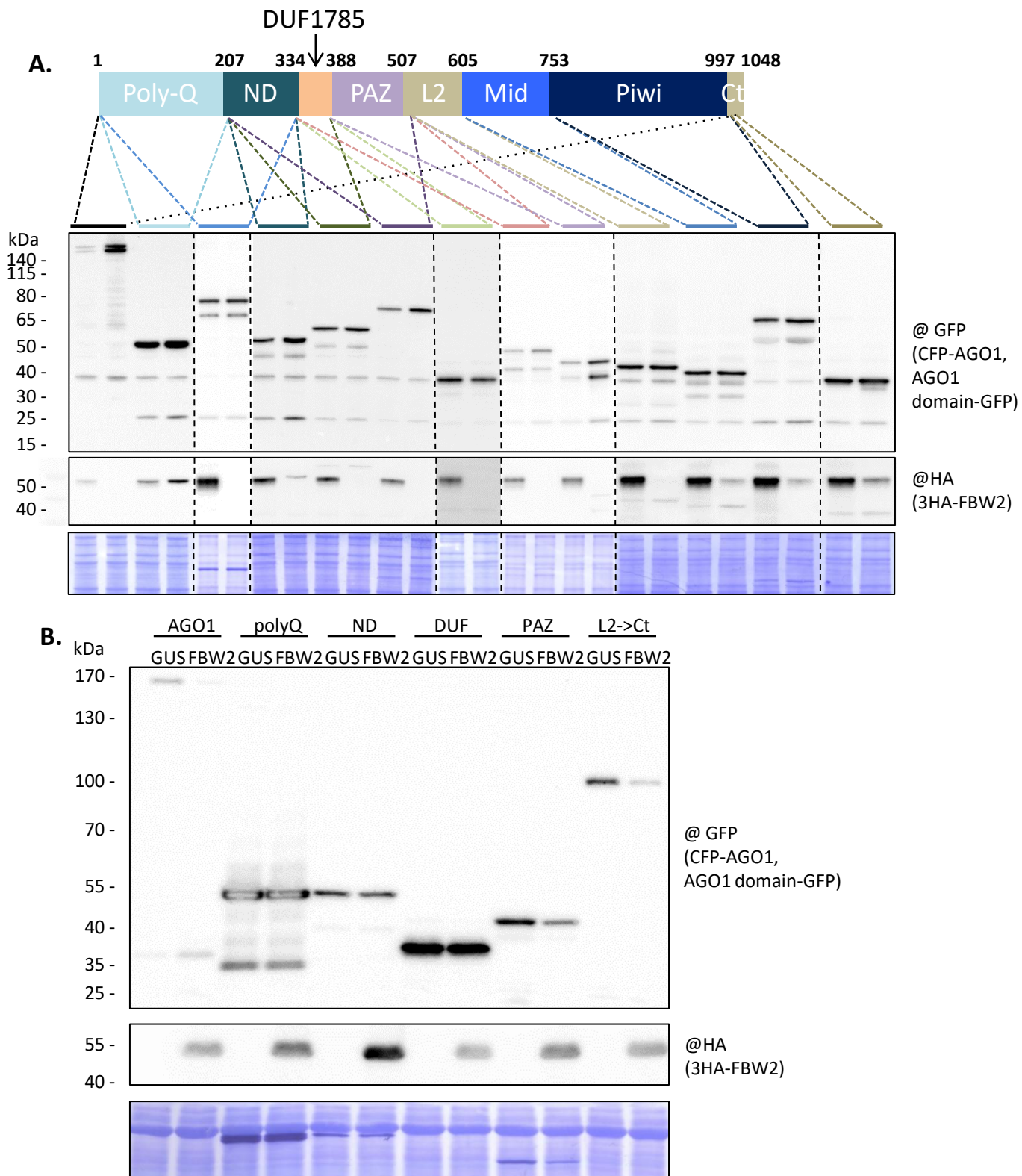
Supplementary Figure 6 : The PAZ and the C-terminal part of AGO1 are targeted by FBW2

A. and B. Western blot of protein extracts from four week-old *Nicotiana benthamiana* agroinfiltrated leaves. Agrobacteria harbouring full length CFP-AGO1 or AGO1 domains, as specified, and C-terminally fused to the GFP and a 35S::3HA-FWB2 constructs were infiltrated at an OD of 0,3 and tissues were sampled 3 days later. Expression of GUS serves as control. Coomassie blue staining was used as a loading control. "@" indicates hybridization with the corresponding antibody.
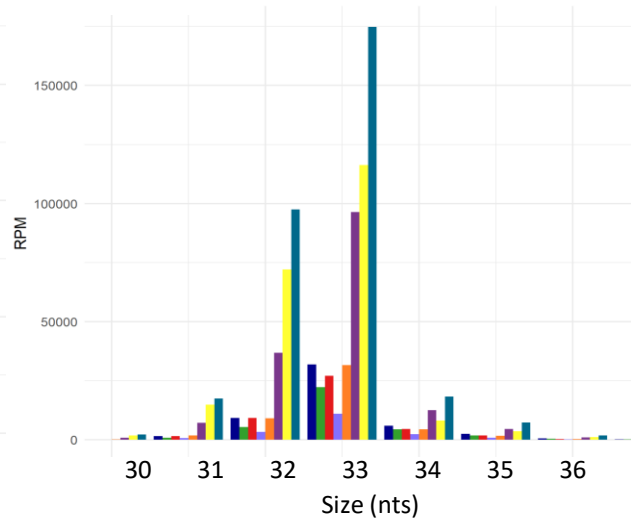
Supplementary Figure 7 : Tryptophan conservation in FBW2 C-terminal end

Protein sequences related to FBW2 were recovered by a BLAST research on the UniProt database (https://www.uniprot.org). These sequences were then aligned with Clustal Omega (https://www.ebi.ac.uk/Tools/msa/clustalo/). Amino acid conservation is displayed in blue, the most intense being the most conserved. The tryptophan residues located at the C-terminal end of FBW2 are shown in red. The dotted bars indicates jumps in the alignment window.
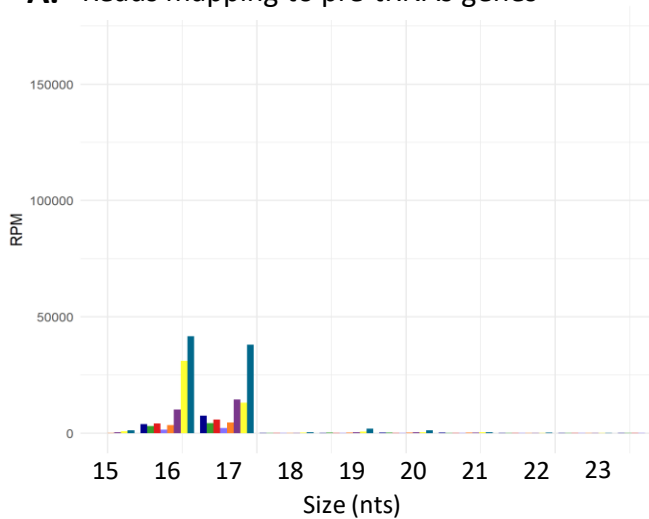
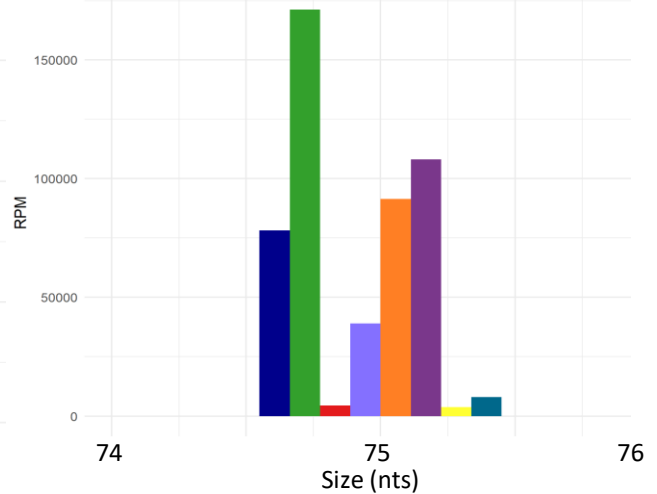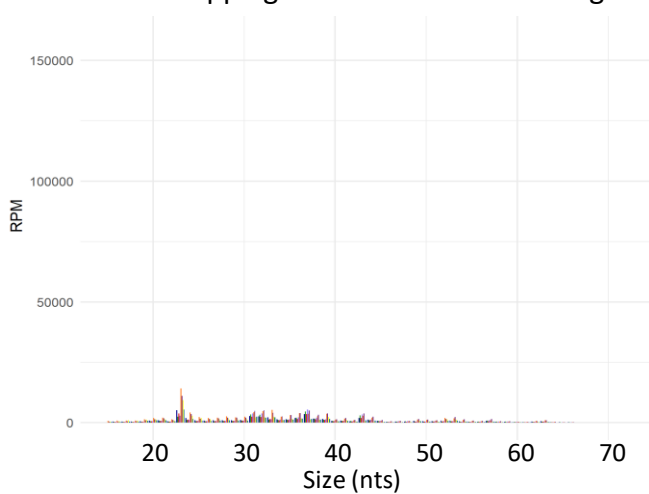**Supplementary Figure 8 : FBW2 induction in *ago1* mutants affects AGO1 protein level and plant growth**

A. Western blot of protein extracts from 7 day-old seedlings XVE:P0-myc and XVE:3HA-FBW2 crossed with the specified *ago1* mutants and grown on MS medium supplemented (+) or not (-) with β-estradiol.
B. Pictures of the same seedlings grown on MS medium supplemented (+) or not (-) with β-estradiol.

Supplementary Figure 9 : AGO1 steady state protein level in diverse mutants

A. Western blot of protein extracts from 12 day-old seedlings grown on MS medium.
B. Western blot of protein extracts from the specified tissues of 40 day-old seedlings grown on soil.

Coomassie blue staining was used as loading control and "@" indicates hybridization with antibody for all western blots. The upper signals observed in the @AGO4 hybridization panel correspond to unstripped antibody directed against AGO1.

A. Reads mapping to pre-tRNAs genes

B. Reads mapping to small nucleolar RNA genes

C. Reads mapping to miRNA genes
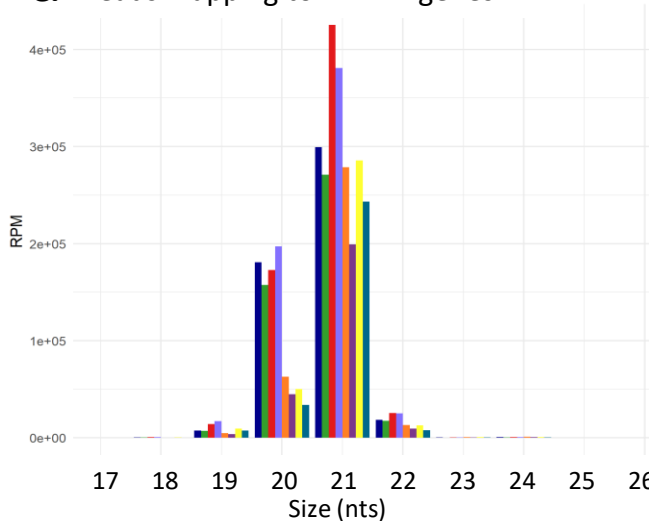
Color code

■ Col0 rep1	■ *hyl1-2* rep2
■ Col0 rep2	■ *hyl1-2* rep1
■ *fbw2-4* rep1	■ *hyl1-2 fbw2-4* rep1
■ *fbw2-4* rep2	■ *hyl1-2 fbw2-4* rep2

Supplementary Figure 10 : miRNA, tRNA fragments and small nucleolar RNAs are deregulated in the *fbw2-4* and *hy1-2* mutants

Abundance and size of differentially represented elements in the raw analysis of the RNA-seq libraries corresponding to the AGO1 immunoprecipitated fractions. Replicate one of Col0 is in dark blue, replicate two in green, replicate one of *fbw2-4* in red, replicate two in light blue, replicate one of *hyl1-2* in orange, replicate two in purple, replicate one of the double mutant *hyl1-2 fbw2-4* in yellow, replicate two in turquoise.

A. Reads mapping to pre-tRNA genes. Short tRNA matching reads are presented on the left. Longer reads are presented on the right.

B. Reads mapping to small nucleolar RNA genes. Reads ranging from 15 to 74 nt are presented on the left. The majority of reads are of 75 nt, are presented on the right.

C. Reads mapping to miRNA genes.

Supplementary Figure 11 : *hen1-6* mutants overexpressing FBW2 present a severely altered development

Picture of 10 week- old *hen1-6* mutant plants harbouring the 35S:3HA-FBW2 construct.

Thibaut Hacquard

Molecular characterization of the F-box protein FBW2 in the RNA silencing in *Arabidopsis thaliana*

L'ARN interférence est un mécanisme moléculaire conservé chez les Eucaryotes dont les principaux acteurs sont les protéines ARGONAUTE (AGO). Chez les plantes, AGO1 est une protéine essentielle à la croissance et la défense antivirale. Elle utilise des petits ARNs comme sondes pour reconnaître et réguler des ARN messagers. Les virus ont développé des suppresseurs de l'ARN interférence pour surmonter cette défense. L'un d'entre eux, P0 du virus de la mosaïque jaune du navet, est comme une protéine F-box qui détourne le complexe SCF, une ubiquitine ligase E3, et conduit AGO1 vers la protéolyse ubiquitine-dépendante. Cette dégradation utilise la vacuole au lieu du protéasome 26S, généralement associé à la dégradation ubiquitine-dépendante. Ce mécanisme de protéolyse n'est pas compris et est aussi apparent quand AGO1 est déstabilisé de manière endogène, suggérant que P0 utilise une voie déjà existante. Une protéine F-box d'Arabidopsis, FBW2, a été décrite comme impactant l'homéostasie d'AGO1 indépendamment du protéasome. Mon projet de thèse visait à caractériser l'activité F-box de FBW2 et à comprendre la relation entre AGO1 et FBW2 ainsi que ses conséquences sur l'ARN interférence.

Les résultats obtenus dans ce manuscrit montrent que le complexe SCF^{FBW2} interagit avec AGO1 et déclenche sa dégradation via un processus indépendant de l'autophagie ou du protéasome, tout en n'affectant que faiblement l'ARN interférence. FBW2 ciblerait en fait un sous-ensemble de protéines AGO1 qui semble ne pas contenir de petits ARNs. Cette régulation jouerait un rôle de surveillance pour prévenir une activité délétère d'AGO1 en absence de petits ARNs.

Mots clés : Arabidopsis, ARN interférence, AGO1, ubiquitine, SCF, FBW2

RNA silencing is a conserved molecular mechanism in eukaryotes, of which the main effectors are the ARGONAUTE (AGO) proteins. In plants, AGO1 is a protein that is essential for growth and antiviral defence. It uses small RNAs as probe to recognize and regulate messenger RNAs. Viruses have developed suppressors of RNA silencing to overcome this defence. One of these, P0 from the Turnip Yellows Virus, acts as an F-box protein to hijack the SCF complex, an E3 ubiquitin ligase, and guide AGO1 to the ubiquitin-dependent proteolysis. This degradation uses the vacuole instead of the 26S proteasome, generally associated with ubiquitin-dependant proteolysis. This proteolysis mechanism is not understood and is also apparent when AGO1 is endogenously destabilized, suggesting that P0 uses an already existing pathway. An Arabidopsis F-box protein, FBW2, has been shown to impact AGO1 homeostasis independently from the proteasome. My PhD project aimed at characterizing FBW2 F-box activity and understanding the relationship between AGO1 and FBW2, as well as its consequences on the RNA silencing.

The results obtained in this manuscript show that the SCF^{FBW2} interacts with AGO1 and triggers its degradation through an autophagy- and proteasome- independent process, while only weakly affecting the RNA silencing. FBW2 would actually target a subset of AGO1 proteins, which appears not to contain small RNAs. This regulation would play a surveillance role in order to prevent a deleterious activity of AGO1 in absence of small RNAs.

Keywords : Arabidopsis, RNA silencing, AGO1, ubiquitin, SCF, FBW2

UNIVERSITE DE STRASBOURG

RESUME DE LA THESE DE DOCTORAT

Discipline : Aspects Moléculaires et Cellulaires de la Biologie

Présentée par : Hacquard Thibaut

Titre : Caractérisation Moléculaire du rôle de la protéine FBW2 dans l'ARN interférence

Unité de Recherche : UPR2357 Institut de Biologie Moléculaire des Plantes

Directeur de Thèse : Genschik Pascal – Directeur de recherche

Localisation : 12 Rue du Général-Zimmer, 67000 Strasbourg

ECOLES DOCTORALES :
(cocher la case)

☐ ED - Sciences de l'Homme et des sociétés	☐ ED 269 - Mathématiques, sciences de l'information et de l'ingénieur
☐ ED 99 – Humanités	☐ ED 270 – Théologie et sciences religieuses
☐ ED 101 – Droit, sciences politique et histoire	☐ ED 413 – Sciences de la terre, de l'univers et de l'environnement
☐ ED 182 – Physique et chimie physique	☒ ED 414 – Sciences de la vie et de la santé
☐ ED 221 – Augustin Cournot	
☐ ED 222 - Sciences chimiques	
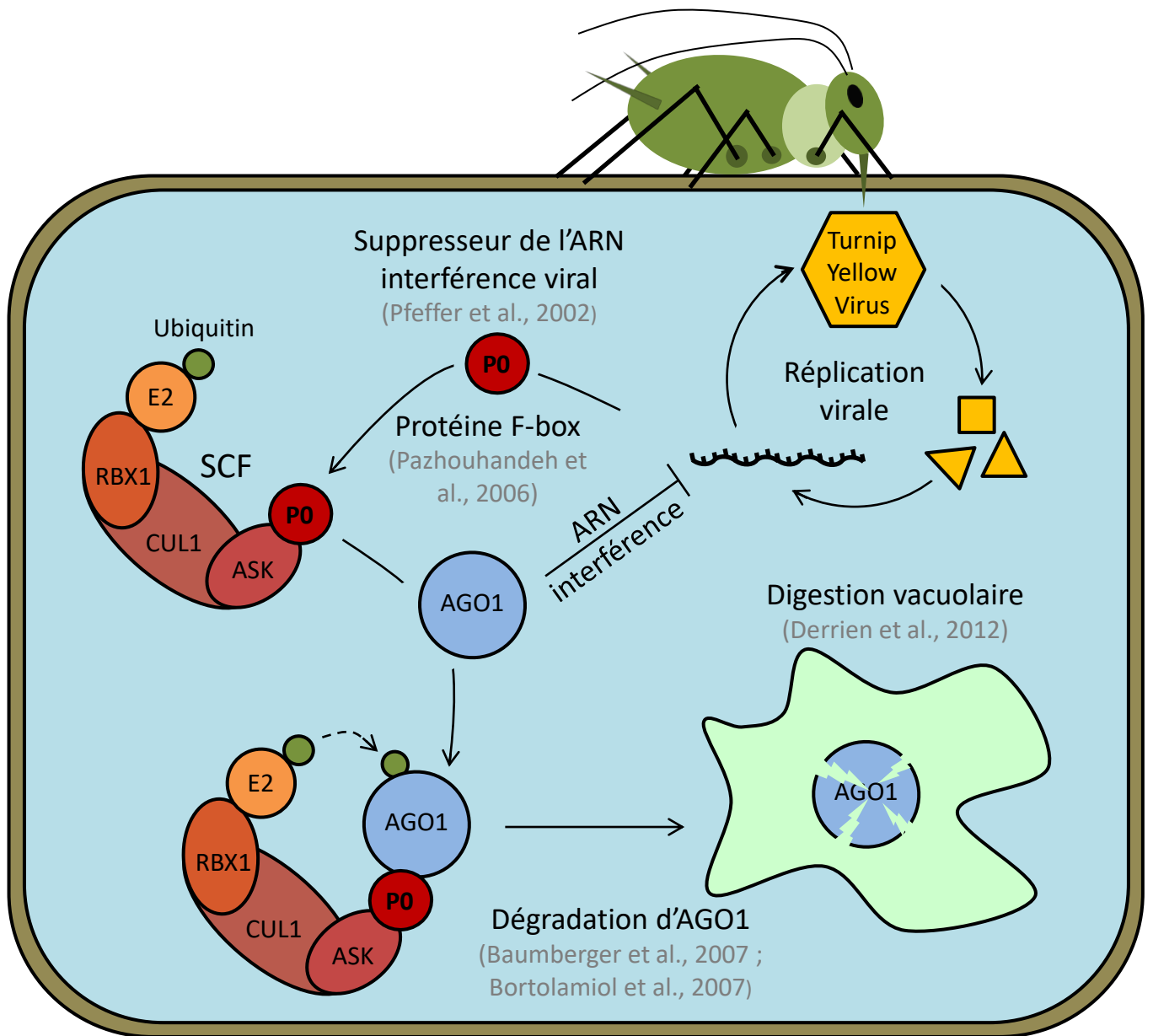
**Figure 1 : Mode d'action du suppresseur de l'ARN interférence P0**

Le virus de la mosaïque jaune du navet est un virus à ARN simple brin transmis par les pucerons. Sa protéine P0 est un suppresseur de l'ARN interférence qui détourne le complexe SCF et déclenche la dégradation AGO1. Au lieu d'être dégradé par le protéasome 26S, AGO1 est dégradé dans la vacuole.

Mon projet de thèse porte sur la régulation post-traductionnelle de ARGONAUTE1 (AGO1) par la protéine F-Box FBW2 chez la plante modèle *Arabidopsis thaliana*.

AGO1 est une protéine de la famille des protéines ARGONAUTE qui joue un rôle clé dans un mécanisme de régulation de l'expression des gènes appelé ARN interférence. AGO1 utilise de petits ARNs non codants pour cibler de manière séquence-spécifique les transcrits de gènes à réprimer (Baulcombe, 2004). L'ARN interférence est nécessaire au développement de la plante et est aussi impliqué dans la défense antivirale (Wang et al., 2011). Pour contrer cette défense, des virus ont développé des protéines inhibant l'ARN interférence. Une protéine F-box de polérovirus, P0, a été découverte à l'IBMP. Elle détourne un mécanisme de dégradation protéique existant chez la plante pour induire la dégradation d'AGO1 et ainsi réprimer la réponse antivirale (Figure 1) (Baumberger et al., 2007; Bortolamiol et al., 2007; Pazhouhandeh et al., 2006). Son domaine F-Box lui permet d'assembler un complexe E3 ubiquitine-ligase de type SCF (Skp, Cullin, F-box containing complex) qui catalyse l'ubiquitination d'AGO1, ce qui conduit cette dernière à la dégradation. Les protéines ubiquitinées sont classiquement éliminées par le protéasome mais AGO1 est dégradé dans la vacuole (Derrien et al., 2012) par une voie encore inconnue. Malgré l'importance d'AGO1 chez les plantes, encore peu de choses concernant sa régulation post-traductionnelle endogène sont connues. Seule la protéine FBW2 (F-box with WD-40 2) a été décrite comme agissant sur l'homéostasie d'AGO1. Comme c'est le cas pour P0, la dégradation d'AGO1 par cette protéine ne semble pas dépendre du protéasome (Earley et al., 2010).

Mon travail de thèse se concentre sur l'étude du mode d'action de FBW2, sa relation avec AGO1 et les possibles conséquences sur l'ARN interférence. J'ai notamment mis en évidence que FBW2 est une protéine instable qui forme une E3 ligase ciblant AGO1. Sa surexpression déstabilise AGO1 et diminue l'activité de l'ARN interférence, cependant moins efficacement que P0. FBW2 révèle son importance physiologique en l'absence de petits ARN ou lorsque l'activité d'AGO1 est anormale.
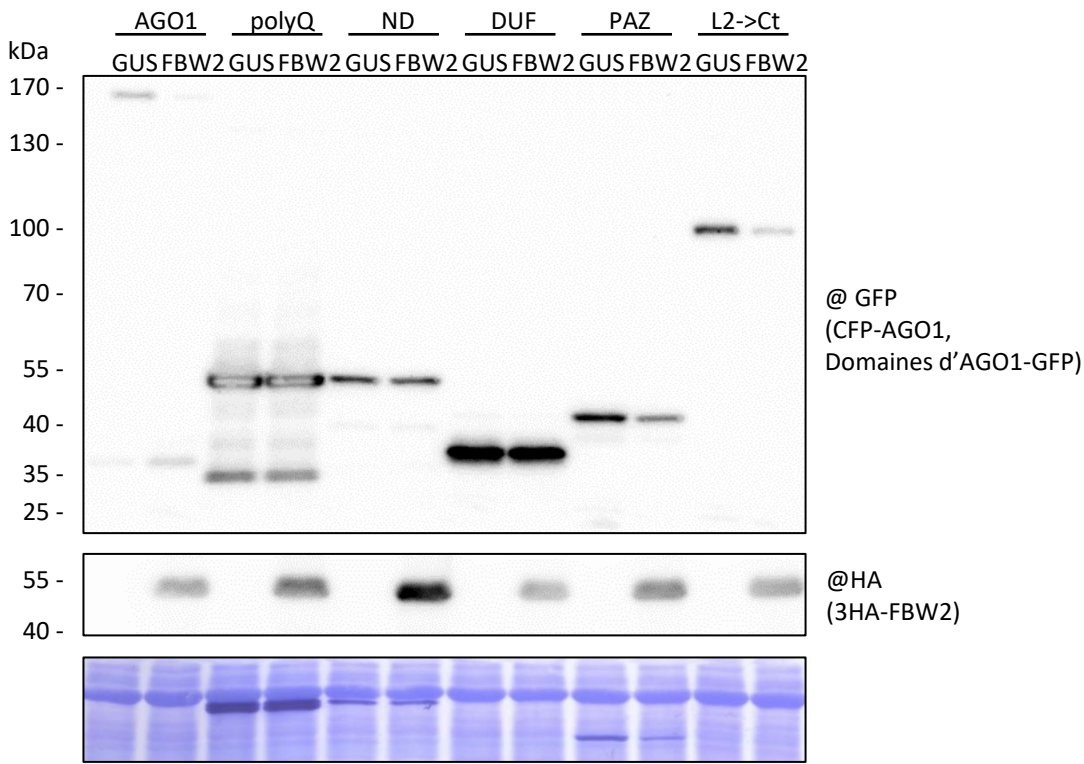
Figure 2 : Les domaines PAZ et Mid Piwi sont ciblés par FBW2

Western blot d'extraits protéiques de feuilles agroinfiltrées de *Nicotiana benthamiana* âgées de 4 semaines. Des agrobactéries contenant des constructions CFP-AGO1, domaines d'AGO1-GFP, et FBW2 sous promoteurs 35S ont été infiltrées à une DO de 0,3. Les tissus ont été échantillonnés 3 jours plus tards. L'expression de la protéine GUS sert de contrôle. La coloration au bleu de Coomassie sert de contrôle de charge. "@" indique une hybridation avec l'anticorps correspondant.

Figure 3 : FBW2 contient un motif GW hypothétique
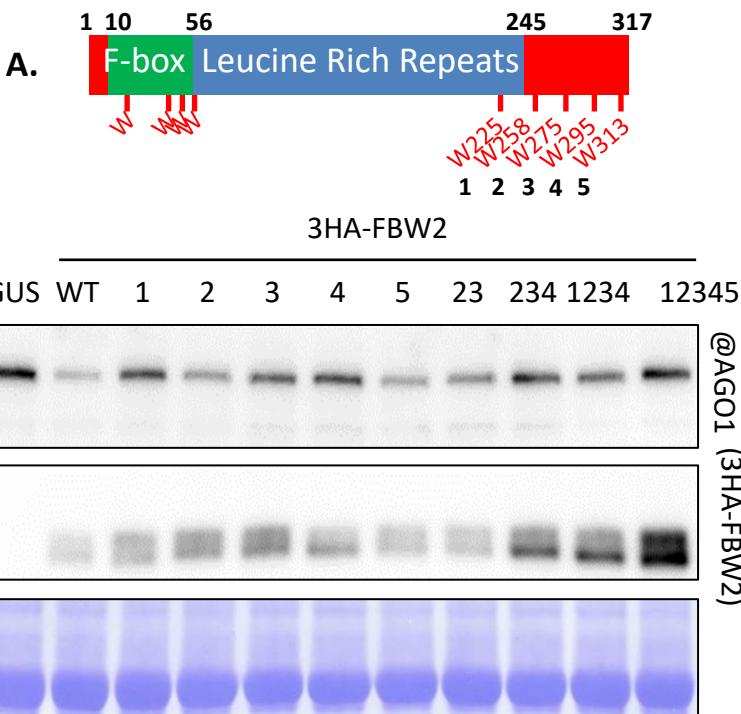
A. Schéma de la répartition de résidus tryptophanes de FBW2. Ils sont localisés soit dans le domaine F-box soit dans la partie C-terminale de FBW2.

B. Western blot d'extraits protéiques de feuilles agroinfiltrées de *Nicotiana benthamiana* âgées de 4 semaines. Des agrobactéries contenant des constructions CFP-AGO1 et FBW2 sauvage (WT) ou muté comme spécifié sous promoteurs 35S ont été infiltrées à une DO de 0,3. Les tissus ont été échantillonnés 3 jours plus tards. L'expression de la protéine GUS sert de contrôle. La coloration au bleu de Coomassie sert de contrôle de charge. "@" indique une hybridation avec l'anticorps correspondant.
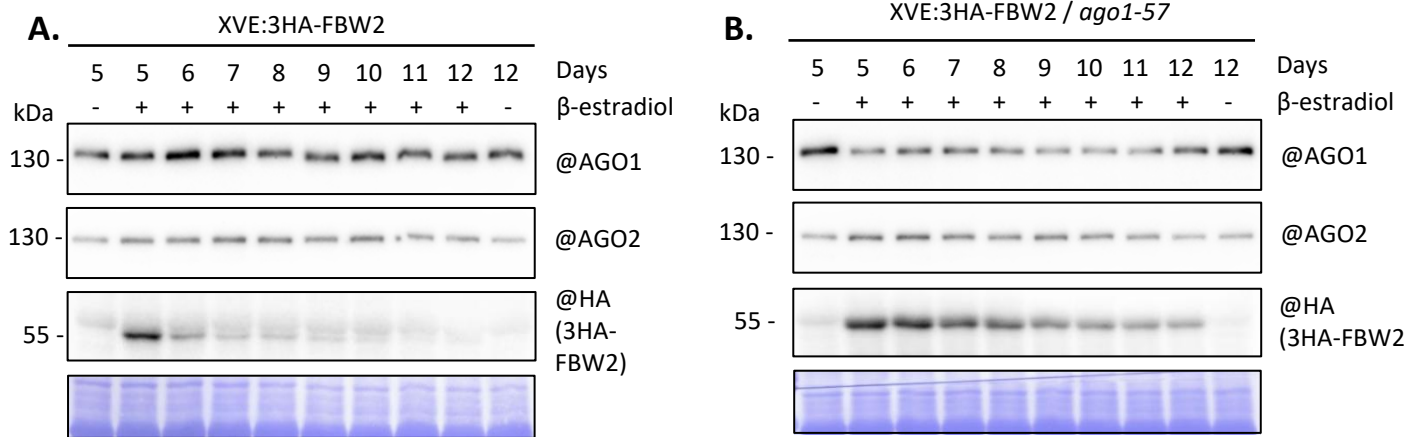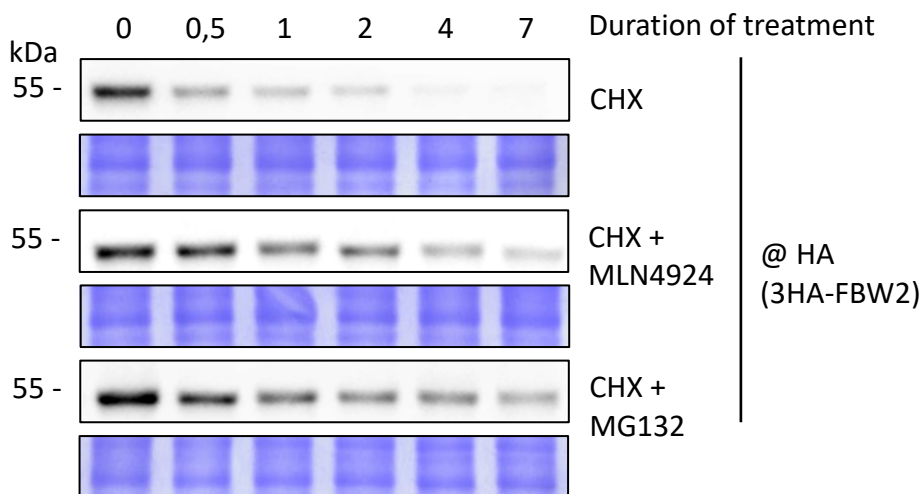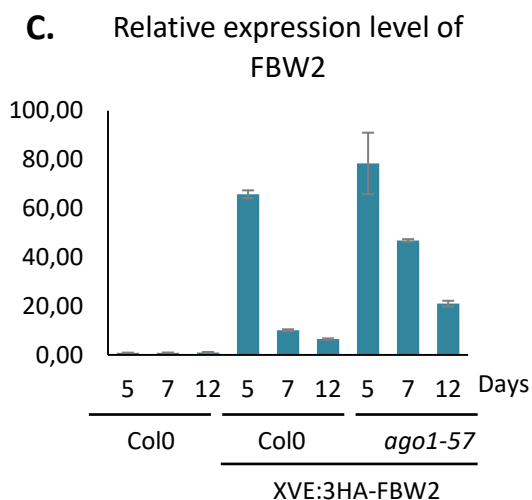
J'ai pu montrer au cours de ces 4 années que FBW2 provoque la dégradation de plusieurs protéines ARGONAUTE lors d'expressions transitoires dans *Nicotiana benthamiana*. De manière similaire, l'expression transitoire de fragments d'AGO1 montre que les domaines impliqués dans la fixation du petit ARN dans AGO1 sont spécifiquement ciblés par FBW2 (Figure 2). Des protéines sont connues pour interagir avec ces domaines via un motif protéique appelé « AGO-hook ». De manière intéressante, ce motif est prédit informatiquement dans la partie C-terminale de FBW2. La délétion ou mutation de ce motif aboli la dégradation d'AGO1, tout comme la mutation d'acides aminés clés du domaine F-box de FBW2 (Figure 3). L'immunoprécipitation d'une protéine de fusion 3HA-FBW2 dans Arabidopsis m'a permis d'isoler le complexe SCF ainsi que AGO1 lorsque l'activité de l'E3 ligase est inhibée chimiquement. L'interaction entre FBW2 et AGO1 a ensuite été validée par des expériences de doubles hybrides en levure. FBW2 cible donc plusieurs protéines ARGONAUTE et induit la dégradation d'AGO1 en la ciblant au sein d'une E3 ligase.

A. XVE:3HA-FBW2

| | 5 | 5 | 6 | 7 | 8 | 9 | 10 | 11 | 12 | 12 | Days |
| kDa | - | + | + | + | + | + | + | + | + | - | β-estradiol |

130 - @AGO1

130 - @AGO2

55 - @HA (3HA-FBW2)

B. XVE:3HA-FBW2 / *ago1-57*

| | 5 | 5 | 6 | 7 | 8 | 9 | 10 | 11 | 12 | 12 | Days |
| kDa | - | + | + | + | + | + | + | + | + | - | β-estradiol |

130 - @AGO1

130 - @AGO2

55 - @HA (3HA-FBW2)

C. Relative expression level of FBW2

Days	5	7	12	5	7	12	5	7	12
	Col0			Col0			*ago1-57*		
				XVE:3HA-FBW2					

Figure 4 : Cinétiques d'induction de FBW2

Induction de l'expression de la construction 3HA-FBW2 sous le contrôle du promoteur XVE inductible au β-estradiol (Zuo et al., 2000). Le bleu de Coomassie sert de contrôle de charge. "@" indique une hybridation avec l'anticorps correspondant.
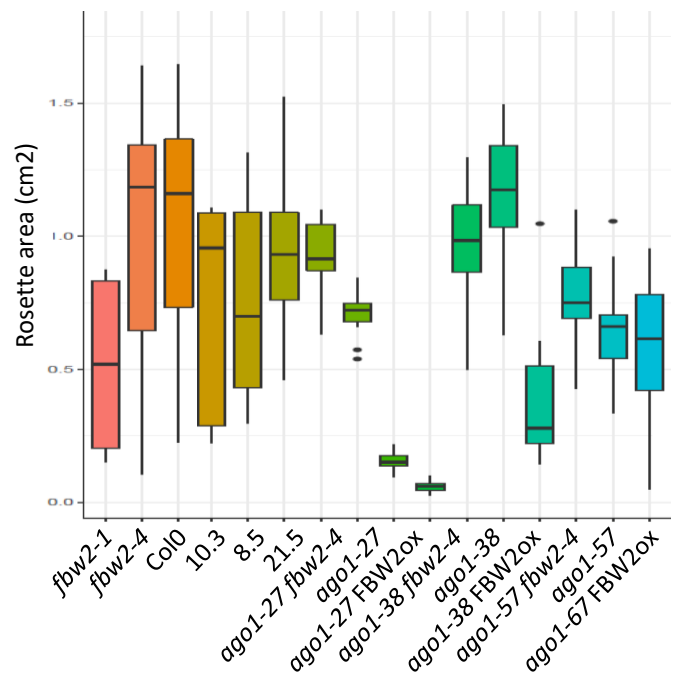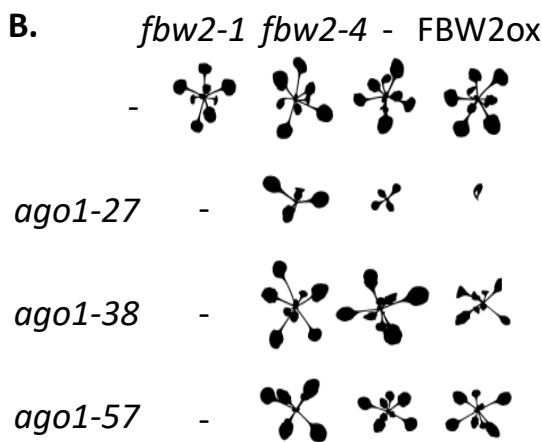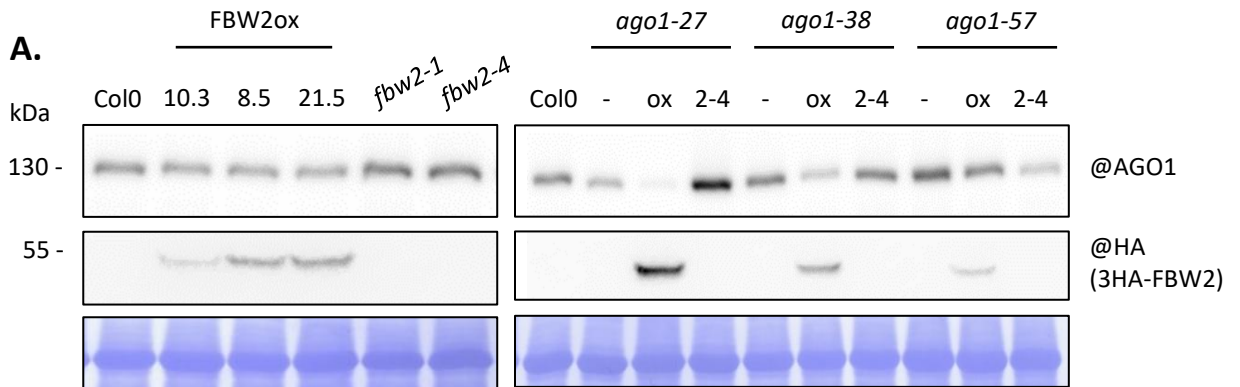
A. et B. Western blots d'extraits protéiques de plantules âgées de 5 à 12 jours de la lignées transgénique spécifiée ayant grandit sur milieu MS supplémenté de DMSO (-) ou de β-estradiol (10 μM) (+).

B. Analyses RT-qPCR du niveau d'expression de *FBW2*, relatif au Col0 âgé de 5 jours, dans des plantules ayant grandit sur milieu MS supplémenté de β-estradiol (10 μM).

| | 0 | 0,5 | 1 | 2 | 4 | 7 | Duration of treatment |
| kDa | | | | | | | |

55 - CHX

55 - CHX + MLN4924

55 - CHX + MG132

@ HA (3HA-FBW2)

Figure 5 : Stabilité de la protéine FBW2

Estimation de la demi-vie de la protéine FBW2 dans des platules 35S::3HA-FBW2 traitées avec du cycloheximide (CHX) qui bloque la traduction des protéines. Western blots d'extraits protéiques de plantules âgées de 10 jours traitées avec du cycloheximide (100 μM) supplémenté de MLN4924 (25 μM) or MG132 (100 μM). Le MNL4924 bloque l'activié des E3 ligase de type CRL. Le MG132 inhibe l'activité du protéasome 26S. Le bleu de Coomassie sert de contrôle de charge. "@" indique une hybridation avec l'anticorps correspondant.

A l'inverse des expériences en expression transitoire, la surexpression de FBW2 dans Arabidopsis induit la dégradation d'AGO1, à priori, moins efficacement. En effet, le transgène de lignées surexprimant FBW2 de manière inductible est rapidement ciblé par l'ARN interférence, ce qui aboli son expression en quelques jours réduisant la capacité de FBW2 à inhiber l'activité d'AGO1 (Figure 4). De plus, l'étude de la demi-vie de FBW2 met en évidence une forte instabilité due à une régulation par le système ubiquitine-protéasome (Figure 5). Ces obstacles ont été surmontés d'une part par le croisement des lignées inductibles avec des mutants affectés dans l'ARN interférence et par la génération de lignées surexprimant de manière constitutive FBW2. Une déstabilisation critique d'AGO1 est visible lorsque FBW2 est surexprimé dans les mutants tandis qu'elle est plus nuancée dans un fond génétique sauvage. Le traitement de ces plantes par des drogues inhibant les mécanismes de protéolyses connus montre que l'ubiquitination d'AGO1 est nécessaire pour sa déstabilisation par FBW2 mais ne permettent pas de définir clairement la voie responsable de sa dégradation. FBW2 induirait donc la dégradation d'AGO1 par une voie non conventionnelle.

Figure 6 : La surexpression ou l'absence de FBW2 affecte les mutants *ago1*

A. Western blots d'extraits protéiques de plantules âgées de 17 jours *ago1-27*, *ago1-38* et *ago1-57*, aussi croisées avec *fbw2-4* ou 35S:3HA-FBW2 (FBW2ox) lignée 10 comme indiqué. 10.3, 8.5 and 21.5 correspondent à des lignées 35S:3HA-FBW2 indépendantes. "ox" indique le croisement avec la lignée surexpresseur 10.3, "2-4" avec le mutant *fbw2-4* et "–" au simple mutant. Le bleu de Coomassie sert de contrôle de charge. "@" indique une hybridation avec l'anticorps correspondant. Le faible niveau d'accumulation d'AGO1 dans *ago1-57 fbw2-4* est probablement causé par une erreur technique étant donné que d'autres Western blots montrent une stabilisation d'AGO1.

B. Gauche : empreinte de la forme des plantules décrit précédemment. Droite : Mesures de l'aire des rosettes des mêmes plantules.

Au niveau physiologique, l'absence ou la surexpression de FBW2 ne produisent pas de phénotypes particuliers sauf dans les mutants affectés dans l'ARN interférence (Figure 6). La perte de FBW2 restaure partiellement le phénotype de mutants *ago1* tandis que sa surexpression accroît leurs défauts développementaux. Ceci suggère que FBW2 module l'activité d'AGO1 en contrôlant son homéostasie. FBW2 n'est néanmoins pas capable d'inhiber l'ARN interférence comme P0 ; la régulation d'une Green Fluorescent Protein (GFP) par l'ARN interférence en expression transitoire dans *benthamiana* est complètement abolie par P0 mais n'est que faiblement affectée par FBW2. Dans d'autres mutants affectés dans la production ou la stabilité des petits ARNs, la perte ou la surexpression de FBW2 accentue considérablement les défauts développementaux tout en restaurant ou déstabilisant davantage AGO1. Ce résultat surprenant peut être expliqué par l'apparition d'une activité délétère d'AGO1 en absence de petits ARNs qui serait normalement éliminée par FBW2. L'analyse du séquençage des petits ARNs dans ces mutants est en cours et met déjà en évidence des ARNs inhabituels davantage présents dans AGO1 en absence de petits ARNs et plus encore en absence de FBW2. FBW2 contrôle donc l'activité d'AGO1 en régulant son homéostasie pour limiter l'utilisation aspécifique d'ARNs par cette dernière.

En conclusion, FBW2 ne se présente pas comme l'alter-ego endogène de la protéine virale P0. FBW2 agit bien comme une protéine F-box qui cible et provoque la dégradation d'AGO1 mais dans un contexte plus spécifique. La voie de dégradation d'AGO1 par FBW2 reste cependant encore inconnue. Il est possible qu'AGO1 soit dégradée dans la vacuole par un processus parallèle de l'autophagie canonique. La complexité de l'autophagie ne fait qu'émerger dans les publications scientifiques et des voies de dégradation candidates sont à l'étude dans le laboratoire. Il est néanmoins certain que FBW2 n'est pas l'unique régulateur post-traductionnel d'AGO1. Le nombre de protéines à motif « AGO-hook » est pour le moment restreint, FBW2 serait donc la première protéine F-box le comportant. De manière intéressante, la nécessité de réguler les protéines ARGONAUTE n'ayant pas fixé de petits ARNs a été proposée en levure mais jamais démontrée (Holoch and Moazed, 2015) alors que l'instabilité des protéines ARGONAUTE en absence de petits ARNs est connue depuis longtemps (Smibert et al., 2013).

Bibliographie

- Baulcombe, D. (2004). RNA silencing in plants. Nature *431*, 356–363.
- Baumberger, N., Tsai, C., Lie, M., Havecker, E., and Baulcombe, D.C. (2007). The Polerovirus silencing suppressor P0 targets ARGONAUTE proteins for degradation. Curr. Biol. *17*, 1609–1614.
- Bortolamiol, D., Pazhouhandeh, M., Marrocco, K., Genschik, P., and Ziegler-Graff, V. (2007). The Polerovirus F box protein P0 targets ARGONAUTE1 to suppress RNA silencing. Curr. Biol. *17*, 1615–1621.
- Derrien, B., Baumberger, N., Schepetilnikov, M., Viotti, C., De Cillia, J., Ziegler-Graff, V., Isono, E., Schumacher, K., and Genschik, P. (2012). Degradation of the antiviral component ARGONAUTE1 by the autophagy pathway. Proc. Natl. Acad. Sci. U. S. A. *109*, 15942–15946.
- Earley, K., Smith, M., Weber, R., Gregory, B., and Poethig, R. (2010). An endogenous F-box protein regulates ARGONAUTE1 in Arabidopsis thaliana. Silence *1*, 15.
- Holoch, D., and Moazed, D. (2015). Small-RNA loading licenses Argonaute for assembly into a transcriptional silencing complex. Nat. Struct. Mol. Biol. *22*, 328–335.
- Pazhouhandeh, M., Dieterle, M., Marrocco, K., Lechner, E., Berry, B., Brault, V., Hemmer, O., Kretsch, T., Richards, K.E., Genschik, P., et al. (2006). F-box-like domain in the polerovirus protein P0 is required for silencing suppressor function. Proc. Natl. Acad. Sci. U. S. A. *103*, 1994–1999.
- Smibert, P., Yang, J.-S., Azzam, G., Liu, J.-L., and Lai, E.C. (2013). Homeostatic control of Argonaute stability by microRNA availability. Nat. Struct. Mol. Biol. *20*, 789–795.
- Wang, X.-B., Jovel, J., Udomporn, P., Wang, Y., Wu, Q., Li, W.-X., Gasciolli, V., Vaucheret, H., and Ding, S.-W. (2011). The 21-Nucleotide, but Not 22-Nucleotide, Viral Secondary Small Interfering RNAs Direct Potent Antiviral Defense by Two Cooperative Argonautes in Arabidopsis thaliana. Plant Cell *23*, 1625–1638.

Thibaut Hacquard

Molecular characterization of the F-box protein FBW2 in the RNA silencing in *Arabidopsis thaliana*

UNIVERSITÉ DE STRASBOURG

École Doctorale des Sciences de la Vie et de la Santé STRASBOURG

L'ARN interférence est un mécanisme moléculaire conservé chez les Eucaryotes dont les principaux acteurs sont les protéines ARGONAUTE (AGO). Chez les plantes, AGO1 est une protéine essentielle à la croissance et la défense antivirale. Elle utilise des petits ARNs comme sondes pour reconnaître et réguler des ARN messagers. Les virus ont développé des suppresseurs de l'ARN interférence pour surmonter cette défense. L'un d'entre eux, P0 du virus de la mosaïque jaune du navet, est comme une protéine F-box qui détourne le complexe SCF, une ubiquitine ligase E3, et conduit AGO1 vers la protéolyse ubiquitine-dépendante. Cette dégradation utilise la vacuole au lieu du protéasome 26S, généralement associé à la dégradation ubiquitine-dépendante. Ce mécanisme de protéolyse n'est pas compris et est aussi apparent quand AGO1 est déstabilisé de manière endogène, suggérant que P0 utilise une voie déjà existante. Une protéine F-box d'Arabidopsis, FBW2, a été décrite comme impactant l'homéostasie d'AGO1 indépendamment du protéasome. Mon projet de thèse visait à caractériser l'activité F-box de FBW2 et à comprendre la relation entre AGO1 et FBW2 ainsi que ses conséquences sur l'ARN interférence.

Les résultats obtenus dans ce manuscrit montrent que le complexe SCF^{FBW2} interagit avec AGO1 et déclenche sa dégradation via un processus indépendant de l'autophagie ou du protéasome, tout en n'affectant que faiblement l'ARN interférence. FBW2 ciblerait en fait un sous-ensemble de protéines AGO1 qui semble ne pas contenir de petits ARNs. Cette régulation jouerait un rôle de surveillance pour prévenir une activité délétère d'AGO1 en absence de petits ARNs.

Mots clés : Arabidopsis, ARN interférence, AGO1, ubiquitine, SCF, FBW2

RNA silencing is a conserved molecular mechanism in eukaryotes, of which the main effectors are the ARGONAUTE (AGO) proteins. In plants, AGO1 is a protein that is essential for growth and antiviral defence. It uses small RNAs as probe to recognize and regulate messenger RNAs. Viruses have developed suppressors of RNA silencing to overcome this defence. One of these, P0 from the Turnip Yellows Virus, acts as an F-box protein to hijack the SCF complex, an E3 ubiquitin ligase, and guide AGO1 to the ubiquitin-dependent proteolysis. This degradation uses the vacuole instead of the 26S proteasome, generally associated with ubiquitin-dependant proteolysis. This proteolysis mechanism is not understood and is also apparent when AGO1 is endogenously destabilized, suggesting that P0 uses an already existing pathway. An Arabidopsis F-box protein, FBW2, has been shown to impact AGO1 homeostasis independently from the proteasome. My PhD project aimed at characterizing FBW2 F-box activity and understanding the relationship between AGO1 and FBW2, as well as its consequences on the RNA silencing.

The results obtained in this manuscript show that the SCF^{FBW2} interacts with AGO1 and triggers its degradation through an autophagy- and proteasome- independent process, while only weakly affecting the RNA silencing. FBW2 would actually target a subset of AGO1 proteins, which appears not to contain small RNAs. This regulation would play a surveillance role in order to prevent a deleterious activity of AGO1 in absence of small RNAs.

Keywords : Arabidopsis, RNA silencing, AGO1, ubiquitin, SCF, FBW2